Effect of the Pliocene closure of the Panamanian Gateway on Caribbean and east Pacific sea surface temperatures and salinities by applying combined Mg/Ca and $\delta^{18}O$ measurements (5.6-2.2 Ma)

Kumulative Dissertation

zur Erlangung des Doktorgrades
der Mathematisch-Naturwissenschaftlichen Fakultät
der Christian-Albrechts-Universität
zu Kiel

vorgelegt von

Jeroen Groeneveld

Kiel, Mai 2005

Referent:		PD Dr. Dirk Nürnberg
Koreferent:		Prof. Dr. Ralph Schneider
Tag der Disputation:		1. Juli 2005
Zum Druck genehmigt:	Kiel, den:	1. Juli 2005
Der Dekan:		Prof. Dr. Wolfgang Kuhnt

Hiermit erkläre ich an Eides statt, dass die vorliegende Abhandlung, abgesehen von der Beratung durch meine akademischen Lehrer, in Inhalt und Form meine eigene Arbeit darstellt. Ferner habe ich weder diese noch eine ähnliche Arbeit an einer anderen Hochschule im Rahmen eines Prüfungsverfahrens vorgelegt.

_____

Jeroen Groeneveld

Recently it has been shown that about thirty per cent of the fishes are the same on the opposite sides of the isthmus of Panama; and this fact has led naturalists to believe that the isthmus was formerly open.
(*Origin of Species, Charles Darwin*, 1*859*)

Abstract

This Ph.D-thesis has been accomplished within the DFG Research Unit "Impact of Gateways on Ocean Circulation, Climate and Evolution" at the Leibniz Institute of Marine Sciences, IFM-Geomar at the University of Kiel. Main objective was to reconstruct Caribbean and Pacific changes in sea surface temperature and salinity that probably resulted from the gradual shoaling of the Isthmus of Panama from 5.6-2.2 Ma. The application of Mg/Ca paleothermometry and the combination with stable oxygen isotopes allowed to determine changes in sea surface temperature (SST) and sea surface salinity (SSS) for mixed layer water masses on both sides of the Isthmus of Panama (ODP Sites 999, 1000, and 1241). A second main objective was the further development of Mg/Ca as a proxy to reconstruct paleo-sea water temperatures. The influence of external factors like diagenesis and salinity on the temperature signal in Mg/Ca was investigated and a high-precision analytical method for the determination of Mg/Ca-ratios was developed.

The divergence of the SST and SSS records between Caribbean Sites 999 and 1000, and east Pacific Site 1241 monitors the progressive closure of the Panamanian Gateway. The divergence of Caribbean-Pacific SSS is first recognized at Site 1000 (at 5.6 Ma) and ~1.4 million years later at Site 999 (at 4.2 Ma), implying a pronounced intra-Caribbean SSS-contrast, especially between 5.6 and 3.7 Ma. This evolution reflects the decreasing inflow of relatively fresh Pacific water masses (Site 1241) into the Caribbean that led to the gradual establishment of the modern Pacific-Caribbean SSS-contrast. By ~2.2 Ma, the Pacific-Caribbean salinity difference equaled ~1‰.

The evolution of Pacific-Caribbean mixed-layer temperatures was different. The northern part of the Caribbean (Site 1000) was ~3°C warmer from 5.6 to 4.4 Ma than the southern Caribbean and the adjacent Pacific (24-26°C). After 4.4 Ma, $SSTs_{Mg/Ca}$ increased at Site 1000 by ~2°C, while $SST_{Mg/Ca}$ close to the gateway region (Sites 999 and 1241) remained relatively constant. The $SST_{Mg/Ca}$ increase at Site 1000 is considered to reflect the progressive development of the Western Atlantic Warm Pool (WAWP).

Although the Pliocene $SSTs_{Mg/Ca}$ are relatively similar between Pacific Site 1241 and Caribbean Site 999, marked differences in the phasing of temperature fluctuations provide hints for the final phase of the closure of the Panamanian Gateway after 2.7 Ma. With the onset of Northern Hemisphere Glaciation at 2.7 Ma, sea level changes started to influence the throughflow through the Panamanian Gateway. Sea level lowstands with 50-80 m during Marine Isotope Stages (MIS) 96, 98, and 100 caused the glacial closure of the Panamanian Gateway. $SST_{Mg/Ca}$ in the east Pacific (Site 1241) followed the global cooling signal, while $SST_{Mg/Ca}$ in the Caribbean (Site 999) increased during glacials due to the cessation of the inflow of colder east Pacific watermasses.

The hypothesis of a permanent El Niño like climate state during the warm Pliocene remains controversial. Support is delivered by a low SST-gradient in the east Pacific between Sites 1239 and 1241 as well as a low SST-gradient between Site 1241 and west Pacific Site 806. In contrast, similar $SSTs_{Mg/Ca}$ at Site 1241 in comparison with modern SSTs do not directly support a permanent El Niño state climate. Therefore, if a permanent El Niño has occurred, the latest Miocene/earliest Pliocene (>5.0 Ma) seems to be the most likely interval.

Extreme high Mg/Ca-ratios and accompanying $SSTs_{Mg/Ca}$ of up to 35°C after 4.5 Ma at Site 1000 suggest the influence of processes other than temperature on the Mg/Ca-signal. Scanning electron microscope (SEM) analyses revealed the presence of crystalline overgrowths on cleaned foraminiferal tests. The analysis of carbonate chemistry and nannoplankton assemblages indicated a diagenetic signal with precessional cyclicity. LA-ICP-MS and pore water data were used to show that the diagenetic overprint, however, is not responsible for the extreme foraminiferal Mg/Ca-ratios. The positive correlation of Mg/Ca with $\delta^{18}O_{G.\ sacculifer}$, instead, suggests a salinity-related Mg/Ca-increase in the foraminiferal tests.

Zusammenfassung

Diese Dissertation wurde durchgeführt innerhalb der DFG Forschergruppe "Impact of Gateways on Ocean Circulation, Climate and Evolution" am Leibniz Institut für Marine Wissenschaften, IFM-Geomar an der Christian-Albrechts Universität in Kiel. Die Hauptfragestellung dieser Dissertation war die Rekonstruktion der Schließung des Panama-Seeweges innerhalb des Zeitintervals 5.6-2.1 Ma an Hand von Änderungen der karibischen und pazifischen Meerswassertemperaturen und Salzgehalte, die die fortschreitende Schließung des Panama-Seeweges kennzeichnen. Untersuchungsmethode war hauptsächlich die Anwendung der Mg/Ca Paläothermometrie in Kombination mit der Analyse von $\delta^{18}O$ für die Bestimmung der Temperaturen und Salzgehalte des Oberflächenwassers an beiden Seite der Landenge von Panama (ODP Sites 999, 1000 und 1241). Ein weiterer Anspruch dieser Arbeit war die Weiterentwicklung von Mg/Ca als Untersuchungsmethode für die Rekonstruktion von Meereswassertemperaturen. Der mögliche Einfluss der externen Faktoren Diagenese und Salzgehalt auf das Temperatursignal in Mg/Ca wurde untersucht. Des weiteren ist eine hoch präzise Methode für die Bestimmung von Mg/Ca entwickelt worden.

Das Auseinanderlaufen der Datensätze von Temperatur und Salzgehalt zwischen den Sites 999, 1000 und 1241 zeigt die fortschreitende Schließung des Panama-Seeweges, wie insbesondere durch die fortschreitende Zunahme des Salzgehaltes von 5.6 bis 3.7 Ma vom Norden der Karibik (Site 1000) zu ihrem Süden (Site 999) angezeigt wird. Dementsprechend ist die Differenz von karibischen und pazifischen Salzgehalten erstmals beobachtbar an Site 1000 (5.6 Ma) und erst 1.4 Millionen Jahre später an Site 999 (4.2 Ma). Diese Entwicklung spiegelt den abnehmenden Zufluss von relativ frischen pazifischen Wassermassen (Site 1241) in die Karibik wieder, die zu der fortschreitenden Anlage des heutigen pazifisch-karibischen Salzgehaltkontrastes führte. Vor 2.2 Ma wurde zwischen Pazifik und Karibik eine Salzgehaltdifferenz von ~1‰ erreicht.

Die Entwicklung der pazifischen und karibischen Oberflächenwassertemperaturen hingegen unterscheidet sich von der Entwicklung der Salzgehaltdifferenz. Der nördliche Teil der Karibik (Site 1000) war etwa 3°C wärmer, im Zeitintervall zwischen 5.6 und 4.4 Ma als der südliche Teil der Karibik und als der angrenzende Pazifik (24-26°C). Vor 4.4 Ma stiegen die durch die Mg/Ca-Paläothermometrie ermittelten Temperaturen bei Site 1000 um etwa 2°C, während die Temperaturen, die auf dieselbe Weise nahe der Gateway Region ermittelt wurden (Sites 999 und 1241), relative konstant blieben. Der genannte Temperaturanstieg bei Site 1000 zeigt wahrscheinlich die fortschreitende Entwicklung des Western Atlantic Warm Pools (WAWP). Obwohl die pliozänen Temperaturen zwischen dem pazifischen Site 1241 und dem karibischen Site 999 relativ ähnlich waren, geben Änderungen in dem Verhältnis der Temperaturzyklen einen Hinweis auf die Phase der endgültigen Schließung ab 2.7 Ma.

Jedoch hatte die vor 2.7 Ma beginnende Vereisung der Nordhemisphäre schon vorher Einfluss auf den Durchstrom durch den Panama-Seeweg, bedingt durch Schwankungen des Meeresspiegels. Meeresspiegelschwankungen von 50-80 m während der Isotopenstadien 96, 98, und 100 verursachten die glazialen Schließungen des Panama-Seeweges. In dem Zusammenhang sanken die Temperaturen des Oberflächenwassers im Ostpazifik, dem globalen Abkühlungstrend folgend, während die Temperaturen des Oberflächenwassers in der Karibik zunahmen, da es zu keinem Zufluss des kälteren Wassers aus dem Pazifik mehr kommen konnte.

Die Hypothese von einem permanenten El Niño während des Pliozäns bleibt umstritten. Gestützt wird diese These durch den geringen Temperaturgradienten sowohl zwischen den Sites 1239 und 1241 als auch zwischen dem Ostpazifik (Site 1241) und dem Westpazifik (Site 806). Allerdings spricht der Vergleich der Wassertemperaturen des Site 1241 mit heutigen Temperaturwerten auf Grund der Ähnlichkeit gegen einen permanenten El Niño während des Pliozän. Auch eine signifikante Verflachung der Thermokline an Site 1241 spricht gegen einer permanenten El Niño zu dieser Zeit. Sollte dieser dennoch existiert haben, so erscheint eine Datierung des Phänomens auf das spätestes Miozän, beziehungsweise das früheste Pliozän am wahrscheinlichsten.

In der zentralen Karibik (Site 1000) ergaben sich nach 4.5 Ma auf Grund der gemessene Mg/Ca-Verhältnisse unrealistisch hohe Temperaturwerte bis 35°C. Dies war ein Hinweis dafür, dass neben der Temperatur noch weitere Faktoren Einfluss auf das Mg/Ca-Signal haben könnten. Die daraufhin durchgeführten Analysen mit dem Raster Elektronen Mikroskop zeigten die Existenz kristalliner Ablagerungen auf den Schalen gereinigter Foraminiferen. Die Analysen von Karbonatchemie und Nannoplanktonvergesellschaftungen zeigten ein diagenetisches Signal mit einer präzessionalen Zyklizität auf. Die Ergebnisse der LA-ICP-MS und die Analyse der Porenwasserdaten zeigten jedoch, dass dieses diagenetisches Signal trotzdem keine ausreichende Erklärung für die extremen Mg/Ca-Verhältnisse liefern kann. Der Vergleich der Mg/Ca-Verhältnisse mit den Werten der Sauerstoffisotope von *G. sacculifer* weist eine positive Korrelation auf. Dies deutet darauf hin, dass die genannten extremen Mg/Ca-Verhältnisse durch den Salzgehalt verursacht wurden.

Contents

Chapter 1

Introduction, objectives, and site selection

Introduction and main objectives of this thesis

This thesis was generated within the DFG Research Unit "Impact of Gateways on Ocean Circulation, Climate and Evolution" at the University of Kiel as part of the sub-project "Impact of low-latitude Gateways on the Formation of Warm Pools, Ocean Circulation, and Climate". The sub-project focused on the Miocene to Pliocene closure history of the Panamanian Gateway. Several studies suggested that the shoaling of the isthmus crossed a threshold in Caribbean/Atlantic SSS increase between 4.6 and 4.2 Ma, thereby leading to profound changes in global ocean circulation and climate. However, the interpreted increase in Caribbean/Atlantic SSS was solely based on planktonic oxygen isotopes and thus was never reliably quantified. When and to what degree the shoaling of the isthmus influenced the Pliocene Northern Hemisphere Glaciation is still in discussion. Arguments vary from either being the cause for the onset (Berggren and Hollister, 1974), the delay (Berger and Wefer, 1996), or setting pre-conditions for the NHG (Driscoll and Haug, 1998; Haug and Tiedemann, 1998).The main objective of this thesis was to reconstruct closure-related effects on Pacific/Caribbean sea surface temperature (SST) and sea surface salinity (SSS) as well as their impact on global thermohaline circulation and climate. The study focused on the time interval 5.6-2.2 Ma and used Mg/Ca in planktonic foraminifera as its main tool in combination with planktonic oxygen isotope records (Steph, 2005) to allow the quantification of SSS.

Major objectives of this thesis are:

* How and when did the modern SSS and SST gradients between the east Pacific and the Caribbean develop?
* Did the progressive closure lead to the development of the WAWP and subsequently to an increased transport of heat and salt into the North Atlantic?
* How did surface ocean circulation in the east Pacific and the Caribbean respond to the progressive closure of the Panamanian Gateway?
* Can the early Pliocene be referred to as a permanent El Niño based climate?
* Can changes in SST and SSS in the east Pacific and the Caribbean be related to global trends in climate?
* Application and verification of Mg/Ca paleothermometry for the Pliocene.
* Improvement and further development of Mg/Ca analytical procedures.

Strategy and structure of this thesis

Sediment samples from three ODP Sites from the Caribbean (999 and 1000) and the east Pacific (1241) were analysed to solve the outlined questions. The planktonic foraminifer *Globigerinoides sacculifer* was selected to reconstruct mixed-layer SST and SSS by means of Mg/Ca and $\delta^{18}O$, as this species is considered to live at 30-80 m water depth (Fairbanks et al., 1982).

To further improve the interpretation additional SST reconstructions from deeper dwelling or high-latitude foraminifers (*N. dutertrei, G. tumida, G. limbata,* (Steph, 2005) and *G. bulloides*), other proxies (Sr/Ca,

aragonite, nannoplankton assemblages, benthic $\delta^{18}O$, and transfer functions), and site locations (ODP Sites 1239, 806, DSDP Site 609) were considered.

The first part of this thesis (Chapters 1-3) contains the introduction to the dissertation with its main objectives (**Chapter 1**), a general introduction to the hydrography of the Caribbean and the east Pacific as well as an overview of the closure history of the Panamanian Gateway (**Chapter 2**), and an introduction into Mg/Ca paleothermometry with additional information on the applied methods and the reliability of the Mg/Ca analyses (**Chapter 3**).

The manuscripts which I have submitted or are in preparation as a first author to internationally peer-reviewed journals are presented in Chapters 4, 5 and 6. **Chapter 4** investigates the development of SST- and SSS-gradients between the Caribbean and the east Pacific and presents the glacial emergence of the Isthmus of Panama. **Chapter 5** examines the development of east Pacific upper ocean water mass signatures in relation to global climate trends as well as the hypothesis of a permanent El Niño-like climate state during the warm Pliocene. **Chapter 6** explores the potential explanations, i.e. SST increase, salinity influence, or diagenesis, for the extremely high Mg/Ca-ratios in the central Caribbean <4.5 Ma by using LA-ICP-MS and pore water data.

Chapter 7 provides a publication to Eos in which a general overview of the closure of the Panamanian Gateway is presented as a result of a workshop which was held by the Ocean Gateway Project in Kiel, 2004. **Chapter 8** summarizes the main conclusions of this thesis by considering the questions previously raised in Chapter 1. In addition, perspectives for future work are suggested. The Appendix includes the data which have been generated within this thesis and which were presented in Chapters 3-6. Supplementary data on the studied cores are presented in the Ph.D theses of S. Steph (2005) and D. Crudeli (2005).

Site selection and age models

Three ODP Sites from the Caribbean (999 and 1000) and the tropical east Pacific (1241) were chosen to provide samples for this study (Fig. 1.1). Due to the close proximity of Sites 999 and 1241 to the former gateway they allow a detailed reconstruction of the progressive closure of the Panamanian Gateway. Since Caribbean Site 1000 is located further away from the former gateway, it provides the opportunity to reconstruct intra-Caribbean gradients in upper water mass signatures that resulted from the decreasing Pacific-Caribbean water mass exchange.

Site 999

ODP Site 999 was recovered during Leg 165 in the Colombian Basin (12°44'N, 78°44'W, Fig. 1) from a water depth of 2828 m (Fig. 1.1). Samples were taken every 10 cm, reflecting a temporal resolution of ~3 kyr per sample. The age model for Site 999 (Haug and Tiedemann, 1998) was established by adjusting the benthic $\delta^{18}O$ fluctuations (*C. wuellerstorfi*) to the astronomical calibrated benthic $\delta^{18}O$ records of ODP Sites 846 (Shackleton et al., 1995) and 659 (Tiedemann et al., 1994).

For a direct comparison, however, we adjusted the benthic $\delta^{18}O$ fluctuations at Site 999 precisely to those at Site 1241 to eliminate phase offsets in the obliquity-related frequency band (41 kyr-cycle) (Chapter 4). This adjustion was performed with the software programm AnalySeries 1.2 (Paillard et al., 1996).

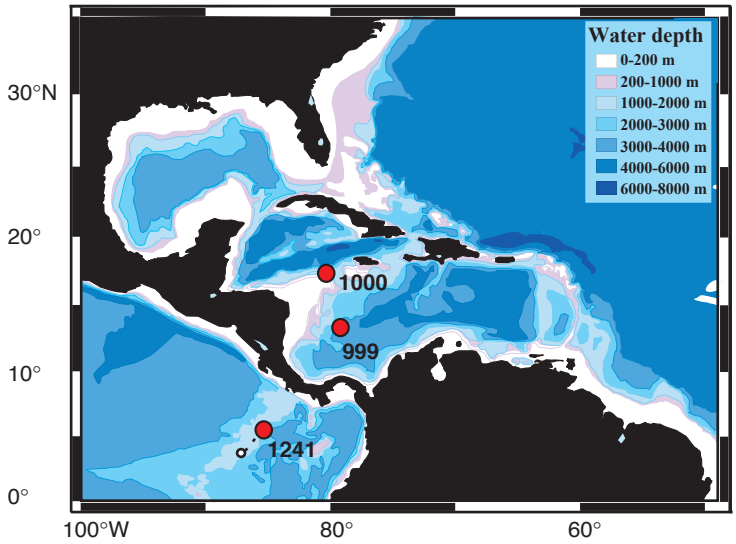

Figure 1.1 Geography and bathymetry of the Caribbean and the east Pacific with the locations of the studied ODP Sites 999, 1000, and 1241.

Site 1000

ODP Site 1000 was cored during Leg 165 on the Nicaraguan Rise (Pedro Channel) (16°33.222'N, 79°52.044'W, Fig. 1.1). Samples were taken every 10 cm, reflecting a temporal resolution of ~3 kyr per sample.

The age model for Site 1000 (Steph et al., submitted) was based on the $\delta^{18}O$ record of the benthic foraminifer *C. wuellerstorfi*. Since no composite depth exists for Site 1000, a preliminary age model was constructed by identifying major $\delta^{18}O$ isotopic stages according to the nomenclature of Shackleton et al. (1995), but using the age model and the $\delta^{18}O$-reference record from ODP Site 925/926 from Ceara Rise (Bickert et al., 1997; Tiedemann and Franz, 1997; Shackleton and Hall, 1997), the final age model revealed the presence of dominant precession cycles in the planktonic $\delta^{18}O$ record, which were then used to fine-tune the age model from Site 1000 (Steph et al., submitted).

Site 1241

ODP Site 1241 was cored during Leg 202 in the Guatemalan Basin on the north flank of the Cocos Ridge (5°50N, 86°26W). The present day location of Site 1241 is within the eastward flowing NECC. A tectonic backtrack of the Cocos Plate, on which Site 1241 is positioned, locates Site 1241 between 4 Ma and 5 Ma at a more southwesterly position around 3°N, 87.7°W (Mix, Tiedemann, Blum et al., 2003; Pisias et al.,1995) (Fig. 1.1). The closer proximity to the equatorial divergence and the SEC suggests that the expected SST and SSS at Site 1241 were about 1°C cooler and 0.35 less saline during the early Pliocene if east Pacific hydrography would have been similar to the modern configuration (Mix, Tiedemann, Blum et al., 2003).

Samples were taken every 10 cm, reflecting a temporal resolution of better than 3 kyr per sample The age model for Site 1241 was constructed by matching patterns of cyclic variation in climate proxy records with patterns of changes in solar radiation that are controlled by cyclic variations in Earth's orbital parameters. This astronomically derived age model is in agreement with the most recent astronomical polarity time scale and with other orbitally tuned age models. The establishment of the age model is described in detail in Tiedemann et al. (submitted).

Chapter 2

Modern hydrography and the closure of the Panamanian Gateway

Tropical east Pacific hydrography

Surface hydrography in the tropical Pacific is strongly controlled by seasonal variations in wind strength, causing seasonal changes in thermocline depth. In general, the North Equatorial Counter Current (NECC) is closely linked to the Intertropical Convergence Zone (ITCZ), the zone of maximal heating and convergence of the northeast and southeast trade winds (Donguy and Meyers, 1996; Huber, 2002). North of the ITCZ, the northeast trade winds drive the North Equatorial Current (NEC) towards the west, while the southeast trade winds drive the South Equatorial Current (SEC) also to the west, but south of the ITCZ. Below the SEC and the equator, the Equatorial Under Current (EUC) flows towards the east from a depth of ~300 m in the Western Pacific Warm Pool (WPWP) to a depth of ~30 m in the east Pacific, parallel to the shallowing thermocline. The EUC is driven by the west-east pressure gradient and confined by the Coriolis force to the equator between 2°N and 2°S (Fig. 2.1).

El Niño-like conditions for the Pacific exist when the warm waters of the WPWP move to the east due to weak easterly winds over the tropical Pacific. This causes the cessation of upwelling, a decreasing temperature gradient between the WPWP and the east Pacific, and a deepening of the thermocline in the east Pacific (Wallace et al., 1998).

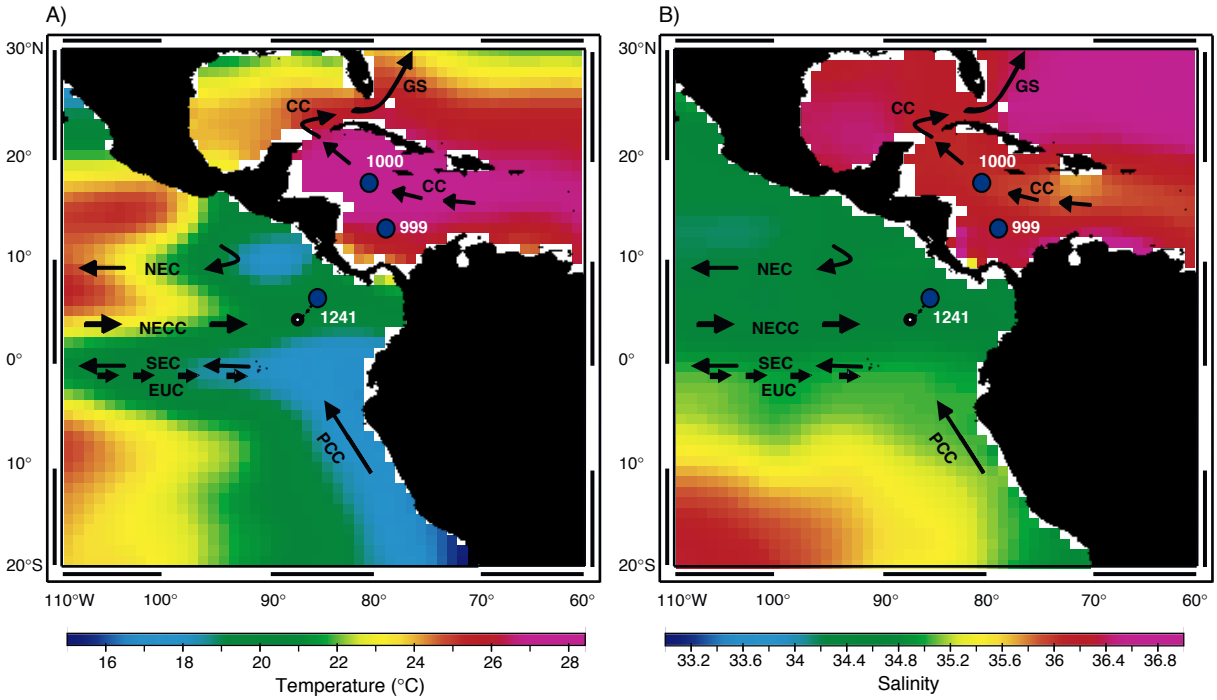

Figure 2.1 Modern hydrography in the Caribbean and the east Pacific, showing annual average sea water temperatures (**A**) and salinities (**B**) at a water depth of 50 m (Levitus and Boyer, 1994), corresponding to the assumed habitat depth of *G. sacculifer* (30-80 m). Blue dots indicate locations of ODP Sites 999, 1000, and 1241 and the tectonic backtrack for Site 1241 (open black dot) (Mix et al., 2003). Major current directions are indicated with arrows: GS: Gulfstream; CC: Caribbean Current; NEC: North Equatorial Current; NECC: North Equatorial Counter Current; SEC: South Equatorial Current; EUC: Equatorial Under Current; PCC: Peru/Chile Current.

Caribbean hydrography

The Caribbean Sea plays an important role as major source region for the Gulfstream in the net export of heat and salt into high northern latitudes. Today, the uppermost water column in the southern part of the Caribbean is composed of relatively fresh Caribbean Water (CW, 0-80 m) and high-salinity Subtropical Under Water (SUW) between ~80-180 m that forms the permanent Caribbean thermocline (Wüst, 1964). The CW represents a mixture of the Amazon and Orinoco River outflow and equatorial Atlantic surface water that mainly enters the Caribbean *via* the Guyana Current through the Lesser Antilles Passages. The salinity enriched SUW originates from the subtropical gyre and mainly enters the Caribbean *via* the North Equatorial Current through the Greater Antilles Passages (Wüst, 1964; Johns et al., 2002). These water masses form the Caribbean Current that passes the Yucatan Channel and the Florida Straits, where it merges with the Antilles Current to form the Gulf Stream (Fig. 2.1).

A significant amount of Amazon freshwater is carried northwestward and can be traced into the central Caribbean Sea to about 70°W (Hellweger and Gordon, 2002). Although the largest river, which drains directly into the western Caribbean, is the Magdalena River, its absolute volume is negligible in comparison with the freshwater provided by the Orinoco and Amazon rivers. In addition to the Amazon and Orinoco rivers, Caribbean SSS is controlled by the seasonal position of the tropical rain belt that follows the ITCZ and determines the evaporation/precipitation ratio.

Modern SSS and SST gradients

The present day east Pacific is characterized by relatively low temperatures (Fig. 2.1). The southeast trade winds cause strong upwelling along the Peruvian coast and along the equator, thus forming the Pacific Cold Tongue, which extends towards the west along the equatorial divergence (Mitchell and Wallace, 1992). Accordingly, the thermocline in these areas is very shallow (<50 m). In contrast, the Caribbean/Western Atlantic Warm Pool (WAWP) is marked by a distinctly deeper thermocline (100-150 m). At a water depth of 50 m (estimated mean habitat depth of *G. sacculifer*), the temperature contrast between the Caribbean and the east Pacific is 5-6°C (Fig. 2.1), while at the surface, SST is about 27°C, both for Site 1241 and the Caribbean (Levitus and Boyer, 1994).

A salinity gradient of 1-1.5 exists between the Atlantic/Caribbean and the east Pacific (Fig. 2.1), which is mainly determined by the net transport of water vapour from the Caribbean over central America into the east Pacific by means of the trade winds (Broecker and Denton, 1989).

The closure history of the Panamanian Gateway

The Neogene tectonic closure of the Panamanian Gateway (12.9-1.8 Ma) resulted from the subduction of the Pacific Cocos and Nazca plates beneath the North and South American plates and later the Caribbean Plate (Fig. 2.2) (Dengo, 1985; Coates and Obando, 1996; Hoernle et al., 2002).

First evidence for the closure of the Panamanian Gateway was provided by Duque-Caro (1990), who showed that distinct benthic foraminiferal faunas developed between the Caribbean and the east Pacific ~12.9-11.8 Ma, suggesting that a deep barrier was formed. Several studies, based on both benthic and planktonic foraminiferal assemblages, showed that the sill shoaled to a depth of ~200-500 m between ~8-5 Ma (Keller et al., 1989;

Collins et al., 1996, Chaisson and Ravelo, 2000). At about 5 Ma, the subduction of the Cocos Ridge, which formed during the passage of the Cocos Plate over the Galapagos hotspot, dramatically elevated the Central

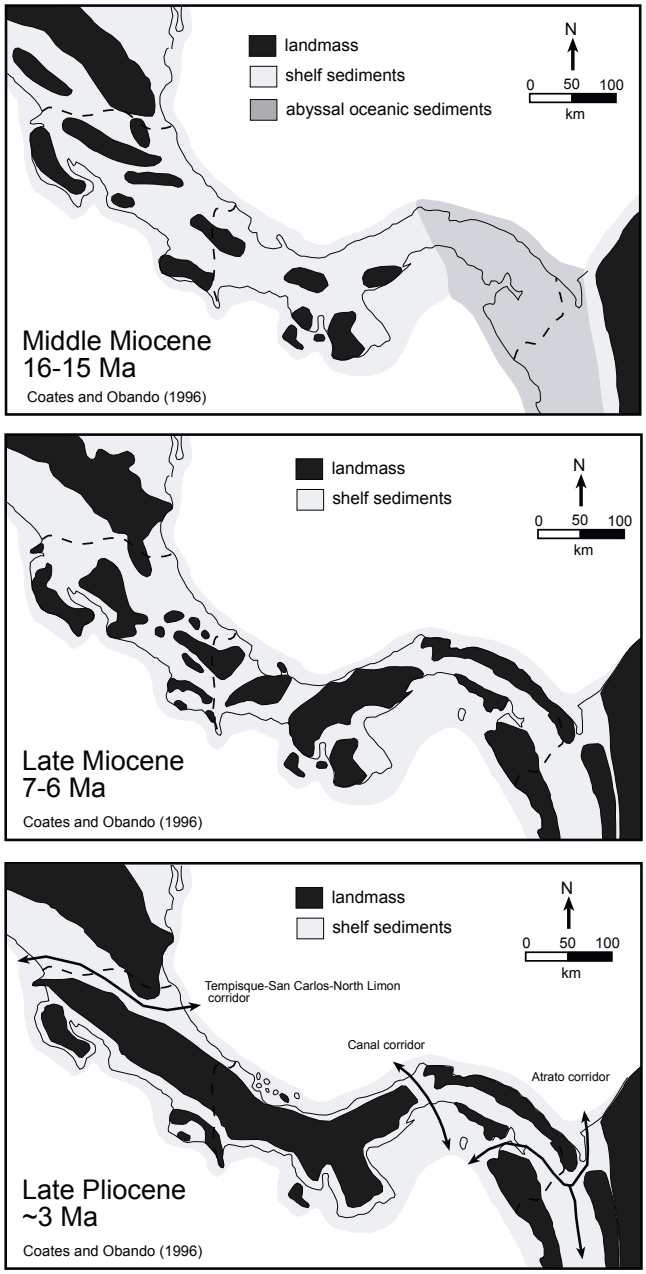

Figure 2.2 A A schematic paleogeographic interpretation of the Central American isthmus 15 million years ago, in the middle of the Miocene period. The dotted pattern indicates the approximate position of the marine shelf. **B** A schematic paleogeographic interpretation of the Central American isthmus 6 million years ago near the end of the Miocene period. The deepest part of the marine shelf along the isthmus is now about 150 meters. **C** A schematic paleogeographic interpretation of the Central American isthmus about 3 million years ago, at the end of the Pliocene period. The probable last marine corridors connecting the Pacific to the Atlantic are indicated. (Figure after Coates and Obando, 1996).

volcanic arc and led to the final phase of the closure (Dengo, 1985; Hoernle et al., 2002). Indeed, Keigwin (1982) and Haug and Tiedemann (1998) suggested that the sill depth of the Panamanian Gateway shoaled to less than 100 m by about 4.6 Ma. This was inferred from a divergence between Pacific-Caribbean planktonic oxygen isotope records indicating the development of the modern Atlantic-Pacific contrast in sea surface salinities (SSS) with higher SSS in the Caribbean.

Collins et al. (1996) concluded that due to the clear distinction in near-shore faunas on both sides of the Isthmus of Panama around 3.8-3.6 Ma, the gateway was effectively closed. The final closure was achieved around the start of the Northern Hemisphere Glaciation (NHG) at 3.0-2.5 Ma. This timing is suggested by the great american biotic interchange (Marshall et al., 1982; Stehli and Webb, 1985; Lundelius et al., 1987; Webb, 1991, 1997) and the divergence of nannoplankton assemblages between the east Pacific and the Caribbean (Kameo and Sato, 2000). Keller et al. (1989) even suggested that the final closure did not occur before 1.8 Ma.

During the early Pliocene the open Panamanian Gateway still allowed free exchange of surface watermasses between the east Pacific and the Caribbean. Most modelling studies indicate that the flow direction was from the east Pacific into the Caribbean (Maier-Reimer et al., 1990; Mikolajewicz et al., 1993; Nisancioglu et al., 2003; Prange and Schulz, 2004) rather than the other way around (Nof and van Gorder, 2002). The inflow of lower salinity waters from the Pacific into the Caribbean, hence, prevented a significant salinity increase in the Caribbean. Haug et al. (2001) showed that $\delta^{18}O_{\textit{G. sacculifer}}$ records of the east Pacific and the Caribbean started to diverge from each other between 4.7 Ma and 4.2 Ma. This was interpreted the way that the Isthmus of Panama had shoaled to a depth of less than 100 m, thereby restricting the inflow of low salinity Pacific surface watermasses into the Caribbean, leading to the formation of the Caribbean-Pacific salinity gradient (see also Chapter 4).

Chapter 3
Mg/Ca paleothermometry

Mg/Ca paleothermometry

The reconstruction of paleo-sea water temperatures is one of the most important issues in paleoceanography in order to understand the atmospheric and oceanographic processes which control developments in the Earth's climate and oceanography. The use of trace metal *versus* calcium ratios in organisms to reconstruct paleo-sea water temperatures, like for example Sr/Ca-ratios in corals, or Mg/Ca-ratios in planktonic foraminifera as performed here, is still a relatively new tool in paleoceanography in comparison with more traditional methods, like oxygen isotopes (Epstein et al., 1953; Shackleton, 1974; Erez and Luz, 1983; Bemis et al., 1998), transfer functions (Imbrie and Kipp, 1971; Pflaumann et al., 2003) and alkenones (Prahl and Wakeham, 1987; Prahl et al., 1988; Müller et al., 1998; Rosell-Melé et al., 1998). Recently, Mg/Ca paleothermometry developed into a powerful tool in paleoceanography (Nürnberg, 2000; Lea, 2003).

The main advantage of using Mg/Ca-ratios in planktonic foraminifera over other paleotemperature proxies is that the Mg/Ca-ratio is measured on the same biotic carrier as oxygen isotopes, which excludes problems on seasonal or habitat variations when different carriers are used. Since oxygen isotopes of planktonic foraminifera depend both on temperature and (regional and global) salinity, the simultaneous analysis of Mg/Ca-ratios allows for the subtraction of the temperature signal from the oxygen isotopes and subsequently the calculation of salinity variations. This is necessary to make reliable reconstructions of the oxygen isotope composition of the seawater and its salinity (Chapter 4, 5; Nürnberg, 2000; Visser et al., 2003; Lea, 2003; Schmidt et al., 2004; Steph, 2005).

Mg/Ca paleothermometry is based on the temperature-dependance of the substitution of magnesium into calcite lattice sites within the foraminiferal tests. From the geographic distribution of skeletal marine magnesium-calcite, Chave (1954) already recognized a covariance of the magnesium content and latitude and thus, suggested a relationship between the substitution of calcium by magnesium and water temperature. Also, it has long been known that tropical calcitic shells of marine organisms are generally more enriched in magnesium than subpolar shells (Savin and Douglas, 1973). Other studies, however, did not always support these results, suggesting major influences from other environmental parameters like light, nutrient content and growth rate (Krinsley, 1960; Duckworth, 1977; Cronblad and Malmgren, 1981; Puechmaille, 1985; Delaney et al., 1985; Izuka, 1988; DeDeckker and Corriège, 1992). Rosenthal and Boyle (1993) even suggested that calcite dissolution may significantly alter the magnesium concentrations within foraminiferal tests and thus, may prevent the applicability of magnesium as a tracer for water mass properties. This caused a temporary use of Mg/Ca as an indicator for dissolution (Russell et al., 1994; Hastings et al., 1996; Rosenthal et al., 2000).

In the last decade, it has been recognized that Mg/Ca-ratios show a species-specific exponential dependance on temperature (Fig. 3.1) (Nürnberg, 1995; Nürnberg et al., 1996a, b; Mashiotta et al., 1999; Lea et al., 1999, 2000; Dekens et al., 2002). Such species-specific Mg/Ca *versus* SST relationships are essential for quantitative paleo-SST reconstructions, although multi-species calibrations are often applied when species-specific calibrations are not available (Elderfield and Ganssen, 2000; Anand et al., 2003).

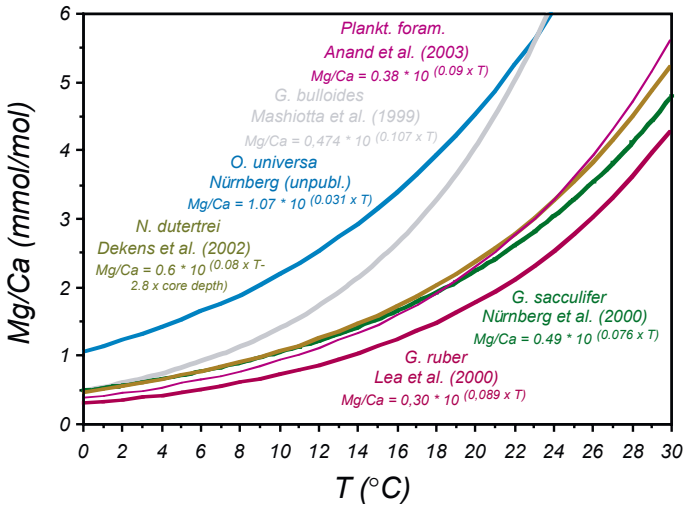

Figure 3.1 Exponential dependance of planktonic foraminiferal Mg/Ca on temperature. Both species-specific calibration curves and the multi-species calibration curve of Anand et al. (2003) are shown as examples.

The significance of additional processes influencing Mg/Ca is still under debate. Several publications discussed dissolution effects on Mg/Ca (Brown and Elderfield, 1996; Dekens et al., 2002; Rosenthal and Lohmann, 2002, de Villiers, 2003; Regenberg et al., submitted). In general, the decreasing CO_3^{2-} concentration with increasing water depth leads to dissolution of calcite. Brown and Elderfield (1996) speculated that calcite with a higher Mg-concentration tends to dissolve more easily than calcite with a lower Mg-concentration. Therefore, samples from greater water depths, being more corrosive, have to be treated with care. To correct for the dissolution induced changes to the original Mg/Ca-ratios, several authors published depth-corrected calibration formulas (Dekens et al., 2002; Regenberg et al., submitted) or used the weight-loss of foraminiferal tests as an indicator for increasing dissolution (Rosenthal and Lohmann, 2002).

Initial cultivating experiments by Nürnberg et al. (1996) and Lea et al. (1999) showed the possible significance of additional factors on Mg/Ca, indicating that changes in salinity and pH do have an influence on Mg/Ca (Fig. 3.2). But, because the effects were opposite from each other and the necessary changes very large in comparison with the then accepted changes between the Last Glacial Maximum and the Holocene, these effects were assumed to cancel each other.

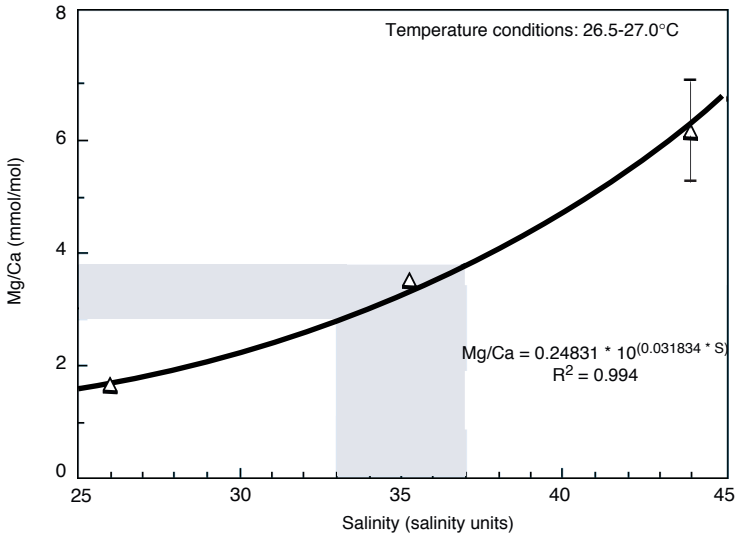

Figure 3.2 Dependance of foraminiferal Mg/Ca on changing salinity. Cultivating experiment was performed on *G. sacculifer* (Nürnberg et al., 1996).

Interlaboratory comparison and consistency

As Mg/Ca paleothermometry is a relatively new method there is still no agreement on a standard method for Mg/Ca-analysis and the cleaning of the foraminiferal tests prior to analysis. A first comparative study was presented by Rosenthal et al. (2004), who provided several laboratories with the same sample material and compared the results. The many different ways in which Mg/Ca was determined, i.e. with or without reductive cleaning or either by ICP-AES or ICP-MS (Rosenthal et al., 2004), showed that the inter-laboratory results varied on a scale which was larger than Last Glacial Maximum *versus* Holocene differences. In the future, the introduction of a common standard, as for example the PDB-standard used for $\delta^{18}O$, is envisioned.

Prepared	Mg/Ca	Sr/Ca
270803	2.92	1.35
220903	2.94	1.41
130404	2.91	1.37
290604	2.89	1.38
270704	2.88	1.38
180804	2.87	1.38
average	2.90	1.38
st. deviation	0.026	0.019
rel. sd (%)	0.91	1.41

Table 3.1 Internal consistency standard as used during this thesis.

The present absence of such a necessary component in the Mg/Ca proxy development is due to the difficulty to acquire a large enough mass of cleaned foraminiferal calcite from the same source and to distribute it among laboratories. Only recently, an artificial solution was shown to be reasonably similar to foraminiferal calcite (Greaves et al., 2005), which may serve as a standard solution. To test the consistency of our measurements, we have used an internal consistency standard, which was analysed after every 5 samples. Since this standard is prepared freshly for each analytical session, it provides us not only with intra- but also with inter-session consistencies (Table 3.1). Use of such an internal consistency standard reveals that matrix effects caused by varying concentrations of Ca were insignificant (Fig. 3.3; Garbe-Schönberg et al., in prep.). The Mg/Ca-ratios were calculated by using a regular standard calibration method, with a constant Mg/Ca-ratio for all standards and varying element concentrations, instead of an intensity calibration method (de Villiers et al., 2002; Garbe-Schönberg et al., in prep.).

All methods are more or less based on the initial procedure by Boyle (1981) for the cleaning of foraminiferal calcite to determine trace metal versus calcium ratios. Presently, the cleaning methods can be divided into two main methods, one including a reductive cleaning step (Martin et al., 2002), and the other without the reductive cleaning (Barker et al., 2003). Reductive cleaning is usually applied for the cleaning of benthic foraminifera or for samples, which were shown to contain large amounts of secondary Mn-carbonate, possibly enriched in magnesium. Commonly, samples which are cleaned reductively show lower Mg/Ca-ratios by about ~0.2-0.3 mmol/mol than those samples cleaned without the reduction step (Ocean Gateway Project; Rosenthal et al., 2004). It was argued that in most cases the Mg-loss due to the reductive cleaning equals the amount of Mg which is present in Mn-coatings. In a case study within the "Ocean Gateway Project", we explored the differences

between reductive and oxidative cleaning (Garbe-Schönberg et al., in prep.) As is also shown in previous studies, reductively cleaned samples are consistently lower by about 0.2 mmol/mol than only oxidatively cleaned samples.

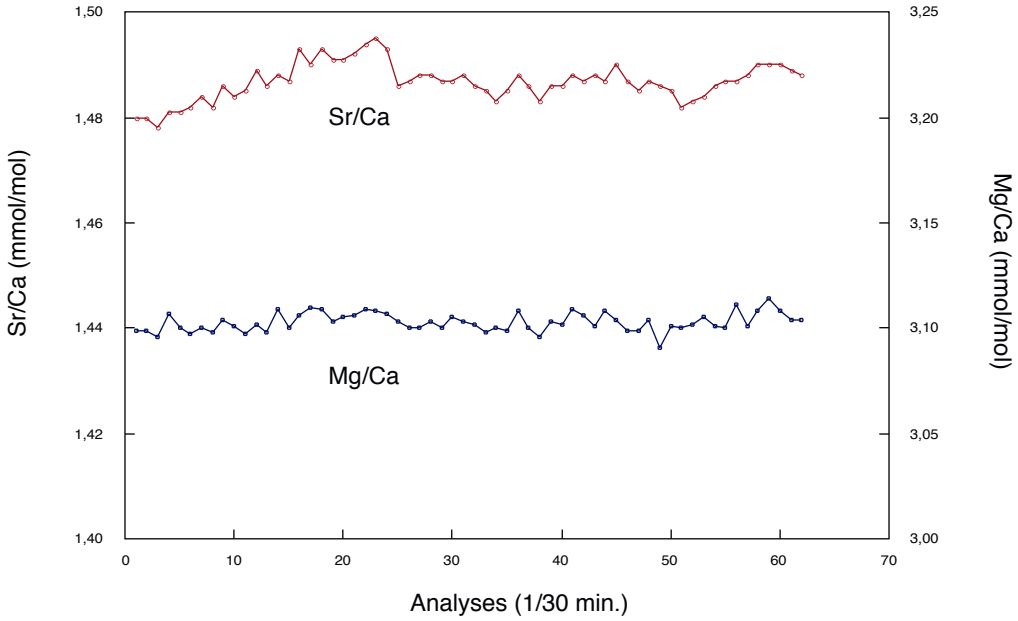

Figure 3.3 Drift of Mg/Ca and Sr/Ca during a typical analytical session as determined on the internal consistency standard. The internal consistency standard was measured after every 5th sample (~30 minutes).

I have cleaned my samples according to the protocol of Barker et al. (2003), i.e. without reductive cleaning. The large differences between the Mg/Ca results from different laboratories make it necessary that every publication is provided with a detailed description of the used methods. Thus, each Chapter contains a detailed description of the method which has been used and its specific adaptations to the involved samples. Therefore, I will not go into detail on the individual cleaning steps in this Chapter. However, I point out that minor changes to the basic method became necessary. Applied changes include the availability and size of the number of foraminifera, the preservation of the foraminiferal tests or the applied analytical method.

The samples of Chapters 4 and 5 were analysed on a different machine than those of Chapter 6. This is due to the installation of a new ICP-OES during this study. The samples from Chapter 6 were measured on an ICP-OES (ISA Jobin Yvon, Spex Instruments S.A. GmbH), while the samples from Chapters 4 and 5 were measured on a ICP-OES (Ciros CCD SOP, Spectro A.I.). Consistency between both ICPs was tested by measuring replicate samples on both machines and showed that a constant offset exists, although this offset is within the error of the measurements (<0.10 mmol/mol). Internationally, we compared our ICP with a set of standards from Cambridge University, which were kindly provided by M. Greaves and H. Elderfield (Garbe-Schönberg et al., in prep.).

The use of the ICP-OES (Ciros CCD SOP) largely improved the analytical results. Firstly, simultaneous measurement of only 6 elements was possible on the ISA Jobin Yvon, including an internal standard, while on the Ciros CCD SOP, an unlimited number of element lines can be measured simultaneously. This means that a series of elements, which are indicative of contamination (Sr, Fe, Mn, Ti), the stability of the machine (Ar), stability of Mg and Ca themselves (alternative lines of Mg and Ca) or the presence of other proxy signals like for example productivity (Ba, Zn) can be measured at the same time. Secondly, the Ciros CCD SOP allows the

employment of an autosampler, while on the ISA Jobin Yvon all samples were introduced manually. The Ciros CCD SOP therefore not only allowed the through-put of much larger numbers of samples (analytical sessions up to 36 hours are no exception), but also guaranteed a much more constant and stable analysis of the samples, resulting in much higher precision. Thirdly, the analytical error of the Ciros CCD SOP is so small, usually 0.1% in comparison with about 1% on the ISA Jobin Yvon that this error can be neglected in the temperature reconstruction.

3.3. The use of Mn and Fe as quality control for sample contamination

To monitor the presence of contaminant clay particles, the Fe/Ca-ratio was used. As reported by Barker et al. (2003), Fe/Ca-ratios of clean foraminifera are usually below 0.1 mmol/mol. Fe/Ca-ratios for Site 1241 are on average <0.2 mmol/mol (Fig. 3.4). Fe/Ca-ratios For Site 1000 were only monitored for samples <4.5 Ma, i.e. potentially diagenetically affected samples (Chapter 6). Fe/Ca-ratios are always lower than 0.4 mmol/mol, although they do show an indication for a linear relationship with Mg/Ca ratios, which might point to the diagenetic inprint on those samples. Fe/Ca ratios for Site 999 are significantly higher but they are not showing a correlation with the Mg/Ca-record, which suggested that the samples were clean (Fig. 3.4). Fe/Ca-ratios of samples which were significantly higher than the average for the respective cores were considered not to be free of clay particles and therefore rejected.

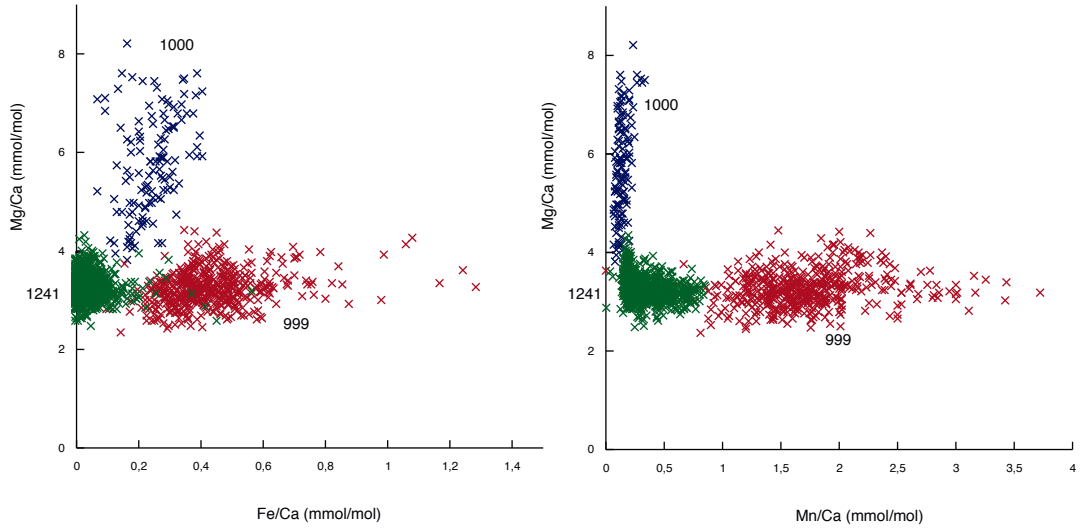

Figure 3.4 Mg/Ca in comparison with Mn/Ca and Fe/Ca as indication for possible contamination due to Mn-carbonates and clays for Sites 999, 1000, and 1241. All data were measured on the Ciros CCD SOP ICP-OES.

Mn/Ca-ratios were analysed to determine the presence of Mn-coatings, which might influence the Mg/Ca-ratios of the foraminiferal tests (Boyle, 1983). Mn/Ca-ratios of samples of Sites 1000 and 1241 were usually lower than 0.5 mmol/mol and not showing any correlation with the Mg/Ca-record (Fig. 3.4). Samples from Site 999, however, did show significantly higher Mn/Ca-ratios with an average of 1.8 mmol/mol and a maximum of >3.0 mmol/mol (Fig. 3.4). Pena et al. (2004) showed that high Mn/Ca-ratios might, under certain circumstances, indicate that contaminant Mg is present and, hence, increase the bulk Mg/Ca-ratios. However, there is no clear correlation between the Mn/Ca- and Mg/Ca-records from Site 999 (Fig. 3.4). To determine what the possible influence on the Mg/Ca-ratios, nevertheless, might have been, we cleaned several replicate samples by using the

reductive cleaning method as described by Martin et al. (2002), in which the Mn-coating is reductively removed. This reduced the Mn/Ca-ratios significantly, although not toward the ‚normal' values (<0.5 mmol/mol) of Sites 1000, and 1241. The Mg/Ca-ratios, however, were hardly changed, matching the results of Rosenthal et al. (2004) who showed that reductively cleaned samples are ~0.2-0.3 mmol/mol lower in Mg/Ca, and thus suggesting that the Mg/Ca-ratios were not contaminated.

Chapter 4

The final phase of the closure of the Panamanian Gateway (5.6-2.2 Ma)

Groeneveld, J. (1), S. Steph (1), R. Tiedemann (1), D. Nürnberg (1), D. Garbe-Schönberg (2), G.H. Haug (3)

Manuscript in preparation for Geology

(1) IFM-Geomar, Leibniz Institute of Marine Sciences, Kiel, Germany
(2) Institut of Earth Sciences, University of Kiel, Germany
(3) GFZ Potsdam, Germany

Abstract

Planktonic Mg/Ca and $\delta^{18}O$ records were established at Caribbean ODP Sites 999 and 1000 and at equatorial east Pacific Site 1241 for the time interval from 5.6 to 2.2 Ma. These records allowed for the first time to quantitatively assess the development of Caribbean/Pacific mixed-layer temperatures and salinities in response to the closure of the Panamanian Gateway. Our data indicate that the Pacific-Caribbean salinity contrast developed gradually during the late Miocene and at least 1 million years earlier than previously suggested. With the Pliocene intensification of the Northern Hemisphere Glaciation, sea level lowstands during glacial isotope stages 96, 98, and 100 probably interrupted the inflow of Pacific watermasses into the Caribbean. This resulted in an anti-phase relationship between Pacific-Caribbean temperature fluctuations. Variations in Pacific $SST_{Mg/Ca}$ followed the global glacial-interglacial temperature pattern, while glacial $SST_{Mg/Ca}$ in the Caribbean increased due to the cessation of the inflow of cooler Pacific water masses. Thus, the first emergence of a landbridge may have resulted from larger sea level drops during the Pliocene NHG.

Introduction

The Neogene tectonic closure of the Panamanian Gateway (12.9-1.8 Ma) resulted from the subduction of the Pacific Cocos and Nazca plates beneath the North and South American plates and later the Caribbean Plate (Dengo, 1985; Hoernle et al., 2002). Much controversy, however, exists on the exact dating of the closure of the Panamanian Gateway. First evidence for the existence of a deep-water barrier was provided by Duque-Caro (1990), who showed that distinct benthic foraminiferal faunas developed between the Caribbean and the east Pacific ~12.9-11.8 Ma. Several studies, based on both benthic and planktonic foraminiferal assemblages, suggested that the sill shoaled to a depth of ~200-500 m between 8 and 5 Ma (Keller et al., 1989; Collins et al., 1996).

Collins et al. (1996) concluded that due to the clear distinction in near-shore faunas on both sides of the Isthmus of Panama around 3.8-3.6 Ma, the gateway was effectively closed. The great american biotic interchange (Marshall et al., 1982; Stehli and Webb, 1985; Lundelius et al., 1987; Webb, 1991, 1997) at ~2.5 Ma is considered to reflect the final closure of the gateway, which is also proposed by the divergence of nannoplankton assemblages between the east Pacific and the Caribbean (Kameo and Sato, 2000). Keller et al. (1989) even suggested that the final closure did not occur before 1.8 Ma.

The major problem with dating the final closure by means of fossil exchanges is the lack of strict stratigraphic control. Hence, Keigwin (1982) and Haug et al. (2001) used deep sea sediments to provide (orbitally tuned) stratigraphic control on time scales better than 20 k.y. They suggested that the sill depth of the Panamanian

Gateway shoaled to less than 100 m by ~4.6 Ma. This was inferred from a divergence between Pacific-Caribbean planktonic oxygen isotope records indicating the development of the modern Atlantic-Pacific contrast in sea surface salinities (SSS) with higher SSS in the Caribbean.

Here, we present evidence to constrain the final phase of the closure of the Panamanian Gateway. Our results are based on a comparison of Pliocene sea surface temperature (SST) records and sea surface salinities (SSS) from east Pacific Site 1241 and Caribbean Sites 999 and 1000 (Fig. 4.1). The SST records were reconstructed from Mg/Ca measurements on the mixed-layer planktonic foraminifer *Globigerinoides sacculifer*. Changes in SSS were obtained by combining Mg/Ca and $\delta^{18}O$ to calculate $\delta^{18}O_{water}$ and $\delta^{18}O_{local\ salinity}$.

The major advantage of Mg/Ca paleothermometry is that it is measured on the same biotic carrier as $\delta^{18}O$ (Nürnberg, 2000). This means that both proxies can be combined to calculate $\delta^{18}O_{water}$ and salinity without any problems on seasonal or habitat variations when different carriers are used (Nürnberg et al., 2000; Lea et al., 2000; Visser et al., 2003; Lea, 2003; Schmidt et al., 2004). Thus, combining Mg/Ca and $\delta^{18}O$ not only provides an excellent age control (<10 kyr), it also allows to differentiate between temperature and salinity related events. Hence, an opportunity is provided to validate and further extend the work of Haug et al. (2001).

Our studies use the two main oceanographic features that distinguish modern east Pacific and Caribbean surface ocean waters from each other. Surface waters which evaporate in the Caribbean are transported by the prevailing trade winds over the isthmus into the east Pacific. This results in a salinity gradient with the Caribbean being more saline than the east Pacific by about 2 units (Broecker, 1989). The other main feature is that warm water is 'collected' in the Western Atlantic/Caribbean Warm Pool (WAWP), while the eastern Pacific is characterized by generally cooler upwelling waters. This leads to an SST gradient between the east Pacific and the Caribbean of about 5°C at the assumed habitat depth of *G. sacculifer* of 30-80 m (Fairbanks et al., 1982).

Materials and Methods

ODP Sites 999 (12°44'N, 78°44'W, 2828 m water depth) and 1000 (16°33.222'N, 79°52.044'W, 916 m water depth) were cored during Leg 165 in the Colombian Basin and the Nicaraguan Rise in the Caribbean (Fig. 4.1). ODP Site 1241 was cored during Leg 202 on the Cocos Ridge in the east Pacific (5°50N, 86°26W, 2027 m water depth) (Fig. 4.1). Mg/Ca and $\delta^{18}O$ analyses were performed on the planktonic foraminifer *Globigerinoides sacculifer*. For Site 999 a new high resolution Mg/Ca record was established, while for Site 1241 the existing Mg/Ca record (Groeneveld et al., submitted) was extended to cover the time interval 5.6-2.2 Ma. For Site 1000, we used existing Mg/Ca (Groeneveld et al., submitted) and $\delta^{18}O$ (Steph et al., submitted) records. Only samples from Site 1000 >4.5 Ma and the minimum values <4.5 Ma were used. As discussed in Groeneveld et al. (submitted) the maximum values <4.5 Ma are most likely affected by salinity. 20-25 Specimens from the 315-400 µm (999) and 355-400 µm (1241) fraction, respectively, were picked. Specimens with a sac-like final chamber or visibly contaminated specimens were not selected for analysis.

After gentle crushing, the samples were cleaned according to the cleaning protocol of Barker et al. (2003). Analyses were performed on a simultaneous, radially viewing ICP-OES (Ciros CCD SOP, Spectro A.I., Germany) at the Institute of Geosciences (Kiel University, Germany) (Garbe-Schönberg et al., in prep.). The analytical error on the analysis of the Mg/Ca-ratios was 0.1% for a total of ~1700 samples. Replicate analyses on the same samples, which were cleaned and analysed during different sessions, showed a standard deviation of 0.09 mmol/mol, introducing a temperature error of ~0.5°C. The conversion of foraminiferal Mg/Ca-ratios into

sea surface temperatures (SST) was carried out by applying the equation of Nürnberg et al. (2000) (SST = (Log(Mg/Ca)-Log 0.491)/0.033). A detailed description of the cleaning and analytical methods is given in Groeneveld et al. (submitted).

For $\delta^{18}O$ we used the record of Haug and Tiedemann (1998) for Site 999, and we extended the $\delta^{18}O$ for Site 1241 (Groeneveld et al., submitted) to cover the time interval 5.6-2.2 Ma. For stable isotope analysis 10 specimens of *G. sacculifer* (without sac-like final chamber) were picked from the 355-400 µm size fraction. All isotope analyses were run at IFM-GEOMAR (Kiel) on a Finnigan Delta-Plus Advantage Mass Spectrometer coupled to a Finnigan gas bench II (Steph, 2005). Analytical precision was better than 0.07‰ for $\delta^{18}O$. The values are reported relative to Pee Dee Belemnite (PDB), based on calibrations directly to National Bureau of Standards (NBS) 19.

The original age model for Site 999 was presented in Haug and Tiedemann (1998), the age model for Site 1241 is discussed in Tiedemann et al. (submitted), and the age model for Site 1000 is discussed in Steph et al. (submitted). For a direct comparison, however, we adjusted the benthic $\delta^{18}O$ fluctuations at Site 999 precisely to those at Site 1241 to eliminate phase offsets in the obliquity-related frequency band (41 kyr-cycle) (Fig. 4.2). Time series analyses were performed with the software programm AnalySeries 1.2 (Paillard et al., 1996).

We calculated $\delta^{18}O_{water}$ by combining the $SST_{Mg/Ca}$ and $\delta^{18}O$ records into the formula of Shackleton (1974). To isolate local variations in SSS, we subtracted an estimate of Pliocene sea level (Groeneveld et al., submitted) from the $\delta^{18}O_{water}$. The residual $\delta^{18}O_{water}$ records for Site 999 and 1241 represent only local variations in SSS (quoted as $\delta^{18}O_{salinity}$). The difference between both $\delta^{18}O_{water}$ records shows the development of the salinity gradient between the east Pacific and the Caribbean

Development of Pacific-Caribbean temperature and salinity gradients

Figure 4.1 provides a comparison of $\delta^{18}O$, $SST_{Mg/Ca}$ and SSS records between equatorial east Pacific Site 1241, Site 999 from the southwestern Caribbean and Site 1000 from the central Caribbean. The comparison of $SST_{Mg/Ca}$ records reflects similar values between the eastern equatorial Pacific and the southwestern Caribbean, ranging between 22° and 27°C from 5.2 to 2.8 Ma, while the temperatures in the central Caribbean were on average ~2°C warmer during the late Miocene and earliest Pliocene. From 4.5 to 4 Ma, central Caribbean $SST_{Mg/Ca}$ increased by ~2°C to 29°C, a trend that is not reflected in the gateway region (Sites 1241 and 999). The Caribbean $SST_{Mg/Ca}$ gradient suggests, that the more northern position of Site 1000 was less affected by the inflow of Pacific water masses than Site 999 since 5.6 Ma.

The comparison of salinity records illustrates that the Pacific-Caribbean salinity contrast already developed during the late Miocene and thus at least about 1 million years earlier than previously suggested (Haug et al., 2001). This is indicated by the divergence between the $\delta^{18}O_{water}$ records from the eastern equatorial Pacific (Site 1241) and the central Caribbean (Site 1000). At 5.5 Ma both records show a short-term event of similar values, whereas the averaged long-term trend points to a bifurcation point prior to 5.5 Ma. After 5.5 Ma, salinities at Pacific Site 1241 decrease by 0.5‰ $\delta^{18}O$ until 4.3 Ma. The inflow of Pacific water masses led to similar values in the southwestern Caribbean (Site 999). The increasing salinity contrast from the gateway region towards the central Caribbean points to the diminishing influence of Pacific water masses since ~5.5 Ma (as also suggested by the $SST_{Mg/Ca}$ difference), allowing salinities to increase in the central Caribbean with respect to the general salinity decrease in the eastern Pacific. The salinity record from the southwestern Caribbean (Site 999)

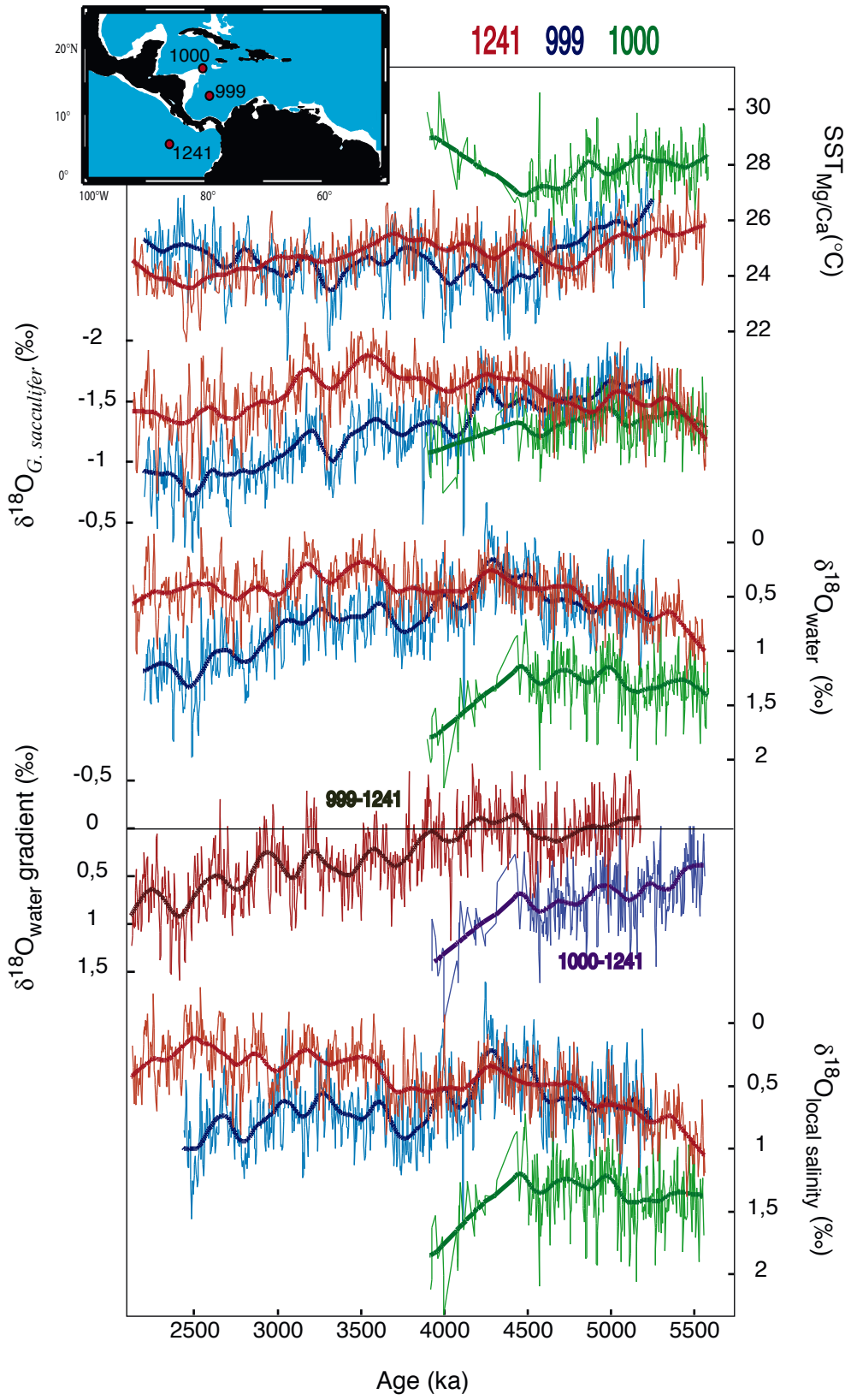

Figure 4.1 Sea surface water properties ($SST_{Mg/Ca}$, $\delta^{18}O_{G.\ sacculifer}$, $\delta^{18}O_{water}$, $\delta^{18}O_{water\text{-}gradient}$, and $\delta^{18}O_{salinity}$) for the Caribbean (Sites 999 and 1000) and the tropical east Pacific (Site1241). Analyses were performed on the planktonic foraminifer *Globigerinoides sacculifer*. Coloured numbers 999, 1000, and 1241 indicate the proxy data for the respective sites. Inlet shows the locations of ODP Sites 999, 1000, and 1241

did not diverge significantly from the Pacific record before 4 Ma, although Caribbean salinities strongly increased from 4.2 to 3.8 Ma. This is best demonstrated by the difference of $\delta^{18}O_{water}$ values between Sites 1241

and 999 (Fig. 4.1). On a long-term view, the Pacific-Caribbean salinity contrast increased from 4 Ma to 2.2 Ma by about 1‰ $\delta^{18}O$, equivalent to about 2 units (Broecker, 1989), which is close to the modern gradient. The assessment of local salinity changes ($\delta^{18}O_{salinity}$) at Pacific Site 1241 and southwestern Caribbean Site 999 reveals that the Pacific-Caribbean salinity contrast is not only characterized by a salinity increase in the Caribbean, but also by a salinity decrease in the east Pacific. These findings partly modify the results of Haug et al. (2001), who suggested that the Caribbean-Pacific salinity contrast increased step-wise at 4.7-4.6 Ma and at 4.3-4.1 Ma, remaining relatively constant afterwards. However, their interpretation was solely based on a Pacific-Caribbean comparison of planktonic $\delta^{18}O$ records (Sites 851 and 999) thereby neglecting temperature variability. The differences can be explained by changes in temperatures (Fig. 4.1).

At Pacific Site 1241, SSS generally decreases throughout the entire time interval from 5.6 to 2.2 Ma. Especially after 3 Ma, the general trend of the local $\delta^{18}O_{salinity}$ records depends on the magnitude of the assumed ice volume correction, as fluctuations in ice volume became more pronounced with the onset of the Northern Hemisphere Glaciation. We assumed a rather conservative approach for the ice volume correction (50 m sea level change for MIS 100), which may, therefore, underestimate the Pacific freshening trend and overestimate the Caribbean salinity increase after 3 Ma. Whether the long-term local freshening at Pacific Site 1241 reflects a salinity decrease of the North Equatorial Counter Current and thus a freshening of the West Pacific Warm Pool remains speculative. The atmospherical moisture transport from the Atlantic across Panama may have provided an additional source of freshwater supply to Site 1241, especially after 4 Ma when the oceanic return flow of fresher water masses into the Caribbean became significantly restricted. The major increase in Caribbean salinities occurred from 4.2 to 3.8 Ma. The development of the Caribbean-Pacific salinity contrast was, however, a gradual process starting well before 5.5 Ma. This early registration of a restricted Pacific-Caribbean water mass exchange is supported by Frank et al. (1999) who used Nd and Pb isotope time series of hydrogenous ferromanganese crusts from the east Pacific and northwestern Atlantic. They observed a shift in isotopic composition between 8 and 5 Ma in the Atlantic, which was explained by diminished supply of Pacific water through the Panamanian gateway.

Glacial closure of the Panamanian Gateway

Although Pacific-Caribbean $SSTs_{Mg/Ca}$ are relatively similar from 5.6 to 2.2 Ma, their comparison on orbital timescales provides surprising evidence for the final phase of the closure when glacial-induced sea level lowstands became important along with the intensification of the Northern Hemisphere Glaciation. Benthic oxygen isotope records are indicative of changes in global ice volume (sea level), which suggest dominant glacial/interglacial variability at cycles of 41 kyr during the Pliocene. At Pacific Site 1241 and Caribbean Site 999, spectral analyses also revealed a strong $SST_{Mg/Ca}$ response to changes in the 41 kyr, obliquity-related, frequency band.

We filtered the 41 kyr signal from the $\delta^{18}O_{benthic}$ and $SST_{Mg/Ca}$ records of Sites 999 and 1241 to expose glacial-interglacial related changes (Fig. 4.2). Comparison between the 41 kyr filters of the $\delta^{18}O_{benthic}$ and $SST_{Mg/Ca}$ records of Site 999 reveals the development of a negative correlation after ~2.65 Ma for Marine Isotope Stages (MIS) 96, 98, and 100 (Fig. 4.2), while at Site 1241 $\delta^{18}O_{benthic}$ and $SST_{Mg/Ca}$ remain in phase. Thus, after ~2.65 Ma, glacial stages (indicative of sea level low-stand) are associated with Pacific minima in $SST_{Mg/Ca}$ (Site 1241)

and maxima in Caribbean $SST_{Mg/Ca}$ (Site 999). This pattern documents the final phase of the closure of the Panamanian Gateway, when the Isthmus of Panama had shoaled to a water depth of 50-80 m. With the onset of

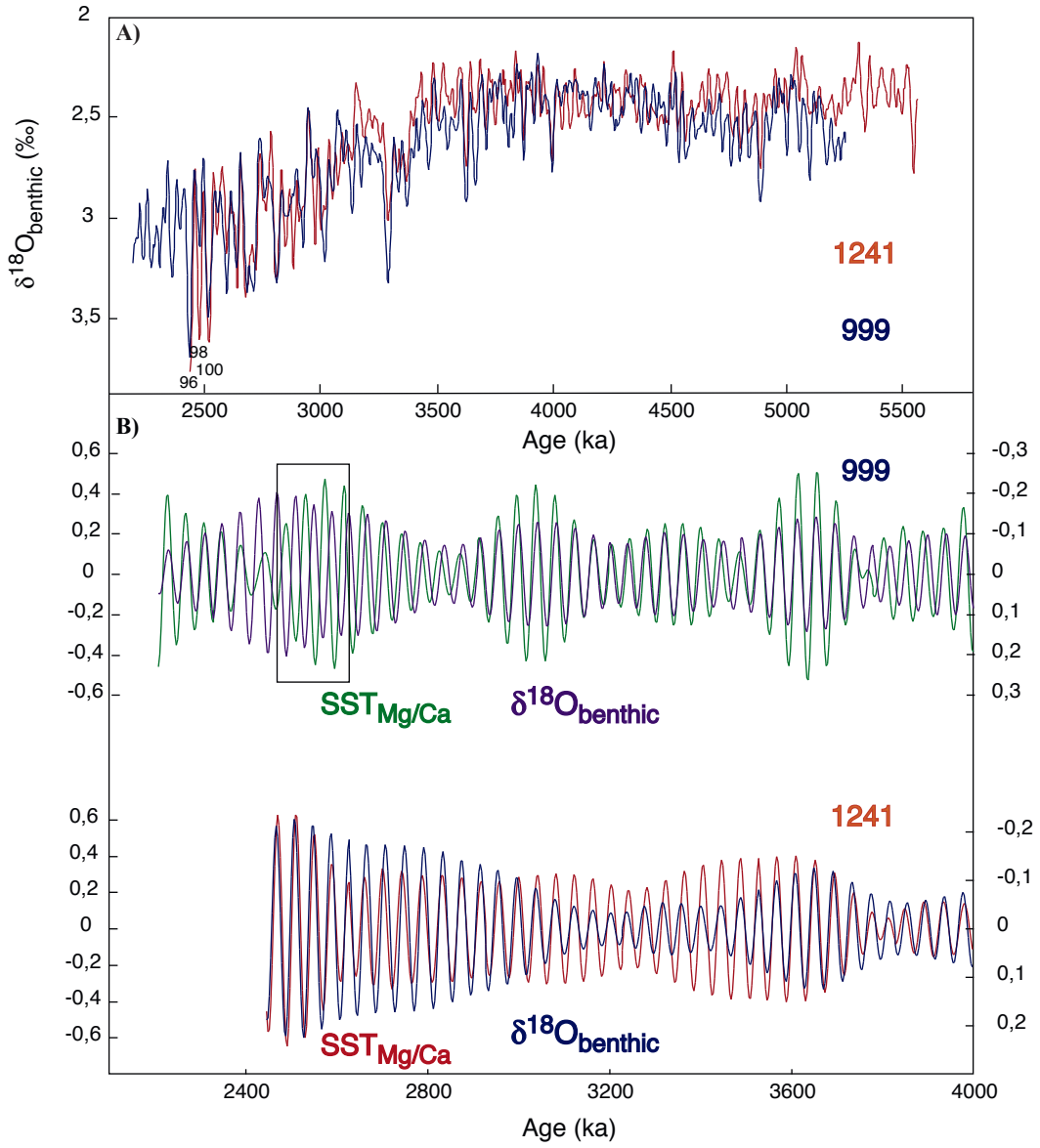

Figure 4.2 **A** Comparison of the tuned $\delta^{18}O_{benthic}$ record of Site 999 to the $\delta^{18}O_{benthic}$ record of Site 1241 (Steph et al., submitted). Numbers 96, 98, and 100 indicate glacial Marine Isotope Stages. **B** 41 k.y. filters, indicating glacial-interglacial oscillations, of the $SST_{Mg/Ca}$ and $\delta^{18}O_{benthic}$ records for Sites 999 and 1241. This reveals the occurance of a negative correlation at Site 999 at 2.5-2.6 Ma (gray square), suggesting the glacial closure of the Panamanian Gateway.

the NHG, sea level fluctuations on the order of 50-80 m started to control the Pacific inflow into the Caribbean. Thus, during glacials the cessation of the throughflow due to sea level low-stand terminated the influence of cooler Pacific surface waters in the Caribbean and subsequently allowed Caribbean SSTs to increase (Fig. 4.3). During interglacial periods with sea level high-stands the Caribbean (Site 999) remained under the influence of the cooler Pacific waters, providing similar $SST_{Mg/Ca}$ between Site 999 and 1241 (Fig. 4.3). As the following MIS 84-94 are characterized by less intense glacials (Lisiecki and Raymo, 2005), and thus, did not result in sea level low-stands typical for MIS96-100, our data do not provide evidence for further exposure of the Isthmus of Panama until 2.2 Ma. Thus, the tectonic closure of the Panamanian Gateway was most likely not finished by 2.2 Ma. Close investigation of the benthic $\delta^{18}O$ stack of Lisiecki and Raymo (2005) suggests that the next glacial

exposure of the land bridge might have occurred during MIS78 and 80. The timing of the glacial exposure of the Panamanian land bridge is consistent with the beginning of the great american interchange of vertebrates (~3.0-2.5 Ma) between North and South America (Webb, 1997).

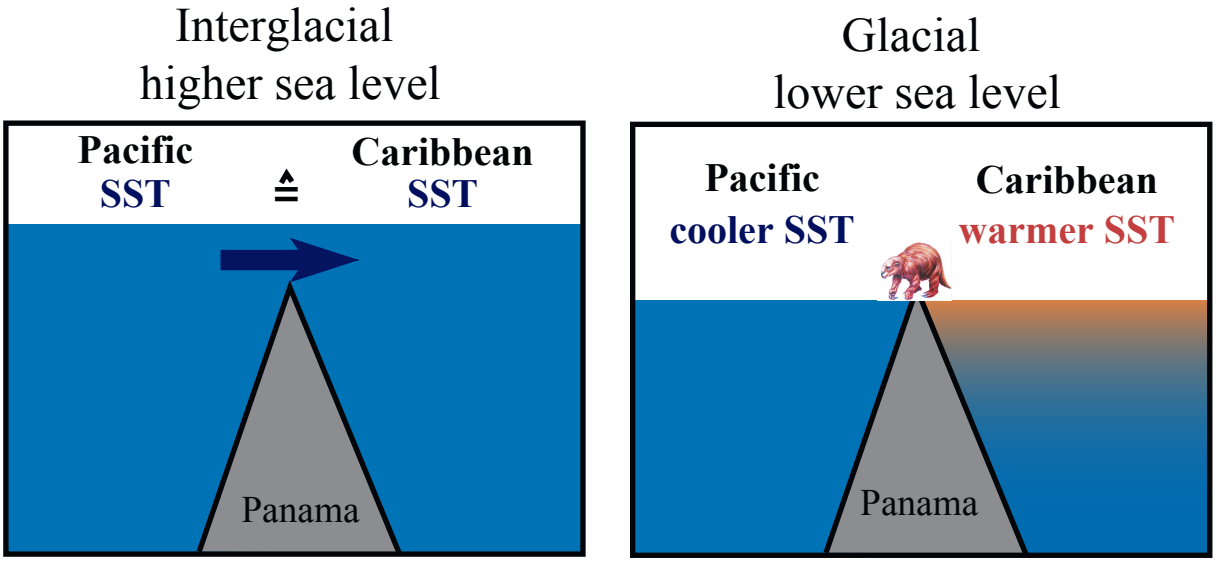

Figure 4.3 Schematic illustration of the glacial closure of the Panamanian Gateway. During glacial time periods (MIS 96, 98, and 100) sea level dropped causing the land bridge to become exposed and leading to a considerable warming of Caribbean surface water masses and allowing vertebrates to migrate from North to South America and the other way around (Webb, 1997).

Chicken or egg problem between Panama and NHG

The impact of the closure of the Panamanian Gateway was of great influence in establishing modern global climate and oceanographic features. The final closure was long given a dominant role in the intensification of Northern Hemisphere Glaciation around 2.7 Ma (Weyl, 1968; Keigwin, 1982; Driscoll and Haug, 1998; Haug et al., 2001). The closure would have led to increased SSS and SST in the Caribbean, generating the WAWP, and subsequently led to an intensified Gulfstream. This resulted in enhanced transport of moisture and heat into the North Atlantic, thereby providing the tools to generate intenser NADW production and ice sheet build-up. Recently however, it has been suggested that the final trigger for NHG might have been delivered by the North Pacific (Haug et al., 2005). They proposed that, based on alkenone saturation ratios and diatom oxygen isotope ratios from a sediment core in the western subarctic Pacific, observed summer warming at 2.7 Ma extended into the autumn, providing water vapour to northern North America, where it precipitated and accumulated as snow, and thus allowed the initiation of the NHG. Thus, although the closure of Panama provided an important pre-condition for the NHG, it seems that the NHG finally provided the necessary positive feedback in the form of sea level low-stands to cause the final closure of the Panamanian Gateway.

Conclusions

Planktonic Mg/Ca and $\delta^{18}O$ records from Caribbean ODP Sites 999 and 1000 and equatorial east Pacific Site 1241 (5.6-2.2 Ma) allowed for the first time to quantitatively assess the development of Caribbean/Pacific mixed-layer temperatures and salinities in response to the closure of the Panamanian Gateway. The data indicate that the Pacific-Caribbean salinity contrast developed gradually during the late Miocene and at least 1 million

years earlier than previously suggested. Significantly warmer $SST_{Mg/Ca}$ and higher saline $\delta^{18}O_{water}$ in the central Caribbean (Site 1000) in comparison with those at Sites 999 and 1241 already occur by 5.6 Ma. Within the direct proximity of the former gateway (Sites 999 (Caribbean) and 1241 (east Pacific)) the SSS contrast commenced to develop at ~4.2 Ma. The progressive closure of the gateway did not only lead to an increase in SSS in the Caribbean (999) as previously suggested (Keigwin, 1982; Haug et al., 2001), but also resulted in a decrease in SSS in the east Pacific (Site 1241) until 2.2 Ma, which significantly contributed to the increasing SSS gradient between the Pacific and the Caribbean.

In contrast to the development of the SSS gradient since the late Miocene, $SSTs_{Mg/Ca}$ at Sites 999 and 1241 remained similar between ~5.2-2.7 Ma. With the onset of Northern Hemisphere Glaciation (~2.7 Ma) sea level lowstands started to control the throughflow, thereby resulting in the glacial emergence of the land bridge of Panama during glacial Marine Isotope Stages (MIS) 96, 98, and 100.

Acknowledgements

This research used samples and data provided by the Ocean Drilling Program, which is sponsored by the U.S. National Science Foundation and participating countries under management of Joint Oceanographic Institutions. This study was performed within DFG-Research Unit „Impact of Gateways on Ocean Circulation, Climate, and Evolution“ (FOR451/1-1 TP B2). We like to thank Silvia Koch, Kerrin Wittmaack, Nicole Gau, Ulrike Nielsen, and Anna Jessusek for sample preparation and laboratory assistence. We gratefully thank Marcus Regenberg, Joachim Schönfeld, Martin Ziegler, and ... anonymous reviewers for their useful comments and the improvement of the manuscript.

Chapter 5

Pliocene mixed-layer oceanography for Site 1241, using combined Mg/Ca and $\delta^{18}O$ analyses of *Globigerinoides sacculifer*

Groeneveld, J. (1), S. Steph (1), R. Tiedemann (1), D. Garbe-Schönberg (2), D. Nürnberg (1), A. Sturm (1)

Manuscript submitted to ODP Scientific Results, Leg 202

(1) IFM-Geomar, Leibniz Institute of Marine Sciences, Kiel, Germany
(2) Institute of Geosciences, University of Kiel, Germany

Abstract

To reconstruct changes in tropical Pacific surface hydrography, we used samples from Site 1241 (5°50N, 86°26W, 2027 m water depth) to establish high-resolution records of Mg/Ca and $\delta^{18}O$ for the mixed-layer dwelling planktonic foraminifer *Globigerinoides sacculifer* for the Pliocene time interval from 4.8 Ma to 2.4 Ma. An increase in average sea surface temperatures (SST) between 4.8 Ma and 3.7 Ma from 24.5°C to 25.5°C can probably be explained by a southward shift of the Intertropical Convergence Zone (ITCZ), thereby increasing the influence of the warmer North Equatorial Counter Current (NECC). MIS Gi24 can be indentified as a global cooling event around 4.0 Ma, while the cooling event between 4.4 Ma and 4.2 Ma is a regional feature, including temporarily freshening less saline waters, and can be explained by regional changes in the precipitation/evaporation budget. The timing of these events suggests that they might be coupled to the progressive closure of the Panamanian Gateway.

The general global cooling trend, a response to the intensification of the Northern Hemisphere Glaciation (NHG) started around 3.2 Ma as shown by the $\delta^{18}O_{benthic}$ record and is paralleled by tropical east Pacific cooling as indicated by $SSTs_{Mg/Ca}$. Tropical east Pacific cooling, however, already commenced around 3.7 Ma, suggesting that global cooling, probably related to decreasing atmospheric CO_2 concentrations, might have started well before the intensification of the NHG.

Local SSS variations as indicated by $\delta^{18}O_{salinity}$ show a decoupling from the global, high latitude processes, as shown by the $\delta^{18}O_{benthic}$ record. Long-term regional freshening started with the decrease in $SSTs_{Mg/Ca}$ around 3.7 Ma, suggesting that changes in the tropical wind field in combination with latitudinal shifts of the tropical rainbelt related with general decrease in tropical east Pacific SST controlled $\delta^{18}O_{salinity}$.

The similarity of Pliocene $SSTs_{Mg/Ca}$ for *G. sacculifer* with modern SSTs in the east Pacific, in combination with the early development of a shallow thermocline (Steph et al., submitted) at Site 1241, gives no direct support to the idea that a permanent El Niño-like Pliocene climate might have existed during the early Pliocene.

Introduction

We present combined high-resolution planktonic Mg/Ca and $\delta^{18}O$ records from the tropical east Pacific Site 1241 that span the interval from 4.8 Ma to 2.4 Ma. Site 1241 (5°50N, 86°26W) is situated at a water depth of 2027 m on the northern side of the Cocos Ridge in the Guatemala Basin (Fig 5.1). We combined the Mg/Ca and $\delta^{18}O$ records to determine $\delta^{18}O_{water}$. By subtracting an estimate of the Pliocene ice volume signal from the $\delta^{18}O_{water}$ record, we reconstructed a $\delta^{18}O_{salinity}$ record, which is assumed to represent local changes in sea surface

salinity (SSS). These results provide important information on Pliocene climate variability and shed light on the hypothesis of a permanent El Niño-like Pliocene climate and the intensification of the NHG.

The Pliocene was affected by two major global events, the intensification of the NHG and the closure of the Panamanian Gateway. Both processes led to marked changes in global oceanography and climate (Maier-Reimer et al., 1990; Tiedemann and Franz, 1997; Billups et al., 1999; Haug et al., 2001). The Pliocene time interval prior to the NHG is often used as a possible near future analogue, because average temperatures were significantly warmer than today with atmospherical CO_2 concentrations probably slightly higher than modern ones (Dowsett et al., 1996; Crowley, 1996; Raymo et al., 1996). If Pliocene atmospheric CO_2 concentrations were higher than today, one could also expect higher tropical sea surface temperatures. More recently, modelling studies suggest the warm Pliocene to represent a permanent El Niño-like state with a suppressed temperature difference between the western tropical Pacific ‚warm pool' and the eastern Pacific Cold Tongue (Molnar and Cane, 2002), which is supported by Pliocene $\delta^{18}O_{G.\ sacculifer}$ gradients between the east and west Pacific (Cannariato and Ravelo, 1997; Chaisson and Ravelo, 2000).

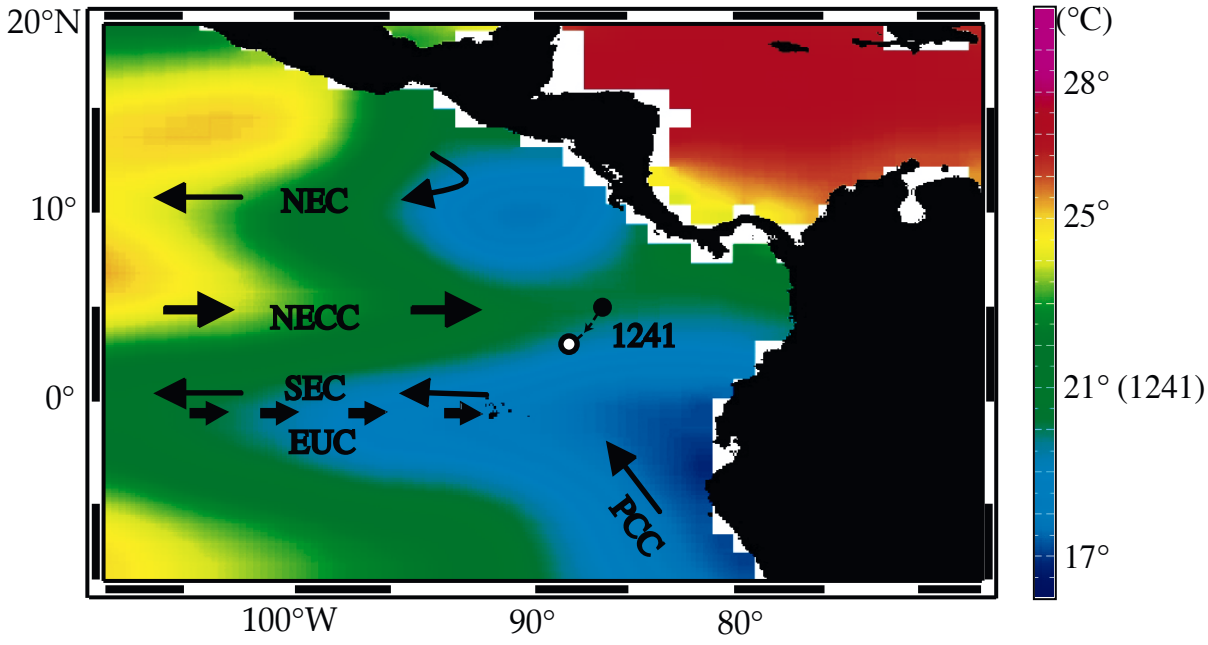

Figure 5.1 Present day oceanography for the tropical eastern Pacific with the major currents and their flow directions as well as the location of Site 1241 (5°50N, 86°26W). Paleolocation (open circle) of Site 1241 is backtracked to 3°N, 87.7°W (Mix, Tiedemann, Blum et al., 2003). Arrows indicate the flow direction of the following currents: NEC = North Equatorial Current, NECC = North Equatorial Counter Current, SEC = South Equatorial Current, EUC = Equatorial Under Current, PCC = Peru Chile Current. SSTs are according to Levitus and Boyer (1994) at a water depth of 50 m.

Tropical Pacific oceanography

The present day location of Site 1241 (5°50N, 86°26W) is within the eastward flowing NECC. A tectonic backtrack of the Cocos Plate, on which Site 1241 is positioned, locates Site 1241 between 4 Ma and 5 Ma at a more southwesterly position around 3°N, 87.7°W (Mix, Tiedemann, Blum et al., 2003; Pisias et al.,1995) (Fig 5.1). The closer proximity to the equatorial divergence and the SEC suggests that the expected SST and SSS at Site 1241 for the early Pliocene were about 1°C cooler and 0.35 less saline if other physical properties would have remained unchanged (Mix, Tiedemann, Blum et al., 2003). Surface hydrography in the tropical Pacific is

strongly controlled by seasonal variations in wind strength, causing seasonal changes in thermocline depth. In general, the NECC is closely linked to the ITCZ, the zone of maximal heating and convergence of the northeast and southeast trade winds (Donguy and Meyers, 1996; Huber, 2002). North of the ITCZ, the northeast trade winds drive the North Equatorial Current (NEC) towards the west, while the southeast trade winds drive the South Equatorial Current (SEC) also to the west, but south of the ITCZ. Below the SEC and the equator, the EUC flows towards the east from a depth of about 300 m in the Western Pacific Warm Pool (WPWP) to a depth of about 30 m in the east Pacific, parallel to the shallowing thermocline. The EUC is driven by the west-east pressure gradient and confined by the Coriolis force to the equator between 2°N and 2°S (Fig 5.1). From August to December, the ITCZ is in its northernmost position and the southeast trade winds are at maximum strength, resulting in a strong SEC and NECC. The SEC carries cool waters from the southeastern upwelling areas to the west and the NECC carries warm, low saline waters to the east out of the WPWP, depressing the thermocline (Donguy and Meyers, 1996). During this interval, the EUC is very weak. From March to May the ITCZ is at its southernmost position and the southeast trade winds are weak. As a result, the SEC and NECC are also weak. The EUC in contrast strengthens and causes the thermocline to shoal (Halpern and Weisberg, 1989; Ravelo and Shackleton, 1995). During El Niño events, easterly winds in the tropical Pacific become very weak, warm waters from the WPWP flow to the east, the thermocline deepens, the EUC is very weak, and SST increases, resulting in a decreased west-east SST-gradient (Wallace et al., 1998).

Between the Atlantic/Caribbean and the east Pacific, a salinity gradient exists of 1-1.5, which is mainly determined by the net transport of water vapour from the Caribbean over central America into the east Pacific by means of the trade winds (Broecker and Denton, 1989). During the early Pliocene free exchange of surface watermasses between the east Pacific and the Caribbean was still possible due to the open Panamanian Gateway. A salinity gradient did not develop because the inflow of lower salinity waters from the Pacific into the Caribbean prevented a significant salinity increase in the Caribbean. Haug et al. (2001) showed that $\delta^{18}O_{\textit{G. sacculifer}}$ records of the east Pacific and the Caribbean started to diverge from each other between 4.7 Ma and 4.2 Ma. This was interpreted as an indication that the Isthmus of Panama had shoaled to a depth of less than 100 m, thereby restricting the inflow of low salinity Pacific surface watermasses into the Caribbean.

Notably, the present day east Pacific is characterized by relatively low temperatures. The southeast trade winds cause strong upwelling along the Peruvian coast and along the equator, thus forming the Pacific Cold Tongue, which extends towards the west along the equatorial divergence (Mitchell and Wallace, 1992). Accordingly, the thermocline in these areas is very shallow, less than 50 m. In contrast, the Caribbean/Western Atlantic Warm Pool (WAWP) is marked by a distinctly deeper thermocline (100-150 m). At a water depth of 50 m, the temperature contrast between the Caribbean and the east Pacific is 5-6°C, while at the surface, SST is about 27°C, both for Site 1241 and the Caribbean (Levitus and Boyer, 1994).

Molnar and Cane (2002) described the early Pliocene as a period of permanent El Niño-like conditions. El Niño-like conditions for the Pacific would mean that the warm waters of the WPWP move to the east because of weak easterly winds over the tropical Pacific. This causes the cessation of upwelling, a decreasing temperature gradient between the WPWP and the east Pacific, and a deepening of the thermocline in the east Pacific (Wallace et al., 1998). A permanent El Niño-like climate state during the Pliocene should thus be characterized by significantly higher $SSTs_{Mg/Ca}$ in the mixed-layer than present day SSTs in the east Pacific, or by lower SSTs in the WPWP. The presence of a deeper thermocline can be determined by using the $\delta^{18}O$ and Mg/Ca records of planktonic foraminifers living at different water depths and calculating their gradients (Steph et al., submitted).

Mg/Ca paleothermometry

Mg/Ca is an independent paleotemperature proxy that is measured on the same biotic carrier as $\delta^{18}O$, which allows to reconstruct $\delta^{18}O_{water}$ and salinity variations without the problems introduced by other temperature proxies like different seasonal signals or different habitat depths of the biotic carriers (Nürnberg, 2000; Lea et al., 2002; Schmidt et al., 2004). Although Mg/Ca-paleothermometry is well established for the last glacial-interglacial cycles, hardly any $SST_{Mg/Ca}$ high-resolution records yet exist for older time periods. The only published, planktonic $SST_{Mg/Ca}$ record existing for older time periods is a record for the Paleocene/Eocene (Tripati et al., 2003). Here, we present the first high-resolution (<5 k.y. per sample) Mg/Ca record for the early Pliocene, covering 2.4 m.y.

The application of Mg/Ca-paleothermometry to Pliocene sample material demands to consider not only dissolution/diagenesis processes, but also possible changes in $Mg/Ca_{seawater}$. Brown (1996) showed in a culturing experiment that a linear dependency between $Mg/Ca_{solution}$ and Mg/Ca_{foram} exists (0.1 mol/mol change in $Mg/Ca_{seawater}$ leads to 0.059 mmol/mol change in Mg/Ca_{foram}). Recently, Ries (2004) showed that for several carbonate building organisms there even exists an exponential relationship between Mg/Ca_{foram} and $Mg/Ca_{solution}$. The residence time of Mg in seawater is about 13 m.y. (Broecker and Peng, 1982), which suggests that paleo sea surface temperature reconstructions on shorter time scales would not be affected by a change in $Mg/Ca_{seawater}$. However, the concentration of Mg and Ca in seawater may change by several factors, like varying continental weathering rates (Berner et al., 1983; Wilkinson and Algeo, 1989), hydrothermal alteration of basalt at mid ocean ridges (Mottle and Wheat, 1994; Elderfield and Schulz, 1996), carbonate deposition (Wilkinson and Algeo, 1989) and ion exchange reactions of Mg with clays (Gieskes and Lawrence, 1981). Several models attempted to reconstruct the Mg/Ca ratio of Cenozoic seawater, suggesting lower $Mg/Ca_{seawater}$ values than today (Wilkinson and Algeo, 1989; Stanley and Hardy, 1998).

Based on the models of Wilkinson and Algeo (1989) and Stanley and Hardie (1998), we assume a lowering in $Mg/Ca_{seawater}$ for the Pliocene time interval from 4.8 Ma to 2.4 Ma of maximum 0.4 mol/mol. Applying the relationship of Brown (1996) between $Mg/Ca_{seawater}$ and Mg/Ca_{foram}, this would imply a maximum underestimation of our temperatures by 0.7-1.0°C. Because this constant offset is within the error estimation for the SST reconstruction, we assess the Pliocene reduction in $Mg/Ca_{seawater}$ of minor importance.

Methods

The Mg/Ca analyses for Site 1241 (5°50N, 86°26W) were performed on the planktonic foraminifer *G. sacculifer*. *G. sacculifer* has a supposed habitat depth within the mixed-layer of 30-50 m (Fairbanks et al., 1982; Curry et al., 1983). For each sample, 20-25 specimens from the 355-400 µm fraction were picked. Specimens with a sac-like final chamber or visibly contaminated specimens were not selected for analysis. In case of insufficient numbers of specimens, the fraction 250-355 µm was used to provide

additional material, from which up to 35 specimens were picked. The shallow water depth of 2028 m of the core in comparison with the depth of the east Pacific lysocline at 3600 m (Lyle et al., 1995) indicates that no significant dissolution has occurred. Fe/Ca and Mn/Ca analyses were performed to monitor contamination with clays or Mn-carbonates and showed that the samples were not contaminated.

After gentle crushing, the samples were cleaned according to the cleaning protocol of Barker et al. (2003). To remove clays, the samples were rinsed 4-6 times with distilled deionized water and twice with methanol

(suprapure) with ultrasonical cleaning steps (2-3 minutes) after each rinse. Samples from several intervals were subject to severe fragmentation during ultrasonic treatment, therefore the duration of ultrasonic treatment was kept at a maximum of one minute per treatment for these samples. Subsequently, samples were treated with a hot (97°C) oxidizing 1% NaOH/ H_2O_2 solution (10 mL 0.1 *N* NaOH (analytical grade); 100 µL 30% H_2O_2 (suprapur)) for 10 minutes to remove organic matter. Every 2.5 minutes, the vials were rapped on the bench top to release any gaseous build-up. After 5 minutes, the samples were placed in an ultrasonic bath for a few seconds in order to maintain contact between reagent and sample. This treatment was repeated after refreshment of the oxidizing solution. Any remaining oxidizing solution was removed by three rinsing steps with distilled deionized water. After transferring the samples into clean vials, a weak acid leach with 250 µL 0.001 M HNO_3 (subboiled distilled) was applied with 30 seconds ultrasonic treatment and subsequent two rinses with distilled deionized water. After cleaning, the samples were dissolved in 0.075 M nitric acid (HNO_3) (subboiled distilled) and diluted several times so that all samples were expected to have Ca-concentrations in the range 30-70 ppm, being the ideal range for analysis (Garbe-Schönberg et al., in prep.).

Analyses were performed on a simultaneous, radially viewing ICP-OES (Ciros CCD SOP, Spectro A.I., Germany) at the Institute of Geosciences (Kiel University, Germany). A cooled cyclonic spraychamber in combination with a microconcentric nebulizer (200 µL/min sample uptake) was optimized for best analytical precision and minimized uptake of sample solution. Automized sample introduction was *via* an autosampler (Spectro A.I.). For Ca, we used the line with the highest stability, being 183.801 nm, providing a truly simultaneous analysis with Mg and Sr within the same detector read-out phase. For the trace elements Mg and Sr, we used the emission lines with the highest signal-to-noise ratios, 279.553 nm for Mg and 407.771 nm for Sr. For Fe and Mn we used the emission lines with the highest sensitivity, 259.940 nm for Fe and 257.610 nm for Mn. Matrix effects caused by varying concentrations of Ca were cautiously checked and were found not to be significant (Garbe-Schönberg et al. in prep.).

Analytical sessions with batches of 200-300 samples usually took between 20 and 30 hours, for which the drift of the machine could be neglected, being less than 0.2% as determined by analysing an internal consistency standard after every 5 samples. The analytical error on the analysis of the Mg/Ca-ratios was 0.1% for a total of 600 samples. Replicate analyses on the same samples, which were cleaned and analysed during different sessions, showed a standard deviation of 0.09 mmol/mol, introducing a temperature error of about 0.5°C.

The conversion of foraminiferal Mg/Ca-ratios into sea surface temperatures was carried out by applying the equation of Nürnberg et al. (2000) ($SST = (\mathrm{Log}(Mg/Ca) - \mathrm{Log}\ 0.491)/0.033$).

For stable isotope analysis 10 specimens of *G. sacculifer* (without sac-like final chamber) were picked from the 355-400 µm size fraction. All isotope analyses were run at IFM-GEOMAR (Kiel) on a Finnigan Delta-Plus Advantage Mass Spectrometer coupled to a Finnigan gas bench II. Analytical precision was better than 0.07‰ for $\delta^{18}O$. The values are reported relative to Pee Dee Belemnite (PDB), based on calibrations directly to National Bureau of Standards (NBS) 19.

The age model for Site 1241 was constructed by matching patterns of cyclic variation in climate proxy records with patterns of changes in solar radiation that are controlled by cyclic variations in Earth's orbital parameters. This astronomically derived age model is in agreement with the most recent astronomical polarity time scale and with other orbitally tuned age models. The establishment of the age model is described in detail in Tiedemann et al. (submitted).

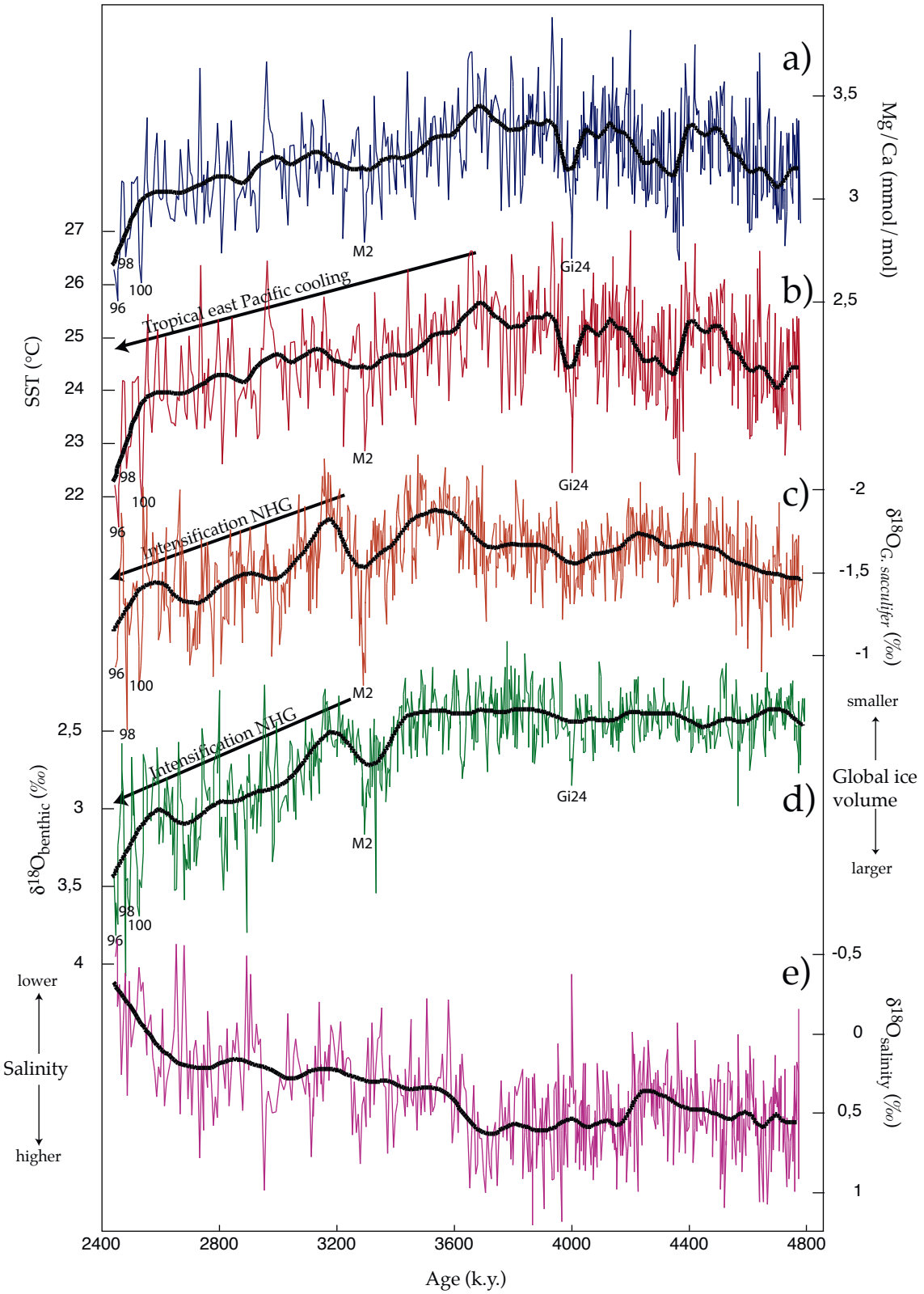

Figure 5.2 Results for Site 1241 for the time interval 4.8 Ma to 2.4 Ma. Arrows indicate trends associated with the intensification of the Northern Hemisphere Glaciation (NHG) and the tropical cooling in the east Pacific. Thick lined curves represent best fits on the data, showing variations on time scales larger than 185 k.y. Numbers 96, 98, 100, M2, and Gi24 indicate Marine Isotope Stages, according to the isotope nomenclature of Shackleton et al. (1995). **A** Mg/Ca ratios, measured in tests of the planktonic foraminifer *G. sacculifer*. **B** SSTs, calculated from the $Mg/Ca_{G.\ sacculifer}$ ratios using the equation of Nürnberg et al. (2000). **C** $\delta^{18}O$, measured in tests of the planktonic foraminifer *G. sacculifer*. D $\delta^{18}O$, measured on benthic foraminifers (Tiedemann et al., submitted). **E** $\delta^{18}O_{salinity}$, calculated by subtracting the normalized $\delta^{18}O_{benthic}$ record from the $\delta^{18}O_{water}$ record.

Results

For the studied time interval from 4.8 Ma to 2.4 Ma, Mg/Ca-ratios of *G. sacculifer* vary between 2.50 and 3.88 mmol/mol (Fig 5.2a), providing $SSTs_{Mg/Ca}$ between 21.4°C and 27.2°C (Fig 5.2b). Short-term $SSTs_{Mg/Ca}$ fluctuations are on the order of 2-2.5°C. A best fit to reveal long-term trends was calculated to show only variations on time scales larger than 185 k.y. (Fig 5.2). The general trend in $SSTs_{Mg/Ca}$ shows a warming between 4.8 Ma and 3.7 Ma from 24.5°C to 25.5°C (Fig 5.2b). After 3.7 Ma and more pronounced after 3.2 Ma, a cooling trend is apparent, paralelled by a continuous increase in $\delta^{18}O_{benthic}$ (Tiedemann et al., submitted). This cooling after 3.2 Ma reflects the irreversible intensification of the NHG (Fig 5.2d). Lowest $SSTs_{Mg/Ca}$ are recorded during marine isotope stages (MIS) 96 and 100 (around 2.5 Ma), when $SSTs_{Mg/Ca}$ dropped to values below 22°C. Highest $SSTs_{Mg/Ca}$ are recorded in the older part , >4.0 Ma, when maxima approached 27°C (Fig 5.2b).

Applying spectral analysis to the Mg/Ca record reveals that the apparent 400 k.y. cycle in the older part of the record, which is suggested by the best fit, shows no relationship to the eccentricity cycle of 400 k.y. (Fig 5.3a). To erase this influence of an artificial cyclicity as well as other long-term trends, like the intensification of the NHG, we filtered the datasets to remove variations on time scales longer than 185 k.y.. In order to do so, we subtracted a best fit with a Gaussian window of 185 k.y. and a time step of 3 k.y. from the different records. Therefore, further results from spectral analyses are based on the detrended datasets.

The Mg/Ca record is dominated by a 41 k.y. cycle between 3.7 Ma and 2.4 Ma (Fig 5.4b), as expected due to its increasing similarity to the $\delta^{18}O_{benthic}$ record (Figs. 2 and 3b). The older part of the record, from 4.8 Ma to 3.7 Ma, shows strong power at 100 k.y. and 23 k.y. periodicities and significantly reduced variance at the 41 k.y. periodicity (Fig 5.5b, Table 5.1). This suggests that regional low-latitude processes significantly contributed to the oceanography at Site 1241 during this period, as the presence of the 41 k.y. cycle, a typical high-latitude signal, is strongly reduced.

The $\delta^{18}O$ values of *G. sacculifer* vary between –0.8‰ and –2.18‰ with short-term fluctuations of about 0.5‰ (Fig 5.2c). From 4.8 Ma to 3.5 Ma, $\delta^{18}O_{G.\ sacculifer}$ values decrease from –1.5‰ to –1.85‰. A rapid increase towards MIS M2 at 3.3 Ma with a maximum of –0.8‰ and a subsequent decrease to –1.8‰ terminate the relatively warm interval of the Pliocene record. After 3.2 Ma, isotopic values increase, according to the global trend of the intensification of the NHG, and culminate at MIS 96, 98 and 100 (>–1.0‰) (Fig. 5c). Spectral analysis of the $\delta^{18}O_{G.\ sacculifer}$ record between 3.7 Ma and 2.4 Ma reveals dominant variability at the obliquity-related 41 k.y. cycle with significant power also in the 100 k.y. eccentricity band and little variability at precession-related cycles (Fig 5.4c and 5c). Spectral variability in the older interval, from 4.8 Ma to 3.7 Ma, is characterized by increased variance at precession-related cyclicities, similar to the Mg/Ca spectrum (Fig 5.5c, Table 5.1). In order to determine temporal changes in local SSS, we combined the $\delta^{18}O$ and Mg/Ca records of *G. sacculifer* to calculate the $\delta^{18}O_{water}$ record, according to Shackleton (1974). In a next step, we subtracted the Pliocene ice volume signal from the $\delta^{18}O_{water}$ record to assess variations in local SSS. To approximate the Pliocene ice volume we used the $\delta^{18}O_{benthic}$ record of Site 1241 (Tiedemann et al., submitted). The $\delta^{18}O_{benthic}$ difference between the Last Glacial Maximum (LGM) and the Holocene for the east Pacific is 1.6‰, while the difference in global ice volume between the LGM and the Holocene is 1.2‰, therefore being 75% of the $\delta^{18}O_{benthic}$ signal for the east Pacific. We assumed that this relationship between ice volume, salinity and temperature is also valid for the Pliocene. This would mean that the 1.1‰ amplitude for MIS 100 (Fig 5.2d) reflects an ice volume signal of about 0.8‰, equivalent to 80 m sea level change (10 m sea level = 0.1‰ $\delta^{18}O$), being two-third of the LGM-Holocene ice volume difference (Raymo et al., 1989). The 1.1‰ amplitude in the

$\delta^{18}O_{benthic}$ record for MIS 100 (Fig 5.2d) was then normalized to an amplitude of 0.8‰ and accordingly extended to the entire $\delta^{18}O_{benthic}$ record. This normalized record was then subtracted from the $\delta^{18}O_{water}$ record leaving a $\delta^{18}O_{salinity}$ record, which provides a first approximation of local SSS changes (Fig 5.2e). We are aware of the fact that this approach to assess SSS might be an oversimplification, but nevertheless gives a reliable first approximation.

Prior to 3.7 Ma, the $\delta^{18}O_{salinity}$ record remains relatively constant around an average value of 0.55‰,

Table 5.1 Cross spectral analysis for Mg/Ca and $\delta^{18}O_{G.\ sacculifer}$ for Site 1241.

Target	Reference	Time interval	Frequency	Cycilicity (k.y.)	Coherency	Phase	Lag (k.y.)
Mg/Ca	insolation 65°N (1)	3.7 - 2.4 Ma	0.024	41	0.90	-0.03	-0.2
$\delta^{18}O_{G.\ sacculifer}$	insolation 65°N (1)	3.7 - 2.4 Ma	0.025	41	0.96	-0.20	-1.3
$\delta^{18}O_{benthic}$ (2)	insolation 65°N (1)	3.7 - 2.4 Ma	0.024	41	0.95	0.13	0.8
Mg/Ca	$\delta^{18}O_{benthic}$ * -1 (2)	3.7 - 2.4 Ma	0.024	41	0.91	-0.19	-1.3
Mg/Ca	$\delta^{18}O_{G.\ sacculifer}$ * -1	3.7 - 2.4 Ma	0.024	41	0.92	0.09	0.6
Mg/Ca	insolation 65°N (1)	4.8 - 3.7 Ma	0.052	19	0.87	0.88	2.7
Mg/Ca	insolation 65°N (1)	4.8 - 3.7 Ma	0.044	23	0.88	0.46	1.7
$\delta^{18}O_{G.\ sacculifer}$	insolation 65°N (1)	4.8 - 3.7 Ma	0.024	41	0.81	1.20	7.8
Mg/Ca	$\delta^{18}O_{G.\ sacculifer}$ * -1	4.8 - 3.7 Ma	0.053	19	0.80	0.23	0.7
Mg/Ca	$\delta^{18}O_{G.\ sacculifer}$ * -1	4.8 - 3.7 Ma	0.042	23	0.87	-0.08	-0.3

(1) Laskar (1990).

(2) Tiedemann et al., submitted.

with the exception of a decrease to 0.4‰ between 4.4 Ma and 4.2 Ma (Fig 5.2e). Between 3.7 Ma and 3.6 Ma, average values decrease from 0.6‰ to 0.35‰. Between 3.6 Ma and 2.7 Ma average values further decrease to 0.2‰, followed by a more pronounced decrease to –0.25‰ until 2.4 Ma. Spectral analysis of the $\delta^{18}O_{salinity}$ record indicates no power in the 41 k.y. frequency band, suggesting a decoupling from the global signal of the intensification of the NHG and high-latitude climate forcing (Fig 5.4d). A weak precession signal for the entire time period indicates that local SSS is mainly controlled by low latitude processes instead of global, high latitude forcing (Fig 5.4d and 5d).

Mixed-layer hydrography during the early Pliocene

The interval between 4.8 Ma and 3.7 Ma reveals an increase in average $SSTs_{Mg/Ca}$ of 1-1.5°C (Fig 5.2b). Comparison with the $\delta^{18}O_{benthic}$ record (Fig 5.2d), which indicates no significant trend during this period, shows that this increase in $SSTs_{Mg/Ca}$ cannot be correlated to a global warming trend. Therefore, the increase in $SSTs_{Mg/Ca}$ between 4.8 Ma and 3.7 Ma represents a regional warming. This suggests an increased influence of the warm NECC and the ITCZ, as is also indicated by the $\delta^{18}O_{salinity}$ record. This might have been achieved either by the plate tectonic movement of Site 1241 towards a more northerly position (Mix, Tiedemann, Blum et al., 2003) or to a southward movement of the ITCZ/NECC.

A southward shift of the ITCZ during this period is supported by several other studies (Billups et al., 1999; Cannariato and Ravelo, 1997). On the other hand, it is also suggested that the ITCZ remained at its position or even moved northwards because of increasing heat piracy to the north Atlantic due to the progressive closure of the Panamanian Gateway (Tiedemann et al., 1989; Maier-Reimer et al., 1990; Haug and Tiedemann, 1998). This, then, would have strengthened the EUC, leading to a shallowing of the thermocline, as is also shown by Steph et

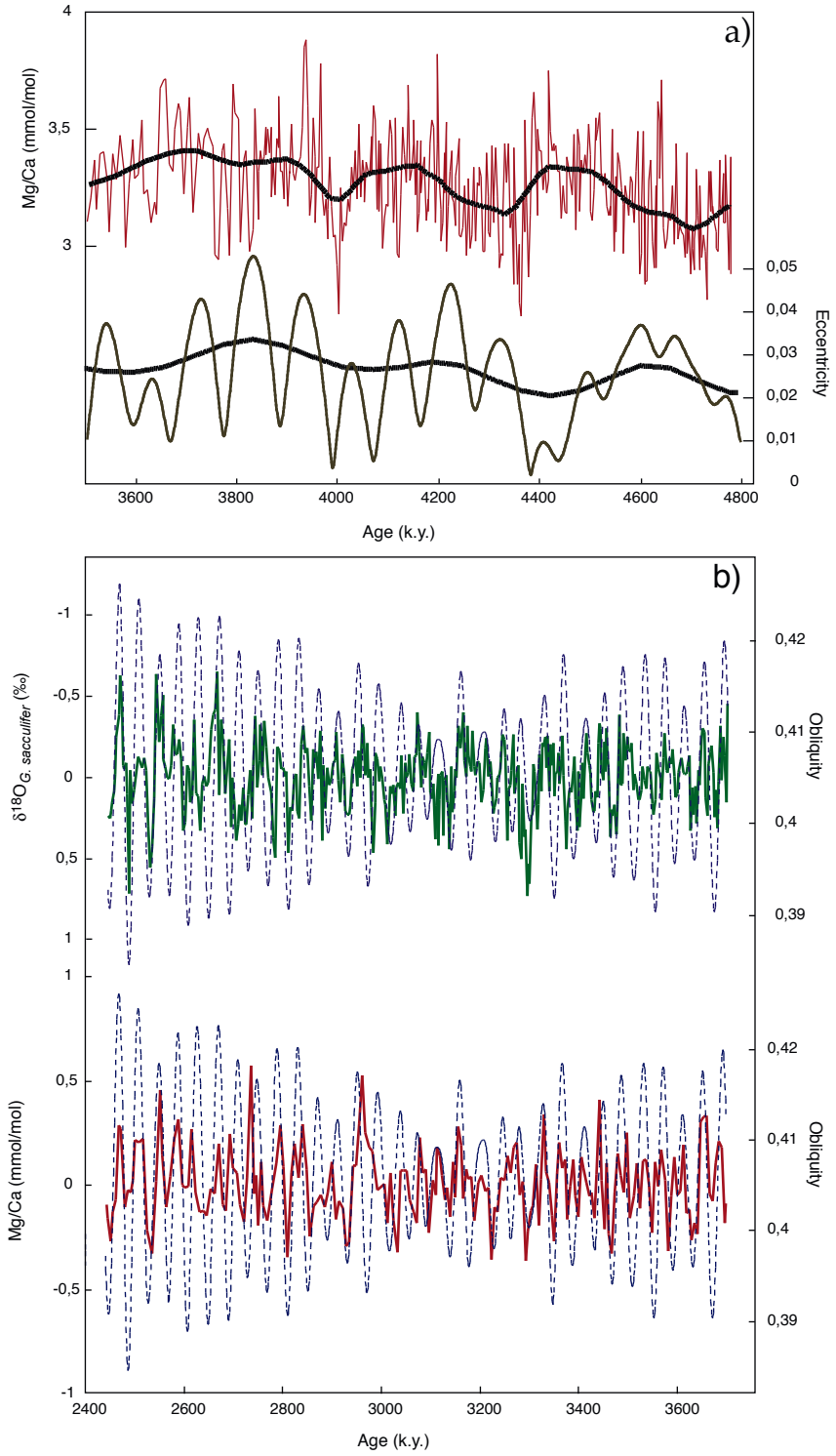

Figure 5.3 Comparison of Mg/Ca and $\delta^{18}O_{G.\ sacculifer}$ with orbital parameters (Laskar, 1990). A Comparison of Mg/Ca with eccentricity for the time interval 4.8 Ma to 3.5 Ma. B Comparison of Mg/Ca and $\delta^{18}O_{G.\ sacculifer}$ with obliquity for the time interval 3.7 Ma to 2.4 Ma. Mg/Ca and $\delta^{18}O_{G.\ sacculifer}$ are shown as detrended (variations longer than 185 k.y. are filtered out) and normalized curves.

al. (submitted). A shallowing of the thermocline might have led to a shallowing of the habitat depth of *G. sacculifer*, since *G. sacculifer* mainly lives in the mixed-layer. A possible imprint on the SST reconstruction, however, would have been a cooling trend, because the whole upper water column is affected when the thermocline significantly shallows. However, our results do not show such a trend in the $SST_{Mg/Ca}$ record of *G.*

sacculifer during this period. Therefore, we conclude that the shallowing of the thermocline between 5.4 Ma and 4.0 Ma had no or only minor effect on average SST in the mixed-layer at the location of Site 1241.

The time interval between 4.8 Ma and 3.7 Ma is further characterized by two significant cooling events around 4.4-4.2 Ma and 4.0 Ma (Fig 5.2b). The event at 4.0 Ma can be clearly correlated with the $\delta^{18}O_{benthic}$ record and can be indentified as MIS Gi24, representing a global cooling event. The event between 4.4 Ma and 4.2 Ma, however, is not present in the $\delta^{18}O_{benthic}$ record and therefore signifies a regional cooling event. This event can be explained either by increasing southeast tradewinds and a resulting northward movement of the ITCZ/NECC or by increasing influence of cooler thermocline waters, as suggested by the shallowing thermocline and the progressive closure of the Panamanian Gateway.

Because the $\delta^{18}O_{benthic}$ record reveals no significant trend for the time period from 4.8 Ma to 3.6 Ma (Fig 5.2d), variations in the $\delta^{18}O_{G.\ sacculifer}$ and $d^{18}O_{salinity}$ records reflect a large portion of variance that has to be ascribed to changes in regional oceanography (Figs. 2c and 2e). The decrease in $\delta^{18}O_{G.\ sacculifer}$ from –1.5‰ to –1.8‰ (Fig 5.2c) is explained by an increase in temperature, as is recorded by the Mg/Ca record (Fig 5.2b). The $\delta^{18}O_{salinity}$ fluctuations (Fig 5.2e) remain relatively constant during this period, except for the interval from 4.4 Ma to 4.2 Ma, when average $\delta^{18}O_{salinity}$ values decrease to 0.4‰. This suggests that between 4.4 Ma and 4.2 Ma Site 1241 bathed in a less saline watermass. This time interval corresponds with the main phase in the shallowing of the thermocline and is paralleled by a decrease in $SST_{Mg/Ca}$. This would suggest an increased influence of cooler thermocline waters because or an increase in southeast trade winds and an intensified EUC. On the other hand, this would not result in decreasing SSS and $SST_{Mg/Ca}$ does not show any changes which can be correlated with the general shoaling of the thermocline. Less saline waters are associated with the tropical rainbelt (ITCZ). Increasing southeast trade winds would move the ITCZ towards the north. Therefore, it seems that this temporarily freshening is due to a decrease in temperatures during this interval, changing the precipitation/evaporation ratio, causing less evaporation and lower saline waters. The synchronousness of this event with the critical threshold in the progressive closure of the Panamanian Gateway during this time might suggest a coupling between these events (Haug et al., 2001).

Permanent El Niño?

The presence of a permanent El Niño-like Pliocene climate has been suggested by several authors (Molnar and Cane, 2002; Ravelo et al., 2004). During a present day El Niño, warm waters originating from the WPWP flow to the east, causing high SSTs in the east Pacific. In consequence, the temperature gradient between the WPWP and the east Pacific diminishes, and the east Pacific thermocline deepens (Wallace et al., 1998). These changes significantly influence extratropical climates, for example they cause warmer and wetter conditions in North America, drier conditions in southeast Asia and Australia and drier conditions over northeastern South America (Molnar and Cane, 2002 and references therein). Several Pliocene reconstructions show similar extratropical conditions as those of present day El Niño (Wolfe, 1994; Dowsett and Poore, 1991; Zarate and Fasana, 1989; Archer et al., 1995). Evidence from the Pliocene tropical Pacific mainly comes from thermocline and SST gradient development. Chaisson (1995), Cannariato and Ravelo (1997) and Chaisson and Ravelo (2000) used $\delta^{18}O$ records of *G. sacculifer* and foraminiferal faunal assemblages for the east and west Pacific to show that the present day SST gradient and the slope of the thermocline depth between the east and the west Pacific did not

fully develop until 1.5 Ma. Although, a first and significant step towards a shallow thermocline occurred between 5.3 Ma and 4.0 Ma (Steph et al., submitted).

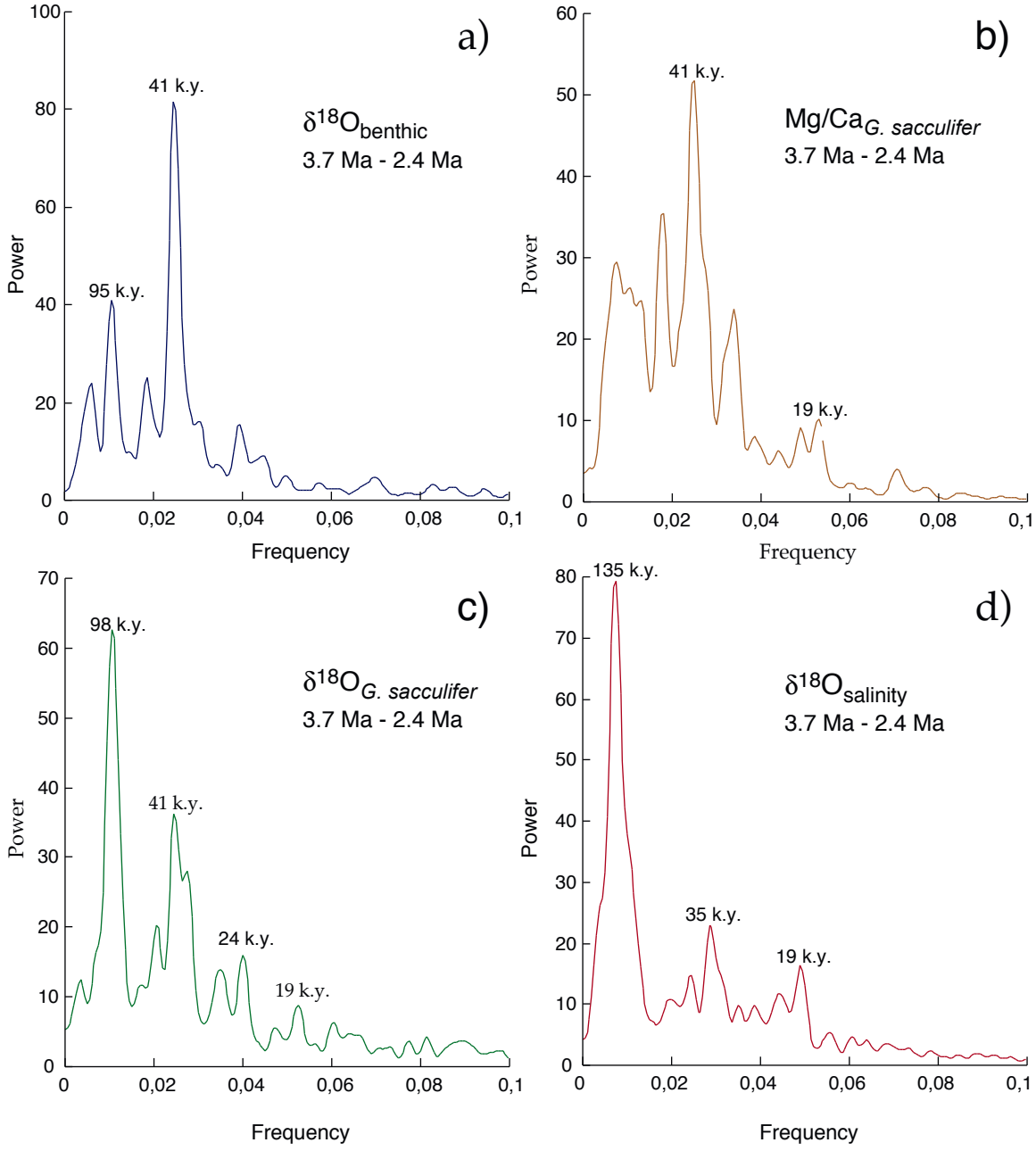

Figure 5.4 Spectral analysis for the time interval 3.7 Ma to 2.4 Ma. Time series analyses were performed with AnalySeries 1.2 (Paillard et al., 1996). **A** Mg/Ca-ratios, measured in foraminiferal tests of the planktonic foraminifer *G. sacculifer*. **B** $\delta^{18}O$, measured in foraminiferal tests of the planktonic foraminifer *G. sacculifer*. C $\delta^{18}O$, measured on benthic foraminifers (Tiedemann et al., submitted). D $\delta^{18}O_{salinity}$, calculated by subtracting the normalized $\delta^{18}O_{benthic}$ record from the $\delta^{18}O_{water}$ record.

The $SST_{Mg/Ca}$ record of *G. sacculifer,* however, is not showing significantly higher temperatures for the early Pliocene in comparison with today, as would be expected. This is also shown by Dowsett et al. (1996), who used foraminifer, diatom and ostracod assemblages for a middle Pliocene time interval to reconstruct SSTs. However, they also show significant warming in mid- and high-latitudes, indicating that a globally warmer climate is not necessarily reflected by higher tropical Pacific SSTs, especially if the Pliocene atmospheric CO_2 concentrations were not significantly higher than modern ones. Present day mixed-layer SSTs in the tropical east Pacific vary

between 24-27°C for the upper 40 m (Levitus and Boyer, 1994), below which the thermocline starts. Taking into account the paleolocation of Site 1241 (Pisias et al., 1995; Mix, Tiedemann, Blum et al., 2003), SSTs would be expected to be lower by about 1°C for the early Pliocene. $SSTs_{Mg/Ca}$ for the early Pliocene indicate variations between 24-26.5°C for the habitat depth of *G. sacculifer*. A study by Lea et al. (2000) from the equatorial east Pacific (core TR163-19, with a comparable position to the paleoposition of Site 1241), showed similar $SST_{Mg/Ca}$ fluctuations between 23-28°C for the surface dwelling *Globigerinoides ruber* for the last 350 k.y.. Since present day SSTs are indicative of interglacial, maximum temperatures, we conclude that the tropical thermal maxima during the early Pliocene were not significantly different than modern interglacial SSTs. Therefore, our east Pacific $SST_{Mg/Ca}$ results do not directly support the idea of an early Pliocene permanent El Niño-like climate. Further evidence against a permanent El Niño-like climate is suggested by the significant shallowing of the thermocline between 5.3 Ma and 4.0 Ma (Steph et al., submitted; Cannariato and Ravelo, 1997; Chaisson and Ravelo, 2000). On the other hand, a typical El Niño-like scenario with a decreased or even reversed east-west Pacific SST gradient might also have been caused by lower SSTs in the west Pacific, as was suggested by Cannariato and Ravelo (1997). Their estimation of SST, however, was based on $\delta^{18}O$ analyses, assuming no influence of salinity on $\delta^{18}O$. Andersson (1997) and Wang (1994) used transfer functions on total planktonic foraminiferal assemblages to reconstruct Pliocene SSTs for the west Pacific. Their SST reconstructions, using three different transfer functions, showed SSTs which are similar to present SSTs in the west Pacific. Andersson (1997) actually investigated the difference between two transfer functions for cold and warm seasons for Ontong Java Plateau ODP Site 806. All estimates were close to present SSTs and significantly higher than our average SSTs for the east Pacific. Anderssons (1997) lowest estimate, using Modern Analog Technique, for the cold season was 27.0°C and the warmest estimate for the warm season, using the Imbrie-Kipp Transfer Function Method, was 29.6°C, while our average SST for the east Pacific is 24.7°C (Fig 5.6). Although the age model of Andersson (1997) is not tuned to our age model, the general trends reveal a strong similarity between the two records between 4.0 Ma and 3.2 Ma with the west Pacific constantly being warmer than the east Pacific by about 3°C. Further comparison between both SST records suggests a strengthening of the tropical west-east Pacific SST gradient along with the major intensification of the NHG after 3.2 Ma.

Therefore, we conclude that a 'normal' SST gradient rather than a very weak, El Niño-like SST gradient between the west and the east Pacific seems most likely to have existed in the early Pliocene. Nevertheless, the closure of the Indonesian Gateway between 4.0 Ma and 3.0 Ma (Cane and Molnar, 2001) and the decrease in east Pacific SST since 3.7 Ma might have played a role in further increasing the SST gradient towards present proportions.

However, the position of Site 1241 is not an ideal place to record El Niño-related changes, as the most pronounced changes in upper ocean water signatures occur along the west coast of South America. Comparison with initial Mg/Ca analyses from Site 1239 from the Peruvian upwelling zone, which is more susceptible to the effects of El Niño, indicates that SST gradients within the east Pacific were much smaller than today, giving an indication for an El Niño-like situation.

Intensification of the NHG

Between 4.8 Ma and 3.4 Ma, the $\delta^{18}O_{benthic}$ record reveals no significant long-term trend, pointing to warm early Pliocene climate conditions without prominent changes in ice volume (Tiedemann et al., 1994). After 3.2 Ma, the $\delta^{18}O_{benthic}$ starts to increase from 2.5‰ to values of over 3.5‰ for MIS 96, 98 and 100 around 2.5 Ma. This increase, which can be globally observed, marks the irreversible intensification of the NHG (Ruddiman and

Raymo, 1988; Raymo et al., 1989; Kwiek and Ravelo, 1999). The preceeding cooling trend (MIS M2), as shown by the $\delta^{18}O_{benthic}$ and $SST_{Mg/Ca}$ records, from 3.4 Ma to 3.3 Ma, that was abruptly terminated by the so-called ‚mid Pliocene warmth period' (Crowley, 1996), may indicate a failed attempt of the climate system to start the NHG (Haug and Tiedemann, 1998).

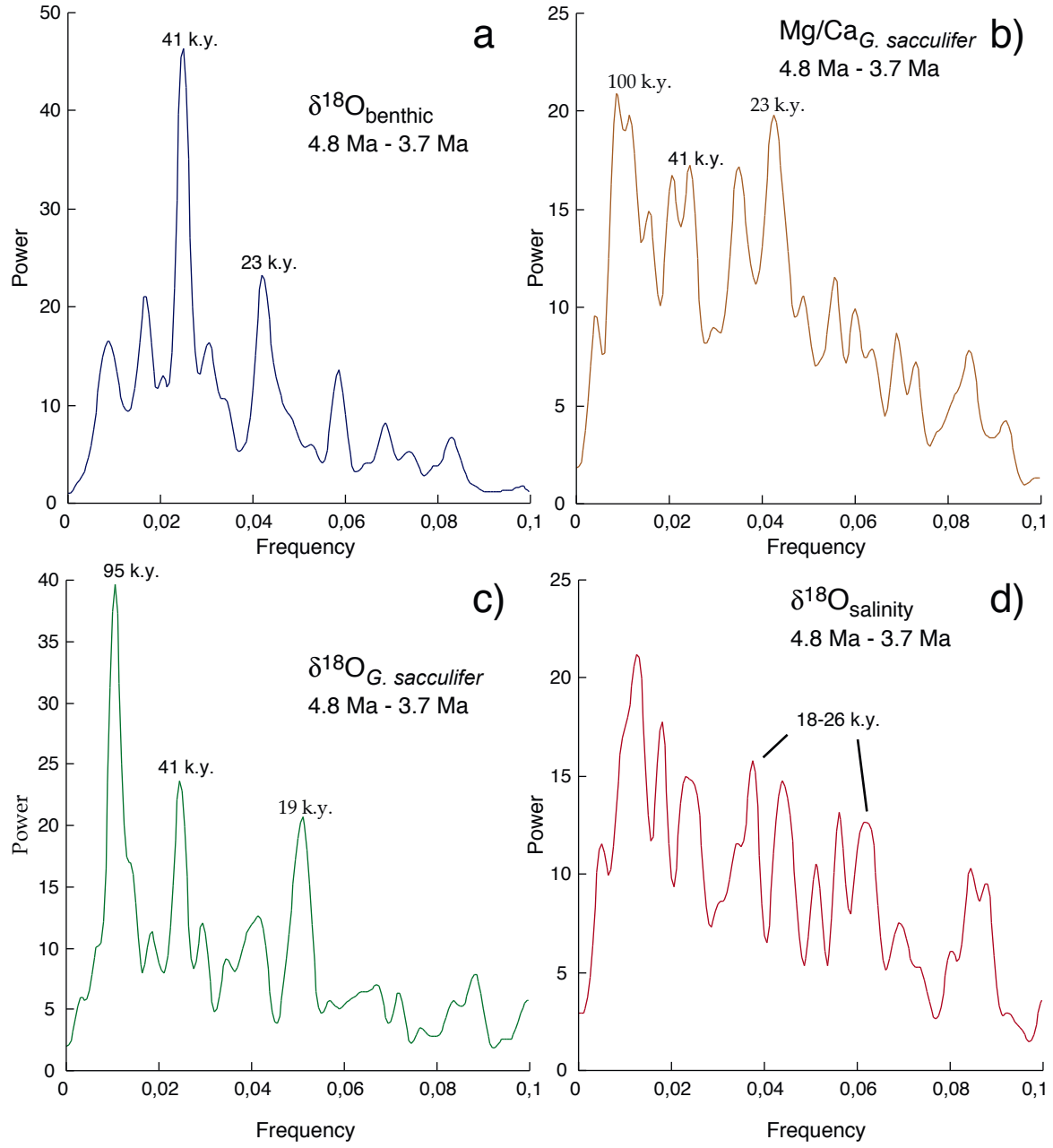

Figure 5.5 Spectral analysis for the time interval 4.8 Ma to 3.7 Ma. Time series analyses were performed with AnalySeries 1.2 (Paillard et al., 1996). **A** Mg/Ca-ratios, measured in foraminiferal tests of the planktonic foraminifer *G. sacculifer*. **B** $\delta^{18}O$, measured in foraminiferal tests of the planktonic foraminifer *G. sacculifer*. **C** $\delta^{18}O$, measured on benthic foraminifers (Tiedemann et al., submitted). **D** $\delta^{18}O_{salinity}$, calculated by subtracting the normalized $\delta^{18}O_{benthic}$ record from the $\delta^{18}O_{water}$ record.

The decrease of $SST_{Mg/Ca}$ since 3.7 Ma starts several 100 k.y. earlier than the start of the intensification of the NHG around 3.2 Ma as generally shown by global $\delta^{18}O_{benthic}$ records, which represent global ice volume. Average $SST_{Mg/Ca}$ decreases by about 2°C between 3.7 Ma and 2.4 Ma. $\delta^{18}O_{G.\ sacculifer}$ increases with 0.8‰, which

agrees with the change expected from the $SST_{Mg/Ca}$ decrease (2°C = 0.5‰) and the ice volume effect of 0.4‰, which would give a total of 0.9‰.

Spectral analyses on the $SST_{Mg/Ca}$ record also indicate a change in spectral character at about 3.7 Ma. The interval from 4.8 Ma to 3.7 Ma is characterized by a concentration of variance at eccentricity- and precession-related frequencies (Fig 5.5b) with limited power at the 41 k.y. cycle. The interval from 3.7 Ma to 2.4 Ma, comprising the tropical cooling trend in $SST_{Mg/Ca}$, in contrast provides a strong 41 k.y. cycle and negligible variability at the precession band. The pronounced dominance of the 41 k.y. cycle after 3.7 Ma indicates that high-latitude climate forcing has played an important role in driving SSTs in the tropical east Pacific, because the presence of a strong obliquity-related cycle typically reflects a high-latitude origin.

The similarity of the Mg/Ca and $\delta^{18}O$ records of *G. sacculifer* with the $\delta^{18}O_{benthic}$ record for the time period younger than 3.4 Ma is expressed by cross spectral analysis between the proxies and the obliquity signal (Laskar, 1990) (Table 5.1). Coherency of all three proxies with obliquity exceeds 0.90 and coherency between $SST_{Mg/Ca}$ and $\delta^{18}O_{benthic}$ is 0.91, while none of the proxies significantly lags or leads obliquity. This suggests that the 41 k.y. rythm in tropical east Pacific $\delta^{18}O_{benthic}$, $SST_{Mg/Ca}$, and $\delta^{18}O_{G.\ sacculifer}$ was mainly driven by variations of global importance, triggered by high-latitude processes which caused the intensification of the NHG (Fig.3 and 4).

Although the tropical cooling trend since 3.7 Ma is not reflected by an increase in ice volume before 3.4 Ma, evidence for early Pliocene high-latitude cooling is provided by sediment records from the Irminger and Norwegian Seas (Kleiven et al., 2002; St. John and Krissek, 2002). These records show significant pulses of ice rafted debris (IRD) back to 3.5 Ma, indicating the existence and development of glaciers large enough to produce icebergs well before the intensification of the NHG.

The warm Pliocene before the intensification of the NHG (Ravelo and Andreasen, 2000) is probably associated with atmospheric CO_2 concentrations which were higher than pre-industrial concentrations by about 100 ppmv (Van der Burgh et al., 1993; Raymo et al., 1996). Although the mid Pliocene warm period is generally assumed to have continued until 3.2 Ma, the initiation of an earlier decrease in atmospheric CO_2 can not be excluded. Therefore, the lead of cooling tropical SSTs over the increase of global ice volume could indicate that a decrease in atmospheric CO_2 concentrations might have played an important role in the intensification of the NHG (Li et al.,1998). Decreasing atmospheric CO_2 concentrations would lead to global cooling, but global ice volume will not start to increase before a certain threshold is reached, thereby resulting in a lag of global ice volume to global temperatures (Raymo, 1998; DeConto and Pollard, 2003).

The expression of the intensification of the NHG is contradicted by Ravelo et al. (2004). The authors argued that the main phase of the intensification of the NHG is not linked to changes in the tropics, but rather to changes in the subtropics. The main changes in the tropics occurred between 4.5 Ma and 4.0 Ma, simultaneously with the critical threshold in the shoaling of the Isthmus of Panama (Haug et al., 2001; Billups et al., 1999) and after 2.0 Ma, when the present day SST gradient between the east and west Pacific became established (Cannariato and Ravelo, 1997; Chaisson and Ravelo, 2000). These changes also suggest that the main influence of the subtropics on the tropics, namely providing the source for cooler upwelling waters, did not develop until 2.0 Ma. If deep water temperatures at high latitudes started to decrease during the middle Pliocene, and then propagated towards the tropics, the thermocline would have to shallow in order to influence SSTs. However, the main phase of shallowing of the thermocline at Site 1241 ended around 4.0 Ma (Steph et al., submitted), showing no significant changes around the period when $SSTs_{Mg/Ca}$ started to decrease at about 3.7 Ma (Fig 5.2). From our data, we

therefore conclude that the intensification of the NHG is paralleled by cooling in the tropical east Pacific, which even preceeded the intensification of the NHG by 500 k.y..

The $\delta^{18}O_{salinity}$ record does not seem to show the intensification of the NHG. Instead of the expected trend towards higher salinity because of increasing global ice volume since 3.2 Ma, a freshening trend is present for this time period (Fig 5.2e), which already started around 3.6 Ma when also $SSTs_{Mg/Ca}$ started to decrease. Also, the global obliquity signal of 41 k.y., which is dominating the $\delta^{18}O_{benthic}$, $\delta^{18}O_{\textit{G. sacculifer}}$ and Mg/Ca records, is not significant in the $\delta^{18}O_{salinity}$ record (Fig 5.4d). This suggests that the variations in local SSS in the Pliocene east Pacific are mainly controlled by low-latitude processes, and can be explained by changes in evaporation/precipitation that are most likely related to latitudinal variations in the tropical rainbelt (ITCZ). The average values of $\delta^{18}O_{salinity}$ for the time period 3.6 Ma to 2.4 Ma are on average 0.4‰ lower than for the time period between 4.8 Ma and 3.6 Ma, indicating generally fresher watermasses at Site 1241. The present day distribution of mixed-layer salinity in the east Pacific shows that lower saline watermasses are related to the position of the ITCZ/NECC and the depth of the thermocline. Therefore, we conclude that between 3.6 Ma and 2.4 Ma, mixed-layer water mass properties at Site 1241 became not only cooler but also less saline. This indicates that with the intensification of the NHG, the ITCZ possibly moved into a more southerly position, with weaker southeast trade winds, a relatively weaker SEC and NECC, a strengthened EUC, and a shallower thermocline in comparison with the period from 4.8

Ma to 3.6 Ma.

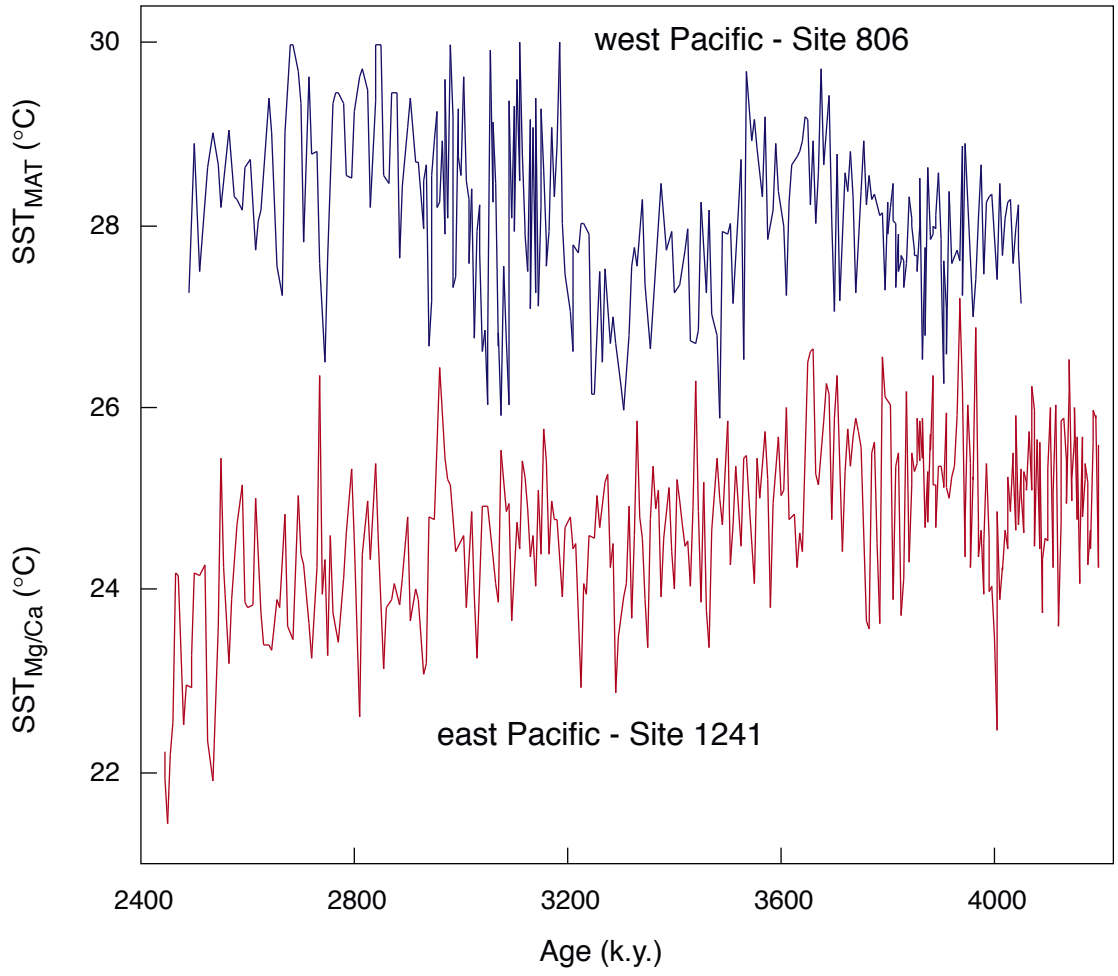

Figure 5.6 Comparison between tropical east and west Pacific SSTs for the time interval 4.2 Ma to 2.4 Ma. East Pacific SSTs are Mg/Ca-SSTs from Site 1241. West Pacific SSTs are results from planktonic foraminiferal transfer functions, Modern Analog Technique (MAT), from Andersson (1997) for Ontong Java Plateau Site 806 (0°19N, 159°21E).

Conclusions

High-resolution analyses of the mixed-layer dwelling planktonic foraminifer *G. sacculifer* for Mg/Ca and $\delta^{18}O$ for Site 1241 reveal the development of east Pacific surface hydrography for the time interval from 4.8 Ma to 2.4 Ma.

An increase in average $SSTs_{Mg/Ca}$ between 4.8 Ma and 3.7 Ma, from 24.5°C to 25.5°C, interrupted by short-term cooler periods, can be explained by a general southward shift of the ITCZ, increasing the influence of the warmer NECC. Between 4.4 Ma and 4.2 Ma, a decrease in $SSTs_{Mg/Ca}$ and SSS suggests a temporarily change in the precipitation/evaporation budget, while around 4.0 Ma the global cooling event MIS Gi24 is clearly present. The timing of these events suggests that they might be coupled to the progressive closure of the Panamanian Gateway.

The general global cooling trend, a response to the intensification of the Northern Hemisphere Glaciation (NHG) started around 3.2 Ma, as shown by the $\delta^{18}O_{benthic}$ record, and is paralleled by tropical east Pacific cooling as indicated by $SSTs_{Mg/Ca}$. Tropical east Pacific cooling, however, already commenced around 3.7 Ma, suggesting that global cooling, probably related to decreasing atmospheric CO_2 concentrations, might have started well before the intensification of the NHG.

Local SSS variations as indicated by $\delta^{18}O_{salinity}$ show a decoupling from the global, high latitude processes, as shown by the $\delta^{18}O_{benthic}$ record. Long-term regional freshening started with the decrease in $SSTs_{Mg/Ca}$ around 3.7 Ma, suggesting that changes in the tropical wind field in combination with latitudinal shifts of the tropical rainbelt related with general decrease in tropical east Pacific SST controlled $\delta^{18}O_{salinity}$.

Considering that Pliocene $SSTs_{Mg/Ca}$ for *G. sacculifer* for Site 1241 are close to modern SSTs in the tropical east Pacific, in combination with the early Pliocene development of a shallow thermocline, give no direct support to the idea that a permanent El Niño-like Pliocene climate might have existed during the early Pliocene.

Acknowledgements

We like to thank S. Koch, K.Wittmaack, N. Gau, A. Jesussek, U. Nielsen and K. Kissling for sample preparation and laboratory assistence. J.G. especially thanks M. Greaves and H. Elderfield (Cambridge University) for introduction into Mg/Ca analyses. We thank C. Andersson Dahl for providing the data for Fig 5.6. We also gratefully thank ..... and .. anonymous reviewers for their useful comments. This research used samples and data provided by the Ocean Drilling Program, which is sponsored by the U.S. National Science Foundation and participating countries under management of Joint Oceanographic Institutions. This study was performed within DFG-Research Unit, FOR 451 (Impact of Gateways on Ocean Circulation, Climate, and Evolution; funding under Ti240/12-2).

Chapter 6

The Pliocene Mg/Ca SST increase in the Caribbean: Western Atlantic Warm Pool formation, salinity influence or diagenetic overprint?

Jeroen Groeneveld (1), Dirk Nürnberg (1), Silke Steph (1), Ralf Tiedemann (1), Gert-Jan Reichart (2), Lars Reuning (1), Daniela Crudeli (3)

Manuscript submitted to Geochemistry, Geophysics, Geosystems

(1) IFM-Geomar, Leibniz Institute of Marine Sciences, Kiel, Germany
(2) Faculty of Earth Sciences, Utrecht University, The Netherlands, and, AWI, Institute for Polar and Marine Research, Bremerhaven, Germany
(3) Institute of Geosciences, University of Kiel, Germany

Abstract

We performed combined analyses of Mg/Ca and $\delta^{18}O$ on the planktonic foraminifer *Globigerinoides sacculifer* from Caribbean ODP Site 1000 in order to reconstruct the effect of the shoaling of the Isthmus of Panama on sea surface temperatures (SST) and salinities (SSS) for the early Pliocene. After 4.5 Ma, the positive, precessional correlation between Mg/Ca and $\delta^{18}O$ suggests that the $\delta^{18}O$ signal is mainly driven by salinity. During maximum SSS, Mg/Ca approaches ~7 mmol/mol (~34-35°C), implying that the large SSS variations exert a profound influence on Mg/Ca, overestimating Mg/Ca by 20-30% (~3-4°C). Foraminiferal Sr/Ca ratios, carbonate mineralogy, calcareous nannofossil analysis, and SEM suggest that diagenetically induced aragonite dissolution and reprecipitation caused crystalline overgrowths on foraminiferal tests with extremely high Mg/Ca-ratios. LA-ICP-MS measurements and pore water data exclude that the overgrowths significantly contributed to the high Mg/Ca-ratios. After correcting the Mg/Ca-ratios after 4.5 Ma for the salinity effect, the $SST_{Mg/Ca}$ record shows an increase by ~2°C due to the progressive shoaling of the Isthmus of Panama.

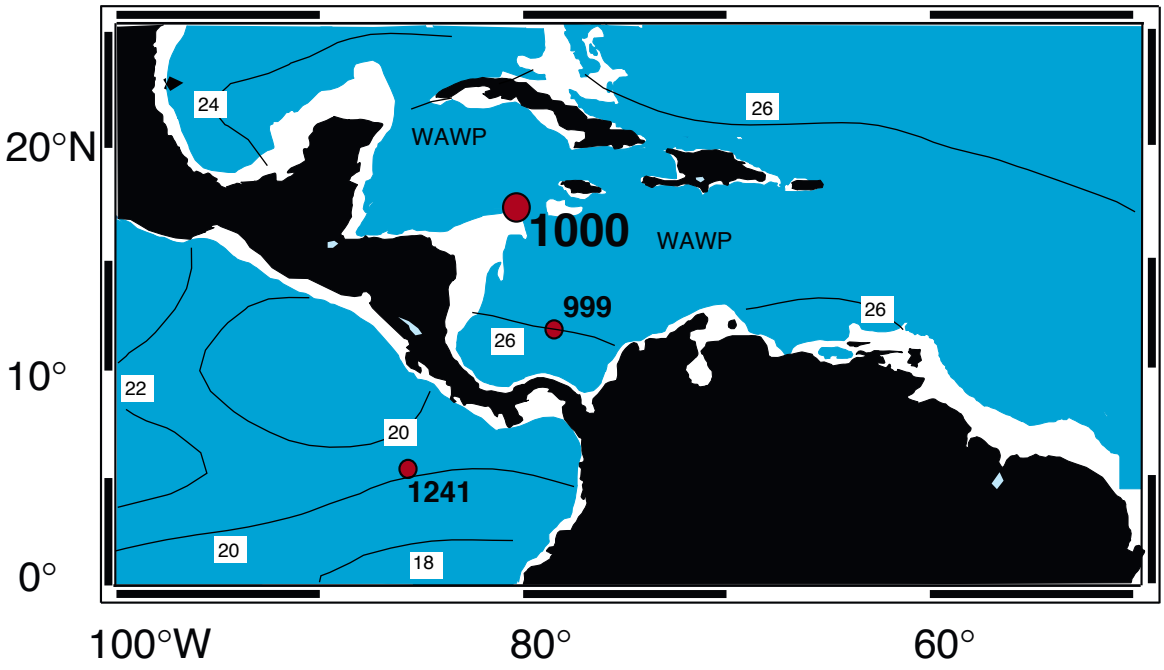

Figure 6.1 Present day configuration of the Caribbean Sea with the location of Site 1000 (16°33.222'N, 79°52.044'W, 916 m water depth). Also indicated are Sites 999 (Haug et al., 2001) and 1241 (Groeneveld et al., submitted). WAWP is the Western Atlantic Warm Pool. Isolines indicate annual average temperatures at a water depth of ~50 m (Levitus and Boyer, 1994), the assumed habitat depth of *G. sacculifer*, showing a temperature difference of ~5°C between the Caribbean and the east Pacific.

Introduction

We present a high-resolution Mg/Ca record for ODP Site 1000 from the Caribbean for the time interval from 5.6 Ma to 3.9 Ma for the planktonic foraminifer *Globigerinoides sacculifer*. Main objective of the study was to investigate what the effect of the restriction of the exchange of upper ocean water masses between the Pacific and the Caribbean, due to the progressive closure of the Panamanian Gateway (Haug et al., 2001; Steph et al., submitted), was on the development of sea surface temperatures (SST) in the Caribbean. Comparison with the $\delta^{18}O$ record of *G. sacculifer* was used to determine the effect of salinity on the Mg/Ca record. To investigate the effect of carbonate diagenesis on the Mg/Ca reconstruction, we established additional records of Sr/Ca on *G. sacculifer*, calcareous nannofossil abundance (*Florisphaera profunda*) and carbonate mineralogy (aragonite), while scanning electron micoscope (SEM) and LA-ICP-MS analyses were performed to further quantify the effect of carbonate diagenesis.

Closure of the Panamanian Gateway

The late Miocene/early Pliocene gradual closure of the Panamanian Gateway effectively changed oceanographic patterns between the Pacific and Atlantic oceans, and thus led to profound changes in global atmospheric circulation and climate. The closure of the Panamanian Gateway was responsible for changing the Pacific, Caribbean, and Atlantic water mass signatures, generating the Western Atlantic Warm Pool (WAWP), and intensifying thermohaline circulation in the North Atlantic via increasing salt and heat transport to high northern latitudes (Maier-Reimer et al., 1990; Tiedemann and Franz, 1997; Haug and Tiedemann, 1998; Billups et al., 1999; Haug et al., 2001). As a consequence, the intensification of the Gulfstream system might have had an important role in the initiation of the northern hemisphere glaciation (NHG), which started during the mid Pliocene (Haug and Tiedemann, 1998; Driscoll and Haug, 1998).

Haug et al. (2001) interpreted the divergent pattern of planktonic $\delta^{18}O$ records from the Caribbean (Site 999) and the tropical Pacific (Site 851) at 4.6 Ma and the subsequent 0.5‰ increase in $\delta^{18}O$ in the Caribbean since ~4.2 Ma as the establishment of the salinity contrast between Pacific and Caribbean surface waters. This hydrographic change was caused by the plate tectonic shoaling of the Panamanian sill to less than 100 m, which effectively restricted the surface water exchange between the Pacific and the Atlantic, and therefore increased SSS in the Caribbean by 1-2 salinity units by means of an increased atmospheric transport of water vapor from the Caribbean into the Pacific. Recent results from Caribbean Site 1000 (Steph et al., submitted) show that, in accordance with this general increase in Caribbean SSS, salinity gradients within the Caribbean increased and varied on precessional timescales. Low SSS gradients occurred during minima in northern hemisphere summer insolation and were interpreted to reflect enhanced inflow of low salinity Pacific surface water into the Caribbean. During maxima in northern hemisphere summer insolation Pacific inflow of low salinity surface waters was reduced, resulting in higher SSS gradients between Sites 999 and 1000.

However, the final closure of the Panamanian Gateway was not established until ~2.7-2.2 Ma, when the major exchange of mammals via the Isthmus between North and South-America took place (Webb, 1997; Stehli and Webb, 1985), and nannofossil assemblages from the Caribbean and the eastern Pacific (Kameo and Sato, 2000),

and $SSTs_{Mg/Ca}$ between the east Pacific (ODP Site 1241) and the Caribbean (ODP Site 999) permanently diverged (Groeneveld et al., manuscript in preparation).

Mg/Ca paleothermometry

The advantage of measuring Mg/Ca and $\delta^{18}O$ on the same biotic carrier is that synchronous estimates of SST and global ice volume can be determined and used to calculate $\delta^{18}O_{seawater}$ and SSS, thereby avoiding the bias of seasonality and/or habitat differences that occur when proxy data from different faunal groups are used. The paired analysis of $\delta^{18}O$ and Mg/Ca on the mixed layer dwelling planktonic foraminifer *G. sacculifer* from ODP Site 1000 provides new insights on the oceanographic evolution of the Caribbean during the shoaling of the Isthmus of Panama as well as clear evidence for complications which may arise when applying Mg/Ca paleothermometry. Our studies concentrate on the late Miocene/early Pliocene time interval between 5.6 Ma and 3.9 Ma.

Commonly, the $\delta^{18}O$ signal of planktonic foraminifers records the combined effects of global ice volume, sea surface temperature, and local salinity. The Mg content of foraminifers is mainly dependant on the temperature of the water in which the foraminifer calcifies as deduced from cultivating work and field studies (Nürnberg, 1995, 2000; Nürnberg et al., 1996, 2000; Lea et al., 1999; Mashiotta et al., 1999; Elderfield and Ganssen, 2000; Dekens et al., 2002). Therefore, the Mg/Ca paleothermometry has become an accepted, powerful tool in paleoceanography for the reconstruction of SSTs. Other factors like salinity (Nürnberg, 1996; Lea et al., 1999) and pH (Lea et al., 1999) additionally affect foraminiferal Mg/Ca, but were hitherto considered to play minor roles since their opposite effects on Mg/Ca would cancel each other and absolute changes are considered to have been small (Lea et al., 2000; Nürnberg et al., 2000). Although the effects of dissolution within the water column have been studied extensively (Dekens et al., 2002; Rosenthal and Lohmann, 2002; de Villiers, 2003; Regenberg et al., manuscript in preparation), the effects of diagenetic processes on Mg/Ca-ratios have only recently become under attention (Reuning et al., in press; Pena et al., submitted).

First efforts to determine high-resolution element ratio profiles through single foraminiferal test chambers were performed by means of microprobe (Nürnberg et al., 1996; McKenna and Prell, 2004), who showed the heterogeneity of Mg/Ca-ratios within single foraminiferal tests. Recent studies have used Laser Ablation Inductively Coupled Mass Spectrometry (LA-ICP-MS) to further investigate inter- and intra-test variability showing the good spatial resolution of this method in determining contaminant phases on foraminiferal tests (Reichart et al., 2003; Hathorne et al., 2003; Eggins et al., 2003; Pena et al., submitted). Here we used LA-ICP-MS to determine the chemistry of the crystal overgrowth which was evident from SEM on the foraminiferal tests after the cleaning process and to investigate to what extent the bulk test chemistry was influenced.

Materials and Methods

ODP Site 1000 was cored during Leg 165 on the Nicaraguan Rise (Pedro Channel) in the Caribbean (16°33.222'N, 79°52.044'W, Fig 6.1). The shallow site location of 916 m in comparison with the depth of the Caribbean lysocline at 4000 m (Archer, 1996) implies that carbonate dissolution is negligible. Samples were taken every 10 cm, reflecting a temporal resolution of ~3 kyr per sample. 20-25 specimens of *Globigerinoides sacculifer* were selected from the 315-400 µm size fraction. Specimens visibly contaminated by ferromanganese oxides and specimens with a final sac-like chamber were not selected for analysis. The age model for Site 1000 was based on the $\delta^{18}O$ record of the benthic foraminifer *C. wuellerstorfi* (Steph et al., submitted). Since no

composite depth exists for Site 1000, a preliminary age model was constructed by identifying major isotopic stages according to the nomenclature of Shackleton et al. (1995). The preliminary age model was then correlated to the orbitally tuned age model of ODP Site 925/926 from Ceara Rise (Bickert et al., 1997; Tiedemann and Franz, 1997; Shackleton and Hall, 1997). The final age model revealed the presence of dominant precession cycles in the planktonic $\delta^{18}O$ record, which were then used to further tune the age model (Steph et al., submitted).

Mg/Ca-analysis

After gentle crushing, the samples were cleaned according to the cleaning protocol of Barker et al. (2003). To remove clays, the samples were rinsed 4-6 times with distilled deionized water and twice with methanol (suprapure) with ultrasonical cleaning steps (2-3 minutes) after each rinse. Subsequently, samples were treated with a hot (97°C) oxidizing 1% NaOH/ H_2O_2 solution (10 mL 0.1 *N* NaOH (analytical grade); 100 µL 30% H_2O_2 (suprapur)) for 10 minutes to remove organic matter. Every 2.5 minutes, the vials were rapped on the bench top to release any gaseous build-up. After 5 minutes, the samples were placed in an ultrasonic bath for a few seconds in order to maintain contact between reagent and sample. This treatment was repeated after refreshment of the oxidizing solution. Any remaining oxidizing solution was removed by three rinsing steps with distilled deionized water. After transferring the samples into clean vials, a weak acid leach with 250 µL 0.001 M HNO_3 (subboiled distilled) was applied with 30 seconds ultrasonic treatment and subsequent two rinses with distilled deionized water. After cleaning, the samples were dissolved in 0.075 M nitric acid (HNO_3) (subboiled distilled) and diluted with distilled deionized water up to 3 mL containing 10 ppm of yttrium as an internal standard.

Analyses were run on an ICP-OES (ISA Jobin Yvon, Spex Instruments S.A. GmbH) with polychromator applying yttrium as an internal standard. We selected element lines for analyses which were most intensive and undisturbed (Ca: 317.93 nm; Mg: 279.55 nm; Sr: 407.77 nm; Fe: 238.21 nm; Mn: 257.61 nm; and Y: 371.03 nm). Element detection was performed with photomultipliers, the high-tension of which was adapted to each element concentration range. The relative standard deviation is 0.45% for magnesium and 0.15% for calcium. The Mg/Ca reproducibility of replicate samples of *G. sacculifer* is good (r^2 = 0.8), giving a temperature error of $\pm$ 0.7°C. The analytical error in temperature is $\pm$ 0.12°C. Fe/Ca and Mn/Ca analyses indicated that contamination with clays or Mn-carbonates after the cleaning procedure was not an issue. The conversion of foraminiferal Mg/Ca-ratios into SST was carried out by applying the equation of Nürnberg et al. (2000) (SST = (Log(Mg/Ca)-Log 0.491)/0.033).

LA-ICP-MS

Laser Ablation Inductively Coupled Mass Spectrometry (LA-ICP-MS) (ICP-MS, Micromass Platform) was used to measure Mg, Sr and Ca chamber profiles of selected cleaned foraminiferal tests. Craters of 80 µm were ablated using an Excimer 193 nm deep ultra violet laser (Lambda Physik) with Geolas optics (Günther et al., 1997). Energy density at the sample surface was kept at 2 mJ/cm^2, shot repetition rate at 8 Hz. Laser ablation of calcite requires ablation at ultra violet wave lengths since higher wave lengths result in uncontrolled cleavage. The ablated material was transported by a continuous He flow and mixed with an Ar make up gas before injection into the Ar plasma of the quadropole ICP-MS instrument (Micromass Platform). A collision and reaction cell was used to give improved results by reducing spectral interferences on the minor isotopes of Ca (^{42}Ca, ^{43}Ca and ^{44}Ca). Interelemental fractionation was insignificant due to the relative low depth to width ratio

of the ablation craters produced. Calibration was performed against U.S. National Institute of Standards and Technology SRM 612 glass using the concentration data of Pearce et al. (1997), with Ca as an internal standard. Calcium carbonate is well suited for LA-ICP-MS because Ca can be used as an internal standard at 40 wt%. For quantifying Ca we used mass 44, monitoring masses 42 and 43 as an internal check. Using Ca as an internal standard allows direct comparison to trace metal to Ca ratios from traditional wet-chemical studies. Magnesium concentrations were calculated using masses 24 and 26. Although the accuracy for mass 24 is higher, both isotopes agree within a few percent. For strontium concentrations mass 88 was used. Analyses were performed at the Faculty of Earth Sciences, University of Utrecht, The Netherlands.

For the laser ablation measurements we selected cleaned *G. sacculifer* fragments from four different samples, two contaminated samples, i.e. with crystalline overgrowths (sample 14-5-115 and sample 14-5-125) and two uncontaminated samples, i.e. without crystalline overgrowths (sample 14-5-95 and sample 14-5-145) (Table 6.1). On each fragment multiple transects were ablated to certify that in-test heterogeneities were avoided and an average signal was produced. In total, 25 profiles were ablated, 11 through the uncontaminated samples, i.e. without crystalline overgrowths, and 14 through the contaminated samples, i.e. with crystalline overgrowths (Fig 6.6)

Carbonate mineralogy

Carbonate mineralogy was determined using a Philips PW1710 diffractometer (IFM-Geomar, Kiel) with a cobalt Kσ tube at 40 KV and 35 mA. The samples were scanned from 25°-40° at a scanning speed of 0.01 steps per second to cover the significant peaks of the various carbonate minerals. The percentage of aragonite and calcite, dolomite was not present in significant amounts, relative to total carbonate content was calculated from peak area ratios using in-house calibration curves. Peak areas were measured using the computer based integration program MacDiff (Petschick, 1999). The non-linear relationship between calcite and aragonite was calculated from ratios calibrated from standards measured on the diffractometer.

Calcareous nannofossil analysis

The relative abundance record of F. profunda was obtained by high-resolution scanning electron microscope (SEM) analysis of calcareous nannofossil assemblages (Crudeli et al., manuscript in preparation). Analyses were conducted at a magnification of 6000X using a CamScan 44-Serie-2-CS-44 SEM (University of Kiel). Methods on sample preparation were reported in Crudeli and Kinkel (2004). An amount of 0.1 g of dry sediment was diluted with carbonate-saturated tap water. The solution was then divided with a rotary splitter device. A final solution with 0.001 g of sediment was filtered with a low-pressure vacuum pump onto a polycarbonate-membrane filter (pore size, 0.40 μm; diameter, 50 mm). A segment of filter was then mounted on a scanning electron microscope (SEM) stub.

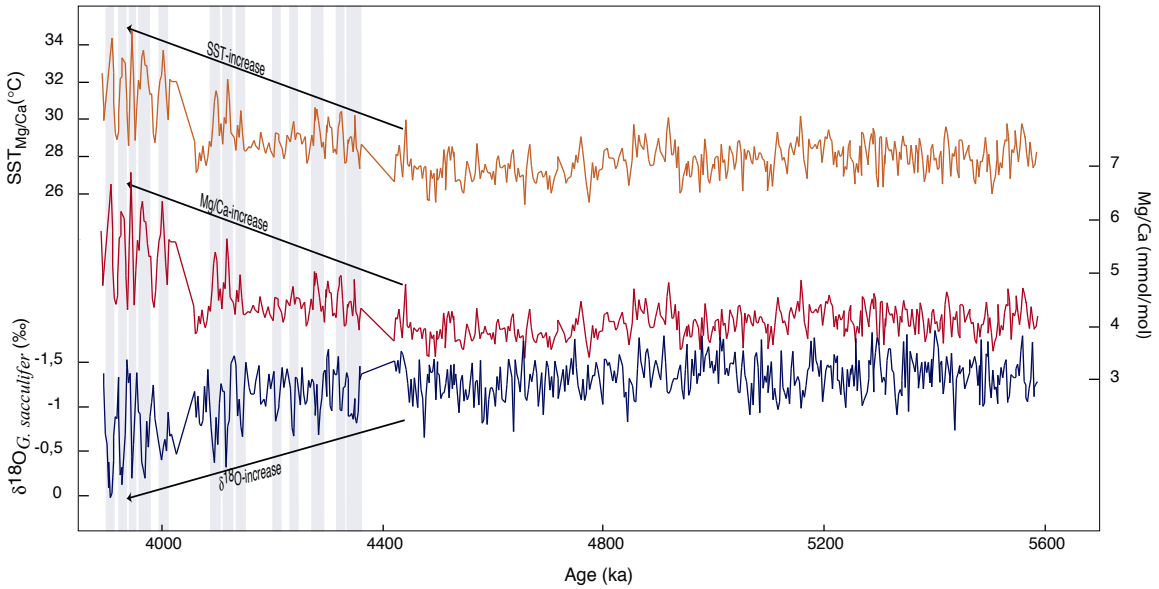

Figure 6.2 Results for Site 1000 for the time interval 5.6 Ma to 3.9 Ma. Arrows indicate trends associated with the restriction of upper ocean water masses between the Pacific and the Caribbean since 4.5 Ma. Mg/Ca-ratios are measured on tests of the planktonic foraminifer *G. sacculifer*. Mg/Ca-ratios are converted into SSTs using the formula of Nürnberg et al. (2000). $\delta^{18}O$ was measured on tests of the planktonic foraminifer *G. sacculifer* (Steph et al., submitted). Bars show the positive correlation between Mg/Ca and $\delta^{18}O$. Note that $\delta^{18}O$ is plotted reversely.

Results and discussion

The total range of Mg/Ca-ratios can be divided into two time intervals, before and after 4.5 Ma. Values before 4.5 Ma are relatively stable and range between 3.5 and 4.5 mmol/mol, translating into $SSTs_{Mg/Ca}$ between 26.5°C and 29°C. The range of Mg/Ca-ratios after 4.5 Ma increases to values between 4 and 7 mmol/mol, providing $SSTs_{Mg/Ca}$ between 28°C and 35°C (Fig 6.2).

The late Miocene to earliest Pliocene Mg/Ca record (5.6-5.0 Ma) implies a relatively uniform $SST_{Mg/Ca}$ pattern of 26.5-29°C (Fig 6.2). This time interval is characterized by a typical negative correlation between Mg/Ca and $\delta^{18}O$, e.g. high SSTs and low $\delta^{18}O$ values. Here, the $\delta^{18}O$ fluctuations, ranging between –1.05‰ and –1.7‰, are mainly related to changes in temperature, because the effects of ice volume and local salinity on the planktonic $\delta^{18}O$ signal are assumed to have remained small during the late Miocene/early Pliocene. Orbital-scale changes in global ice volume affected the late Miocene/early Pliocene $\delta^{18}O$ signal by less than 0.15‰ (Tiedemann et al., 1994). Large changes in salinity affecting planktonic $\delta^{18}O$ can be largely excluded for this time interval, as the free exchange between Pacific and Caribbean surface water masses prohibited the establishment of salinity gradients (Haug et al., 2001). Hence, we translated the late Miocene/early Pliocene $\delta^{18}O$ amplitude fluctuations of ~0.65 ‰ directly into temperature, providing isotopic SST changes of ~2°C. Such amplitude corresponds to those calculated from the Mg/Ca signal.

The time interval from 5.0-4.5 Ma (Fig 6.2) is characterized by both positive and negative correlations between $SST_{Mg/Ca}$ and $\delta^{18}O$. A positive correlation between $\delta^{18}O$ and Mg/Ca, e.g. high $SSTs_{Mg/Ca}$ are paralleled by high $\delta^{18}O$ values, was not reported before and we interpret such a scenario in the way that $\delta^{18}O$ is no longer solely reflecting changes in temperature, but is becoming dominated by salinity. Since a synchronous increase in SST and SSS influences the $\delta^{18}O$ signal in opposite directions, the effect of temperature on $\delta^{18}O$ appears to be fully compensated and even overprinted by the strong SSS signal. The onset of the positive correlation between $SST_{Mg/Ca}$ and $\delta^{18}O$ suggests that the shoaling of the Isthmus of Panama started to affect the continuous

throughflow of low salinity waters from the Pacific into the Caribbean, leading to increased influence of higher saline Atlantic/Caribbean waters.

After the critical threshold at ~4.5 Ma, when the salinity contrast between Pacific and Caribbean became established (Haug et al., 2001) and salinity gradients between the southern and central Caribbean increased (Steph et al., submitted), we observe a nearly perfect positive correlation in the paired Mg/Ca and $\delta^{18}O$ records of *G. sacculifer* (r = 0.71) (Fig 6.2). Maximum $SSTs_{Mg/Ca}$ and maximum SSSs are occurring at the same time. Starting at 4.5 Ma, the $SSTs_{Mg/Ca}$ imply a warming of ~4°C until 3.9 Ma, an increase in $SST_{Mg/Ca}$ amplitudes up to 5°C, and $SST_{Mg/Ca}$ maxima of up to 35°C (Fig 6.2).

The extreme $SST_{Mg/Ca}$ maxima of up to 35°C and amplitudes of up to 5°C appear to be very unlikely for the early Pliocene. Firstly, modern SSTs at ~30-50 m water depth, the assumed habitat depth of *G. sacculifer* (Fairbanks et al., 1982), do not exceed 30-31°C in open ocean conditions (Levitus and Boyer, 1994), and it is unreasonable to expect significantly higher SSTs during the early Pliocene. Secondly, this time interval is known to represent a globally warm and stable climate of unipolar glaciation with a pole-equator temperature gradient, which was smaller than today. Hence, amplitudes in $SST_{Mg/Ca}$ as large as 5°C appear to be rather unlikely. Recently, Molnar and Cane (2002) suggested permanent El Niño-like conditions throughout the early Pliocene. In addition, studies in the high-latitudinal Atlantic indicated that SSTs might have been warmer by up to 8°C than today, while the tropical SSTs remained the same or were, due to increased heat transport to higher latitudes, even slightly cooler than today (Cronin et al., 1993; Crowley, 1996; Dowsett et al., 1996; Billups et al., 1998; Groeneveld et al., submitted).

How do we explain the extremely high $SSTs_{Mg/Ca,}$ the large $SST_{Mg/Ca}$ amplitude variations and the positive correlation to $\delta^{18}O$ during the time interval 4.5-3.9 Ma? Factors potentially affecting the Mg/Ca-signal will be discussed below.

Impact of Pliocene salinity changes on foraminiferal Mg/Ca and $\delta^{18}O$

Both the positive relationship between the Mg/Ca and $\delta^{18}O_{G.\ sacculifer}$ records (Fig 6.2), and the suggested increase in Caribbean SSS after 4.5 Ma (Haug et al., 2001; Steph et al., submitted) basically suggest that the planktonic $\delta^{18}O$ record is dominated by variations in SSS. In a first approach we simply assumed that the $\delta^{18}O$ fluctuations of up to 1.3‰ for the time interval 4.5-3.9 Ma (Fig 6.2), only reflect salinity variations, on the order of three salinity units, when applying Broeckers (1989) rule of thumb; 1‰ $\delta^{18}O$ = 2 salinity units (Fig 6.3b). By doing so, possible temperature and ice effects on $\delta^{18}O_{G.\ sacculifer}$ are ignored. On average, the corresponding SSS record would thus imply an increase of 1.5 salinity units in the Caribbean since 4.5 Ma. Subsequently, we corrected the Mg/Ca record for the effect of these potential salinity changes. Cultivating experiments with *G. sacculifer* revealed a positive relationship between foraminiferal Mg/Ca and salinity (Nürnberg et al., 1996) ($Mg/Ca = 0.248*10^{(0.031*Sal)}$, $R^2 = 0.994$), suggesting a 7% to 10% increase in Mg/Ca per salinity unit. Similar results were found by Lea et al. (1999), who concluded from cultivating experiments with *Globigerina bulloides* that a salinity change of 1 salinity unit results in a 4 $\pm$ 3% increase in Mg/Ca. Salinity variations of ~3 salinity units deduced from the planktonic $\delta^{18}O$ record would therefore result in a $SST_{Mg/Ca}$ overestimation of 3.0-3.6°C (7% increase in Mg/Ca per one unit salinity increase). After correcting the Mg/Ca record for changes in salinity $SST_{Mg/Ca}$ shows maximum amplitudes of ~4.5°C, and maximum $SST_{Mg/Ca}$ estimates up to 32°C. The average $SST_{Mg/Ca}$ increase from 4.5-3.9 Ma is ~3°C (Fig 6.3c).

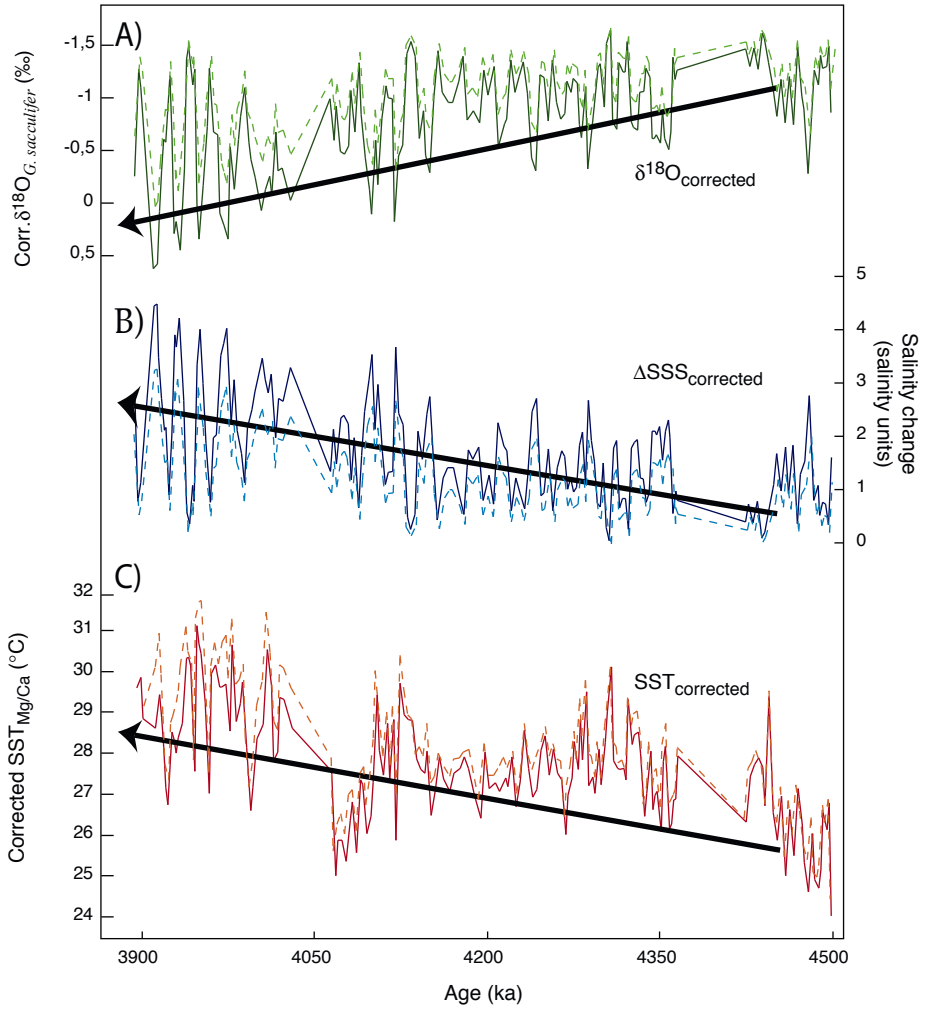

Figure 6.3 Correction of the $SST_{Mg/Ca}$ record for the influence of salinity. Arrows indicate trends associated with the restriction of upper ocean water masses between the Pacific and the Caribbean since 4.5 Ma. **A** $\delta^{18}O$ of *G. sacculifer*, corrected for a temperature cyclicity of 2.5°C. Dotted line shows the original $\delta^{18}O$ record. **B** Change in salinity, calculated using the basic rule that $\Delta 1‰$ $\delta^{18}O = \Delta 2$ salinity units salinity (Broecker, 1989). Dotted line shows the result from the first approach. **C** Corrected $SST_{Mg/Ca}$ record. Mg/Ca-ratios were corrected by using a 7% increase in Mg/Ca per 1 unit increase in salinity. Dotted line shows the result from the first approach.

In a second approach, we additionally consider potential temperature and ice effects on the $\delta^{18}O_{G.\ sacculifer}$ signal. Furtermore we assume $SST_{Mg/Ca}$ fluctuations of ~2.5°C during the earlier part of the record (5.6-5.0 Ma) persisting to 3.9 Ma. Such an assumption is reasonable because large glacial-interglacial temperature amplitudes did not occur before the intensification of the Northern Hemisphere Glaciation. To subtract the 2.5°C temperature cyclicity from the $\delta^{18}O_{G.\ sacculifer}$ record, we interprete the positive correlation between the two proxies (4.5-3.9 Ma) in such a way that the highest $\delta^{18}O$ values represent both highest salinity and highest temperatures. The temperature effect on $\delta^{18}O$ can then be assessed for each data point, using the value in individual data points relative to the maximum value and using the (fundamental) relationship that a shift of 1‰ $\delta^{18}O$ represents 4∝C. This value is subsequently subtracted from the $\delta^{18}O_{G.\ sacculifer}$ record, resulting in larger $\delta^{18}O$ amplitudes.

As a next step, we correcte the $\delta^{18}O_{G.\ sacculifer}$ record for the global ice volume effect. From terrestrial settings it is known that an ice cap of limited extend existed on Antarctica during the early Pliocene (Webb and Harwood, 1991), and minor ice sheets existed on Greenland (Jansen et al., 1990). Glacial to interglacial variations in global

ice volume during the Pliocene, nevertheless, were only on the order of 0.15-0.25‰ (Hodell and Warnke, 1991; Kennett and Hodell, 1993; Shackleton et al., 1995; Mix et al., 1995; Tiedemann et al., submitted) with average values of about 0.6-0.7‰ lower than present day values (Shackleton et al., 1995). Such a shift in isotopic values was explained by a deep water warming of ~1°C and a global ice volume effect equivalent to 20-25 m sea level change (Kennett and Hodell, 1993; Shackleton et al., 1995). We use the benthic $\delta^{18}O$ record of ODP Site 1241 from the east Pacific to estimate early Pliocene changes in global ice volume, thereby assuming that Marine Isotope Stage (MIS) 100 represents two-third of the change in global ice volume between the Last Glacial Maximum and the Holocene (Raymo et al., 1989; Tiedemann et al., submitted; Groeneveld et al., submitted). The resulting sea level record is then normalized and subtracted from the $\delta^{18}O_{G.\ sacculifer}$ record of Site 1000 (Groeneveld et al., submitted). However, precession dominated periodicities in planktonic Mg/Ca and $\delta^{18}O$ are not significantly influenced by the obliquity dominated Pliocene glacial to interglacial sea level changes. Sea level changes can, therefore, be ignored in our further calculations.

The resulting temperature corrected $\delta^{18}O_{G.\ sacculifer}$ record for the time interval 4.5-3.9 Ma the amplitude in $\delta^{18}O_{G.\ sacculifer}$ now is ~2‰, equivalent to 4 salinity units (Fig 6.3a, b). As a final step, we correct the $SST_{Mg/Ca}$ record for these salinity effects, similar as in the first approach. The maximum Mg/Ca-ratios were corrected by as much as 20-30%, which corresponds to temperature corrections of 3-4°C. The corrected $SST_{Mg/Ca}$ record now shows reduced amplitude fluctuations of ~3°C, absolute values ranging from 25-31°C, and a general warming trend of ~2°C since 4.5 Ma (Fig 6.3c). These results provide the first evidence that the restricted exchange of surface water between the east Pacific and the Caribbean due to the progressive shoaling of the Isthmus of Panama led to a considerable warming of Caribbean surface waters, and hence to the initiation of the Western Atlantic Warm Pool. Because the Caribbean is the source region of the Gulf Stream, the resulting northward transport of warmer and saltier water masses increased, which might have contributed to an intensified formation of North Atlantic Deep Water.

Diagenetic alteration of the foraminiferal tests

Sediments with high calcium carbonate contents are prone to diagenetic overprinting, dissolution and reprecipitation, especially when the carbonate is present as metastable aragonite or high-Mg calcite (Swart and Guzikowski, 1988; Malone et al., 1990; Munnecke et al., 1997; Melim et al., 2002). Site 1000 is surrounded by carbonate platforms, which supply high amounts of aragonite to the core location (Sigurdsson et al., 1997). Aragonite in sediments is susceptible to dissolution, which subsequently can result in reprecipitation as inorganic calcite. Aragonite is not present in the studied samples before 4.5 Ma, i.e. the interval with normal Mg/Ca-ratios (Fig 6.4). However, after 4.5 Ma alternations between aragonite-rich (up to 60%) and cemented aragonite-poor layers (<30%) occur, showing precessional cyclicity (Fig 6.4). This precessional variation in aragonite negatively correlated with the foraminiferal Mg/Ca record ($r = -0.80$, <4.05 Ma), which points into the direction of a diagenetic imprint, related to carbonate chemistry. Periods of aragonite dissolution, reprecipitation of inorganic calcite could have resulted in diagenetic Mg-rich overgrowth on the foraminiferal tests, resulting in abnormally high foraminiferal Mg/Ca-ratios (up to ~7 mmol/mol) (Fig 6.2).

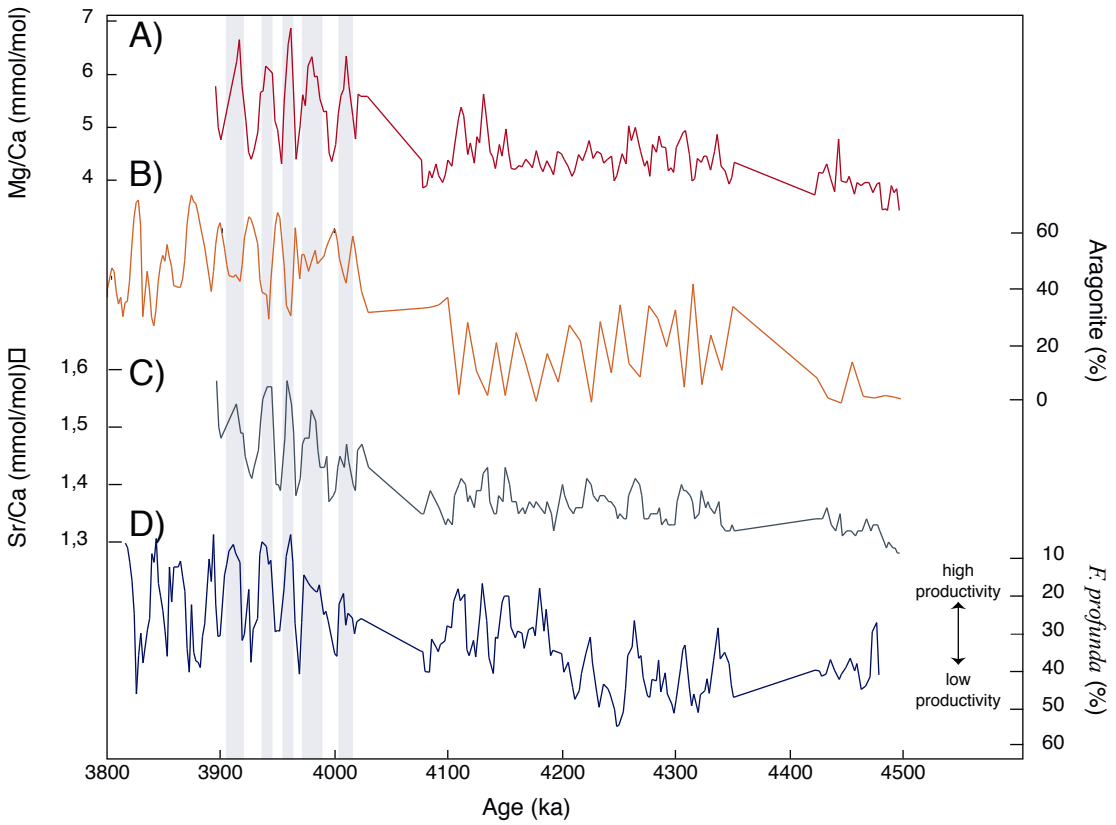

Figure 6.4 Mg/Ca results in comparison with $Sr/Ca_{G.\ sacculifer}$, aragonite content, and relative abundance of *F. profunda* for the time interval from 4.5 Ma to 3.9 Ma. Bars show the correlation between the individual records. **A** Mg/Ca-ratios, measured on tests of the planktonic foraminifer *G. sacculifer.* **B** Aragonite content, measured on bulk sediment by XRD analysis. **C** Sr/Ca-ratios, measured on tests of the planktonic foraminifer *G. sacculifer,* indicative of diagenetic alteration. **D** Relative abundance (plotted reversely) of *F. profunda*, indicative of variation in primary productivity.

SEM studies indeed show that crystalline overgrowths are present on the inner surfaces of foraminiferal tests after 4.5 Ma (Fig 6.5), corresponding to the high Mg/Ca-ratios (Fig 6.2). These crystals resilient to the cleaning procedures normally applied before Mg/Ca analyses. Foraminiferal tests with low Mg/Ca-ratios after 4.5 Ma, as well as tests from the older part of the core (>4.5 Ma), do not show these crystalline overgrowths (Fig 6.5). Together this strongly suggests that diagenetic overgrowth, originating from partial dissolution of aragonite which contributed to the unusually elevated foraminiferal Mg/Ca-ratios.

Previously, Sr/Ca of bulk sediment has been used as an indicator of sediment diagenesis (Baker et al., 1982; Swart and Guzikowski, 1988; Hampt and Delaney, 1997). Since in the record of Site 1000 foraminiferal Sr/Ca and Mg/Ca-ratios are positively correlated after 4.5 Ma (r = 0.76, <4.05 Ma), we exploited the possibility to use foraminiferal Sr/Ca as an indication for diagenetic overprinting via aragonite dissolution. Maximum values of foraminiferal Mg/Ca and lower sedimentary aragonite correspond to foraminiferal Sr/Ca increasing to values between 1.35-1.58 mmol/mol. Typical Sr/Ca ratios for foraminiferal tests are generally lower, ranging from 1.25-1.40 mmol/mol, similar to the older part of the record. This suggests dissolution of Sr-rich aragonite and subsequent carbonate reprecipitation from pore waters with elevated Sr/Ca ratios.

Temporal variations in aragonite diagenesis are closely related to changes in marine productivity, which are reflected in the relative abundance of the coccolithophorid *Florisphaera profunda*, which lives at the bottom of the photic zone (Molfino and McIntyre, 1990; Beaufort et al., 1997; de Garidel-Thoron et al., 2001) (Fig 6.4). Variations in the coccolithophorid *F. profunda* at Site 1000 are positively correlated with the aragonite record (r = 0.71), showing that at times of enhanced aragonite dissolution reflected by high Sr/Ca ratios, relative abundances of *F. profunda* are low (Fig 6.4). These low relative abundances reflect high marine productivity at

the surface of the mixed layer, which enhances nutrient utilization and relatively reduces nutrient flux to the bottom of the photic zone, hence, resulting in decreased relative abundances of *F. profunda* (Crudeli et al., manuscript in preparation).

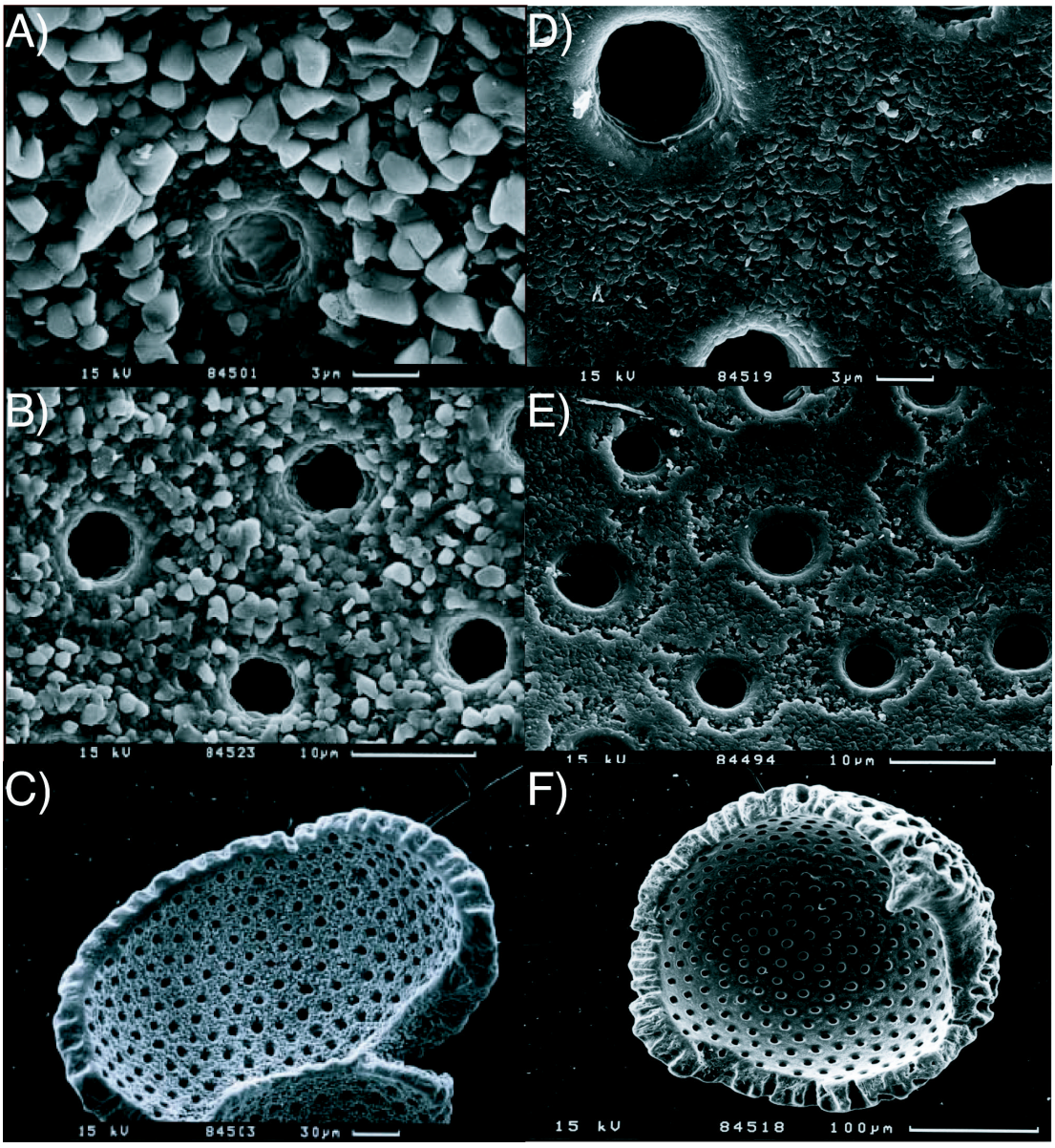

Figure 6.5 Scanning electron microscope images (CAMSCAN-Serie-2-CS-44, Univ. of Kiel, Germany) of cleaned tests of the planktonic foraminifer *G. sacculifer*. Bars indicate the scale of the images. For comparison, couples of two photos of about the same size scale are plotted together, one from a contaminated test and one from an uncontaminated test. **A-C** Foraminiferal tests containing an overgrowth of diagenetic crystals. **D-F** Cleaned foraminiferal tests without the presence of diagenetic crystals. Slight indications of dissolution are visible, most likely caused by the intense cleaning procedure.

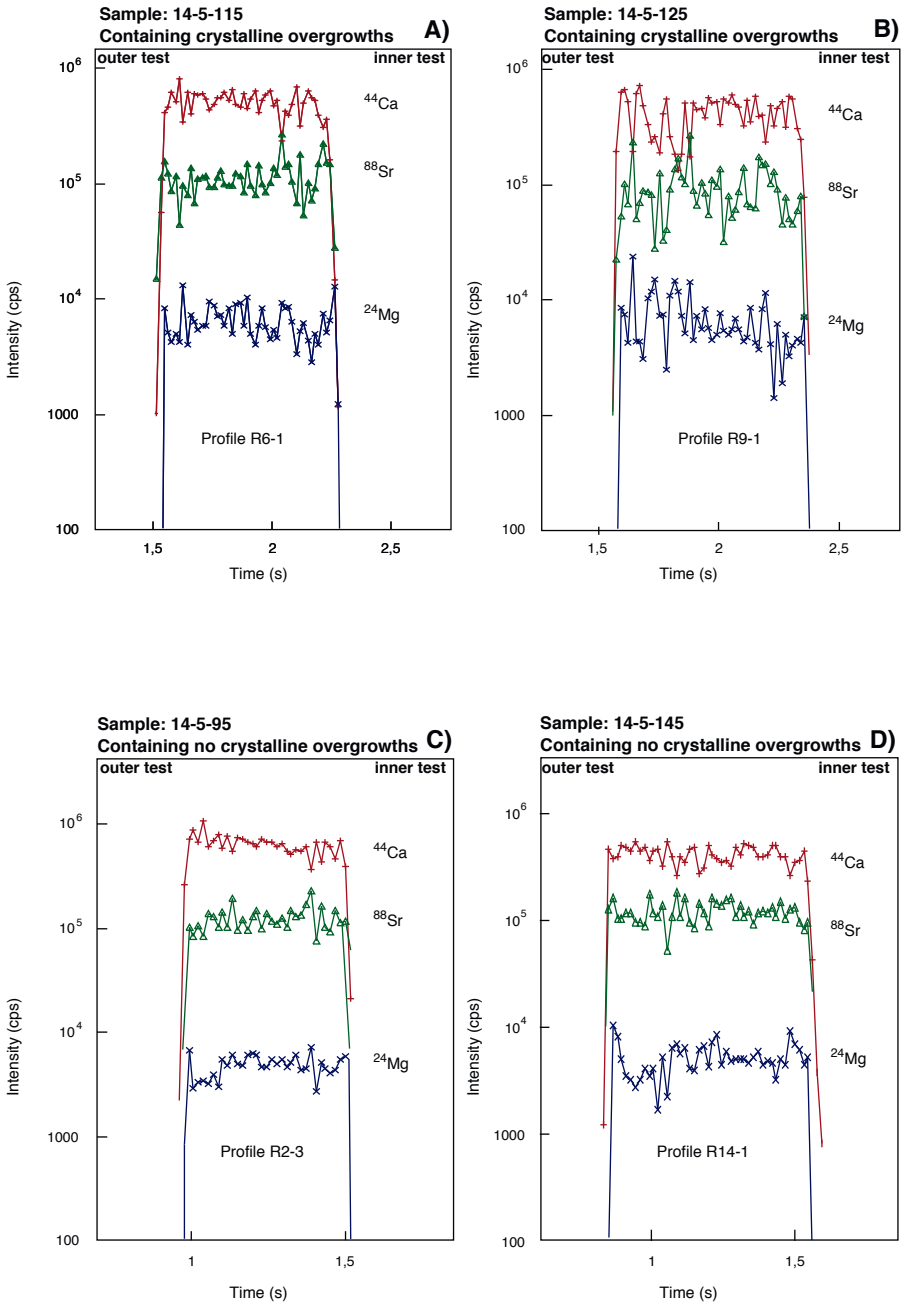

Figure 6.6 Results from LA-ICP-MS for selected contaminated, i.e. with crystalline overgrowths, and uncontaminated, i.e. without crystalline overgrowths, samples. Measurements performed on tests of the planktonic foraminifer *G. sacculifer*. All profiles are ablated from the outer side of the test toward the inner site. **A-B** Typical ablation profiles for Mg and Sr through the contaminated, i.e. with crystalline overgrowths, samples 14-5-115 and 14-5-125. All intensities are normalized to ^{44}Ca. Time (s) represents the duration of the measurement. **C-D** Typical ablation profiles for Mg and Sr through the uncontaminated, i.e. without crystalline overgrowths, samples 14-5-95 and 14-5-145. All intensities are normalized to ^{44}Ca. Time (s) represents the duration of the measurement.

How is marine productivity affecting aragonite dissolution? During microbial sulphate reduction reactive organic material becomes oxidized, reducing interstitial sulphate concentration and releasing CO_2 and H_2S to the pore water. The concomitant pH lowering leads to the undersaturation of the pore water with respect to metastable carbonate phases and hence, to carbonate dissolution, which increases alkalinity. Continuing sulphate reduction eventually causes an increase in the ion activity product of $CaCO_3$ (Ben-Yaakov, 1973) and subsequently leads to the precipitation of inorganic calcite. This inorganic calcite primarily reflects porewater chemistry and can, therefore, deviate considerably from the biogenic calcite. Alkalinity increases during the initial stage of sulphate

reduction due to the dissolution of carbonate, whereas in a later phase further alkalinity increase is reduced by the precipitation of inorganic calcite (Morse and Mackenzie, 1990) (Fig 6.7). This means that during periods with relatively high productivity, more organic matter is decomposed, thereby lowering the pH of the pore water, favoring aragonite dissolution, and subsequently reprecipitation as inorganic calcite (Reuning et al., submitted).

Whether such diagenetic processes affect the $\delta^{18}O$ composition of foraminiferal tests needs to be considered (Killingley, 1983; Schrag et al., 1995). In fact, the positive correlation between Mg/Ca and $\delta^{18}O$ after 4.5 Ma (see chapter 3.2), and the fact that $\delta^{18}O$ exhibits the same precessional variations as the diagenetically induced oscillations in aragonite and Sr/Ca, might imply that $\delta^{18}O$ is potentially also affected by carbonate diagenesis. However, as the benthic $\delta^{18}O$ record of Site 1000 closely matches those of ODP Site 925 (Ceara Rise) and 999 (Caribbean) (Steph et al., submitted), we suspect that the primary signal of the planktonic $\delta^{18}O$ record is preserved. If the $\delta^{18}O$ record would contain a diagenetic component, such an effect would increase the $\delta^{18}O$ signal of the diagenetically affected samples, resulting in increased $\delta^{18}O$ amplitudes (Killingley, 1983; Schrag et al., 1995). Further work needs to be done to decipher the diagenetic effect on $\delta^{18}O$.

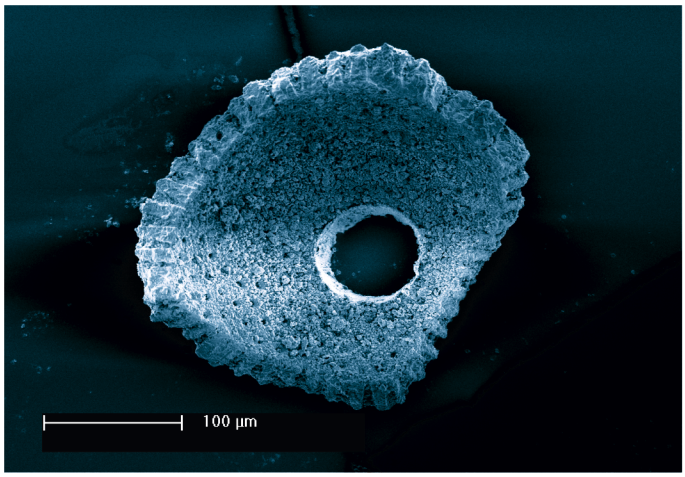

Figure 6.7E *G. sacculifer* test, showing an ablation crater formed by LA-ICP-MS analysis (Photo taken at Utrecht Univ., The Netherlands).

Quantifying the effect of carbonate diagenesis by LA-ICP-MS

To quantify the Mg content of these diagenetic crystalline overgrowths, Laser Ablation Inductively Coupled Plasma Mass Spectrometry (LA-ICP-MS) (Eggins et al., 2003; Reichart et al., 2003; Hathorne et al., 2003) was applied. A laser ablation profile through a foraminiferal chamber wall allows the investigation of both internal heterogeneities of element-incorporation and concentration anomalies related to possible crystalline overgrowths. Since SEM showed the size of the single crystals to be 2-3 µm (Fig 6.5), they are within the spatial depth resolution of LA-ICP-MS, in view of the laser pulse rate (6 pulses per second) and the ICP-MS quadropole mass scanning rate. Energy density at the sediment surface was set at 2 J/cm^2, resulting in less than 200 nm of material in depth removed per pulse.

Laser ablation measurements of profiles across the foraminiferal tests with/without crystalline overgrowths show relatively similar Ca-normalized Mg distribution patterns (Fig 6.6). It is important to note that the calculated Mg/Ca-ratios derived from the LA-ICP-MS measurements agree, within the method standard deviation of 5-10%, to the traditional whole test ICP-OES measurements performed on the same samples (Table 6.1). There is no significant change in the LA-ICP-MS Mg signal of the chamber walls with depth, although these profiles

include measurements directly performed within the crystalline overgrowths. In view of the ablation rate and the ICP-MS mass scanning it is reasonable to assume that the innermost 2 to 3 datapoints represent the crystalline overgrowths. When average test Mg concentrations are calculated excluding these data points no significant different values are obtained for Mg/Ca-ratios. Evidently, the crystalline overgrowths do not contribute significantly to the high Mg/Ca-ratios. Still, foraminiferal tests after 4.5 Ma and most prominent after 4.05 Ma, for samples with the maxima in $\delta^{18}O$, are enriched in Mg. These Mg/Ca-ratios, remaining high throughout the entire test, cannot be explained by partial (or total) recrystallization of the foraminiferal tests, as diagenetic overgrowths at the test surfaces and slight dissolution signs (Fig 6.5), most likely caused by the rigorous cleaning procedure, were the only visible disturbances.

Similar to the laser ablation Mg-profiles, Sr is not showing any significant concentration changes within the chamber walls, although one would expect higher Sr/Ca levels in the inorganic crystalline overgrowths (see Chapter 3.3) (Fig 6.6). However, the relatively high standard deviation of the laser ablation Sr measurements (5-10%) is of the same order as the absolute increase in foraminiferal Sr/Ca (~8%) after 4.05 Ma in comparison with the older samples.

Table 6.1 Comparison between bulk ICP-OES measurements and LA-ICP-MS analyses for Mg/Ca and Sr/Ca. Shown are average results from multiple ablation profiles through cleaned *G. sacculifer* tests from two contaminated, i.e. with crystalline overgrowths, samples (14-5-115 and 14-5-125) and two uncontaminated, i.e. without crystalline overgrowths, samples (14-5-95 and 14-5-145).

Sample	Age (ka)	State	Number of profiles (analyses/profile)	Mg/Ca (mmol/mol) ICP-OES	Mg/Ca-uncont.interval (mmol/mol) LA-ICP-MS*
1000,14-5-95	3952	no crystalline overgrowth	4 (37)	4.30	3.84
1000,14-5-145	3965	no crystalline overgrowth	4 (38)	4.39	4.29
1000,14-5-115	3958	crystalline overgrowth	5 (45)	6.57	6.89
1000,14-5-125	3960	crystalline overgrowth	4 (47)	6.87	6.23

* relative standard deviation is 5-10%

Sample	Age (ka)	State	Number of profiles (analyses/profile)	Sr/Ca (mmol/mol) ICP-OES	Sr/Ca-uncont.interval (mmol/mol) LA-ICP-MS*
1000,14-5-95	3952	no crystalline overgrowth	4 (37)	1.39	1.45
1000,14-5-145	3965	no crystalline overgrowth	4 (38)	1.38	1.44
1000,14-5-115	3958	crystalline overgrowth	5 (45)	1.58	1.66
1000,14-5-125	3960	crystalline overgrowth	4 (47)	1.54	1.55

* relative standard deviation is 5-10%

Quantifying the impact of pore water chemistry on foraminiferal Mg/Ca and Sr/Ca

We used pore water data of Site 1000 (Fig 6.7, (Lyons et al., 2000)) to calculate the potential Mg/Ca and Sr/Ca ratios of precipitated inorganic calcite. The elemental composition of a diagenetic phase precipitating from pore water is dependent on the pore water element composition and the inorganic distribution coefficient. In fact, the calculation of the Mg/Ca ratio in the inorganically precipitated crystalline overgrowths is dependant on the distribution coefficient used for Mg (Tripati et al., 2003; Reuning et al., in press; Table 6.2b). There is a large variety of Mg distribution coefficients either assessed from sediments or experimentally derived ranging between

Table 6.2 Measured properties of Site 1000, possible distribution coefficients for Mg and Sr and calculated compositions of the inorganic calcite. **A** Pore water data (Sample 15-3-145, 4.202 Ma) are from Lyons et al. (2000) and are used to calculate the composition of the inorganic calcite. ‚Average maximum of the contaminated Sr/Ca_{foram}' refers to the average Sr/Ca ratio of those samples which show the diagenetic overprint. ‚Average maximum of the uncontaminated Sr/Ca_{foram}' refers to the average Sr/Ca ratio of the samples from the older, uncontaminated part of the record, but only those from the maximum values. ‚Average maximum of the contaminated Mg/Ca_{foram}' refers to the average Mg/Ca ratio of those samples which show the diagenetic overprint. **B** By using different distribution coefficients for Mg and the pore water composition, the possible Mg/Ca-ratios of the inorganic calcite are calculated. **C** By using different distribution coefficients for Sr and the pore water composition, the possible Sr/Ca ratios of the inorganic calcite are calculated. Using these compositions in combination with the measured Sr/Ca_{foram}, the mass percentage of the diagenetic overprint of the bulk analysed foraminifer is calculated (Mc = ((Cb* Mb) - (Mp* Cp))/ Cc, see text for explanation; Lohmann, 1995). **D** Original Mg/Ca-ratios of the contaminated foraminiferal tests. Combining the mass percentage of the diagenetic overprint with the calculated Mg/Ca-ratios of the overgrowth, the Mg/Ca-ratios of the original contaminated foraminiferal tests are calculated (Cp = ((Cb*Mb)-(Cc*Mc))/Mp, see text for explanation, Lohmann, 1995). Shaded area shows the range of values which are considered to be realistic estimates. These values result in SSTs between 32.4°C and 33.9°C, indicating that the carbonate diagenesis is not able to explain the extreme measured Mg/Ca-ratios.

a)

Specifications Site 1000:	**Value**	**Reference**
Sr pore water	1771 µM	Lyons et al. 2000
Ca pore water	10.5 mM	Lyons et al. 2000
Mg pore water	33.9 mM	Lyons et al. 2000
Sr/Ca pore water	168.7 mmol/mol	Lyons et al. 2000
Mg/Ca pore water	3230 mmol/mol	Lyons et al. 2000
averaged maximum Sr/Ca_{foram} <4.05 Ma	1.55 mmol/mol	this study
averaged maximum Sr/Ca_{foram} >4.5 Ma	1.36 mmol/mol	this study
averaged maximum Mg/Ca_{foram} <4.05 Ma	6.33 mmol/mol	this study

b)

Distribution coefficient Mg (1) (inorganic calcite)	**Reference**	**$Mg/Ca_{crystal}$ mmol/mol**
0.0008	Baker et al., 1982	2.58
0.004	Delaney, 1989	12.92
0.012	Mucci and Morse, 1983	38.76

(1) $D = Mg/Ca_{mineral} / Mg/Ca_{solution}$

c)

Distribution coefficient Sr (2) (inorganic calcite)	**Reference**	**$Sr/Ca_{crystal}$ mmol/mol**	**Mass percentage crystal (%)**
0.015	Delaney, 1989	2.53	16.1
0.040	Baker et al., 1982	6.75	3.4
0.050	Delaney, 1989	8.43	2.7
0.060	Katz et al., 1972	10.12	2.1

(2) $D = Sr/Ca_{mineral} / Sr/Ca_{solution}$

d)

	Mass percentage of the crystals (%)				
		16.1	**3.4**	**2.7**	**2.1**
Mg/Ca of the	**2.58**	7.05	6.46	6.43	6.41
crystals (mmol/mol)	**12.92**	5.06	6.10	6.15	6.19
	38.76	0.11	5.18	5.43	5.63

$0.8 * 10^{-3}$ and $12.3 * 10^{-3}$ (Baker et al., 1982; Mucci and Morse, 1983; Delaney, 1989; Morse and Bender, 1990; Andreasen and Delaney, 2000) (Table 6.2b). Morse and Bender (1990) and Delaney (1989) demonstrated that such variability can be explained by changing element concentrations in pore water during the recrystallization process.

There are several arguments for using Sr/Ca for our calculations instead of Mg/Ca. Firstly, the pore water composition for the studied interval of Site 1000 is mainly determined by selective dissolution of aragonite, which is relatively enriched in Sr (1000-10,000 ppm) (Fig 6.7). Secondly, the distribution coefficient of Sr is much better constrained (0.015-0.06) than the distribution coefficient of Mg (Baker et al., 1982; Delaney, 1989; Morse and Bender, 1990; Table 6.2c). Thirdly, the range of Sr/Ca ratios in modern planktonic foraminifers is moderate (1.25-1.40 mmol/mol). Such a range in Sr/Ca is typically found in samples >4.5 Ma having no

crystalline overgrowths. We therefore assume that excess Sr in the samples <4.05 Ma showing crystalline overgrowths (~1.55 mmol/mol) is due to aragonite dissolution and subsequent reprecipitation. In this way the significant increase in foraminiferal Sr/Ca ratios is considered to indicate diagenetic overprinting. The averaged maximum Sr/Ca ratio in the aragonite-free interval >4.5 Ma is 1.36 mmol/mol. The interval <4.05 Ma, instead, shows an increase in Sr/Ca of 12% to an averaged maximum of 1.55 mmol/mol. The assumption that this increase is solely due to diagenesis allows us to estimate the portion of diagenetic calcite with respect to the initial foraminiferal calcite (Reuning et al., in press).

First, we calculated the potential Sr/Ca ratio of the diagenetically precipitated inorganic calcite by using the pore water Sr- and Ca-concentrations (Fig 6.7; Table 6.2; Lyons et al. (2000)). Depending on the existing Sr-distribution coefficients, the expected Sr/Ca ratios of the inorganically precipitated overgrowths vary between 2.5-10.1 mmol/mol (Table 6.2). Subsequently, we used the Lohmann (1995) equation to calculate the mass percentage of the inorganic diagenetic calcite:

$$Mc = ((Cb * Mb) - (Mp * Cp))/ Cc \qquad (1)$$

with Cp = averaged maximum Sr/Ca_{foram} >4.5 Ma (1.36 mmol/mol), Cb = averaged maximum Sr/Ca_{foram} <4.05 Ma (1.55 mmol/mol), Cc = the calculated $Sr/Ca_{crystal}$ (2.5-10.1 mmol/mol), Mb = the mass percentage of the analysed foraminifer (1), Mp = the mass percentage of the original foraminiferal test (Mb-Mc), and Mc = the mass percentage of the inorganic, diagenetic calcite. Accordingly, the amount of diagenetically precipitated calcite is 2.1-3.4% of the entire foraminiferal sample, with a maximum value of >16% when applying the lowest Sr-distribution coefficient (Table 6.2c). This extreme value clearly does not correspond to the distribution pattern of the diagenetic overgrowths, consisting of small crystals (~2-3 µm) mainly attached to the inner test surfaces (Fig 6.5).

Knowing both the amount of diagenetically precipitated calcite and the expected Mg/Ca-ratios of these overgrowths (Table 6.2b), we are able to correct the measured Mg/Ca-ratios for the diagenetic effect. Table 6.2d combines the different assumptions on the portion (2.1-16.1%) and on the Mg/Ca-ratios of the diagenetic overgrowths (2.58-38.76 mmol/mol) in dependance of the different distribution coefficients, and provides Mg/Ca-ratios of the diagenetically unaffected foraminiferal tests. These Mg/Ca-ratios range from unrealistically low 0.11 mmol/mol (16.1% diagenetic overprint with Mg/Ca = 38.76 mmol/mol) to maximum 7.05 mmol/mol (16.1% diagenetic overprint with Mg/Ca = 2.58 mmol/mol) (Table 6.2d).

As the distribution coefficients for naturally precipitated inorganic calcite tend to be lower than those for experimentally precipitated calcite (Baker et al., 1982; Delaney, 1989), we conclude that the Mg/Ca-ratios for the unaffected foraminiferal calcite most likely range between 6.10 and 6.46 mmol/mol. These calculated Mg/Ca-ratios, corrected for the diagenetic imprint, are similar to the measured averaged maximum value of 6.33 mmol/mol after 4.05 Ma, and convert into $SSTs_{Mg/Ca}$ of 33.2-33.9°C still being unrealistically high. We conclude that the observed crystalline overgrowths do not provide enough Mg to shift the foraminiferal Mg/Ca-ratios to high values.

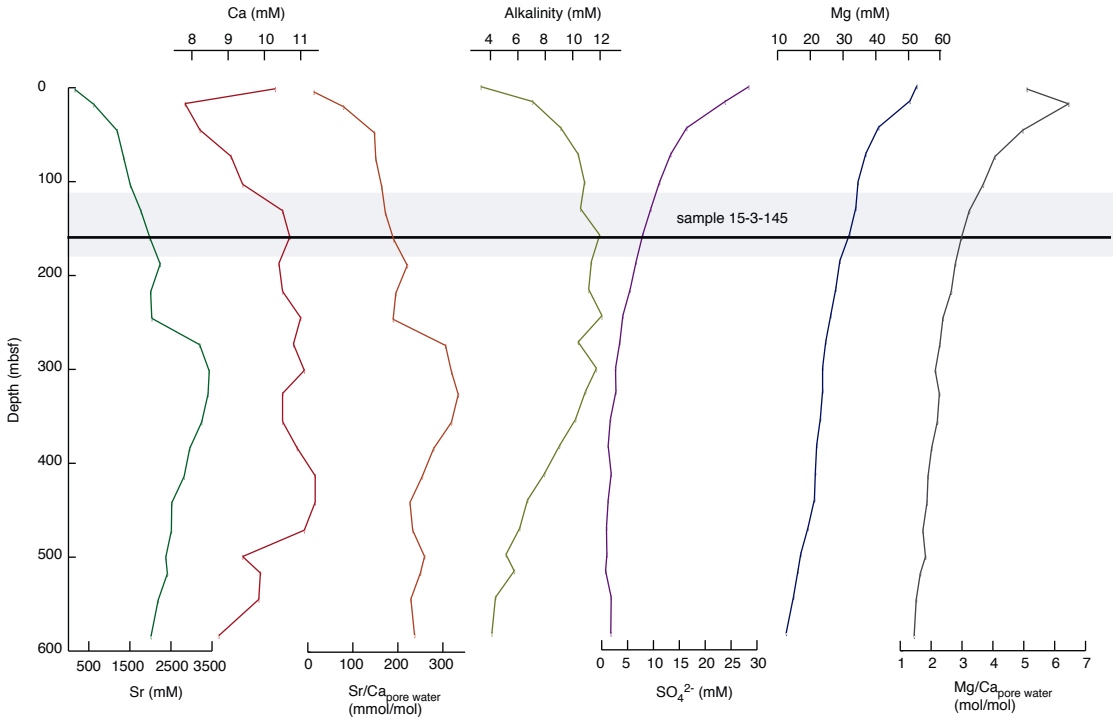

Figure 6.7 Pore water profiles of Site 1000 for magnesium (Mg), strontium (Sr), calcium (Ca), sulfate (SO_4^{2-}), alkalinity, and Mg/Ca and Sr/Ca of the pore water, reflecting shallow burial diagenetic reactions. Data are from Lyons et al. (2000). Shaded interval indicates the interval which provided samples for this study. Solid black line shows the position of the pore water sample (15-3-145) which was used for the calculation of the inorganic calcite Mg/Ca- and Sr/Ca-ratios.

Pliocene change in seawater Mg/Ca

The application of Mg/Ca paleothermometry to sample material from older time slices, for example in this study the Pliocene, requires to consider possible changes in $Mg/Ca_{seawater}$ (Lear et al., 2000; Billups and Schrag, 2002; Tripati et al., 2003). From cultivating experiments Brown (1996) concluded that Mg/Ca_{foram} is linearly dependent on $Mg/Ca_{solution}$ (0.1 mol/mol change in $Mg/Ca_{seawater}$ leads to 0.059 mmol/mol change in Mg/Ca_{foram}). Recently, Ries (2004) showed that several carbonate building organisms exhibit an exponential relationship between Mg/Ca_{foram} and $Mg/Ca_{solution}$. The residence time of Mg in seawater is ~13 m.y. (Broecker and Peng, 1982), which basically suggests that paleo sea surface temperature reconstructions on much shorter time scales would not be affected by a change in $Mg/Ca_{seawater}$. However, on long time scales Mg and Ca in seawater might have changed due to varying continental weathering rates (Berner et al., 1983; Wilkinson and Algeo, 1989), hydrothermal alteration of basalt at mid ocean ridges (Mottle and Wheat, 1994; Elderfield and Schulz, 1996), carbonate deposition (Wilkinson and Algeo, 1989), and ion exchange reactions of Mg with clays (Gieskes and Lawrence, 1981). Based on the models of Wilkinson and Algeo (1989) and Stanley and Hardie (1998), $Mg/Ca_{seawater}$ was lowered by maximum 0.4 mol/mol during the early Pliocene. When applying the calibration formula introduced by Lear et al. (2000) to correct for this change in $Mg/Ca_{seawater}$, the resulting $SST_{Mg/Ca}$ record is offset to even higher $SST_{Mg/Ca}$ by maximum 1°C in comparison to the original $SST_{Mg/Ca}$ dataset.

This consideration, in combination with the relatively short time interval of our record which excludes large variations in $Mg/Ca_{seawater}$, and the resemblance of the $SSTs_{Mg/Ca}$ >4.5 Ma with modern Caribbean SSTs, suggests that the Pliocene drop in $Mg/Ca_{seawater}$ cannot explain the extreme $SSTs_{Mg/Ca}$ observed after 4.05 Ma and therefore, made us decide not to apply a correction for changed $Mg/Ca_{seawater}$.

Conclusions

Combined analyses of Mg/Ca and $\delta^{18}O$ on the planktonic foraminifer *G. sacculifer* from ODP Site 1000 allowed to study changes in Caribbean surface hydrography during the effective restriction of surface throughflow through the Panamanian Gateway between 5.6-3.9 Ma. The reconstruction of $SST_{Mg/Ca}$ and SSS from combined foraminiferal Mg/Ca and $\delta^{18}O$ measurements implies a relatively uniform $SST_{Mg/Ca}$ pattern of 26.5°C-29°C for the time interval 5.6-5.0 Ma. This period is characterized by the typical negative correlation between Mg/Ca and $\delta^{18}O$. This pattern changes after 5.0 Ma, when both positive and negative correlations between $SST_{Mg/Ca}$ and $\delta^{18}O$ occur.

After 4.5 Ma, we show a nearly perfect positive correlation between Mg/Ca and $\delta^{18}O$, i.e. high $SST_{Mg/Ca}$ are paralleled by high $\delta^{18}O$ values, on a precessional timescale. Such a positive correlation was not reported before. We interpret such a positive relationship between $SST_{Mg/Ca}$ and $\delta^{18}O$ the way that the salinity effect on the $\delta^{18}O$ signal dominates those of global ice volume and temperature. Converting the $\delta^{18}O$ record into SSS yields salinity amplitudes of up to 4 salinity units. At times of peak SSS, foraminiferal Mg/Ca increase to up to ~7 mmol/mol, transferring to unrealistically high $SST_{Mg/Ca}$ of up to 35°C with amplitudes of up to 5°C. We suspect that the large variations in SSS have a profound influence on the Mg/Ca record overestimating Mg/Ca-ratios by 20-30% and $SST_{Mg/Ca}$ by 3-4°C.

SEM analyses of foraminiferal tests of *G. sacculifer* showing anomalously high Mg/Ca-ratios reveal crystalline overgrowths. Foraminiferal Sr/Ca ratios, carbonate mineralogy, and calcareous nannofossil analysis suggest that diagenetically induced aragonite dissolution and reprecipitation caused these overgrowths. LA-ICP-MS measurements and pore water data, however, exclude the possibility that the diagenetic overgrowths provide enough Mg to generate the extremely high foraminiferal Mg/Ca-ratios observed after 4.5 Ma. According to our estimation, the diagenetic overprint may account for a potential error on Mg/Ca of maximum -0.1 to 0.3 mmol/mol (-0.3°C to 1°C in temperature).

After correcting the foraminiferal Mg/Ca-ratios after 4.5 Ma for the salinity effect, the reconstructed $SST_{Mg/Ca}$ record shows an increase in Caribbean SST by ~2°C due to the progressive shoaling of the Isthmus of Panama, possibly indicating the initiation of the Western Atlantic Warm Pool.

Acknowledgements

This research used samples and data provided by the Ocean Drilling Program, which is sponsored by the U.S. National Science Foundation and participating countries under management of Joint Oceanographic Institutions. This study was performed within DFG-Research Unit „Impact of Gateways on Ocean Circulation, Climate, and Evolution“ (FOR451/1-1 TP B2). We like to thank Silvia Koch, Kerrin Wittmaack, Nicole Gau, Jutta Heintze, Kristin Nass, Beate Bader, Ute Schuldt, Paul Mason, and Gijs Nobbe for sample preparation and laboratory assistence. We gratefully thank Marcus Regenberg, Joachim Schönfeld, Martin Ziegler, and ... anonymous reviewers for their useful comments and the improvement of the manuscript.

Chapter 7

Global impact of the Panamanian Seaway closure

A. Schmittner, M. Sarnthein, H. Kinkel, G. Bartoli, T. Bickert, M. Crucifix, D. Crudeli, **J. Groeneveld**, F. Kösters, U. Mikolajewicz, C. Millo, D. Schmidt, B. Schneider, M. Schulz, S. Steph, R. Tiedemann, M. Weinelt, M. Zuvela and the other participants of the workshop "Pliocene Closure of the Panama Gateway and its Effect on Ocean Circulation, Climate and Evolution".

Eos 85-49. 526

Closure of the Isthmus of Panama about 3 million years ago (Ma) was accompanied by dramatic changes in the Earth's climate and biosphere. The Greenlandic ice sheet grew to continental extent and the great cycles of ice ages that dominated climate variability henceforth started around the same time as the final closure of the seaway. Disruption of water mass exchange between the Atlantic and the Pacific oceans led to different evolution of marine species on either side of the land bridge while land based organisms like mammals and other animals took the advantage to colonize an entire subcontinent. A two-day workshop at the University of Kiel (Germany) was held on June 11-12, 2004 to summarize our current knowledge of this time period and to identify areas where new research is needed. The main scientific questions asked were:

_What was the timing of events associated with the restriction of the seaway?

_What were the effects of changed ocean circulation patterns on climate, marine productivity and evolution?

_Did the closure of the seaway trigger the intensification of northern hemisphere glaciation?

The definitive answer to the last question remains open. However, a great deal of information is now available both from the geological record and from climate modeling studies concerning the timing and the effect of the closure on climate and biology.

Timing of the closure

Marine carbon isotope records ($\delta^{13}C$) from Atlantic and Pacific sediments below 1000 m depth show parallel variability until 14-11 Ma when a first divergence is observed as reported by T. Bickert (Bremen). This suggests that the deep ocean passage began to shoal around that time. Between 10.5 and 9 Ma the carbonate content in sediments from the eastern tropical Pacific began to decline dramatically (the so called "carbonate crash"). This is generally interpreted as a reduced inflow of less corrosive North Atlantic Deep Water (NADW) through the seaway into the Pacific. The first recorded intermingling of terrestrial faunas (racoons) between North and South America at 8-9.3 Ma suggests the existence of an extended archipelago in Central America. After about 7 Ma the modern distribution of deep water masses with NADW advection into the South Atlantic seems to be established. Indeed, ocean-climate models (MIT, UVic, LSG) in which the sill depth becomes shallower than the depth of NADW flow (1-3 km) demonstrate that NADW no longer escapes westward through the gateway into the Pacific but penetrates into the South Atlantic. This suggests that at about 7 Ma the sill depth was shallower than 1 km.

Restriced surface water exchange through the gateway marks the time interval from 4.7 to 4.2 Ma. Comparisons of planktonic $\delta^{18}O$ records (Ocean Drilling Program (ODP) Sites 1241, 999, 1000 and 1006) (S.Steph/L.Reuning, Kiel) demonstrate the establishment of the modern Pacific-Caribbean salinity contrast and the formation of the Caribbean Warm Pool. The general increase in Caribbean SST (3°C) and SSS (up to 3 psu) was associated with pronounced variations on precessional periodicities. Correlation between Pacific and Caribbean $\delta^{18}O$ signals of deep dwelling

foraminifers (70-150 m) indicates the existence of deeper leakages until ~3.6 Ma, although the volume transport of upper surface waters through the gateway was significantly reduced after 4.2 Ma.

In the eastern tropical Pacific a distinct south-eastward shift in the locus of maximum opal accumulation rates at ~4.4 Ma was accompanied by a decrease in the thermocline depth (ODP Site 1241). This is consistent with increased upwelling between 5 and 4 Ma and a southward shift of the intertropical convergence zone (ITCZ) in the east Pacific as deduced from eolian grain size and flux studies. These changes document a reorganization of the tropical Pacific circulation most probably in response to the restriction of the Panama seaway. In the tropical Atlantic, major changes in surface hydrography at 4.4-4.0 Ma were also linked to changes in the tropical wind field.

Evidence of further shoaling of the seaway is provided by Pacific-Caribbean Mg/Ca-derived SST reconstructions (ODP Sites 999 and 1241) of shallow-dwelling foraminifers (*G. sacculifer*) (J.Groeneveld, Kiel). Similar SST values and fluctuations persisted on both sides until about 2.8 Ma, before larger-scale sea level variations became important in response to the amplification of northern hemisphere glaciation. After about 2.8 Ma, glacial stages (indicative of sea level low-stands) are associated with Pacific minima in SST (ODP Site 1241) and maxima in Caribbean SST. Thus, the cessation of the throughflow during glacials terminated the imprint of cooler Pacific surface waters in the Caribbean and allowed Caribbean temperatures to increase. This documents the final phase of the seaway closure, when sea level fluctuations on the order of 50-70 m controlled the Pacific water leakage into the Caribbean. The ebbing of the interglacial throughflow remains unclear since presently available records end at 2.5 Ma and will be subject to future investigations.

Exchanges of land mammals and oak trees between North and South America, albeit less well dated, indicate the full emergence of the isthmus. The time of the final closure of the gateway coincides with massive increases in ice rafted detritus in northern hemisphere high-latitude ocean sediments (e.g. ODP Site 907 in the North Atlantic and ODP Site 882 in the North Pacific). This detritus indicates the intensification of northern hemisphere glaciation with large continental-size ice sheets crossing the shoreline. This interpretation is supported by a drop in sea level as indicated by increased concentrations of the heavy oxygen isotope ($\delta^{18}O$) in benthic fossils after the beginning of marine isotope stage G6 at 2.75 Ma. Subsequently, changes in the Earth's orbit around the sun and associated variations in the seasonal cycle of insolation controlled the waxing and waning of these ice sheets that dominated northern hemisphere climate variability during the most recent period of Earth's history, the Quaternary.

Impact on marine productivity

Enigmatic changes were also recorded in sediments from the subarctic North Pacific. Following a phase of gradually increasing opal accumulation to the sediments an abrupt collapse occurred at 2.75 Ma. The drop of the opal accumulation rates is generally interpreted as the inception of the halocline (strong vertical stratification) and/or a strong decline in productivity. While some researchers believe that this was due to a reduction in upwelling in the North Pacific others think it might have been caused by decreased downwelling and lower rates of intermediate water formation accompanied by a shutdown of a meridional overturning in the North Pacific. The later hypothesis seems to be supported by oxygen isotope records from the Northeast Pacific which suggest that SSTs dropped by 7°C at 2.75 Ma. Nevertheless, a consistent and unambiguous explanation of these records remains one of the major open questions concerning the closure of the Panamanian seaway warranting further investigations by both the reconstructing community as well as from climate modelers.

In the North Atlantic productivity appears to have been decreasing during the final closure of the seaway as suggested by changes in benthic foraminiferal species composition. At ODP Site 984 south of Iceland, *Bolivina pacifica,* a high carbon flux indicator species which is common prior to 2.75 Ma disappears completely thereafter (M. Weinelt, Kiel).

This is consistent with model simulations showing that reduced inflow of nutrient rich Pacific surface waters into the North Atlantic decreases productivity there, while in the eastern equatorial Pacific productivity increases due to intensified upwelling after the closure of the seaway (B. Schneider, Kiel). The consequences of these changes in productivity and upwelling on the marine carbon cycle and atmospheric CO_2 concentration will be subject to future investigations.

Impact on evolution of marine organisms

The closure led to the separation of marine organisms now living on both sides of the isthmus, providing classical textbook examples for allopatric speciation. Since most of these examples come from benthic shallow water organisms (e.g. corals) the geological record is too inaccurate to determine the exact timing of the separation. Planktonic microfossils are better suitable for studies on the biological response to environmental change, since they can be examined in high-resolution sediment cores with well constrained stratigraphy. First studies indicate that phytoplankton evolution (coccolithophores) might be controlled by changes in the surface water circulation pattern as similar trends are observed on both sides of the isthmus prior to 3.8 Ma and support a model in which evolution is a direct result of physical environmental selective forces (D. Crudeli, Kiel). Until this time, this evolution is in agreement with sympatric speciation models, where organisms evolve in new ecological niches. However, since the changes in surface water circulation and ecological restructuring are a consequence of the gateway closure at 2.7 Ma, the evolutionary steps similar to those in the benthic communities still need to be investigated.

An unresolved question remains in the timing of first and last appearances of planktonic organisms commonly used for biostratigraphy in ODP cores. The data available so far do not permit a clear picture of what happened when, but indicate that there are no major differences in timing before and after the closure of the gateway, as pointed out by D. Schmidt (London) and H. Kinkel (Kiel), with the exception of the first occurrence of *G. truncatulinoides* (2.5-2 Ma) in the South Pacific which gradually spread westward into the Atlantic. One of the reasons for present uncertainties is that age models and biostratigraphic data have a too coarse resolution, but this will improve with ongoing studies on high resolution sediment cores and age models, that now are available from both sides of the gateway (ODP Leg 202). A previously unknown biodiversity among selected coccolithophores has been shown from the early Pliocene which is of significance for regional correlations and could be of support to classical biostratigraphy.

Impact on ocean circulation

How did the closure of this tropical seaway affect global ocean circulation patterns and heat transport? The use of climate models shows that the main water mass transport in the upper ocean has been from the Pacific into the Atlantic despite the trade winds which blow in the opposite direction (U. Mikolajewicz, Hamburg). The reason for this unexpected behavior lies in the different sea surface elevations with respect to the geoid. Due to the density contrast of the underlaying water column, the sea surface in the Pacific is higher by 10-20 cm compared with the Atlantic. This small difference is sufficient to exert a pressure gradient and the water flows “downhill” from the Pacific into the Atlantic against the winds (at least in an annual mean sense). This is a robust result in different models and the flow rate depends on the sill depth with more than 10 Sv ($=10^6 m^3/s$) for a 700 m deep passage and reduces to still around 5 Sv for a sill depth of 100 m (A. Schmittner, Kiel). However, new results from a model with higher vertical resolution suggest that there might have existed a shallow surface layer (10 m) in which the transport may be seasonally reversed (from the Atlantic into the Pacific) as reported by M. Prange (Bremen). Moreover it is likely that the flow direction varied on seasonal and interannual timescales as well as on spatial scales not resolved by the coarse resolution models.

Pacific waters are less saline than Atlantic waters and therefore its reduced inflow concentrates salinities in the North

Atlantic. This in turn increases the density of surface waters in the sinking regions of NADW and hence its rate of formation. All climate models agree on this point but the degree of increase depends on the sill depth and on other weakly constrained model parameters like vertical diffusivities. These findings suggest that as a consequence of the closure NADW formation and the associated northward heat transport intensified. Indeed epibenthic $d^{13}C$ records and better carbonate preservation in the Atlantic after 4.6 Ma suggest increasing influence of NADW. A mega-hiatus (lack of sediments) in the eastern low-latitude Atlantic (ODP Leg 108) around the same time (4.5-3.8 Ma) probably indicates a super-conveyor (stronger NADW or AABW incursion than today) and associated strong bottom currents (M. Sarnthein, Kiel).

New reconstructions of North Atlantic sea surface temperatures and deep ocean ventilation ($\delta^{13}C$) reported by G. Bartoli and M. Sarnthein (Kiel) indeed show a warming of 2-3^{o}C and increased NADW flow around 2.85 Ma, just prior to the final closure confirming increasing ocean heat transport. The areas of deep water formation were probably much different from today. In the Nordic- and Labrador Seas, where today freshly ventilated deep water leads to good carbonate preservation, carbonate concentrations were much lower throughout the Pliocene. Moreover, the rates of deep water formation and their changes remain to be quantified in future studies combining proxy records with ocean-climate models.

Impact on northern hemisphere glaciation

How could a warmer North Atlantic trigger the glaciation? At first glance this seems to be a paradox. However, warmer temperatures will also lead to increased snowfall at high altitudes. Thus if higher snowfall rates outweigh the increased melting at lower altitudes mountain glaciers can grow in a warmer climate. It is obvious that this subtle balance depends on the topography. This is the reason why recent modeling efforts use a realistic preglacial Greenland topography as reported by B. Schneider (Kiel). However, so far no model could simulate glacial inception due to changes in ocean heat transport triggered by the closure of Panama only.

Another hypothesis suggests that a warmer North Atlantic leads to increased moisture supply to high latitudes. This would increase Siberian river runoff into the Arctic and decrease salinity and hence increase stratification and sea ice cover eventually leading to high latitude cooling and glacial inception. This hypothesis is not supported by climate models, which suggests a small effect of increased NADW on high latitude precipitation (U. Mikolajewicz). So far there are no proxy records for the evolution of surface salinity in the Arctic. However, this issue will be addressed with new sediment cores from the IODP Arctic Coring Expedition (ACEX) Leg 302 in this summer 2004.

Other forcing mechanisms invoked for the glacial inception are changes in orbital parameters and atmospheric CO_2 concentrations. Increasing amplitude variations of the Earth's axis tilt with respect to the ecliptic led to enhanced maxima and minima in the seasonal insolation. In fact, changes in orbital parameters have a much larger effect on the perennial snow cover distribution than changes in ocean heat transport in models of intermediate complexity (ECBILT/CLIO, UVic) as pointed out by A. Klocker (Bremen). However, similar configurations of Earth's orbit also occurred well before and well after 2.7 Ma. This suggests that the climate system must have been preconditioned by some other process. Model experiments with a zonally averaged atmosphere-ice sheet model forced with varying orbital parameters simulate the inception of glaciation around the correct time only if atmospheric CO_2 is decreasing as reported by M. Crucifix (Exeter, UK). Reconstructions of past CO_2 levels, however, do not support this theory as they indicate relatively stable CO_2 concentrations of between 200 and 400 ppmv back to the Oligocene (25 Ma) although the uncertainty in the reconstructions leaves some room for speculations. How did the reorganisation of the ocean circulation associated with the gateway closure influence the carbon cycle and hence atmospheric CO_2? This was identified as another pressing issue that needs to be addressed with future modeling of the coupled climate-carbon cycle

system.

Acknowledgments

We are grateful to all participants who contributed to the lively discussions during the meeting. The workshop was supported by the German Founding Agency (Deutsche Forschungsgemeinschaft) through the research unit (Forschergruppe 451) on ocean gateways in Kiel.

Chapter 8

Conclusions and perspectives

Within the framework of this thesis high resolution sea surface temperature (SST) and sea surface salinity (SSS) records were generated for ODP Sites 999, 1000, and 1241 using Mg/Ca paleothermometry in combination with stable oxygen isotopes (Steph, 2005). This allowed for the first time in high detail and at high temporal resolution to distinguish between the effects on sea surface temperature (SST) and sea surface salinity (SSS) caused by the progressive closure of the Panamanian Gateway (5.6-2.2 Ma) in the east Pacific and the Caribbean. Further development of Mg/Ca as a paleo-sea water temperature proxy in combination with the installation of a new ICP-OES resulted in a high precision analytical method for the determination of biogenic carbonates.

The following paragraphs summarize the major conclusions from the previous chapters, answer the questions from the introductory Chapter 1, and provide some perspectives for future work.

How and when did the modern SSS and SST gradients between the east Pacific and the Caribbean develop?

Planktonic Mg/Ca and $\delta^{18}O$ records from Caribbean ODP Sites 999 and 1000 and equatorial east Pacific Site 1241 (5.6-2.2 Ma) allowed for the first time to quantitatively assess the development of Caribbean/Pacific mixed-layer temperatures and salinities in response to the closure of the Panamanian Gateway. The data indicate that the Pacific-Caribbean salinity contrast developed gradually during the late Miocene and at least 1 million years earlier than previously suggested. Significantly warmer $SST_{Mg/Ca}$ and higher saline $\delta^{18}O_{water}$ in the central Caribbean (Site 1000) in comparison with those at Sites 999 and 1241 already occur by 5.6 Ma. Within the direct proximity of the former gateway (Sites 999 (Caribbean) and 1241 (east Pacific)) the SSS contrast commenced to develop at ~4.2 Ma. Also, the progressive closure of the gateway did not only lead to an increase in SSS in the Caribbean (999) as previously suggested (Keigwin, 1982; Haug et al., 2001), but also resulted in a decrease in SSS in the east Pacific (Site 1241) until 2.2 Ma, which significantly contributed to the increasing SSS gradient between the Pacific and the Caribbean (Chapter 4).

In contrast to the development of the SSS gradient since the late Miocene, $SSTs_{Mg/Ca}$ at Sites 999 and 1241 remained similar between ~5.2-2.7 Ma. With the onset of Northern Hemisphere Glaciation (~2.7 Ma) sea level lowstands started to control the throughflow, thereby creating for the first time similar to modern temperature gradients during Marine Isotope Stages (MIS) 96, 98, and 100 (Chapter 4).

Did the progressive closure of the Panamanian Gateway lead to the development of the WAWP and subsequently to an increased transport of heat and salt into the North Atlantic?

The location of Site 1000 in the central Caribbean provided the ideal opportunity to trace the formation of the WAWP. After 4.5 Ma, $SSTs_{Mg/Ca}$ of the planktonic foraminifer *G. sacculifer* increase by ~2°C during a threshold in the progressive shoaling of the Isthmus of Panama (Chapter 6). This probably reflects the initiation of the Western Atlantic Warm Pool (WAWP). Accompanying this increase in $SST_{Mg/Ca}$, SSS also increased at Site 1000, both in comparison with the east Pacific and with the southern Caribbean Site 999. The difference in SSS betwen Sites 999 and 1000 implies the formation of an intra-Caribbean SSS gradient (Chapter 4; Steph, 2005).

Since the central Caribbean is the source region of the Gulfstream, these developments in $SST_{Mg/Ca}$ and SSS indicate that the progressive closure might have led to an intensified transport of heat and salt into the North Atlantic. This effect was proposed as a possible trigger or necessary pre-condition for the onset of Northern Hemisphere Glaciation (Berggren and Hollister, 1974; Haug and Tiedemann, 1998; Driscoll and Haug, 1998). Enhanced evaporation in the North Atlantic would provide the necessary water vapour to build ice

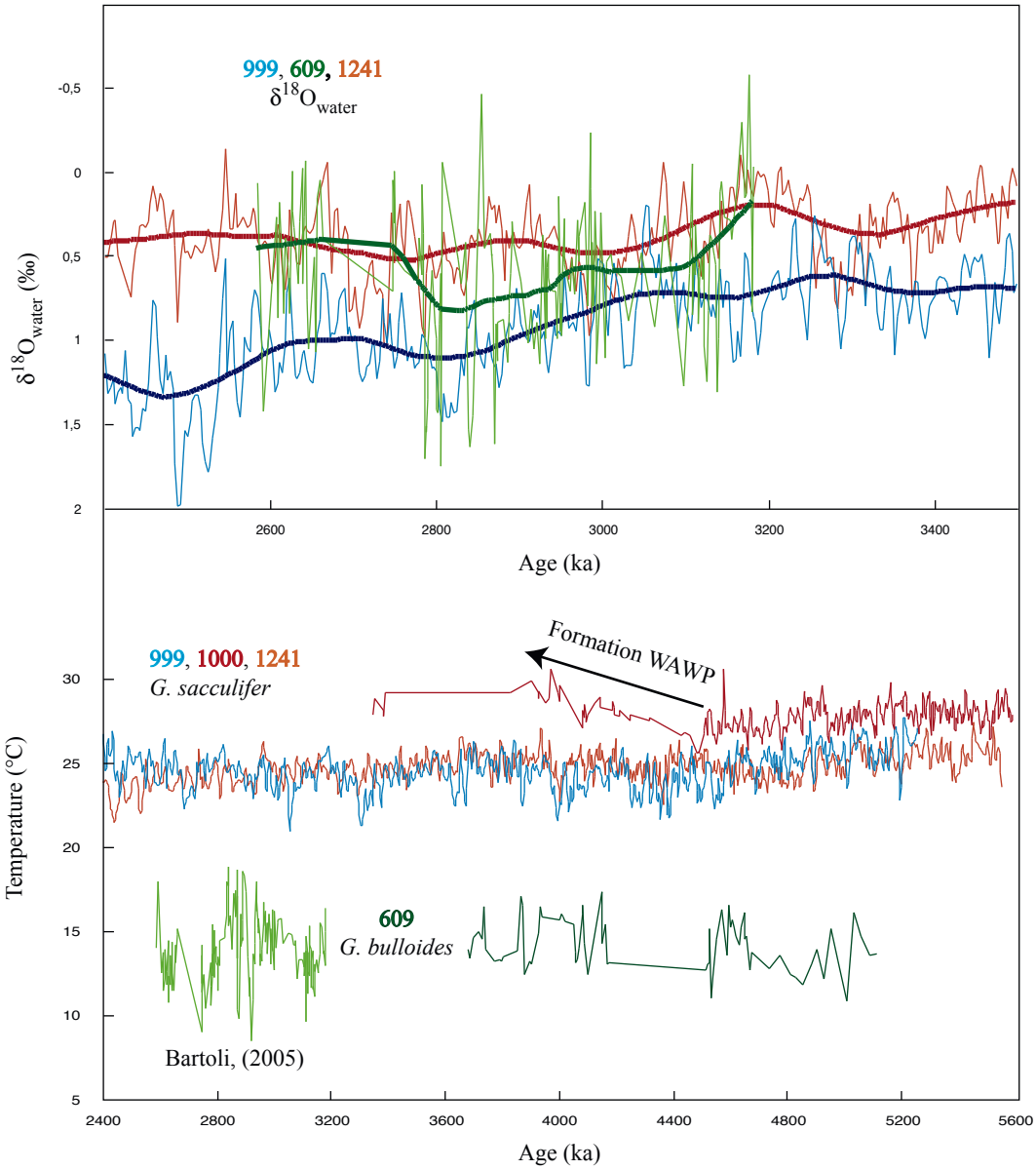

Figure 8.1 Comparison of $\delta^{18}O_{water}$ and seawater temperatures of low-latitude Sites 999, 1000, and 1241 with high-latitude Site 609 (Bartoli, 2005).

sheets, while the increased density of the remaining water would further intensify thermohaline circulation (Maier-Reimer et al., 1990; Tiedemann and Franz, 1997; Haug and Tiedemann, 1998; Whitehead and Bohaty, 2003; Nisancioglu et al., 2003; Prange and Schulz, 2004). On the other hand, Berger and Wefer (1996) argued that this increased transport of heat into the North Atlantic would instead delay the onset of NHG.

A pilot study within this thesis tried to trace these effects from the Caribbean into the North Atlantic. Mg/Ca analyses on the planktonic foraminifer *Globigerina bulloides* were performed on North Atlantic DSDP Site 609B (49°52.66'N, 24°14.28'W, 3884 m water depth) for the time interval from 4.8 Ma to 4.0 Ma, i.e. when $SSTs_{Mg/Ca}$ in the central Caribbean (Site 1000) significantly increased (Fig. 8.1). Site 609B is located in the

center of the modern Gulfstream and is thus expected to react on changes in Caribbean SST and SSS. In the North Atlantic, however, no significant change in $SSTs_{Mg/Ca}$ could be seen during this time interval. Also on Site 609B, Bartoli (2005) performed a high resolution study on North Atlantic $SST_{Mg/Ca}$ and SSS for the time interval <3.3 Ma. The comparison of the Mg/Ca analyses on *G. bulloides* between the older interval (5.1-3.7 Ma) and the work of G. Bartoli (3.2-2.6 Ma) reveals no significant long-term change until 2.8 Ma, after which Mg/Ca starts to decrease, probably as a result of the onset of NHG (Fig. 8.1). Assuming that both *G. sacculifer* from the low-latitude Caribbean (Site 999) and *G. bulloides* from the high-latitude North Atlantic (Site 609) represent the watermass signature of the Gulfstream, we may directly compare $\delta^{18}O_{water}$ values derived from the combined analysis of Mg/Ca and $\delta^{18}O$ (Fig. 8.1). The comparison shows that average $\delta^{18}O_{water}$ values from North Atlantic (Site 609B) are intermediate between those from the Caribbean (Site 999) and the east Pacific (Site 1241). $\delta^{18}O$ values at Site 609B follow the same trend between 3.2-2.8 Ma as seen at the higher saline Site 999, although the values are clearly lower. After 2.8 Ma $\delta^{18}O_{water}$ at Site 609B indicates a freshening along with the onset of NHG (Bartoli, 2005).

To better understand the direct influence of SST and SSS changes along the pathway of the Gulfstream due to the closure of the Panamanian Gateway high resolution and continuous combined Mg/Ca and $\delta^{18}O$ records are needed for the entire time interval from 6.0-2.0 Ma.

How did surface ocean circulation in the east Pacific and the Caribbean respond to the progressive closure of the Panamanian Gateway?

The most pronounced changes in surface ocean circulation did occur in the Caribbean rather than in the east Pacific. During the critical time interval 4.6-4.0 Ma, the only change at Site 1241 was a significant shoaling of the thermocline (Steph, 2005). In the Caribbean, instead, this interval is characterized by major changes in both $SST_{Mg/Ca}$ and SSS. A significant $SST_{Mg/Ca}$ incease in the central Caribbean (Site 1000) led to the formation of the WAWP (Chapter 6). Simultaneously, a pronounced Caribbean-Pacific salinity gradient was established (Chapter 4; Steph, 2005). Since SSS fluctuates at precessional cycles with the larger amplitudes at Site 1000, an intra-Caribbean salinity gradient is formed as well (Steph, 2005), suggesting an oscillating dominance of Pacific and Atlantic watermasses at Site 1000. The similarity in $SST_{Mg/Ca}$ between Sites 999 and 1241 implies that the southern Caribbean remained under influence of Pacific watermasses until ~2.5 Ma, when glacial induced sea level lowstands start to control the throughflow (Chapter 4).

Can the early Pliocene be referred to as a permanent el Niño-like based climate?

Molnar and Cane (2002) described the early Pliocene as a period of permanent El Niño-like conditions. For the Pacific El Niño-like conditions mean that the warm waters of the WPWP move to the east because of weak easterly winds over the tropical Pacific, causing the cessation of upwelling along the equator and the coast of South America and result in reduced productivity and enhanced SST.

As was discussed in Chapter 5, $SSTs_{Mg/Ca}$ at Site 1241 compare to modern SSTs at that location. The position of Site 1241, however, is probably not the best place to record El Niño-related changes, as the most pronounced changes in upper ocean water signatures occur along the west coast of South America and the equator. Site 1239 from the Peruvian upwelling zone is, therefore, more suitable to monitor the effects of El Niño. Initial $Mg/Ca_{G. sacculifer}$ analyses from Site 1239 indicate that $SSTs_{Mg/Ca}$ were similar to those of Site 1241 around 4.0 Ma (Fig. 8.2), suggesting a much smaller SST gradient between the east Pacific sites. This may be interpreted as an

indication for El Niño-like conditions. Measurements from <3.0 Ma show that $SSTs_{Mg/Ca}$ had decreased at Site 1239 in comparison to those at Site 1241 (Fig. 8.2), which points to a situation more similar to the modern situation.

To further investigate the scenario of a permanent El Niño-like situation during the early Pliocene, a high resolution Mg/Ca record on *G. sacculifer* at Site 1239 will be established to reveal when the presence of the temperature gradient in the east Pacific started to develop. Additional information can be generated by the analysis of opal accumulation rates, reflecting productivity changes, which would provide knowledge on the initiation of upwelling along the Peruvian Coast.

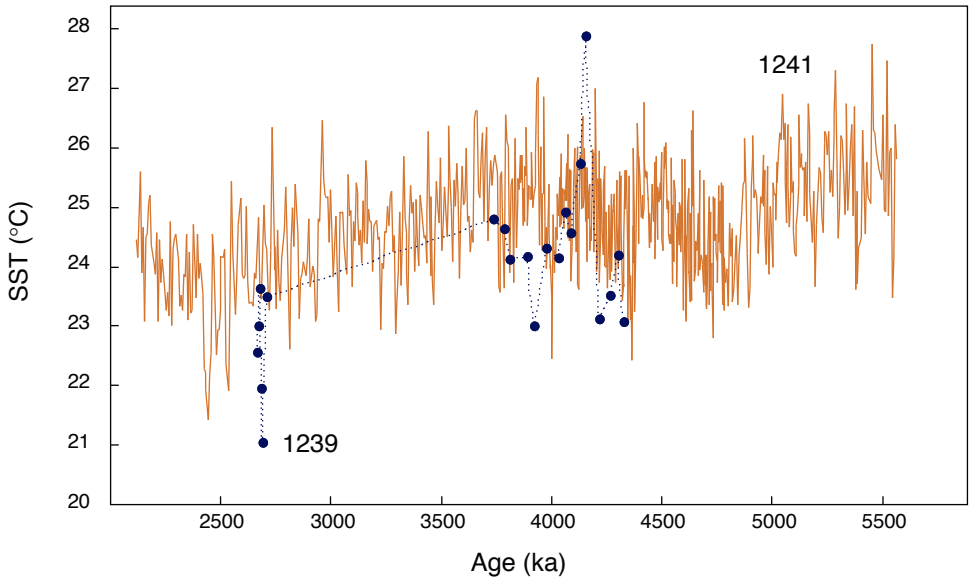

Figure 8.2 Comparison between $SST_{Mg/Ca}$ from the Peruvian upwelling zone (Site 1239, blue dots) and Site 1241 (orange curve), north of the equator outside the equatorial upwelling areas. Analyses were performed on the planktonic foraminifer *G. sacculifer*.

Can changes in SST and SSS in the east Pacific and the Caribbean be related to global trends in climate?

The global cooling trend, a response to the intensification of the Northern Hemisphere Glaciation (NHG), started at ~3.2 Ma as shown by the $\delta^{18}O_{benthic}$ records of Sites 999 and 1241 (Haug and Tiedemann, 1998; Steph, 2005). This trend is also reflected by tropical east Pacific cooling of surface water masses as indicated by $SSTs_{Mg/Ca}$ at Site 1241. Cooling, however, already commenced at ~3.7 Ma here, suggesting that global cooling, possibly related to decreasing atmospheric CO_2 concentrations, might have started well before the intensification of the NHG (Chapter 5). Glacial-interglacials oscillations, which are reflected by the obliquity-related 41 kyr filters, reveal that Caribbean $SSTs_{Mg/Ca}$ generally followed the global trend. But, with the onset of NHG, $SSTs_{Mg/Ca}$ at Site 999 show a negative correlation with the global trend due to the glacial closure of the gateway, resulting in a warming of the Caribbean during glacial periods rather than the expected cooling (Chapter 4).

Application and verification of Mg/Ca paleothermometry for the Pliocene.

Mg/Ca as a proxy for the determination of paleo-sea water temperatures proved to be applicable for the Pliocene. Reconstructed temperatures are reasonable and compare to modern values. Seawater Mg/Ca was only slightly different than today, and most Pliocene species of planktonic foraminifer are still present today (Chapter 4 and 5).

The results from Site 1000 showed, however, that large salinity variations seem to affect foraminiferal Mg/Ca significantly, resulting in high Mg/Ca-ratios, which convert to unrealistically high temperatures (Chapter 6).

Indeed, cultivating experiments revealed that salinity exerts an significant influence on foraminiferal Mg/Ca of 4-10% per salinity unit (Nürnberg et al., 1996; Lea et al., 1999). Ferguson et al. (2005) even suggested a salinity influence on Mg/Ca as large as 30% per salinity unit. The impact of salinity on the Pliocene Mg/Ca-values was suggested by the nearly perfect positive correlation between Mg/Ca and $\delta^{18}O$, i.e. extremely high Mg/Ca-ratios were paralleled by high $\delta^{18}O$ values for samples <4.5 Ma from Site 1000. Such a relationship which was never reported before. Taking into account the above mentioned salinity effect, the high Mg/Ca-ratios at times of a positive correlation with $\delta^{18}O$ appear to be perturbed to higher ratios by 20-30%, equivalent to a temperature increase of 3-4°C. Further constraints on the influence of salinity on Mg/Ca are needed and might be provided by cultivating experiments.

Scanning electron microscope (SEM) analyses of foraminiferal tests of *G. sacculifer* showing anomalously high Mg/Ca-ratios revealed crystalline overgrowths. Foraminiferal Sr/Ca-ratios, carbonate mineralogy, and calcareous nannofossil analysis (Crudeli, 2005) suggested that diagenetically induced aragonite dissolution and reprecipitation caused these overgrowths. LA-ICP-MS measurements and pore water data, however, exclude the possibility that the diagenetic overgrowths provided enough Mg to generate the extremely high foraminiferal Mg/Ca-ratios observed <4.5 Ma. According to our estimation, the diagenetic overprint may account for a potential error on Mg/Ca of maximum -0.1 to 0.3 mmol/mol (-0.3°C to 1°C in temperature) (Chapter 6). Nevertheless, these overgrowths suggest that in environments which are under the influence of carbonate platforms, care should be taken with the analysis of Mg/Ca, especially when high-Mg calcite is part of the sediment.

Improvement and further development of Mg/Ca analytics.

The installation of a new ICP-OES at the Institute of Earthsciences in Kiel within the scope of the „Ocean Gateway Project“ led to the establishment of a high precision method for the analysis of biogenic carbonates. Multiple experiments and comparisons with ICPs at IFM-Geomar and the University of Cambridge were used to calibrate and optimize the machine (Chapter 3). An upcoming publication (Garbe-Schönberg et al.) describes the applied experiments and accompanying problems, which had to be considered.

Publications

Garbe-Schönberg, D., **J. Groeneveld**, G. Bartoli, D. Nürnberg, (2005). High-precision Mg/Ca and Sr/Ca ratios of biogenic carbonate and seawater by simultaneous ICP-OES. Manuscript in preparation for Geochemistry, Geophysics, Geosystems.

Groeneveld, J., R. Tiedemann, S. Steph, D. Nürnberg, D. Garbe-Schönberg, G.H. Haug, (2005). The final phase of the closure history of the Panamanian Gateway and the onset of global cooling. Manuscript in preparation for Geology.

Groeneveld, J., S. Steph, R. Tiedemann, D. Garbe-Schönberg, D. Nürnberg, A. Sturm, (2004).Pliocene development of east-Pacific hydrology as revealed by Mg/Ca analyses on the planktic foraminifer Globigerinoides sacculifer. Submitted to ODP Scientific Results, Leg 202.

Groeneveld, J., D. Nürnberg, S. Steph, R. Tiedemann, G.J. Reichart, D. Crudeli, L. Reuning, (2005). Increasing Mg/Ca-SSTs in the Pliocene Caribbean: Diagenetical overprint, salinity influence or initiation of the Western Atlantic Warm Pool? Submitted to Geochemistry, Geophysics, Geosystems.

Nürnberg, D., **J. Groeneveld.** (2005). Pleistocene variability of the Subtropical Convergence at East Tasman Plateau – Evidence from planktonic foraminiferal Mg/Ca (ODP Site 1172A). Submitted to Geochemistry, Geophysics, Geosystems

Regenberg, M., D. Nürnberg, S. Steph, **J. Groeneveld**, W.-Chr. Dullo, D. Garbe-Schönberg, R. Tiedemann (2005). Assessing the dissolution effect on planktonic foraminiferal Mg/Ca: Evidence from Caribbean core-tops. Submitted to Geochemistry, Geophysics, Geosystems

Schmittner, A., M. Sarnthein, H. Kinkel, G. Bartoli, T. Bickert, M. Crucifix, D. Crudeli, **J. Groeneveld**, F. Kösters, U. Mikolajewicz, C. Millo, J. Reijmer, P. Schäfer, D. Schmidt, B. Schneider, M. Schulz, S. Steph, R. Tiedemann, M. Weinelt, M. Zuvela, (2004). Global impact of the Panamanian Seaway Closure. Eos 85-49: 526

Steph, S., R. Tiedemann, **J. Groeneveld**, D. Nürnberg, (2004). Changes in Caribbean surface hydrography during the Pliocene shoaling of the Central American Seaway. Submitted to Paleoceanography

Steph, S., R. Tiedemann, **J. Groeneveld**, A. Sturm, D. Nürnberg, (2004). Pliocene changes in tropical east Pacific upper ocean stratification: Response to tropical gateways? Submitted to ODP Scientific Results, Leg 202.

Steph, S., R. Tiedemann, **J. Groeneveld**, D. Nürnberg. Thermocline development during the closure history of the Panamanian Gateway. Manuscript in preparation.

Presentations

- EGS-AGU-EUG Joint Assembly 2003, Nice, April 6-11
Poster presentation: **Groeneveld, J.,** Nürnberg, D., Steph, S. Tiedemann, R. Effect of the closure of the Panamanian Gateway on Carribbean sea surface temperature and salinity as indicated by foraminiferal Mg/Ca-ratios and salinity in the upper water column, 4-6 million years ago

Oral presentation: Crudeli, D., **Groeneveld, J**., Kinkel, H., Nürnberg, D., Schäfer, P., Steph, S., Tiedemann, R. Investigation on controls on microevolutionary trends of *Gephyrocapsa* and *Pseudoemiliania* coccoliths during the closure of the Panamanian Seaway (Early Pliocene)

Poster presentation: Kinkel, H., Crudeli, D., **Groeneveld, J**., Nürnberg, D., Steph, S., Tiedemann, R. Impact of Ocean Gateways on ocean circulation, climate and evolution: a multidisciplinary approach to the closing of the Isthmus of Panama.

- TMS-FG Spring Meeting 2003, Kiel, April 25-26
Poster presentation: **Groeneveld, J**., Nürnberg, D., Steph, S. Tiedemann, R. Effect of the closure of the Panamanian Gateway on Carribbean sea surface temperature and salinity as indicated by foraminiferal Mg/Ca-ratios and salinity in the upper water column, 4-6 million years ago

- DMG Annual Meeting 2003, Bochum, 22-25 September
Poster presentation: Nürnberg, D., **Groeneveld, J**., Regenberg, M., Steph, S., Tiedemann, R., Bijma, J. Constraining Mg/Ca in foraminiferal calcite as a proxy in paleoceanography.

- GSA 2003 Seattle Annual Meeting, November 2-5
Oral presentation: **Groeneveld, J**., Nürnberg, D., Steph, S. Tiedemann, R. Influence of salinity on planktic foraminiferal Mg/Ca as deducted from a reconstruction of the shoaling of the Isthmus of Panama.

- AGU Fall Meeting 2003, San Francisco, 8-12 December
Poster presentation: Regenberg, M., Nürnberg, D., Steph, S., **Groeneveld, J**., Tiedemann, R. Paired Mg/Ca and $\delta^{18}O$ in planktonic foraminifers from Caribbean and (sub-) tropical South Atlantic core-top sediments – Assessing the dissolution effect.

- EGU 1st General Assembly 2004, Nice, 25-30 April
Oral presentation: **Groeneveld, J**., Nürnberg, D., Steph, S. & Tiedemann, R. Paleo-SST reconstruction for the shoaling of the Isthmus of Panama 4.8 - 3.8 Ma, deduced from Mg/Ca-ratios from the planktic foraminifer *G.sacculifer.*

- IODP/ICDP Euroforum, March 17-19, 2004 Bremen, Germany
Poster presentation: Steph, S., Tiedemann, R., **Groeneveld, J.,** Nürnberg, D. Pliocene changes in Caribbean and tropical east Pacific upper ocean stratification.

- International Conference of Paleoceanography 8, Biarritz, 5-10 September 2004
Poster presentation: **Groeneveld, J.**, D. Nürnberg, S. Steph R. Tiedemann, G.J. Reichart, L. Reuning, D. Crudeli. Increasing Mg/Ca-SSTs in the Pliocene Caribbean: Initiation of the Western Atlantic Warm Pool, salinity influence or diagenetic overprint?

Poster presentation: Steph, S., Tiedemann, R., **Groeneveld, J.**, Nürnberg, D. Pliocene changes in Caribbean and tropical east Pacific upper ocean stratification: Evidence for a deeper passage in the Central American Seaway?

- AGU Fall Meeting 2004, San Francisco, 8-12 December
Poster presentation: **Groeneveld, J**., S. Steph, R. Tiedemann, D. Nürnberg. The Pliocene evolution of E-Pacific and Caribbean SST reveals the final phase of the closure of the Panamanian Gateway.

Oral presentation: Steph, S., Tiedemann, R., **Groeneveld, J.**, Nürnberg, D. Pliocene Shoaling of the Central American Seaway and its effect on Caribbean and tropical east Pacific upper ocean stratification.

- European Geosciences Union General Assembly April 24-29, 2005, Vienna, Austria

Poster presentation: Tiedemann, R., J. **Groeneveld, J**., Steph, S. Sturm A., Nürnberg, D., Schmittner A. Pliocene shoaling of the Central American Seaway and its effect on Caribbean and tropical east Pacific upper ocean stratification.

Poster presentation: R. Kozdon, A. Eisenhauer, D. Hippler, M. Meland, M. Weinelt, **J. Groeneveld**. A changing $\delta^{44/40}$Ca temperature sensitivity of *N. pachyderma* (sin.) in the Nordic Seas reveals new insights in Mg/Ca temperature overestimations.

Acknowledgements

I would like to thank Dirk Nürnberg and Ralf Tiedemann for their supervision and Silke Steph for the cooperation within our sub-project. I thank professor Sarnthein for leading the project.

I thank Daniela Crudeli, Gretta Bartoli, Claudia Sieler, Jenny Lezius, Hanno Kinkel, Andreas Schmittner, Christian Millo, Maja Zuvela, Frank Kösters, Andrea Lorenz, Bettina Kaste and everybody else from the Ocean Gateway Project.

From Geomar I thank Marcus Regenberg, Joachim Schönfeld, Arne Sturm, Lester Lembke, Martin Ziegler, Lars Reuning for all their discussions and comments.

Further I would like to thank Gert-Jan Reichart, Carsten Rühlemann, Kristin Nass, Natasja Brughmans, Shungo Kawagata, Hiroshi Kawamura, Reinhard Kozdon, Carin Andersson, Wolf-Christian Dullo, John Reijmer, and the rest of Geomar.

Many thanks go to Silvia Koch for all the laboratory and other assistance and to Kerrin Wittmaack for picking all those forams and cleaning endless numbers of vials as well as to Nicole Gau, Anna Jessusek, Ulrike Nielsen, and Carolin Herbon.

Thank you very much also to Dieter Garbe-Schönberg and Karin Kissling for help and assistance with the ICP.

I gratefully thank Mervyn Greaves and Harry Elderfield, University of Cambridge, for introducing me into the Mg/Ca cleaning methods.

Last but definitely not least I thank my family and friends who have long awaited this finish and endured all the stories on tiny, millions of years old, fossilized foraminifers whose Mg-content is apparently telling the temperature of seawater.

And ofcourse, I thank everybody else I have accidentally forgotten.

References

Anand, P., Elderfield, H., and Conte, M., 2003. Calibration of Mg/Ca thermometry in planktonic foraminifera from a sediment trap time series. *Paleoceanography,* 18: doi:10.1029/2002PA000846

Andersson, C., 1997. Transfer function vs. Modern analog technique for estimating Pliocene sea-surface temperatures based on planktic foraminiferal data, western equatorial Pacific Ocean. *J. Foraminiferal Res.,* 27-2: 123-132.

Archer, M., Hand, S.J., and Godthelp, H., 1995. Tertiary environmental and biotic change in Australia. In Jain, D.V.S. et al., (Eds). *Paleoclimate and evolution with emphasis on human origins*, Yale Univ. Press, New Haven. 77-90.

Archer, D.E., 1996. An atlas of the distribution of calcium carbonate in sediments of the deep sea. *Global Biogeochem. Cycles*, 10: 159-174

Baker, P., Gieskes, J.M., and Elderfield, H., 1982. Diagenesis of carbonates in deep-sea sediments evidence from Sr/Ca ratios and interstitial dissolved Sr^{2+} data, *J. Sediment. Petrol*., 52: 71-82

Barker, S., Greaves, M., and Elderfield, H., 2003. A study of cleaning procedures used for foraminiferal Mg/Ca paleothermometry. *Geochem., Geophys., Geosys.,* 4-9. doi:10.1029/2003GC000559.

Bartoli, G., 2005. Short-term climate variability in the North Atlantic during the onset of northern hemisphere glaciation and the final closure of the Panamanian seaways, 3.3-2.5 Ma. *Ph.D-thesis*, University of Kiel.

Beaufort, L., Lancelot, Y., Camberlin, P., Cayre, O., Vincent, E., Bassinot, F., and Labeyrie, L., 1997. Insolation cycles as a major control of equatorial Indian Ocean primary production. *Science*, 278: 1451-1454

Bemis, B.E., Spero, H.J., Bijma, J., and Lea , D.W., 1998. Reevaluation of the oxygen isotopic composition of planktonic foraminifera: Experimental results and revised paleotemperature equations. *Paleoceanography,* 13: 150-160

Ben-Yaakov, S., 1973. pH Buffering of pore water of recent anoxic marine sediments. *Limnology and Oceanography*, 18: 86-94.

Berger, W.H. and Wefer, G., 1996. Central themes of South Atlantic circulation, in *The South Atlantic: Present and Past Circulation*, edited by G. Wefer et al., Springer-Verlag Berlin: 1-11

Berggren, W.A., and Hollister, C.D., 1974. Paleogeography, paleobiogeography, and the history of circulation of the Atlantic Ocean, in Studies in Paleoceanography, edited by W.W. Hay, *Spec. Publ.-Soc. Econ. Paleontol. Mineral*., 20: 126-186

Berner, R.A., Lasaga, A.C., and Garrels, R.M., 1983. The carbonate-silicate geochemical cycle and its effect on atmospheric carbon dioxide over the past 100 million years. *Am. J. Sci*., 283: 641-683.

Bickert, T., Curry,W.B., and Wefer, G., 1997. Late Pliocene to Holocene (2.6-0 Ma) western equatorial Atlantic deep-water circulation: Inferences from benthic stable isotopes, Leg 154. *Proc. Ocean Drill. Programm Sci. Results,* 154: 239-254

Billups, K., Ravelo, A.C., and Zachos, J.C., 1998a. Early Pliocene deep water circulation in the western equatorial Atlantic: implications for high-latitude climate change. *Paleoceanography*, 13: 84-95

Billups, K., Ravelo, A.C., and Zachos, J.C., 1998b. Early Pliocene climate: A perspective from the western equatorial Atlantic warm pool. *Paleoceanography*, 13: 459-470

Billups, K., Ravelo, A.C., Zachos, J.C., and Norris, R.D., 1999. Link between oceanic heat transport, thermohaline circulation, and the Intertropical Convergence Zone in the early Pliocene Atlantic. *Geology*, 27: 319-322.

Billups, K., and Schrag, D.P., 2002. Paleotemperature and ice volume of the past 27 Myr revisted with paired Mg/Ca and $^{18}O/^{16}O$ measurements on benthic foraminifera. *Paleoceanography*, 17 doi:10.1029/2000PA000567

Boyle, E.A., 1981. Cadmium, Zinc, Copper and Barium in foraminiferal tests. *Earth Planet. Sci. Lett*., 53: 11-35

Boyle, E.A. 1983. Manganese carbonate overgrowths on foraminiferal tests. *Geochim. Cosmochim. Acta*. 47: 1815-1819

Broecker, W.S., and Peng, T.H., 1982. Tracers in the Sea: Palisades, New York. 1-690.

Broecker, W.S., and Denton, G.H., 1989. The role of ocean-atmosphere reorganizations in glacial cycles. *Geochim. Cosmochim. Acta*, 53: 2465-2501.

Broecker, W.S., 1989. The salinity contrast between the Atlantic and Pacific oceans during glacial time. *Paleoceanography*, 4: 207-212

Broecker, W.S., and Clark, E., 2003. Role of sonification in shell weight measurements. *Geochem., Geophys., Geosys*., 4-11. doi:10.1029/2003GC000569

Brown, S.J., 1996. Controls on the trace metal chemistry of foraminiferal calcite and aragonite (Ph.D. dissert.). Univ. of Cambridge, UK.

Brown, S.J., and Elderfield, H., 1996. Variations in Mg/Ca and Sr/Ca ratios of planktonic foraminifers caused by postdepositional dissolution: Evidence of shallow Mg-dependant dissolution. *Paleoceanography*, 11: 543-551

Burgh, J.van der, Visscher, H., Dilcher, D.L., and Kürschner, W.M., 1993. Paleoatmospheric signatures in Neogene fossil leaves. *Science*, 260: 1788-1790.

Cane, M.A., and Molnar, P., 2001. Closing of the Indonesian seaway as a precursor to east African aridification around 3-4 million years ago. *Nature*, 411: 157-162.

Cannariato, K.G., and Ravelo, A.C., 1997. Pliocene-Pleistocene evolution of eastern tropical Pacific surface water circulation and thermocline depth. *Paleoceanography*, 12-6: 805-820.

Chaisson, W.P., 1995. Planktonic foraminiferal assemblages and paleoceanographic change in the trans-tropical Pacific Ocean: a comparison of west (leg 130) and east (leg 138), latest Miocene to Pleistocene. In Pisias, N.G., Mayer, L.A., Palmer-Julson, A., Janecek, T.R., and Andel, T.H.van (Eds). *Proc. ODP, Sci. Results*, 138: College Station, TX (Ocean Drilling Program), 555-581.

Chaisson, W.P., and Ravelo, A.C., 2000. Pliocene development of the east-west hydrographic gradient in the equatorial Pacific. *Paleoceanography*, 15-5: 497-505.

Chave, K. E., 1954. Aspects of biochemistry of magnesium: 1. Calcareous marine organisms, *J. Geol*., 62: 266-283

Coates, A.G., Jackson, J.B.C., Collins, L.S., Cronin, T.M., Dowsett, H.J., Bybell, L.M., Jung, P., and Obando, J.A., 1992. Closure of the Isthmus of Panama: The near-shore marine record of Costa Rica and western Panama, *Geol. Soc. Am. Bull.,* 104: 814-828

Coates, A.G., and Obando, J.A., 1996. The geological evolution of the Central American Isthmus. In Jackson, J.B.C., Budd, A.F., Coates, A.G. (eds). *Evolution and environment in tropical America*. Univ. of Chicago Press, Chicago, Illinois: 21-56

Coates, A.G., Collins, L.S., Aubry, M-P., Berggren, W.A., 2004. The Geology of the Darien, Panama, and the late Miocene-Pliocene collision of the Panama arc with northwestern South America. *Geol. Soc. Am. Bull*, 116: 1327-1344

Collins, L.S, Coates, A.G., Berggren, W.A., Aubry, M.P., and Zhang, J., 1996. The Late Miocene Panama isthmiam strait. *Geology*, 24: 687-690

Cronblad H.G., and Malmgren, B.A., 1981. Climatically controlled variation of Sr and Mg in Quaternary planktic foraminifera. *Nature*, 291: 61-64

Cronin, T.M., Whatley, R., Wood, A., Tsukagoshi, A., Ikeya, N., Brouwers, E.M., and Briggs Jr., W.M., 1993. Microfaunal evidence for elevated Pliocene temperatures in the Arctic Ocean. Paleoceanography, 8: 161-173

Crowley, T.J., 1991. Past CO2 changes and tropical sea surface temperatures. *Paleoceanography*, 6: 387-394

Crowley, T.J., 1992. North Atlantic Deep Water cools the Southern Hemisphere. *Paleoceanography*, 7: 489-497

Crowley, T.J., 1996. Pliocene climates: the nature of the problem. *Mar. Micropaleontol*., 27: 3-12

Crudeli, D., and Kinkel, H., 2004. Reticulofenestra calicis n. sp., an unusual small reticulofenestrid coccolith from the Lower Pliocene of the South Caribbean Sea. *Micropaleontology*, 50: 369-379

Crudeli, D., 2005. Evolution of coccolithophores during the early Pliocene: Implication ofr taxonomy, biostratigraphy, paleoecology and paleoceanography (Caribbean Sea). *Ph.D-thesis*, University of Kiel.

Curry, W.B., Thunell, R.C., and Honjo, S., 1983. Seasonal changes in the isotopic composition of planktonic foraminifera collected in Panama Basin sediment traps. *Earth Planet. Sci. Lett*., 64: 33-43

DeConto, R.M., and Pollard, D., 2003. Rapid Cenozoic glaciation of Antarctica induced by declining atmospheric CO_2. *Nature*, 421: 245-249

DeDeckker, P., and Corriège, T., 1992. A new palaeothermometer: The magnesium to calcium ratio in benthic ostracod valves, Abstract, *Fourth International Conference on Paleoceanography ICP IV*, September 21.-25, 1992, Kiel, 92

de Garidel-Thoron, T., Beaufort, L., Linsley, B.K., and Dannenmann, S., 2001. Millennial-scale dynamics of the East Asian winter monsoon during the last 200,000 years. *Paleoceanography* 16: 1-12

Dekens, P.S., Lea, D.W., Pak, D.K., and Spero, H.J., 2002. Core top calibration of Mg/Ca in tropical foraminifera: Refining paleotemperature estimation. *Geochem., Geophys., Geosys*., 3: doi:10.1029/2001GC000200

Delaney, M.L., Bé, A.W.H., and Boyle, E.A., 1985. Li, Sr, Mg, Na in foraminiferal calcite shells from laboratory culture, sediment traps, and sediment cores. *Geochim. Cosmochim. Acta*, 49: 1327-1341

Delaney, M.L., 1989. Temporal changes in interstitial water chemistry and calcite recrystallization in marine Sediments. *Earth Planet. Sci. Lett.,* 95: 23-37

Dengo, G., 1985. Tectonic setting for the Pacific margin from southern Mexico to Northwestern Columbia. In Nairn, A.E., Stehli, F.G., and Uyeda, S. (eds), *The Pacific Ocean: The ocean basins and margins,* 7A. Plenum Press, New York: 123-180

Donguy, J.R., and Meyers, G., 1996. Mean annual variation of transport of major currents in the tropical Pacific Ocean. *Deep-Sea Res. Part I*, 43-7: 1105-1122.

Dowsett, H.J., and Poore, R.Z., 1991. Pliocene sea surface temperatures of the North Atlantic Ocean at 3.0 Ma. *Quat. Sci. Rev*., 10: 189-204.

Dowsett, H.J., Barron, J., and Poore, R., 1996. Middle Pliocene sea surface temperatures: a global reconstruction. *Mar. Micropaleontology*, 27: 13-25.

Driscoll, N.W., and Haug, G.H., 1998. A short circuit in thermohaline circulation: A cause for Northern Hemisphere Glaciation? *Science*, 282: 436-438

Duckworth, D.L., 1977. Magnesium concentration in the tests of the planktic foraminifer Globorotalia truncatulinoides. *J. Foram. Res.*, 7: 304-312

Duque-Caro, H., 1990. Neogene stratigraphy, paleoceanograpy and paleobiogeography in northwest South America and the evolution of the Panama Seaway. *Palaeogeogr., Palaeoclimat., Palaeoecol*., 77: 203-234

Eggins, S., De Deckker, P., and Marshall, J., 2003. Mg/Ca variation in planktonic foraminifera shells: Implications for reconstruction of paleoseawater temperature and habitat migration, *Earth Planet. Sci. Lett*., 212: 291-306

Elderfield, H., and Schultz, A., 1996. Mid-ocean ridge hydrothermal fluxes and the chemical composition of the ocean. *Ann. Rev. Earth Plan. Sci*., 24: 191-224.

Elderfield, H., and Ganssen, G., 2000. Past temperature and $\delta^{18}O$ of surface ocean waters inferred from foraminiferal Mg/Ca ratios. *Nature*, 405: 442-445

Epstein , S., Buchsbaum, R., Lowenstamm, H.A., and Urey, H.C., 1953. Revised carbonate-water isotopic temperature scale. *Geol. Soc. Am. Bull*., 64: 1315-1325

Erez, J., and Luz, B., 1983. Experimental paleotemperature equation for planktonic foraminifera. *Geochim. Cosmochim. Acta*, 47: 1025-1031

Fairbanks, R.G., Sverdlove, M., Free, R., Wiebe, P.H., and Be, A.W.H., 1982. Vertical distribution and isotopic fractionation of living planktonic foraminifera from the Panama Basin. *Nature*, 298: 841-844.

Ferguson, J.E., Henderson, G.M., Kucera, M., and Rickaby, R.E.M., 2005. Control of trace element incorporation into planktonic foraminifera across a strong salinity and nutrient gradient in the Mediterranean Sea. *Geophysical Research Abstracts*, 7: EGU05-A-07302

Frank, M., Reynolds, B.C., and O'Nions, R.K., 1999. Nd and Pb isotopes in Atlantic and Pacific water masses before and after closure of the Panama gateway: *Geology*, 27: 1147-1150

Gieskes, J.M., and Lawrence, J.R., 1981. Alteration of volcanic matter in deep sea sediments, evidence from the chemical composition of interstitial waters from deep sea drilling cores. *Geochim. Cosmochim. Acta*, 45: 1687-1703.

Given, R.K., and Wilkinson, B.H., 1985. Kinetic control of morphology, composition, and mineralogy of abiotic sedimentary carbonates. *J. Sediment. Petrol*., 55: 109-119

Greaves, M., Barker, S., Daunt, C., and Elderfield, H., 2005. Accuracy, standardization, and interlaboratory calibration standards for foraminiferal Mg/Ca thermometry. Geochem., Geophys., Geosys. 6: Q02D13. doi:10.1029/2004GC000790

Günther, D., Frischknecht, R., Heinrich, C.A., and Kahlert, H.J., 1997. Capabilities of a 193 nm ArF excimer laser for LA-ICP-MS micro analysis of geological materials, *J. Analyt. Atom. Spectrom*., 12: 939-944.

Halpern, D., and Weisberg, R., 1989. Upper ocean thermal and flow fields at 0°, 28°W (Atlantic) and 0°, 140W (Pacific) during 1983-1985. *Deep-Sea Res. Part A*, 36: 407-418.

Hampt, G., and Delaney, M.L., 1997. Influences of calcite Sr/Ca records from Ceara Rise and other regions: Distinguishing ocean history and calcite recrystallization, *Proc. ODP Sci. Results*, 154: 491-500

Hastings, D.W., Emerson, S., Erez, J., and Nelson, B.K., 1996. Vanadium in foraminiferal calcite: Evaluation of a method to determine paleo seawater vanadium concentrations. *Geochim. Cosmochim. Acta*, 60: 3701-3715

Hastings, D., Russell, A.D., and Emerson, S.R., 1998. Foraminiferal magnesium in Globeriginoides sacculifer as a paleotemperature proxy. Paleoceanography, 13: 161-169

Hathorne, E.C., Alard, O., James, R.H., and Rogers, N.W., 2003. Determination of intratest variability of trace elements in foraminifera by Laser Ablation ICP-MS. *Geochem., Geophys., Geosys*., 4: doi:10.1029/2003GC000539

Haug, G.H., and Tiedemann, R., 1998. Effect of the formation of the Isthmus of Panama on Atlantic Ocean thermohaline circulation. *Nature*, 393: 673-676.

Haug, G.H., Hughen, K.A., Sigman, D.M., Peterson, L.C., and Röhl, U., 2001. Southward migration of the Intertropical Convergence Zone through the Holocene. *Science*, 293: 1304-1308

Haug, G.H., Tiedemann, R., Zahn, R., and Ravelo, A.C., 2001. Role of Panama uplift on Oceanic freshwater balance. *Geology*, 29-3: 207-210.

Haug, G.H., Ganopolski, A., Sigman, D.M., Rosell-Mele, A., Swann, G.E.A., Tiedemann, R., Jaccard, S.L., Bollmann, J., Maslin, M.A., Leng, M.J., and Eglinton, G., 2005. North Pacific seasonality and the glaciation of North America 2.7 million years ago. *Nature*, 433: 821-825

Hellweger, F.L., and Gordon, A.L., 2002. Tracing Amazon River water into the Caribbean Sea. *J. Mar. Res*., 60: 537-549

Hodell, D.A., and Warnke, D.A., 1991. Climate evolution of the Southern Ocean during the Pliocene epoch from 4.8 to 2.6 million years ago. *Quatern.Sci.Rev*., 10: 205-214

Hoernle, K., Bogaard, P. v.d., Werner, R., Lissinna, B., Hauff, F., Alverado, G., and Garbe-Schönberg, D., 2002. Missing history (16-71 Ma) of the Galápagos hotspot: Implications for the tectonic and biological evolution of the Americas. *Geology*, 30: 795-798.

Hovan, S.A. 1995. Late Cenozoic atmospheric circulation intensity and climatic history recorded by eolian deposition in the eastern equatorial Pacific Ocean, leg 138 In Pisias, N.G., Mayer, L.A., Palmer-Julson, A., Janecek, T.R., and Andel, T.H.van (Eds). *Proc. ODP, Sci. Results*, 138: College Station, TX (Ocean Drilling Program), 615-625.

Huber, M., 2002. Straw Man 1: A preliminary view of the tropical Pacific from a global coupled climate model simulation of the early Paleogene. In Lyle, M., Wilson, P.A., and Janecek, T.R. (Eds). *Proc. ODP, Init. Repts.,* 202: College Station, TX (Ocean Drilling Program), Chap. 3.

Imbrie, J., and Kipp, N.G., 1971. A new micropaleontological method for quantitative paleo-climatology: Application to a late Pleistocene Caribbean core, in K.K. Turekian (ed.), *The Late Cenozoic Glacial Ages*, Yale Univ. Press, New Haven, C.T.: 1-81

Izuka, S.K., 1988. Relationship of magnesium and other minor elements in tests of *Cassidulina subglobosa* and *corriangulata* to physical oceanic properties. *J. Foram. Res*., 18: 151-157

Jansen, E., Sjoholm, S., Bleil, U., and Erichsen, J.A., 1990. Neogene and Pleistocene glaciations in the northern hemisphere and late Miocene-Pliocene global ice volume fluctuations: Evidence from the Norwegian Sea. In: Geological history of the polar oceans: Arctic versus Antarctic. U.Bleil, J.Thiede (eds). Kluwer Acad. Norwell. Mass. 677-5

Johns, W.E., Townsend, T.L., Fratantoni, D.M., and Wilson, W.D., 2002. On the Atlantic inflow to the Caribbean Sea. *Deep-Sea Res.* 49: 211-243

Kameo, K., and Sato, T., 2000. Biogeography of Neogene calcareous nannofossils in the Caribbean and the eastern equatorial Pacific – floral response to the emergence of the Isthmus of Panama. *Mar. Micropaleontology*, 39: 201-218

Katz, A., Sass, E., Starinsky, A., and Holland, H.D., 1972. Strontium behavior in the aragonite-calcite transformation: an experimental study at 40-98°C, *Geochim. Cosmochim. Acta*, 36: 481-496

Keigwin, L., 1982. Isotopic paleoceanography of the Caribbean and east Pacific: Role of Panama uplift in Late Neogene time. *Science*, 217: 350-353

Keller, G., Zenker, C.E., and Stone, S.M., 1989. Late Neogene history of the Pacific-Caribbean gateway. *J. South Am. Earth Sci*., 2: 73-108

Kennett, J.P., and Hodell, D.A., 1993. Evidence for relative climate stability of Antarctica during the early Pliocene: A marine perspective. *Geograph. Ann*., 75: 205-220

Killingley, J.S., 1983. Effects of diagenetic recrystallization on $^{18}O/^{16}O$ values of deep-sea sediments. *Nature*, 301: 594-597

Kleiven, H.F., Jansen, E., Fronval, T., and Smith, T.M., 2002. Intensification of Northern Hemisphere glaciations in the circum Atlantic region (3.5-2.4 Ma) – ice-rafted detritus evidence. *Palaeogeogr., Palaeoclimatol., Palaeocol*., 184: 213-223.

Krinsley D., 1960. Trace elements in the tests of planktic foraminifera. *Micropal*., 63: 297-300

Kwiek, P.B., and Ravelo, A.C., 1999. Pacific Ocean intermediate and deep water circulation during the Pliocene. *Palaeogeogr., Palaeoclimatol., Palaeocol*., 154: 191-217.

Laskar, J., 1990. The chaotic motion of the solar system: A numerical estimate of the size of the chaotic zones. *Icarus*, 88: 266-291.

Lea, D.W., Mashiotta, T.A., and Spero, H.J., 1999. Controls on magnesium and strontium uptake in planktonic foraminifera determined by live culturing. *Geochim. Cosmochim. Acta*, 63: 2369-2379

Lea, D.W., Pak, D.K., and Spero, H.J., 2000. Climate impact of Late Quaternary Equatorial Pacific sea surface temperature variations. *Science*, 289: 1719-1724.

Lea, D.W., Martin, P.A., Pak, D.K., and Spero, H.J., 2002. Reconstructing a 350 k.y. history of sea level using planktonic Mg/Ca and oxygen isotope records from a Cocos Ridge core. *Quat. Sci. Rev*., 21: 283-293.

Lea, D.W., 2003. Elemental and isotopic proxies of past ocean temperatures. in H. Elderfield (ed), *The oceans and marine geochemistry*, Elsevier-Pergamon, Oxford: 365-390

Lear, C.H., Elderfield, H., and Wilson, P.A., 2000. Cenozoic deep-sea temperatures and global ice volumes from Mg/Ca in benthic foraminiferal calcite. *Science*, 287: 269-272

Levitus, S., and Boyer, T.P., 1994. *World Ocean Atlas 1994, (Vol. 3): Salinity*. NOAA Atlas NESDIS 4.

Levitus, S., and Boyer, T.P, 1994. *World Ocean Atlas 1994, (Vol. 4): Temperature*. NOAA Atlas NESDIS 4.

Li, X.S., Berger, A., Loutre, M.F., Maslin, M.A., Haug, G.H., and Tiedemann, R., 1998. Simulating late Pliocene Northern Hemisphere climate with the LLN 2-D model. *Palaeogeogr., Palaeoclimatol., Palaeocol*., 25-6: 915-918.

Lisiecki, L.E., and Raymo, M.E., 2005. A Pliocene-Pleistocene stack of 57 globally distributed benthic $\delta^{18}O$ records. *Paleoceanography*, 20: doi:10.1029/2004PA001071

Lohmann, G.P., 1995. A model for variation in the chemistry of planktonic foraminifera due to secondary calcification and selective dissolution. *Paleoceanography*, 10: 445-457

Lundelius, E.L. Jr., Churcher, C.S., Downs, T., Harrington, C.R., Lindsay, E., Schultz, G.E., Holmes, A. Semken, Jr., Webb, S.D., and Zakrzewski, R.J., 1987. The North American Quaternary Sequence, 211-235. in M.O. Woodburne, ed., *Cenozoic Mammals of North America: Geochronology and Biostratigraphy*. University of California Press. Berkeley: 336 pp.

Lyle, M., Dadey, K.A., and W.Farrell, J., 1995. The Late Miocene (11-8 Ma) eastern Pacific carbonate crash: Evidence for reorganization of deep-water circulation by the closure of the Panama Gateway. In Pisias, N.G., Mayer, L.A., Palmer-Julson, A., Janecek, T.R., and Andel, T.H.van (Eds). *Proc. ODP, Sci. Results* 138: College Station, TX (Ocean Drilling Program), 821-838.

Lyons, T.W., Murray, R.W., and Pearson, D.G., 2000. A comparative study of diagenetic pathways in sediments of the Caribbean Sea: Highlights from pore-water results. In: Leckie, R.M., H. Sigurdsson, G.D. Acton, G. Draper (eds). *Proc. ODP, Sci. Results*, 165: 287-298

Maier-Reimer, E., Mikolajewicz, U., and Crowley, T., 1990. Ocean general circulation model sensitivity experiment with an open central american isthmus. *Paleoceanography*, 5-3: 349-366.

Malone, M.J., Baker, P., Burns, S., and Swart, P., 1990. Geochemistry of periplatform carbonate sediments, Ocean Drilling Programm Site 716 (Maldives Archipelago, Indian Ocean). *Proc. ODP, Sci. Results*, 115, 647-659.

Marshall, L.G., Webb, S.D., Sepkosko Jr., J.J., and Raup, D.M., 1982. Mammalian evolution and the great american interchange. *Science*, 215: 1351-1357

Martin, P.A., and Lea, D.W., 2002. A simple evaluation of cleaning procedures on fossil benthic foraminiferal Mg/Ca. *Geochem., Geophys., Geosys*., 3: doi:2001GC000280

Mashiotta, T.A., Lea, D.W., and Spero, H.J., 1999. Glacial-interglacial changes in Subantarctic sea surface temperature and $\delta^{18}O$-water using foraminiferal Mg. *Earth Planet. Sci. Letters*, 170: 417-432

McKenna, V.S., and Prell, W.L., 2004. Calibration of the Mg/Ca of *Globorotalia truncatulinoides* (right) for the reconstruction of marine temperature gradients. *Paleoceanography*, 19: doi:10.1029/2000PA000604

Melim, L.A., Westphal, H., Swart, P.K., Eberli, G.P., and Munnecke, A., 2002. Questioning carbonate diagenetic paradigms: evidence from the Neogene of the Bahamas. *Mar. Geol*., 185: 27-53

Mikolajewicz, U., and Crowley. T.J., 1997. Response of a coupled ocean/energy balance model to restricted flow through the Central American Isthmus. *Paleoceanography* 12: 429-441

Mitchell, T.P., and Wallace, J.M., 1992. The annual cycle of equatorial convection and sea surface temperature. *J. Clim*., 5: 1140-1156.

Mix, A. C., Pisias, N.G., Rugh, W., Wilson, J., Morey, A., and Hagelberg, T. K., 1995. Benthic foraminifer stable isotope record from Site 849 (0-5 Ma): Local and global climate changes. *Proc. ODP, Sci. Results*, 138: 371-412

Mix, A.C., Tiedemann, R., and Blum, P., 2003. *Proc. ODP, Init. Repts*., 202: College Station, TX (Ocean Drilling Program).

Molfino, B., and McIntyre, A., 1990. Precessional forcing of nutricline dynamics in the equatorial Atlantic. *Science*, 249: 766-769

Molnar, P., and Cane, M.A., 2002. El Niño's tropical climate and teleconnections as a blueprint for pre-Ice Age climates. *Paleoceanography*, 17: 10.1029/2001PA000663.

Morse, J.W., and Bender, M.L., 1990. Partition coefficients in calcite: Examination of factors influencing the validity of experimental results and their application to natural systems. *Chem. Geol*., 82: 265-277

Morse, J.W., and Mackenzie, F.T., 1990. *Geochemistry of Sedimentary Carbonates*, 707 pp., New York, Elsevier.

Mottle, M.J., and Wheat, G., 1994. Hydrothermal circulation through mid-ocean ridge flanks: Fluxes of heat and magnesium. *Geochim. Cosmochim. Acta*, 58: 2225-2237.

Mucci, A., and Morse, J.W., 1983. The incorporation of Mg^{2+} and Sr^{2+} into calcite overgrowths: influences of growth rate and solution composition, *Geochim. Cosmochim. Acta*, 47: 217-233

Müller, A., 2000. Mg/Ca- und Sr/Ca-Verhältnisse in biogenem Carbonat planktischer Foraminiferen und benthischer Ostracoden. PhD-thesis, University of Kiel, Germany

Müller, P.J., Kirst, G., Ruhland, G., Storch, I.V., and Rosell-Melé, A., 1998. Calibration of the alkenone paleotemperature index $U^{K'}_{37}$ based on core-tops from the eastern South Atlantic and the global ocean (60°N-60°S). *Geochim. Cosmochim. Acta*, 62: 1757-1772

Munnecke, A., Westphal, H., Reijmer, J.J.G., and Samtleben, C., 1997. Microspar development during early marine burial diagenesis: a comparison of Pliocene carbonates from the Bahamas with Silurian limestones from Gotland (Sweden). *Sedimentology*, 44: 977-990.

Nisancioglu, K.H., Raymo, M.E., and Stone, P.H., 2003. Reorganization of Miocene deep water circulation in response to the shoaling of the Central American Seaway. *Paleoceanography*, 18: doi:10.1029/2002PA000767

Nof, D., and van Gorder, S., 2002. Did an open Panama Isthmus correspond to an invasion of pacific water into the Atlantic? *J. Phys. Oceanogr*., 33: 1324-1336

Nürnberg, D., 1995. Magnesium in tests of *Neogloboquadrina Pachyderma* sinistral from high northern and southern latitudes, *J. Foraminiferal Res*., 25: 350-368

Nürnberg, D., Bijma, J., and Hemleben, C., 1996. Assessing the reliability of magnesium in foraminiferal calcite as a proxy for water mass temperatures. *Geochim. Cosmochim. Acta*, 60: 803-814

Nürnberg, D., 2000. Taking the temperature of past ocean surfaces. *Science*, 289: 1698-1699.

Nürnberg, D., Müller, A., and Schneider, R.R., 2000. Paleo-sea surface temperature calculations in the equatorial east Atlantic from Mg/Ca ratios in planktic foraminifera: A comparison to sea surface temperature estimates from Uk37, oxygen isotopes, and foraminiferal transfer function. *Paleoceanography*, 15-1: 124-134.

Paillard, D., Labeyrie, L., and Yiou, P., 1996. Macintosh program performs time-series analysis. *EOS Trans*. AGU, 77: 379.

Pearce, N. J. G., Perkins, W.T., Westgate, J.A., Gorton, M.P., Jackson, S.E., Neal, C.R., and Chenery, S.P., 1997. A compilation of new and published major and trace element data for NIST SRM 610 and NIST SRM 612 glass reference materials, *Geostandards Newsletter*, 21: 115-144

Pena, L. D., Calvo, E., Cacho, I., Eggins, S., and Pelejero, C., submitted. Identification and removal of Mn-Mg-rich contaminant phases in foraminiferal tests: Implications for Mg/Ca past temperature reconstructions. *Geochem. Geophys. Geosyst*., doi:10.1029/2005GC000930

Petschick, R., 1999. *MacDiff*, Johann Wolfgang von Goethe-Universität, Frankfurt am Main.

Pflaumann, U., Sarnthein, M., Chapman, M., d'Abreu, L., Funnel, B., Huels, M., Kiefer, T., Maslin, M., Schulz, H., Swallow, J., van Krefeld, S., Vautravers, M., Vogelsang, E., and Weinelt, M., 2003. Glacial North Atlantic: Sea-surface conditions reconstructed by GLAMAP 2000. *Paleoceanography*, 18: 1065, doi:10.1029/2002PA000774

Pisias, N.G., Mayer, L.A., and Mix, A.C., 1995. Paleoceanography of the eastern equatorial Pacific during the Neogene: Synthesis of Leg 138 drilling results. In Pisias, N.G., Mayer, L.A., Palmer-Julson, A., Janecek, T.R., and Andel, T.H.van (Eds). *Proc. ODP, Sci. Results*: College Station, TX (Ocean Drilling Program), 5-21.

Prahl, F.G., and Wakeham, S.G., 1987. Calibration of unsaturation patterns in long-chain ketone compositions for paleotemperature assessment. *Nature*, 330: 367-369

Prahl, F.G., Muehlhausen, L.A., and Zahnle, D.I., 1988. Further evaluation of long-chain alkenones as indicators of paleoceanographic conditions. *Geochim. Cosmochim. Acta*, 52: 2303-2310

Prange, M., and Schulz. M., 2004. A coastal upwelling seesaw in the Atlantic Ocean as a results of the closure of the Central American Seeway. *Geophys. Res. Lett*., 31: L17207. doi:10.1029/2004GL020073

Puechmaille, C., 1985. Teneurs en strontium et magnésium dans les tests de foraminifères planctoniques - Premiers indices de l´altération post-mortem. *Bull. Inst. Geol. Bassin d'Aquitaine*, 38: 81-94

Ravelo, A.C., and Shackleton, N.J., 1995. Evidence for surface-water circulation changes at Site 851 in the eastern tropical Pacific Ocean. In Pisias, N.G., Mayer, L.A., Palmer-Julson, A., Janecek, T.R., and Andel, T.H.van (Eds). *Proc. ODP, Sci. Results*, 138: College Station, TX (Ocean Drilling Program), 503-514.

Ravelo, A.C., and Andreasen, D.H., 2000. Enhanced circulation during a warm period. *Geophys. Res. Lett*., 27-7: 1001-1004.

Ravelo, A.C., Andreasen, D.H., Lyle, M., Lyle, A.O., and Wara, M.W., 2004. Regional climate shifts caused by gradual global cooling in the Pliocene epoch. *Nature*, 429: 263-267.

Raymo, M.E., Ruddiman, W.F., Backman, J., Clement, B.M., and Martinson, D.G., 1989. Late Pliocene variation in Northern Hemisphere ice sheets and North Atlantic deep water circulation. *Paleoceanography*, 4-4: 413-446.

Raymo, M.E., Grant, B., Horowitz, M., and Rau, G.H., 1996. Mid-Pliocene warmth: stronger greenhouse and stronger conveyor. *Mar. Micropaleontol*., 27: 313-326.

Raymo, M.E., 1998. Glacial Puzzles. *Science*, 281: 1467-1468.

Regenberg, M., Nürnberg, D., Steph, S., Groeneveld, J., Garbe-Schönberg, D., Tiedemann, R., Dullo, W.-F., submitted. Assessing the dissolution effect on planktonic foraminiferal Mg/Ca: Evidence from Caribbean core-tops.

Reichart, G.J., Jorissen, F., Anschutz, P., and Mason, P.R.D., 2003. Single foraminiferal test chemistry records the marine environment. *Geology*, 31: 355-358

Reuning, L., Reijmer, J.J.G., Betzler, C., Swart, P., and Bauch, T., 2005. The use of paleoceanographic proxies in carbonate periplatform settings – opportunities and pitfalls, *Sediment. Geol*., in press

Ries, J.B., 2004. Effect of ambient Mg/Ca ratio on Mg fractionation in calcareous marine invertebrates: A record of the oceanic Mg/Ca ratio over the Phanerozoic. *Geology*, 32: 981-984.

Rosell-Mélé, A., Bard, E., Emeis, K.-C., Farrimond, P., Grimalt, J., Müller, P.J., and Schneider, R., 1998. Project takes a new look at past sea surface temperatures, *EOS*, Transactions AGU, 79(33): 393-394

Rosenthal, Y., and Boyle, E., 1993. Factors controlling the fluoride content of planktonic foraminifera: An evaluation of its paleoceanographic applicability. *Geochim. Cosmochim. Acta*, 57: 335-346

Rosenthal, Y., Lohmann, G.P., Lohmann, K.C., and Sherrell, R.M., 2000. Incorporation and preservation of Mg in *Globigerinoides sacculifer*: Implications for reconstructing the temperature and $^{18}O/^{16}O$ of seawater. *Paleoceanography*, 15: 135-145

Rosenthal, Y., and Lohmann, G.P., 2002. Accurate estimation of sea surface temperatures using dissolution-corrected calibrations for Mg/Ca paleothermometry. *Paleoceanography*, 17: doi:10.1029/2001PA000749

Rosenthal, Y., Perron-Cashman, S., Lear, C.H., Bard, E., Barker, S., Billups, K., Bryan, M., Delaney, M.L., deMenocal, P., Dwyer, G.S., Elderfield, H., German, C.R., Greaves, M., Lea, D.W., Marchitto Jr., T.M., Pak, D.K., Paradis, G.L., Russell, A.D., Schneider, R.R., Scheiderich, K., Stott, L., Tachikawa, K., Tappa, E., Thunell, R., Wara, M., Weldeab, S., and Wilson, P.A. (2004). Interlaboratory comparison study of Mg/Ca and Sr/Ca measurements in planktonic foraminifera for paleoceanographic research. *Geochem., Geophys., Geosys*., 5-4: Q04D09, doi: 10.1029/2003GC000650

Ruddiman, W.F., and Raymo, M., 1988. Northern Hemisphere climate regimes during the past 3 Ma: possible tectonic connections. *Phil. Trans. R. Soc. London B*, 318: 411-430.

Russell, A.D., Emerson, S., Nelson, B.K, Erez, J., and Lea, D.W., 1994. Uranium in foraminiferal calcite as a recorder of seawater uranium concentrations. *Geochim. Cosmochim. Acta*, 58: 671-681

Sanyal, A., Hemming, N.G., Hanson, G.N., and Broecker, W.S., 1995. Evidence for a higher pH in the glacial ocean from boron isotopes in foraminifera. *Nature*, 373: 234-236

Savin, S. M., and Douglas, R.G., 1973. Stable isotope and magnesium geochemistry of Recent planktic foraminifera from the South Pacfic. *Geol. Soc. Am. Bull.,* 84: 2327-2342

Savin, S.M., and Douglas, R.G., 1985. Sea level, climate, and the Central American Land Bridge. in The Central American *Land Bridge*, edited by F. G. Stehli and S. D. Webb, Plenum Press, 303-324

Schmidt, M.W., Spero, H.J., and Lea, D.W., 2004. Links between salinity variation in the Caribbean and North Atlantic thermohaline circulation. *Nature*, 428: 160-163.

Schrag, D.P., DePaolo, D.J., and Richter, F.M., 1995. Reconstructing past sea surface temperatures: Correcting for diagenesis of bulk marine carbonate, *Geochim. Cosmochim. Acta*, 59: 2265-2278

Shackleton, N.J., 1974. Attainment of isotope equilibrium between ocean water and the benthonic foraminiferal genus *Uvigerina*. Isotopic changes in the ocean during the last glacial. *Cent. Nat.Rech.Sci.Colloq.Int*., 219: 203-209.

Shackleton, N.J., Hall, M.A., and Pate, D., 1995. Pliocene stable isotope stratigraphy of site 846. In Pisias, N.G., Mayer, L.A., Palmer-Julson, A., Janecek, T.R., and Andel, T.H.van (Eds). *Proc. ODP, Sci. Results*, 138: College Station, TX (Ocean Drilling Program), 337-353.

Shackleton, N.J. and M.A. Hall, 1997. The Late Miocene stable isotope record, site 926. *Proc. Ocean Drill. Program, Sci. Results*, 154: 367-373

Sigurdsson, H., Leckie, R.M., Acton, G.D., et al., 1997. *Proc. ODP, In. Repts*, 165, College Station, TX (Ocean Drilling Program)

Stanley, S.M., and Hardie, L.A., 1998. Secular oscillations in the carbonate mineralogy of reef-building and sediment-producing organisms driven by tectonically forced shifts in seawater chemistry. *Palaeogeogr., Palaeoclimatol., Palaeoecol*., 144: 3-19.

Stehli, F.G., and Webb, S.D., eds., 1985. *The Great American Biotic Interchange*. Plenum Press, New York: 523 pp

Steph, S., Tiedemann, R., Groeneveld, J., Nürnberg, D., Reuning, L., and Haug, G.H. submitted. Changes in Caribbean surface hydrography during the Pliocene shoaling of the Central American Seaway. *Paleoceanography*

Steph, S., 2005. Pliocene stratigraphy and the impact of Panama uplift on changes in Caribean and tropical east Pacific upper ocean stratification (6-2.5 Ma). *Ph.D-thesis*. University of Kiel.

St. John, K., and Krissek, L.A., 2002. The late Miocene to Pleistocene ice-rafting history of southeast Greenland. *Boreas*, 31: 28-35.

Stott, L., Poulsen, C., Lund, S., and Thunell, R., 2002. Super ENSO and global climate oscillations at millenial time scales. *Science*, 297: 222-226

Swart, P.K., and Guzikowski, M., 1988. Interstitial water chemistry and diagenesis of periplatform sediments from the Bahamas, ODP Leg 101. *Proc. ODP, Sci. Results*, 101: 363-380

Tiedemann, R., Sarnthein, M., and Stein, R., 1989. Climatic changes in the western Sahara: Paleomarine sediment record of the last 8 million years (Sites 657-661). In Ruddiman, W., Sarnthein, M., et al. (Eds) *Proc. ODP, Sci. Results*, 108: College Station, TX (Ocean Drilling Program), 108, 241-277.

Tiedemann, R., Sarnthein, M., and Shackleton, N.J., 1994. Astronomic timescale for the Pliocene Atlantic $\delta^{18}O$ and dust flux records of Ocean Drilling Program Site 659. *Paleoceanography*, 9-4: 619-638.

Tiedemann, R., and Franz, S.O., 1997. Water circulation, chemistry, and terrigenous sediment supply in the Equatorial Atlantic during the Pliocene, 3.3-2.6 Ma and 5-4.5 Ma. In Shackleton, N.J., Curry, W.B., and Bralower, T.J. (Eds). *Proc. ODP, Sci. Results*, 154: College Station, TX (Ocean Drilling Program), 299-318.

Tiedemann, R., Sturm, A., Steph, S., Lund, S.P., and Stoner, J.S., submitted. Astronomically calibrated time scales from 6-2.5 Ma and benthic isotope stratigraphies of Sites 1236, 1237, 1239, and 1241.

Tripati, A.K., Delaney, M.L., Zachos, J.C., Anderson, L.D., Kelly, D.C., and Elderfield, H., 2003. Tropical sea-surface temperature reconstruction for the early Paleogene using Mg/Ca ratios of planktonic foraminifera. *Paleoceanography*, 18-4. doi:10.1029/2003PA000937.

Villiers, S. de, Greaves, M., and Elderfield, H., 2002. An intensity method for the accurate determination of Mg/Ca and Sr/Ca of marine carbonates by ICP-AES. *Geochem., Geophys., Geosyst*., 3: doi:10.1029/2001GC000169

Villiers, S. de (2003). Dissolution effects on foraminiferal Mg/Ca records of sea surface temperature in the western equatorial Pacific. *Paleoceanography,* 18: doi:10.1029/2002PA000802

Villiers, S. de (2003). A 425 kyr record of foraminiferal shell weight variability in the western equatorial Pacific. *Paleoceanography*, 18: doi:10.1029/2002PA000801

Visser, K., Thunell, R., and Stott, L., 2003. Magnitude and timing of temperature change in the Indo-Pacific warm pool during deglaciation. *Nature*, 421: 152-155

Wallace, J.M., Rasmusson, E.M., Mitchell, T.P., Kousky, V.E., Sarachik, E.S., and Storch, H.von, 1998. On the structure and evolution of ENSO-related climate variability in the tropical Pacific: Lessons from Toga. *J. Geophys. Res*., 103: 14.241-14.259.

Wang, L., 1994. Sea surface temperature history of the low latitude western Pacific during the last 5.3 million years. *Palaeogeogr., Palaeoclimatol., Palaeoecol*., 108: 379-436.

Webb, S.D, 1985. Late Cenozoic mammal dispersals between the Americas. In: Stehli, F.G., and Webb, S.D., (Eds.), *The Great American Biotic Interchange*, New York (Plenum Press): 357-386

Webb, P.N., and Harwood, D.M., 1991. Late Cenozoic glacial history of the Ross Embayment, Antarctica. *Quatern. Sci. Rev*., 10: 215-223

Webb, S.D., 1991. Ecogeography and the Great American Interchange. *Paleobiology*, 17: 266-280.

Webb, S.D., 1997. The great american faunal interchange. In: Coates, A.G. (ed). *Central America: A natural and cultural history*, New Haven, Connecticut, Yale Univ.. 97-122

Weyl, P.K., 1968. The role of the oceans in climate change; a theory of the ice ages. *Meteorol. Monogr*., 8: 37-62.

Whitehead, J.M., and S.M. Bohaty, 2003. Pliocene summer sea surface temperature reconstruction using silicoflagellates from Southern Ocean ODP Site 1165. *Paleoceanography*, 18: doi:10.1029/2002PA000829

Wilkinson, B.H., and Algeo, T.J., 1989. Sedimentary carbonate record of calcium-magnesium cycling. *Am. J. Sci*., 289: 1158-1194.

Wolfe, J.A., 1994. An analysis of Neogene climates in Beringia. *Palaeogeogr., Palaeoclimatol., Palaeoecol*.,108: 207-216.

Wüst G., 1964. Stratification and Circulation in the Antillean-Caribbean Basins, Part 1: *Spreading and Mixing of the Water Types with an Oceanographic Atlas*. Columbia University Press, London and New York

Zarate, M.A., and Fasana, J.I., 1989. The Plio-Pleistocene record of the central eastern Pampas, Buenos Aires, Province, Argentina: the Chapadmalal Case Study. *Palaeogeogr., Palaeoclimatol., Palaeoecol*., 72: 27-52.

Appendix

The Appendices provide the data, which were presented in this thesis. Supplementary data on the studied cores are presented in the Ph.D-theses of Steph (2005) and Crudeli (2005).

Appendix A Mg/Ca and temperature data for Site 999. Mg/Ca-ratios were converted into temperatures by applying the calibration equation of Nürnberg et al. (2000). The age model of Site 999 was originally published in Haug and Tiedemann (1998) and adapted by Steph (2005). Sr/Ca, Mn/Ca, and Fe/Ca were monitored as quality control.

Appendix B Uncorrected Mg/Ca and temperature data for Site 1000. Mg/Ca-ratios were converted into temperatures by applying the calibration equation of Nürnberg et al. (2000). The age model of Site 1000 was established by Steph (2005). Sr/Ca, Mn/Ca, and Fe/Ca were monitored as quality control. The aragonite data were generated by L. Reuning (IFM-Geomar). Analyses on nannoplankton assemblages were performed by D. Crudeli (Crudeli, 2005).

Appendix C Mg/Ca and temperature data for Site 1241. Mg/Ca-ratios were converted into temperatures by applying the calibration equation of Nürnberg et al. (2000). $\delta^{18}O_{G.\ sacculifer}$ and the age model of Site 1241 were was established by Steph (2005). Sr/Ca, Mn/Ca, and Fe/Ca were monitored as quality control.

Appendix D Correction of Mg/Ca of Site 1000 (<4.5 Ma) for the influence of salinity. $\delta^{18}O_{G.\ sacculifer}$ (Steph et al., submitted) was corrected for a temperature cyclicity of 2.5°C, assuming a perfect positive correlation between $\delta^{18}O_{G.\ sacculifer}$ and the temperature fluctuations. Salinity changes were calculated according to the basic rule that $\Delta 1‰\delta^{18}O = \Delta 2$ salinity units (Broecker, 1989). Mg/Ca-ratios were then corrected using a 7% increase in Mg/Ca per 1 unit salinity increase (Nürnberg et al., 1996).

Appendix E $\delta^{18}O_{water}$ and $\delta^{18}O_{salinity}$ for Site 1241. $\delta^{18}O_{water}$ was calculated inserting $SST_{Mg/Ca}$ and $\delta^{18}O_{G.\ sacculifer}$ (Steph, 2005) into the equation of Shackleton (1974). $\delta^{18}O_{salinity}$ was calculated by subtracting the Pliocene ice volume (sea level) estimate (Chapter 5) from the $\delta^{18}O_{water}$ record. The ice volume/sea level estimate was based on the smoothed benthic $\delta^{18}O$ of Site 1241 (Tiedemann et al., submitted) assuming that the amplitude for Marine Isotope Stage 100 represents 50 m sea level change. To allow calculation the data were 'resampled' on 3 kyr time-steps. Time series analyses were performed with the software programm AnalySeries 1.2 (Paillard et al., 1996).

Appendix F $\delta^{18}O_{water}$ and $\delta^{18}O_{salinity}$ for Sites 999 and 1000 and the their $\delta^{18}O_{water}$-gradients with respect to Site 1241. $\delta^{18}O_{water}$ was calculated inserting $SST_{Mg/Ca}$ and $\delta^{18}O_{G.\ sacculifer}$ (Steph, 2005) into the equation of Shackleton (1974). $\delta^{18}O_{salinity}$ was calculated by subtracting the Pliocene ice volume (sea level) estimate (Chapter 5) from the $\delta^{18}O_{water}$ record. To allow calculation the data were 'resampled' on 3 kyr time-steps. Time series analyses were performed with the software programm AnalySeries 1.2 (Paillard et al., 1996).

Appendix A Mg/Ca and temperature data for Site 999. Sr/Ca, Mn/Ca, and Fe/Ca were monitored as quality control.

Site	Hole	Core	Sec.	Top (cm)	Bot (cm)	Depth (corr. msbf)	Age (ka)	Mg/Ca (mmol/mol)	Temperature (°C)	Sr/Ca (mmol/mol)	Mn/Ca (mmol/mol)	Fe/Ca (mmol/mol)
999	A	8	6	45	47	72.21	2202.1	3.41	25.5	1.35	1.28	0.43
999	A	8	6	65	67	72.40	2208.3	3.49	25.8	1.38	2.15	0.67
999	A	8	6	85	87	72.59	2214.6	3.22	24.7	1.38	1.52	0.45
999	A	8	6	105	107	72.78	2220.9	3.46	25.7	1.38	1.49	0.42
999	A	8	6	125	127	72.97	2227.1	3.34	25.2	1.38	1.44	0.35
999	A	8	6	145	147	73.16	2233.4	3.29	25.1	1.39	1.20	0.34
999	A	8	7	15	17	73.35	2239.7	3.41	25.5	1.41	1.04	0.36
999	A	8	7	35	37	73.55	2246.3	3.05	24.0	1.36	1.20	0.30
999	A	8	7	55	57	73.74	2252.5	3.08	24.2	1.37	0.94	0.23
999	A	8	0	5	7	73.93	2258.8	3.24	24.8	1.39	1.20	0.36
999	A	8	0	15	17	74.02	2261.8	3.49	25.8	1.38	1.59	0.38
999	A	9	1	15	17	74.24	2269.0	3.24	24.8	1.37	1.22	0.37
999	A	9	1	35	37	74.43	2275.3	3.08	24.2	1.42	1.07	0.43
999	A	9	1	55	57	74.62	2281.6	3.29	25.1	1.41	1.24	0.31
999	A	9	1	75	77	74.81	2287.8	3.60	26.2	1.41	1.46	0.46
999	A	9	1	95	97	75.00	2294.1	3.19	24.6	1.39	1.41	0.36
999	A	9	1	115	117	75.19	2300.4	3.26	24.9	1.39	1.49	0.31
999	A	9	1	135	137	75.38	2307.0	3.54	26.0	1.40	1.42	0.38
999	A	9	2	5	7	75.57	2313.6	2.95	23.6	1.37	1.20	0.26
999	A	9	2	25	27	75.76	2320.3	3.29	25.0	1.36	1.28	0.37
999	A	9	2	45	47	75.95	2326.9	2.90	23.4	1.27	1.12	0.45
999	A	9	2	65	67	76.14	2333.5	3.01	23.9	1.38	1.04	0.25
999	A	9	2	85	87	76.33	2340.1	3.51	25.9	1.39	1.54	0.37
999	A	9	2	105	107	76.52	2346.7	3.19	24.6	1.38	1.36	0.29
999	A	9	2	125	127	76.71	2353.3	2.99	23.8	1.35	1.23	0.28
999	A	9	2	145	147	76.90	2360.0	3.27	25.0	1.37	1.06	0.26
999	A	9	3	15	17	77.09	2366.6	3.18	24.6	1.37	1.11	0.35
999	A	9	3	35	37	77.28	2372.9	3.38	25.4	1.37	1.13	0.34
999	A	9	3	55	57	77.47	2378.9	3.55	26.0	1.34	1.14	0.38
999	A	9	3	75	77	77.66	2385.0	3.20	24.7	1.37	1.36	0.36
999	A	9	3	95	97	77.85	2390.3	3.24	24.8	1.35	1.18	0.29
999	A	9	3	115	117	78.04	2395.6	3.43	25.6	1.40	1.32	0.34
999	A	9	3	125	127	78.13	2398.1	3.88	27.2	1.52	1.41	0.40
999	A	9	3	135	137	78.23	2400.9	3.60	26.2	1.52	1.23	0.42
999	A	9	3	143	145	78.30	2402.8	3.46	25.7	1.48	1.25	0.36
999	A	9	4	15	17	78.51	2408.6	3.07	24.1	1.34	0.85	1.29
999	A	9	4	35	37	78.70	2413.9	3.72	26.6	1.38	1.31	0.39
999	A	9	4	45	47	78.80	2416.7	3.65	26.4	1.34	1.29	0.43
999	A	9	4	65	67	78.99	2422.0	3.40	25.5	1.32	1.72	0.27
999	A	9	4	85	87	79.18	2427.3	3.38	25.4	1.33	1.78	0.33
999	A	9	4	105	107	79.37	2432.6	3.58	26.2	1.34	1.40	0.35
999	A	9	4	115	117	79.46	2435.1	4.00	27.6	1.38	1.54	0.39
999	A	9	4	135	137	79.65	2440.3	3.11	24.3	1.32	0.93	0.30
999	A	9	4	145	147	79.75	2443.1	3.01	23.9	1.32	0.77	0.18
999	A	9	5	15	17	79.94	2448.4	3.17	24.5	1.32	1.26	0.26
999	A	9	5	25	27	80.03	2450.8	3.20	24.7	1.29	1.53	0.29
999	A	9	5	55	57	80.32	2458.5	2.78	22.8	1.31	0.99	0.17
999	A	9	5	95	97	80.70	2468.7	3.39	25.4	1.29	1.64	0.27
999	A	9	5	125	127	80.98	2476.2	3.00	23.8	1.30	1.82	0.32
999	A	9	5	145	147	81.17	2481.2	3.12	24.3	1.36	1.35	0.34
999	A	9	6	15	17	81.36	2486.3	3.59	26.2	1.35	1.20	0.32
999	A	9	6	65	67	81.84	2504.6	3.24	24.8	1.32	1.76	0.33
999	A	9	6	85	87	82.03	2511.9	3.40	25.4	1.34	1.75	0.43
999	A	9	6	105	107	82.21	2518.8	3.36	25.3	1.36	0.99	0.29
999	A	9	6	125	127	82.40	2526.0	3.42	25.5	1.33	1.26	0.30
999	A	9	6	145	147	82.59	2532.0	3.47	25.7	1.35	1.35	0.30
999	A	9	7	15	17	82.78	2537.9	3.13	24.4	1.32	1.66	0.77
999	A	9	7	35	37	82.97	2543.9	3.33	25.2	1.43	1.69	0.42
999	A	9	7	55	57	83.16	2549.8	2.86	23.2	1.28	1.02	0.11
999	A	9	0	5	7	83.35	2555.8	3.29	25.0	1.30	1.58	0.37
999	A	9	0	25	27	83.54	2561.7	3.57	26.1	1.32	1.39	0.33
999	A	10	1	15	17	83.74	2568.0	3.21	24.7	1.31	1.46	0.27
999	A	10	1	35	37	83.93	2574.0	3.39	25.4	1.33	1.50	0.37

Appendix A (continued)

Site	Hole	Core	Sec.	Top (cm)	Bot (cm)	Depth (corr. msbf)	Age (ka)	Mg/Ca (mmol/mol)	Temperature (°C)	Sr/Ca (mmol/mol)	Mn/Ca (mmol/mol)	Fe/Ca (mmol/mol)
999	A	10	1	55	57	84.12	2579.9	3.02	23.9	1.31	1.39	0.22
999	A	10	1	95	97	84.50	2591.8	2.96	23.6	1.33	1.39	0.25
999	A	10	1	125	127	84.78	2600.6	3.04	24.0	1.33	1.60	0.37
999	A	10	1	145	147	84.97	2607.7	3.48	25.8	1.44	1.59	0.30
999	A	10	2	15	17	85.16	2614.8	3.72	26.7	1.48	2.01	0.38
999	A	10	2	35	37	85.35	2621.9	2.85	23.1	1.33	1.45	0.10
999	A	10	2	55	56	85.54	2628.9	3.38	25.4	1.34	1.54	0.28
999	A	10	2	75	77	85.73	2636.0	3.27	25.0	1.35	1.42	0.25
999	A	10	2	95	97	85.92	2643.1	3.07	24.1	1.33	1.72	0.29
999	A	10	2	115	117	86.11	2650.2	3.50	25.8	1.34	1.67	0.35
999	A	10	2	135	137	86.30	2655.3	3.46	25.7	1.35	1.68	0.34
999	A	10	3	15	17	86.58	2662.7	3.09	24.2	1.32	1.71	0.37
999	A	10	3	35	37	86.77	2667.8	3.13	24.4	1.31	1.92	0.37
999	A	10	3	55	57	86.96	2672.8	3.25	24.9	1.33	1.78	0.37
999	A	10	3	75	77	87.15	2677.9	2.97	23.7	1.34	1.50	0.31
999	A	10	3	95	97	87.34	2682.9	2.64	22.1	1.30	1.51	0.26
999	A	10	3	115	117	87.53	2688.7	2.77	22.8	1.29	1.62	0.32
999	A	10	3	135	137	87.72	2695.0	2.82	23.0	1.31	1.52	0.26
999	A	10	4	5	7	87.91	2701.4	2.83	23.1	1.32	1.62	0.30
999	A	10	4	25	27	88.10	2707.7	3.00	23.8	1.33	1.17	0.31
999	A	10	4	45	47	88.28	2713.7	2.91	23.4	1.37	1.38	0.37
999	A	10	4	65	67	88.47	2720.1	2.76	22.7	1.37	1.75	0.34
999	A	10	4	75	77	88.57	2723.4	2.86	23.2	1.32	1.10	0.21
999	A	10	4	85	87	88.66	2726.4	3.36	25.3	1.38	1.88	0.37
999	A	10	4	105	107	88.85	2732.8	3.14	24.4	1.35	1.72	0.29
999	A	10	4	125	127	89.04	2739.2	3.30	25.1	1.28	1.18	0.37
999	A	10	4	145	147	89.23	2745.5	3.27	25.0	1.31	1.59	0.29
999	A	10	5	15	17	89.42	2751.7	3.39	25.4	1.28	1.89	0.36
999	A	10	5	35	37	89.61	2758.0	2.99	23.8	1.33	1.68	0.31
999	A	10	5	55	57	89.80	2764.2	3.51	25.9	1.37	1.92	0.38
999	A	10	5	75	77	89.99	2770.5	3.13	24.4	1.37	1.33	0.23
999	A	10	5	95	97	90.18	2776.7	3.20	24.7	1.33	1.64	0.38
999	A	10	5	115	117	90.37	2783.0	3.22	24.8	1.33	1.46	0.35
999	A	10	5	135	137	90.56	2789.2	3.38	25.4	1.33	1.63	0.37
999	A	10	6	5	7	90.74	2795.2	3.37	25.4	1.36	1.60	0.30
999	A	10	6	25	27	90.93	2801.4	3.27	25.0	1.34	1.38	0.27
999	A	10	6	45	47	91.12	2807.7	3.43	25.6	1.38	1.35	0.34
999	A	10	6	65	67	91.31	2813.9	3.47	25.7	1.40	1.66	0.43
999	A	10	6	85	87	91.50	2820.9	3.61	26.3	1.37	1.69	0.61
999	A	10	6	105	107	91.69	2828.6	3.20	24.6	1.29	1.48	0.29
999	A	10	6	125	127	91.88	2836.4	3.14	24.4	1.32	1.64	0.37
999	A	10	6	145	147	92.07	2844.1	3.18	24.6	1.33	1.80	0.52
999	A	10	7	15	17	92.26	2851.8	3.28	25.0	1.34	1.75	0.39
999	A	10	7	35	37	92.45	2859.6	3.24	24.8	1.34	1.51	0.20
999	A	10	7	55	57	92.64	2867.3	3.04	24.0	1.33	1.41	0.29
999	A	10	0	5	7	92.83	2875.1	3.35	25.3	1.35	2.00	0.59
999	A	10	0	25	27	93.02	2882.8	3.15	24.4	1.36	1.42	0.28
999	A	11	1	15	17	93.24	2891.8	3.14	24.4	1.34	1.41	0.37
999	A	11	1	35	37	93.43	2899.5	2.85	23.2	1.34	1.47	0.24
999	A	11	1	55	57	93.63	2906.8	3.10	24.2	1.32	1.54	0.39
999	A	11	1	75	77	93.82	2912.8	3.14	24.4	1.36	1.55	0.39
999	A	11	1	95	97	94.01	2918.9	3.07	24.1	1.36	1.58	0.35
999	A	11	1	115	117	94.20	2924.9	2.74	22.6	1.31	1.28	0.27
999	A	11	1	135	137	94.39	2931.0	3.16	24.5	1.33	1.42	0.35
999	A	11	2	5	7	94.58	2937.0	3.05	24.0	1.35	1.54	0.29
999	A	11	2	25	27	94.77	2943.1	3.08	24.2	1.32	1.86	0.38
999	A	11	2	45	47	94.96	2949.2	3.37	25.4	1.34	1.90	0.42
999	A	11	2	65	67	95.15	2955.2	3.18	24.6	1.35	1.67	0.48
999	A	11	2	85	87	95.34	2960.9	3.46	25.7	1.36	1.64	0.37
999	A	11	2	105	107	95.54	2966.9	3.24	24.8	1.33	1.66	0.39
999	A	11	2	125	127	95.73	2972.6	2.79	22.9	1.33	1.56	0.33
999	A	11	2	145	147	95.92	2978.3	3.28	25.0	1.37	1.91	0.42
999	A	11	3	15	17	96.11	2984.0	3.31	25.1	1.39	2.01	0.41

Appendix A (continued)

Site	Hole	Core	Sec.	Top (cm)	Bot (cm)	Depth (corr. msbf)	Age (ka)	Mg/Ca (mmol/mol)	Temperature (°C)	Sr/Ca (mmol/mol)	Mn/Ca (mmol/mol)	Fe/Ca (mmol/mol)
999	A	11	3	35	37	96.30	2989.7	2.92	23.5	1.33	1.62	0.47
999	A	11	3	75	77	96.68	3001.1	2.81	22.9	1.34	1.65	0.31
999	A	11	3	95	97	96.87	3006.8	3.18	24.6	1.36	1.38	0.26
999	A	11	3	115	117	97.06	3012.5	2.74	22.6	1.32	1.40	0.25
999	A	11	3	135	137	97.25	3018.4	2.93	23.5	1.36	1.52	0.35
999	A	11	4	5	7	97.44	3024.2	3.27	24.9	1.36	1.59	0.49
999	A	11	4	25	27	97.64	3030.4	3.20	24.7	1.34	1.30	0.24
999	A	11	4	45	47	97.83	3036.2	3.41	25.5	1.36	1.68	0.34
999	A	11	4	65	67	98.02	3042.1	3.07	24.1	1.36	1.99	0.49
999	A	11	4	85	87	98.21	3047.9	3.10	24.2	1.36	1.80	0.40
999	A	11	4	105	107	98.40	3053.8	2.36	20.7	1.29	0.81	0.15
999	A	11	4	125	127	98.59	3059.6	2.61	22.0	1.29	1.14	0.23
999	A	11	4	145	147	98.78	3065.5	2.77	22.8	1.35	1.70	0.31
999	A	11	5	15	17	98.97	3071.3	3.11	24.3	1.32	1.48	0.34
999	A	11	5	25	27	99.07	3074.4	2.88	23.3	1.31	1.26	0.23
999	A	11	5	55	57	99.35	3083.0	2.97	23.7	1.33	1.88	0.33
999	A	11	5	75	77	99.55	3089.2	2.91	23.4	1.36	1.67	0.33
999	A	11	5	95	97	99.74	3095.0	3.03	24.0	1.30	1.94	0.47
999	A	11	5	115	117	99.93	3100.9	3.31	25.1	1.34	1.63	0.34
999	A	11	5	135	137	100.12	3106.7	3.27	25.0	1.35	1.86	0.40
999	A	11	6	5	7	100.31	3112.6	3.02	23.9	1.34	1.62	0.56
999	A	11	6	25	27	100.50	3118.4	3.19	24.6	1.32	1.78	0.40
999	A	11	6	45	47	100.69	3124.3	3.25	24.9	1.34	1.59	0.61
999	A	11	6	65	67	100.88	3130.1	3.06	24.1	1.32	2.01	0.39
999	A	11	6	85	87	101.07	3136.0	3.14	24.4	1.33	1.81	0.43
999	A	11	6	105	107	101.26	3141.8	2.92	23.5	1.32	1.33	0.31
999	A	11	6	125	127	101.45	3148.6	2.89	23.3	1.35	1.60	0.27
999	A	11	6	145	147	101.65	3155.8	3.33	25.2	1.34	1.60	0.36
999	A	11	7	15	17	101.84	3162.6	3.31	25.1	1.31	1.61	0.31
999	A	11	7	35	37	102.03	3169.4	3.37	25.4	1.36	2.02	0.38
999	A	11	7	55	57	102.22	3176.2	3.39	25.4	1.33	1.56	0.32
999	A	11	0	5	7	102.41	3183.0	3.44	25.6	1.35	1.85	0.42
999	A	12	1	5	7	102.65	3191.6	3.60	26.2	1.32	1.91	0.41
999	A	12	1	25	27	102.84	3198.4	3.10	24.2	1.32	1.58	0.31
999	A	12	1	45	47	103.02	3204.8	3.28	25.0	1.32	1.72	0.37
999	A	12	1	65	67	103.21	3211.6	3.12	24.3	1.33	1.81	0.46
999	A	12	1	85	87	103.40	3218.4	3.35	25.3	1.36	1.75	0.39
999	A	12	1	105	107	103.59	3225.2	3.18	24.6	1.33	1.71	0.36
999	A	12	1	125	127	103.78	3232.0	2.78	22.8	1.32	1.52	0.33
999	A	12	1	145	147	103.97	3238.8	3.08	24.2	1.34	1.88	0.39
999	A	12	2	15	17	104.16	3245.6	3.41	25.5	1.37	1.85	0.39
999	A	12	2	35	37	104.35	3252.4	2.97	23.7	1.32	1.41	0.27
999	A	12	2	55	57	104.53	3258.9	2.87	23.2	1.36	1.65	0.32
999	A	12	2	75	77	104.72	3265.7	3.15	24.5	1.34	1.75	0.32
999	A	12	2	95	97	104.91	3272.5	3.05	24.0	1.35	1.60	0.34
999	A	12	2	115	117	105.10	3279.3	2.95	23.6	1.35	1.49	0.36
999	A	12	2	135	137	105.29	3286.1	3.11	24.3	1.35	1.35	0.35
999	A	12	3	5	7	105.48	3292.9	2.83	23.1	1.34	1.42	0.37
999	A	12	3	25	27	105.67	3299.6	2.51	21.5	1.29	1.20	0.30
999	A	12	3	45	47	105.85	3305.8	2.46	21.2	1.28	1.21	0.30
999	A	12	3	65	67	106.04	3312.4	2.62	22.0	1.25	1.23	0.25
999	A	12	3	85	87	106.23	3318.9	2.97	23.7	1.33	1.60	0.34
999	A	12	3	105	107	106.42	3325.5	2.61	22.0	1.28	1.29	0.26
999	A	12	3	125	127	106.61	3332.1	2.79	22.9	1.29	1.47	0.30
999	A	12	3	142	144	106.77	3337.6	2.96	23.6	1.31	1.59	0.29
999	A	12	4	15	17	106.99	3345.2	2.65	22.2	1.27	1.41	0.36
999	A	12	4	35	37	107.18	3351.8	3.36	25.3	1.29	1.64	0.29
999	A	12	4	55	57	107.36	3358.0	3.00	23.8	1.30	1.74	0.38
999	A	12	4	75	77	107.55	3364.6	3.00	23.8	1.32	1.55	0.39
999	A	12	4	95	97	107.74	3371.1	2.97	23.7	1.29	1.73	0.42
999	A	12	4	105	107	107.84	3374.6	2.64	22.1	1.33	1.77	0.39
999	A	12	4	125	127	108.02	3384.0	3.15	24.5	1.32	1.67	0.36
999	A	12	4	135	137	108.12	3389.2	3.28	25.0	1.31	2.09	0.45

Appendix A (continued)

Site	Hole	Core	Sec.	Top (cm)	Bot (cm)	Depth (corr. msbf)	Age (ka)	Mg/Ca (mmol/mol)	Temperature (°C)	Sr/Ca (mmol/mol)	Mn/Ca (mmol/mol)	Fe/Ca (mmol/mol)
999	A	12	5	5	7	108.31	3399.1	3.18	24.6	1.33	1.69	0.54
999	A	12	5	25	27	108.50	3409.0	2.92	23.5	1.28	1.74	0.31
999	A	12	5	45	47	108.68	3418.4	3.13	24.4	1.32	1.44	0.38
999	A	12	5	65	67	108.87	3427.2	3.43	25.6	1.35	2.11	0.74
999	A	12	5	85	87	109.06	3434.8	2.93	23.5	1.29	2.02	0.41
999	A	12	5	105	107	109.25	3442.3	3.28	25.0	1.32	2.00	0.40
999	A	12	5	125	127	109.44	3449.9	3.21	24.7	1.28	1.56	0.27
999	A	12	5	145	147	109.63	3457.5	3.04	24.0	1.26	1.31	0.25
999	A	12	6	15	17	109.82	3465.0	3.17	24.6	1.28	1.82	0.32
999	A	12	6	35	37	110.01	3472.6	2.91	23.4	1.29	1.61	0.32
999	A	12	6	55	57	110.19	3479.3	3.21	24.7	1.31	1.57	0.38
999	A	12	6	75	77	110.38	3485.8	3.02	23.9	1.29	1.80	0.24
999	A	12	6	95	97	110.57	3492.4	3.08	24.1	1.28	1.64	0.38
999	A	12	6	115	117	110.76	3498.9	3.18	24.6	1.31	1.67	0.30
999	A	12	6	135	137	110.95	3505.4	3.34	25.2	1.31	1.49	0.32
999	A	12	7	5	7	111.14	3511.2	3.10	24.3	1.30	1.87	0.45
999	A	12	7	25	27	111.33	3517.0	3.07	24.1	1.30	1.42	0.33
999	A	12	7	45	47	111.52	3522.7	3.23	24.8	1.31	1.89	0.38
999	A	12	7	64	66	111.69	3527.9	3.29	25.0	1.32	1.62	0.26
999	A	12	0	15	17	111.89	3534.0	3.21	24.7	1.31	1.76	0.32
999	A	13	1	15	17	112.24	3544.6	3.10	24.3	1.28	1.18	0.37
999	A	13	1	35	37	112.43	3550.4	3.18	24.6	1.33	1.11	0.24
999	A	13	1	55	57	112.62	3556.5	3.46	25.7	1.33	1.43	0.40
999	A	13	1	75	77	112.81	3562.6	3.49	25.8	1.36	1.43	0.40
999	A	13	1	95	97	113.00	3568.7	3.37	25.4	1.32	1.41	0.41
999	A	13	1	115	117	113.19	3574.8	3.46	25.7	1.36	1.38	0.36
999	A	13	1	135	137	113.37	3580.6	3.15	24.4	1.29	1.43	0.36
999	A	13	2	15	17	113.66	3590.0	3.28	25.0	1.39	1.41	0.55
999	A	13	2	35	37	113.85	3596.1	3.07	24.1	1.30	1.24	0.37
999	A	13	2	55	57	114.04	3602.2	3.05	24.1	1.35	1.44	0.38
999	A	13	2	75	77	114.22	3608.0	3.03	23.9	1.29	1.10	0.37
999	A	13	2	95	97	114.41	3614.1	3.38	25.4	1.38	1.33	0.38
999	A	13	2	115	117	114.60	3620.2	2.97	23.7	1.28	0.92	0.31
999	A	13	3	5	7	114.98	3632.7	2.67	22.3	1.27	0.88	0.27
999	A	13	3	25	27	115.17	3639.4	2.91	23.4	1.34	0.96	0.32
999	A	13	3	45	47	115.36	3646.2	2.85	23.2	1.27	0.90	0.26
999	A	13	3	65	67	115.55	3652.9	3.63	26.3	1.41	1.76	0.66
999	A	13	3	85	87	115.74	3659.6	3.14	24.4	1.29	1.14	0.34
999	A	13	3	105	107	115.92	3666.0	2.87	23.2	1.34	1.06	0.43
999	A	13	3	125	127	116.11	3672.6	2.65	22.2	1.29	1.04	0.33
999	A	13	3	145	147	116.30	3679.2	3.34	25.2	1.39	1.39	0.41
999	A	13	4	15	17	116.49	3685.8	3.57	26.1	1.31	1.56	0.65
999	A	13	4	35	37	116.68	3692.4	3.10	24.3	1.32	0.94	0.35
999	A	13	4	55	57	116.87	3699.0	3.66	26.4	1.34	1.53	0.51
999	A	13	4	75	77	117.06	3705.5	3.54	26.0	1.42	1.77	0.49
999	A	13	4	95	97	117.25	3712.1	3.09	24.2	1.28	1.03	0.34
999	A	13	4	115	117	117.44	3719.9	3.27	24.9	1.38	1.28	0.36
999	A	13	4	135	137	117.62	3727.6	3.05	24.1	1.31	1.43	0.41
999	A	13	5	15	17	117.91	3740.0	3.29	25.0	1.28	1.21	0.43
999	A	13	5	35	37	118.10	3748.2	3.49	25.8	1.27	1.61	0.48
999	A	13	5	55	57	118.29	3756.4	3.21	24.7	1.26	0.88	0.26
999	A	13	5	75	77	118.47	3764.1	3.37	25.4	1.30	1.21	0.38
999	A	13	5	95	97	118.66	3772.2	3.12	24.3	1.27	1.12	0.36
999	A	13	5	115	117	118.85	3780.4	3.36	25.3	1.29	1.22	0.35
999	A	13	5	135	137	119.04	3786.0	2.95	23.6	1.27	1.12	0.32
999	A	13	6	5	7	119.23	3791.6	3.38	25.4	1.30	1.24	0.45
999	A	13	6	25	27	119.42	3797.3	3.59	26.2	1.28	1.28	0.35
999	A	13	6	45	47	119.61	3802.9	3.40	25.5	1.30	1.29	0.38
999	A	13	6	65	67	119.80	3808.5	3.48	25.8	1.32	1.53	0.51
999	A	13	6	85	87	119.99	3814.1	2.94	23.6	1.28	1.28	0.39
999	A	13	6	105	107	120.17	3819.4	3.41	25.5	1.31	1.40	0.36
999	A	13	6	125	127	120.36	3825.0	3.30	25.1	1.32	1.29	0.44
999	A	13	6	145	147	120.55	3831.0	3.01	23.9	1.27	1.21	0.48

Appendix A (continued)

Site	Hole	Core	Sec.	Top (cm)	Bot (cm)	Depth (corr. msbf)	Age (ka)	Mg/Ca (mmol/mol)	Temperature (°C)	Sr/Ca (mmol/mol)	Mn/Ca (mmol/mol)	Fe/Ca (mmol/mol)
999	A	13	7	15	17	120.74	3837.3	3.70	26.6	1.31	1.60	0.48
999	A	13	7	35	37	120.93	3843.6	3.63	26.3	1.31	1.63	0.43
999	A	13	7	55	57	121.12	3849.9	3.09	24.2	1.28	1.33	0.42
999	A	13	7	75	77	121.31	3856.2	3.07	24.1	1.26	1.26	0.46
999	A	13	0	15	17	121.50	3862.5	3.62	26.3	1.33	1.59	0.43
999	A	14	1	5	7	121.65	3867.5	2.71	22.5	1.27	1.06	0.36
999	A	14	1	25	27	121.84	3873.8	2.70	22.4	1.28	0.97	0.23
999	A	14	1	45	47	122.03	3880.2	3.12	24.3	1.33	1.39	0.42
999	A	14	1	65	67	122.21	3886.2	3.30	25.1	1.32	1.46	0.42
999	A	14	1	85	87	122.40	3892.6	3.02	23.9	1.32	1.61	0.59
999	A	14	1	105	107	122.59	3899.0	2.97	23.7	1.30	1.16	0.35
999	A	14	1	125	127	122.78	3905.4	3.31	25.1	1.31	1.56	0.49
999	A	14	1	145	147	122.97	3911.8	3.17	24.5	1.28	1.45	0.39
999	A	14	2	15	17	123.16	3918.2	3.26	24.9	1.30	1.33	0.37
999	A	14	2	35	37	123.35	3924.6	3.18	24.6	1.25	1.24	0.40
999	A	14	2	55	57	123.54	3931.0	3.08	24.1	1.30	1.30	0.62
999	A	14	2	75	77	123.73	3937.4	3.20	24.7	1.28	1.21	0.42
999	A	14	2	95	97	123.92	3943.8	3.47	25.7	1.30	1.33	0.67
999	A	14	2	115	117	124.10	3949.8	3.31	25.1	1.29	1.39	0.54
999	A	14	2	135	137	124.29	3956.2	3.32	25.2	1.32	1.57	0.61
999	A	14	3	5	7	124.48	3962.6	3.28	25.0	1.28	1.43	0.41
999	A	14	3	25	27	124.67	3969.0	3.15	24.5	1.28	1.44	0.43
999	A	14	3	45	47	124.86	3975.4	2.84	23.1	1.26		
999	A	14	3	65	67	125.05	3981.8	3.00	23.8	1.29	1.39	0.39
999	A	14	3	85	87	125.24	3988.2	2.65	22.2	1.27	1.44	0.36
999	A	14	3	105	107	125.43	3994.6	2.50	21.4	1.24		
999	A	14	3	124	126	125.61	4000.6	2.77	22.8	1.27	1.20	0.47
999	A	14	3	145	147	125.81	4007.4	2.72	22.5	1.25	1.43	0.40
999	A	14	4	15	17	126.00	4013.8	3.30	25.1	1.31	1.54	0.50
999	A	14	4	35	37	126.18	4019.9	2.54	21.6	1.25	0.90	0.32
999	A	14	4	55	57	126.37	4026.3	2.92	23.5	1.26		
999	A	14	4	75	77	126.56	4032.8	2.59	21.9	1.25		
999	A	14	4	95	97	126.75	4039.2	3.05	24.0	1.31	1.69	0.49
999	A	14	4	115	117	126.94	4045.6	2.69	22.4	1.26		
999	A	14	4	135	137	127.13	4052.1	3.22	24.8	1.30	1.52	0.60
999	A	14	5	5	7	127.35	4059.6	3.36	25.3	1.31	1.85	0.43
999	A	14	5	15	17	127.44	4062.6	2.83	23.1	1.25		
999	A	14	5	25	27	127.54	4066.0	2.94	23.6	1.26	1.40	0.36
999	A	14	5	45	47	127.73	4072.5	2.99	23.8	1.28	1.68	0.50
999	A	14	5	65	67	127.91	4078.6	2.91	23.4	1.29	1.56	0.45
999	A	14	5	85	87	128.10	4085.0	3.00	23.8	1.24		
999	A	14	5	105	107	128.29	4091.5	2.79	22.9	1.26	1.32	0.35
999	A	14	5	125	127	128.48	4097.9	2.91	23.4	1.24		
999	A	14	5	145	147	128.67	4105.9	3.19	24.6	1.29	1.68	0.43
999	A	14	6	15	17	128.86	4113.9	3.14	24.4	1.30	1.74	0.52
999	A	14	6	35	37	129.05	4121.8	3.19	24.6	1.29	1.51	0.46
999	A	14	6	55	57	129.24	4129.8	3.27	24.9	1.32	1.43	0.51
999	A	14	6	65	67	129.33	4133.6	3.19	24.6	1.28		
999	A	14	6	75	77	129.43	4137.8	3.25	24.9	1.31	1.59	0.49
999	A	14	6	95	97	129.62	4145.8	3.11	24.3	1.27		
999	A	14	6	115	117	129.80	4153.3	2.94	23.6	1.26	1.23	0.88
999	A	14	6	135	137	129.99	4161.3	3.00	23.8	1.30		
999	A	14	7	5	7	130.18	4169.3	3.14	24.4	1.30	1.59	0.50
999	A	14	7	15	17	130.28	4173.5	2.80	22.9	1.25		
999	A	14	7	25	27	130.37	4177.2	3.48	25.8	1.32	1.44	0.44
999	A	14	7	45	47	130.56	4185.2	3.18	24.6	1.27		
999	A	14	7	64	66	130.74	4192.8	3.09	24.2	1.31	1.56	0.55
999	A	14	0	5	7	130.84	4197.0	3.08	24.2	1.27		
999	A	14	0	15	17	130.94	4201.2	3.20	24.7	1.29	2.03	0.49
999	A	14	0	25	27	131.03	4205.0	2.99	23.8	1.27		
999	A	15	1	15	17	131.24	4213.8	3.39	25.4	1.26		
999	A	15	1	35	37	131.43	4221.7	3.56	26.1	1.31	1.73	0.48
999	A	15	1	55	57	131.62	4229.7	3.06	24.1	1.29	1.74	0.38

Appendix A (continued)

Site	Hole	Core	Sec.	Top (cm)	Bot (cm)	Depth (corr. msbf)	Age (ka)	Mg/Ca (mmol/mol)	Temperature (°C)	Sr/Ca (mmol/mol)	Mn/Ca (mmol/mol)	Fe/Ca (mmol/mol)
999	A	15	1	75	77	131.81	4237.7	3.33	25.2	1.29		
999	A	15	1	95	97	132.00	4245.7	2.93	23.5	1.29	1.81	0.47
999	A	15	1	115	117	132.18	4253.2	2.64	22.1	1.33	1.43	0.49
999	A	15	1	135	137	132.37	4261.2	3.05	24.1	1.31	1.74	0.49
999	A	15	2	5	7	132.56	4269.2	2.74	22.6	1.30	2.01	0.56
999	A	15	2	25	27	132.75	4277.2	2.78	22.8	1.29	1.91	0.58
999	A	15	2	35	37	132.85	4281.4	2.94	23.6	1.27		
999	A	15	2	45	47	132.94	4285.2	2.64	22.1	1.27	1.76	0.58
999	A	15	2	65	67	133.13	4293.3	2.84	23.1	1.32	2.02	0.51
999	A	15	2	75	77	133.22	4297.1	3.06	24.1	1.29		
999	A	15	2	85	87	133.32	4301.3	3.01	23.9	1.29	1.99	0.49
999	A	15	2	105	107	133.51	4309.3	3.51	25.9	1.30	2.17	0.47
999	A	15	2	125	127	133.69	4316.9	2.72	22.5	1.30	1.80	0.48
999	A	15	2	145	147	133.88	4324.9	2.80	22.9	1.30	1.82	0.44
999	A	15	3	15	17	134.07	4332.9	3.36	25.3	1.32	1.98	0.60
999	A	15	3	35	37	134.26	4340.9	2.79	22.9	1.27	1.76	0.45
999	A	15	3	45	47	134.35	4344.7	2.74	22.6	1.30	2.50	0.47
999	A	15	3	55	57	134.45	4349.0	2.96	23.7	1.29	1.82	0.42
999	A	15	3	65	67	134.54	4352.8	2.48	21.3	1.29	1.76	0.41
999	A	15	3	75	77	134.64	4357.0	2.80	22.9	1.26	1.61	0.43
999	A	15	3	95	97	134.83	4365.0	3.00	23.8	1.23		
999	A	15	3	115	117	135.02	4373.0	3.16	24.5	1.26	1.83	0.44
999	A	15	3	125	127	135.11	4376.8	2.51	21.5	1.25	2.01	0.37
999	A	15	3	135	137	135.20	4380.6	2.90	23.4	1.23		
999	A	15	3	145	147	135.30	4384.8	2.57	21.8	1.26	1.92	0.29
999	A	15	4	5	7	135.39	4388.6	2.55	21.7	1.27	1.56	0.34
999	A	15	4	25	27	135.58	4396.6	3.12	24.3	1.33	1.97	0.73
999	A	15	4	35	37	135.68	4400.9	3.27	25.0	1.25		
999	A	15	4	45	47	135.77	4404.7	2.97	23.7	1.31	1.89	0.52
999	A	15	4	65	67	135.96	4412.7	3.25	24.9	1.32	2.12	0.64
999	A	15	4	75	77	136.05	4416.5	2.74	22.6	1.27		
999	A	15	4	95	97	136.24	4424.5	3.51	25.9	1.30	2.00	0.50
999	A	15	4	125	127	136.52	4436.3	2.95	23.6	1.30	2.53	0.45
999	A	15	4	135	137	136.62	4440.2	3.12	24.3	1.34	1.84	0.48
999	A	15	5	5	7	136.84	4448.6	2.87	23.2	1.31	1.53	0.54
999	A	15	5	25	27	137.02	4455.6	3.03	24.0	1.32	1.64	0.49
999	A	15	5	45	47	137.21	4462.9	3.73	26.7	1.27	1.80	0.51
999	A	15	5	55	57	137.31	4466.8	3.03	24.0	1.23		
999	A	15	5	65	67	137.40	4470.2	3.41	25.5	1.31	2.48	0.68
999	A	15	5	75	77	137.50	4474.1	3.15	24.5	1.25		
999	A	15	5	85	87	137.59	4477.5	3.01	23.9	1.29	1.87	0.38
999	A	15	5	95	97	137.68	4481.0	3.02	23.9	1.30	3.42	0.50
999	A	15	5	105	107	137.78	4484.9	2.72	22.5	1.28	2.43	0.54
999	A	15	5	115	117	137.87	4488.3	2.79	22.9	1.23	1.29	0.33
999	A	15	5	125	127	137.97	4491.7	3.04	24.0	1.30		
999	A	15	5	145	147	138.16	4497.5	2.72	22.6	1.28	1.44	0.54
999	A	15	6	15	17	138.37	4503.9	2.95	23.6	1.24		
999	A	15	6	35	37	138.56	4509.8	2.95	23.6	1.26	2.33	0.64
999	A	15	6	55	57	138.75	4515.6	3.35	25.3	1.32	2.28	0.68
999	A	15	6	75	77	138.94	4521.4	3.28	25.0	1.31	2.03	0.47
999	A	15	6	95	97	139.13	4527.2	3.32	25.2	1.29	2.16	0.46
999	A	15	6	115	117	139.32	4533.0	3.12	24.4	1.28		
999	A	15	6	125	127	139.41	4535.7	2.81	22.9	1.29	3.11	0.59
999	A	15	6	135	137	139.51	4538.8	2.87	23.3	1.29	1.77	0.42
999	A	15	6	145	147	139.60	4541.5	2.66	22.2	1.29	2.50	0.49
999	A	15	7	5	7	139.69	4545.3	2.65	22.2	1.27	1.60	0.60
999	A	15	7	15	17	139.79	4549.6	2.95	23.6	1.24		
999	A	15	7	25	27	139.88	4553.5	2.69	22.4	1.27	1.77	0.50
999	A	15	7	35	37	139.98	4557.8	3.19	24.6	1.27	3.17	0.60
999	A	15	7	45	47	140.07	4561.7	2.70	22.4	1.27	1.88	0.60
999	A	15	7	55	57	140.17	4566.0	2.81	23.0	1.22		
999	A	15	7	65	67	140.26	4569.9	2.89	23.3	1.31	1.62	0.51
999	A	15	0	5	7	140.35	4573.8	2.80	22.9	1.29	2.00	0.37

Appendix A (continued)

Site	Hole	Core	Sec.	Top (cm)	Bot (cm)	Depth (corr. msbf)	Age (ka)	Mg/Ca (mmol/mol)	Temperature (°C)	Sr/Ca (mmol/mol)	Mn/Ca (mmol/mol)	Fe/Ca (mmol/mol)
999	A	15	0	15	17	140.45	4578.1	3.38	25.4	1.32	1.67	1.17
999	A	15	0	25	27	140.54	4582.0	3.14	24.4	1.32	2.81	0.48
999	A	16	1	5	7	140.65	4597.0	3.53	26.0	1.30	1.88	0.50
999	A	16	1	15	17	140.74	4600.1	2.98	23.7	1.29	2.25	0.41
999	A	16	1	25	27	140.84	4603.5	2.95	23.6	1.27	1.89	0.45
999	A	16	1	39	41	140.97	4607.9	3.05	24.0	1.27	3.00	0.46
999	A	16	1	45	47	141.03	4609.9	2.96	23.6	1.27	1.86	0.49
999	A	16	1	55	57	141.13	4613.3	3.26	24.9	1.29	2.60	0.58
999	A	16	1	65	67	141.22	4616.4	3.31	25.1	1.27	1.81	0.58
999	A	16	1	75	77	141.32	4619.8	3.34	25.2	1.31	2.75	0.40
999	A	16	1	85	87	141.42	4623.2	3.76	26.8	1.31	2.07	0.56
999	A	16	1	95	97	141.51	4626.3	3.38	25.4	1.33	2.61	0.56
999	A	16	1	115	117	141.70	4632.7	3.45	25.7	1.34	3.25	0.61
999	A	16	1	125	127	141.80	4636.1	3.33	25.2	1.29	1.94	0.56
999	A	16	1	145	147	141.99	4642.6	3.28	25.0	1.30	2.23	0.63
999	A	16	2	15	17	142.18	4649.1	3.48	25.8	1.33	2.39	0.54
999	A	16	2	25	27	142.28	4652.5	3.18	24.6	1.30	3.73	0.62
999	A	16	2	35	37	142.38	4655.9	3.64	26.4	1.29	2.07	1.24
999	A	16	2	45	47	142.47	4658.6	3.34	25.2	1.30	2.84	0.46
999	A	16	2	55	57	142.57	4661.5	3.53	26.0	1.32	2.02	0.47
999	A	16	2	65	67	142.66	4664.1	3.18	24.6	1.30	3.01	0.46
999	A	16	2	75	77	142.76	4667.0	3.40	25.5	1.33	2.16	0.51
999	A	16	2	85	87	142.86	4669.9	3.19	24.6	1.32	2.86	0.39
999	A	16	2	95	97	142.95	4672.6	3.32	25.1	1.31	2.44	0.63
999	A	16	2	115	117	143.14	4678.1	3.19	24.6	1.29	1.73	0.52
999	A	16	2	125	127	143.24	4681.0	3.09	24.2	1.28	2.85	0.51
999	A	16	2	135	137	143.33	4683.6	3.03	23.9	1.28	1.68	0.52
999	A	16	3	5	7	143.53	4689.4	2.82	23.0	1.31	2.22	0.52
999	A	16	3	15	17	143.62	4692.2	2.91	23.4	1.30	2.50	0.41
999	A	16	3	25	27	143.72	4696.8	3.25	24.9	1.27	2.15	0.46
999	A	16	3	35	37	143.81	4700.9	3.08	24.1	1.27	2.81	0.54
999	A	16	3	45	47	143.91	4705.6	3.21	24.7	1.31	1.52	0.53
999	A	16	3	55	57	144.01	4710.2	3.39	25.4	1.31	3.43	0.37
999	A	16	3	65	67	144.10	4714.3	3.32	25.2	1.33	1.93	0.49
999	A	16	3	75	77	144.20	4718.9	3.53	26.0	1.30	3.15	0.55
999	A	16	3	85	87	144.29	4723.1	3.33	25.2	1.34	1.85	0.48
999	A	16	3	95	97	144.39	4726.3	3.36	25.3	1.28	2.61	0.40
999	A	16	3	105	107	144.49	4729.6	3.28	25.0	1.32	1.66	0.62
999	A	16	3	115	117	144.58	4732.5	3.65	26.4	1.31	2.78	0.49
999	A	16	3	125	127	144.68	4735.7	3.48	25.8	1.32	2.26	0.56
999	A	16	3	135	137	144.77	4738.6	3.44	25.6	1.32	2.45	0.49
999	A	16	3	145	147	144.87	4741.8	3.31	25.1	1.31	2.05	0.68
999	A	16	4	5	7	144.97	4745.1	3.25	24.9	1.31	2.39	0.44
999	A	16	4	15	17	145.06	4748.0	3.15	24.5	1.31	1.74	0.63
999	A	16	4	25	27	145.16	4751.2	3.69	26.6	1.31	2.47	0.54
999	A	16	4	35	37	145.25	4754.1	3.09	24.2	1.32	1.89	0.51
999	A	16	4	45	47	145.35	4757.4	3.22	24.8	1.30	2.94	0.43
999	A	16	4	55	57	145.45	4760.6	3.52	25.9	1.31	2.26	0.71
999	A	16	4	65	67	145.54	4763.5	3.16	24.5	1.29	2.68	0.40
999	A	16	4	75	77	145.64	4766.8	3.06	24.1	1.30	1.72	0.80
999	A	16	4	85	87	145.73	4769.7	2.93	23.5	1.30	2.01	0.51
999	A	16	4	95	97	145.83	4773.1	3.53	26.0	1.31	1.88	0.53
999	A	16	4	105	107	145.93	4776.4	3.06	24.1	1.28	2.66	0.42
999	A	16	4	115	117	146.02	4779.4	3.34	25.2	1.29	1.96	0.48
999	A	16	4	125	127	146.12	4782.7	3.39	25.4	1.31	2.31	0.76
999	A	16	4	135	137	146.21	4785.7	3.59	26.2	1.32	1.80	0.57
999	A	16	4	145	147	146.31	4789.1	3.77	26.8	1.32	2.43	0.40
999	A	16	5	5	7	146.41	4792.4	3.17	24.5	1.31	3.00	0.57
999	A	16	5	15	17	146.50	4795.4	3.35	25.3	1.30	3.00	0.51
999	A	16	5	25	27	146.60	4798.7	3.05	24.1	1.31	1.75	0.50
999	A	16	5	35	37	146.69	4801.7	3.05	24.0	1.29	2.03	0.20
999	A	16	5	45	47	146.79	4805.1	3.04	24.0	1.32	1.88	0.98
999	A	16	5	55	57	146.89	4808.5	3.19	24.6	1.30	2.53	0.59

Appendix A (continued)

Site	Hole	Core	Sec.	Top (cm)	Bot (cm)	Depth (corr. msbf)	Age (ka)	Mg/Ca (mmol/mol)	Temperature (°C)	Sr/Ca (mmol/mol)	Mn/Ca (mmol/mol)	Fe/Ca (mmol/mol)
999	A	16	5	65	67	146.98	4811.6	3.60	26.2	1.33	2.70	0.50
999	A	16	5	75	77	147.08	4815.0	3.42	25.5	1.31	2.40	0.50
999	A	16	5	85	87	147.17	4818.1	3.37	25.4	1.30	1.96	0.55
999	A	16	5	95	97	147.27	4821.6	3.34	25.2	1.30	1.57	0.75
999	A	16	5	105	107	147.37	4825.0	3.28	25.0	1.34	2.03	0.61
999	A	16	5	125	127	147.56	4831.6	3.39	25.4	1.32	1.79	0.62
999	A	16	5	135	137	147.65	4834.7	3.18	24.6	1.32	2.53	0.38
999	A	16	5	145	147	147.75	4838.1	3.34	25.2	1.30	2.07	0.49
999	A	16	6	25	27	148.04	4846.2	3.31	25.1	1.36	1.81	0.52
999	A	16	6	45	47	148.23	4851.4	3.12	24.4	1.35	1.95	0.83
999	A	16	6	65	67	148.42	4856.7	3.51	25.9	1.36	0.67	0.16
999	A	16	6	85	87	148.61	4862.0	3.44	25.6	1.40	1.79	0.48
999	A	16	6	105	107	148.80	4867.2	3.81	27.0	1.36	1.90	0.46
999	A	16	6	125	127	149.00	4872.8	3.53	25.9	1.36	2.18	0.57
999	A	16	6	145	147	149.19	4878.1	4.09	27.9	1.35	2.26	0.46
999	A	16	7	14	16	149.37	4883.1	3.29	25.0	1.37	2.42	0.40
999	A	16	0	15	17	149.57	4888.6	2.99	23.8	1.33	2.18	0.46
999	A	16	0	25	27	149.67	4891.6	3.01	23.8	1.35	2.37	0.52
999	A	16	0	35	37	149.76	4894.6	3.10	24.3	1.37	2.05	0.46
999	A	16	0	55	57	149.96	4901.1	3.65	26.4	1.39	2.40	0.63
999	A	17	1	5	7	150.14	4907.0	3.54	26.0	1.38	2.21	0.62
999	A	17	1	25	27	150.34	4913.6	3.74	26.7	1.37	2.09	0.47
999	A	17	1	45	47	150.53	4919.8	3.71	26.6	1.39	2.04	0.46
999	A	17	1	65	67	150.73	4926.4	3.37	25.4	1.37	1.87	0.38
999	A	17	1	85	87	150.92	4932.6	3.68	26.5	1.38	2.27	0.44
999	A	17	1	105	107	151.11	4938.8	3.11	24.3	1.35	2.00	0.76
999	A	17	1	115	117	151.21	4942.1	3.57	26.1	1.37	2.35	0.40
999	A	17	1	125	127	151.31	4945.4	3.27	24.9	1.37	2.17	0.51
999	A	17	1	145	147	151.50	4951.6	3.78	26.9	1.38	2.14	0.44
999	A	17	2	14	16	151.68	4957.5	3.49	25.8	1.35	1.91	0.43
999	A	17	2	34	36	151.88	4964.1	3.44	25.6	1.37	1.81	0.50
999	A	17	2	55	57	152.08	4970.6	3.36	25.3	1.35	2.02	0.48
999	A	17	2	74	76	152.26	4976.5	3.25	24.9	1.35	1.88	0.47
999	A	17	2	95	97	152.47	4983.4	3.32	25.2	1.35	1.97	0.42
999	A	17	2	114	116	152.65	4989.3	3.33	25.2	1.32	1.90	0.37
999	A	17	2	134	136	152.84	4995.5	3.67	26.5	1.38	2.20	0.99
999	A	17	3	5	7	153.05	5002.4	3.53	26.0	1.36	2.24	0.44
999	A	17	3	15	17	153.14	5005.3	3.27	25.0	1.37	1.97	0.42
999	A	17	3	25	27	153.24	5008.8	2.91	23.4	1.31	1.39	0.36
999	A	17	3	45	47	153.43	5016.7	3.10	24.3	1.29	0.62	0.34
999	A	17	3	55	57	153.53	5020.9	3.59	26.2	1.38	2.18	0.70
999	A	17	3	65	67	153.63	5025.1	4.00	27.6	1.36	1.85	1.09
999	A	17	3	85	87	153.82	5033.0	3.68	26.5	1.36	1.68	0.72
999	A	17	3	105	107	154.01	5040.9	3.46	25.7	1.35	1.86	0.38
999	A	17	3	125	127	154.21	5049.2	3.73	26.7	1.33	2.17	0.36
999	A	17	3	145	147	154.40	5057.1	3.63	26.3	1.37	1.70	0.71
999	A	17	4	15	17	154.59	5063.9	3.87	27.2	1.34	1.96	1.06
999	A	17	4	35	37	154.79	5070.9	3.72	26.7	1.35	2.37	0.63
999	A	17	4	55	57	154.98	5077.5	3.81	27.0	1.36	2.07	0.70
999	A	17	4	75	77	155.17	5084.2	3.12	24.3	1.32	1.80	0.53
999	A	17	4	95	97	155.37	5091.2	3.62	26.3	1.37	1.92	0.44
999	A	17	4	135	137	155.75	5105.3	3.12	24.4	1.33	1.62	0.26
999	A	17	4	145	147	155.85	5109.3	3.37	25.4	1.32	0.00	0.01
999	A	17	5	5	7	155.95	5113.4	3.22	24.8	1.34	1.58	0.43
999	A	17	5	25	27	156.14	5121.2	3.53	26.0	1.35	2.37	0.48
999	A	17	5	45	47	156.33	5128.9	3.44	25.6	1.36	1.97	0.85
999	A	17	5	65	67	156.53	5137.1	3.12	24.3	1.35	1.85	0.86
999	A	17	5	85	87	156.72	5144.9	3.77	26.8	1.36	2.05	0.56
999	A	17	5	105	107	156.91	5152.6	3.13	24.4	1.30	1.82	0.51
999	A	17	5	125	127	157.11	5160.8	3.44	25.6	1.33	1.88	0.46
999	A	17	5	145	147	157.30	5168.6	3.57	26.1	1.35	2.36	0.45
999	A	17	6	15	17	157.49	5176.3	3.91	27.3	1.37	2.01	0.42
999	A	17	6	35	37	157.69	5184.5	3.72	26.7	1.37	1.95	0.79

Appendix A (continued)

Site	Hole	Core	Sec.	Top (cm)	Bot (cm)	Depth (corr. msbf)	Age (ka)	Mg/Ca (mmol/mol)	Temperature (°C)	Sr/Ca (mmol/mol)	Mn/Ca (mmol/mol)	Fe/Ca (mmol/mol)
999	A	17	6	45	47	157.78	5188.2	3.63	26.3	1.36	2.16	0.71
999	A	17	6	55	57	157.88	5192.3	2.71	22.5	1.30	1.63	0.49
999	A	17	6	75	77	158.07	5200.1	3.22	24.7	1.33	1.94	0.48
999	A	17	6	95	97	158.27	5208.3	4.12	28.0	1.35	2.00	0.39
999	A	17	6	115	117	158.46	5216.1	3.86	27.1	1.35	1.95	0.48
999	A	17	6	135	137	158.65	5223.9	3.65	26.4	1.33	1.83	0.29
999	A	17	7	5	7	158.85	5232.1	3.55	26.0	1.36	2.05	0.41
999	A	17	7	25	27	159.04	5240.0	3.59	26.2	1.35	2.02	0.40
999	A	17	7	45	47	159.23	5247.8	3.64	26.4	1.35	2.18	0.38
999	A	17	0	5	7	159.43	5256.0	3.86	27.1	1.36	1.94	0.36

Appendix B Mg/Ca, temperature, aragonite content and relative abundance of *F. profunda* for Site 1000. Sr/Ca, Mn/Ca, and Fe/Ca were monitored as quality control.

Site	Hole	Core	Type	Sec.	Top (cm)	Bot (cm)	Depth (corr. msbf)	Age (ka)	Mg/Ca (mmol/mol)	Temperature (°C)	Sr/Ca (mmol/mol)	Mn/Ca (mmol/mol)	Fe/Ca (mmol/mol)	Aragonite <63 (%)	*F.profunda* (%)
1000	A	9	H	4	55	57	75.05	2721.3	7.11	35.2	1.55	0.20	0.09		
1000	A	9	H	5	5	7	76.05	2738.2	7.09	35.1	1.56	0.20	0.07		
1000	A	9	H	5	145	147	77.45	2761.6	5.20	31.1	1.49	0.14	0.07		
1000	A	9	H	6	75	77	78.25	2775.2	8.22	37.1	1.61	0.23	0.16		
1000	A	9	H	6	135	137	78.85	2785.3	7.61	36.1	1.53	0.26	0.15		
1000	A	9	H	0	5	7	79.65	2799.7	6.85	34.7	1.54	0.14	0.09		
1000	B	1	R	1	25	27	79.95	2806.0	5.75	32.4	1.49	0.14	0.13		
1000	B	1	R	1	125	127	80.95	2827.2	7.28	35.5	1.58	0.20	0.13		
1000	B	1	R	2	56	58	81.75	2844.2	7.52	35.9	1.56	0.30	0.18		
1000	B	1	R	2	135	137	82.55	2861.1	7.45	35.8	1.60	0.26	0.21		
1000	B	1	R	4	55	57	84.75	2915.4	7.44	35.8	1.56	0.32	0.25		
1000	B	1	R	5	65	67	86.35	2957.5	5.83	32.6	1.57	0.23	0.24		
1000	B	1	R	5	125	127	86.95	2972.7	7.51	35.9	1.57	0.33	0.34		
1000	A	11	H	1	5	7	88.85	3027.0						53.90	
1000	A	11	H	1	35	37	89.15	3033.7						51.14	
1000	A	11	H	1	45	47	89.25	3036.0	6.94	34.9	1.56	0.24	0.23		
1000	A	11	H	1	65	67	89.45	3040.7						43.99	
1000	A	11	H	1	95	97	89.75	3047.4						53.38	
1000	A	11	H	1	105	107	89.85	3049.7	6.75	34.5	1.55	0.21	0.24		
1000	A	11	H	1	125	127	90.05	3054.3						69.91	
1000	A	11	H	2	5	7	90.35	3061.3						38.56	
1000	A	11	H	2	35	37	90.65	3068.0						42.09	
1000	A	11	H	2	65	67	90.95	3074.9	4.78	30.0	1.49	0.15	0.15		
1000	A	11	H	2	75	77	91.05	3077.0						63.46	
1000	A	11	H	2	105	107	91.35	3083.9	6.31	33.6	1.63	0.19	0.20	48.31	
1000	A	11	H	2	135	137	91.65	3090.6						57.84	
1000	A	11	H	3	5	7	91.85	3095.3	5.05	30.7	1.55	0.16	0.12		
1000	A	11	H	3	15	17	91.95	3097.6						67.12	
1000	A	11	H	3	45	47	92.25	3104.3	6.02	33.0	1.61	0.20	0.20	56.91	
1000	A	11	H	3	75	77	92.55	3111.2						49.80	
1000	A	11	H	3	105	107	92.85	3118.2	6.26	33.5	1.60	0.19	0.16	58.76	
1000	A	11	H	3	135	137	93.15	3124.9						66.69	
1000	A	11	H	4	15	17	93.47	3132.3	6.57	34.1	1.56	0.22	0.24	56.88	
1000	A	11	H	4	45	47	93.77	3139.0	6.21	33.4	1.56	0.20	0.18	53.19	
1000	A	11	H	4	75	77	94.07	3146.0	4.79	30.0	1.47	0.13	0.13	72.45	
1000	A	11	H	4	106	108	94.38	3152.9						46.84	
1000	A	11	H	4	135	137	94.67	3159.8						45.20	
1000	A	11	H	4	145	147	94.77	3162.0	6.49	34.0	1.62	0.17	0.14		
1000	A	11	H	5	15	17	94.97	3166.8						71.89	
1000	A	11	H	5	45	47	95.27	3174.1	5.62	32.1	1.57	0.17	0.16	61.86	
1000	A	11	H	5	75	77	95.57	3181.1						58.14	
1000	A	11	H	5	105	107	95.87	3188.3						59.68	
1000	A	11	H	5	115	117	95.97	3190.7	5.42	31.6	1.57	0.13	0.16		
1000	A	11	H	5	135	137	96.17	3195.3						59.19	
1000	A	11	H	5	145	147	96.27	3197.7	6.00	32.9	1.59	0.16	0.18		
1000	A	11	H	6	15	17	96.47	3202.5						52.47	
1000	A	11	H	6	45	47	96.77	3209.5						47.59	
1000	A	11	H	6	75	77	97.07	3216.8	5.50	31.8	1.59	0.14	0.17	66.42	
1000	A	11	H	6	105	107	97.37	3223.8						56.18	
1000	A	11	H	6	125	127	97.57	3228.6	6.23	33.4	1.58	0.15	0.21		
1000	A	11	H	6	135	137	97.67	3231.0						59.24	
1000	A	11	H	7	15	17	97.97	3238.0						58.79	
1000	A	11	H	7	25	27	98.07	3240.4	6.53	34.1	1.62	0.17	0.31		
1000	A	11	H	7	45	47	98.27	3245.2						60.72	
1000	A	11	H	0	5	7	98.3	3247.4	6.41	33.8	1.63	0.15	0.20		
1000	A	12	H	1	5	7	98.35	3250.8	6.80	34.6	1.56	0.19	0.38		
1000	A	12	H	1	15	17	98.45	3253.2	6.92	34.8	1.66	0.10	0.31	57.93	
1000	A	12	H	1	25	27	98.55	3255.6	6.50	34.0	1.61	0.11	0.31		
1000	A	12	H	1	35	37	98.65	3258.0	6.64	34.3	1.61	0.11	0.20		
1000	A	12	H	1	45	47	98.75	3260.5	7.05	35.1	1.58	0.12	0.29	56.60	
1000	A	12	H	1	55	57	98.85	3262.9			1.64	0.13	0.30		
1000	A	12	H	1	65	67	98.95	3265.3	7.09	35.1	1.62	0.14	0.28		
1000	A	12	H	1	75	77	99.05	3267.7	7.33	35.6	1.61	0.11	0.26	54.64	
1000	A	12	H	1	85	87	99.15	3270.1	7.17	35.3	1.63	0.13	0.39		
1000	A	12	H	1	95	97	99.25	3272.5	6.80	34.6	1.55	0.13	0.28		

Appendix B (continued)

Site	Hole	Core	Type	Sec.	Top (cm)	Bot (cm)	Depth (corr. msbf)	Age (ka)	Mg/Ca (mmol/mol)	Temperature (°C)	Sr/Ca (mmol/mol)	Mn/Ca (mmol/mol)	Fe/Ca (mmol/mol)	Aragonite <63 (%)	*F.profunda* (%)
1000	A	12	H	1	105	107	99.35	3274.9	6.79	34.6	1.58	0.12	0.35	59.71	
1000	A	12	H	1	115	117	99.45	3277.4	6.66	34.3	1.56	0.12	0.28		
1000	A	12	H	1	125	127	99.55	3279.8	7.19	35.3	1.58	0.13	0.35		
1000	A	12	H	1	135	137	99.65	3282.2	7.61	36.1	1.58	0.12	0.39	49.68	
1000	A	12	H	1	145	147	99.75	3284.6	6.97	34.9	1.53	0.10	0.34		
1000	A	12	H	2	5	7	99.85	3287.0	6.05	33.1	1.50	0.08	0.28		
1000	A	12	H	2	15	17	99.95	3290.6	4.79	30.0	1.48	0.07	0.18	65.08	
1000	A	12	H	2	25	27	100.05	3294.1	5.52	31.8	1.51	0.08	0.23		
1000	A	12	H	2	35	37	100.15	3297.6	5.25	31.2	1.47	0.08	0.21		
1000	A	12	H	2	45	47	100.25	3301.2	5.67	32.2	1.49	0.10	0.27	48.10	
1000	A	12	H	2	54	56	100.35	3304.7	5.85	32.6	1.55	0.09	0.32		
1000	A	12	H	2	65	67	100.45	3308.3	5.91	32.7	1.57	0.08	0.40		
1000	A	12	H	2	75	77	100.55	3311.8	4.86	30.2	1.52	0.07	0.22	61.63	
1000	A	12	H	2	85	87	100.65	3315.4	5.57	32.0	1.55	0.09	0.20		
1000	A	12	H	2	95	97	100.75	3318.9	6.30	33.6	1.59	0.10	0.27		
1000	A	12	H	2	105	107	100.85	3322.4	6.97	34.9	1.61	0.12	0.30	42.19	
1000	A	12	H	2	115	117	100.95	3326.0	7.48	35.8	1.70	0.14	0.34		
1000	A	12	H	2	125	127	101.05	3328.6	6.54	34.1	1.66	0.11	0.31		
1000	A	12	H	2	135	137	101.15	3331.2	5.34	31.4	1.54	0.08	0.23	60.81	
1000	A	12	H	2	145	147	101.25	3333.7	5.24	31.2	1.53	0.08	0.31		
1000	A	12	H	3	5	7	101.35	3336.3	5.30	31.3	1.53	0.09	0.22		
1000	A	12	H	3	15	17	101.45	3338.9	6.16	33.3	1.61	0.12	0.26	59.48	
1000	A	12	H	3	25	27	101.55	3341.5	6.26	33.5	1.60	0.11	0.28		
1000	A	12	H	3	35	37	101.65	3344.1	5.25	31.2	1.55	0.10	0.29		
1000	A	12	H	3	45	47	101.75	3346.6	4.10	27.9	1.36	0.11	0.19	63.29	
1000	A	12	H	3	55	57	101.85	3349.2	4.40	28.9	1.36	0.09	0.19		
1000	A	12	H	3	65	67	101.95	3351.8	5.92	32.8	1.55	0.12	0.27		
1000	A	12	H	3	75	77	102.05	3354.4	5.64	32.1	1.51	0.10	0.25	65.15	
1000	A	12	H	3	85	87	102.15	3357.0	4.98	30.5	1.49	0.09	0.18		
1000	A	12	H	3	95	97	102.25	3359.6	5.30	31.3	1.51	0.11	0.30		
1000	A	12	H	3	105	107	102.35	3362.1	6.11	33.2	1.58	0.14	0.39	64.27	
1000	A	12	H	3	115	117	102.45	3364.7	6.48	34.0	1.59	0.13	0.29		
1000	A	12	H	3	124	126	102.54	3367.0	6.79	34.6	1.60	0.15	0.33		
1000	A	12	H	3	135	137	102.65	3369.9	6.67	34.3	1.64	0.14	0.34	51.09	
1000	A	12	H	3	142	144	102.72	3371.7	7.24	35.4	1.66	0.15	0.40		
1000	A	12	H	4	5	7	102.85	3375.0	6.45	33.9	1.61	0.12	0.29		
1000	A	12	H	4	15	17	102.95	3377.6	5.82	32.5	1.54	0.13	0.29	57.97	
1000	A	12	H	4	25	27	103.05	3380.2	4.89	30.2	1.48	0.08	0.22		
1000	A	12	H	4	35	37	103.15	3382.8	4.17	28.2	1.38	0.07	0.17		
1000	A	12	H	4	45	47	103.25	3385.4	4.05	27.8	1.37	0.09	0.18	71.13	
1000	A	12	H	4	55	57	103.35	3387.9	4.53	29.2	1.41	0.08	0.17		
1000	A	12	H	4	65	67	103.45	3390.5	4.75	29.9	1.42	0.08	0.17		
1000	A	12	H	4	75	77	103.55	3393.1	4.97	30.5	1.46	0.10	0.17	63.78	
1000	A	12	H	4	85	87	103.65	3395.7	5.90	32.7	1.54	0.13	0.27		
1000	A	12	H	4	94	96	103.74	3398.0	5.82	32.5	1.58	0.12	0.24		
1000	A	12	H	4	107	109	103.87	3400.9	5.90	32.7	1.58	0.12	0.27	48.23	
1000	A	12	H	4	115	117	103.95	3402.6	5.83	32.6	1.59	0.14	0.27		
1000	A	12	H	4	125	127	104.05	3404.8	5.82	32.5	1.56	0.10	0.26		
1000	A	12	H	4	135	137	104.15	3407.0	4.93	30.4	1.50	0.11	0.20	62.83	
1000	A	12	H	4	145	147	104.25	3409.2	4.98	30.5	1.48	0.11	0.24		
1000	A	12	H	5	15	17	104.45	3413.5						54.13	
1000	A	12	H	5	35	37	104.65	3417.9	5.89	32.7	1.63	0.18	0.28		
1000	A	12	H	5	45	47	104.75	3420.1						46.84	
1000	A	12	H	5	55	57	104.85	3422.3	5.52	31.8	1.58	0.16	0.27		
1000	A	12	H	5	75	77	105.05	3426.7						69.11	
1000	A	12	H	5	95	97	105.25	3431.1	4.09	27.9	1.44	0.15	0.16		
1000	A	12	H	5	105	107	105.35	3433.2						56.88	
1000	A	12	H	5	115	117	105.45	3435.4	5.31	31.3	1.58	0.23	0.23		
1000	A	12	H	5	135	137	105.65	3439.8						34.60	
1000	A	12	H	6	15	17	105.95	3446.9						56.02	
1000	A	12	H	6	45	47	106.25	3454.1	5.05	30.7	1.53	0.18	0.27	50.55	
1000	A	12	H	6	65	67	106.45	3459.0	4.62	29.5	1.50	0.19	0.22		
1000	A	12	H	6	75	77	106.55	3461.4						48.97	
1000	A	12	H	6	85	87	106.65	3463.8	4.22	28.3	1.41	0.11	0.11		
1000	A	12	H	6	105	107	106.85	3468.7						63.99	
1000	A	12	H	6	115	117	106.95	3471.1	4.24	28.4	1.41	0.20	0.17		

Appendix B (continued)

Site	Hole	Core	Type	Sec.	Top (cm)	Bot (cm)	Depth (corr. msbf)	Age (ka)	Mg/Ca (mmol/mol)	Temperature (°C)	Sr/Ca (mmol/mol)	Mn/Ca (mmol/mol)	Fe/Ca (mmol/mol)	Aragonite <63 (%)	*F.profunda* (%)
1000	A	12	H	6	135	137	107.15	3475.9						40.38	
1000	A	12	H	7	5	7	107.35	3480.8	6.34	33.7	1.57	0.25	0.39		
1000	A	12	H	7	15	17	107.45	3483.2						38.09	
1000	B	2	R	1	15	17	107.95	3495.4	4.16	28.1	1.42	0.13	0.26		
1000	B	2	R	1	45	47	108.25	3502.6	5.20	31.1	1.53	0.15	0.24		
1000	B	2	R	1	85	87	108.65	3512.3	5.47	31.7	1.55	0.19	0.27		
1000	B	2	R	1	125	127	109.05	3522.0	5.24	31.2	1.55	0.16	0.28		
1000	B	2	R	1	145	147	109.25	3526.9	5.09	30.8	1.56	0.16	0.26		
1000	B	2	R	2	25	27	109.55	3534.1	4.60	29.5	1.52	0.16	0.21		
1000	B	2	R	2	55	57	109.85	3541.1	5.09	30.8	1.53	0.14	0.25		
1000	B	2	R	2	95	97	110.25	3549.3	5.51	31.8	1.63	0.15	0.30		
1000	B	2	R	2	135	137	110.65	3557.5	5.45	31.7	1.61	0.16	0.28		
1000	B	2	R	3	45	47	111.25	3569.8	4.56	29.3	1.49	0.14	0.21		
1000	B	2	R	3	85	87	111.65	3578.1	4.15	28.1	1.45	0.11	0.12		
1000	B	2	R	3	105	107	111.85	3582.2	4.31	28.6	1.47	0.14	0.17		
1000	B	2	R	4	35	37	112.65	3598.6	5.38	31.5	1.56	0.15	0.33		
1000	B	2	R	4	65	67	112.95	3604.8	5.60	32.0	1.58	0.16	0.31		
1000	B	2	R	4	125	127	113.55	3617.1	4.16	28.1	1.42	0.11	0.28		
1000	B	2	R	5	35	37	114.15	3630.1	4.75	29.9	1.50	0.13	0.32		
1000	B	2	R	5	105	107	114.85	3649.1	4.20	28.2	1.40	0.12	0.17		
1000	B	2	R	5	145	147	115.25	3660.0	5.92	32.8	1.55	0.17	0.39		
1000	A	14	H	1	5	7	117.35	3797.0						43.33	
1000	A	14	H	1	15	17	117.45	3799.0						37.01	
1000	A	14	H	1	24	26	117.54	3800.9						39.83	
1000	A	14	H	1	35	37	117.65	3803.1						47.28	
1000	A	14	H	1	45	47	117.75	3805.3						46.13	
1000	A	14	H	1	55	57	117.85	3807.3						38.96	
1000	A	14	H	1	65	67	117.95	3809.5						34.73	
1000	A	14	H	1	75	77	118.05	3811.4						37.01	
1000	A	14	H	1	85	87	118.15	3813.6						30.24	
1000	A	14	H	1	95	97	118.25	3815.6						35.39	6.00
1000	A	14	H	1	104	106	118.34	3817.6						35.63	7.24
1000	A	14	H	1	115	117	118.45	3819.8						42.54	11.08
1000	A	14	H	1	126	128	118.56	3821.9						54.45	15.90
1000	A	14	H	1	135	137	118.65	3823.9						64.46	24.49
1000	A	14	H	1	144	146	118.74	3825.9	4.52	29.2	1.40	0.11	0.21	70.17	45.97
1000	A	14	H	2	5	7	118.85	3828.1						71.08	35.87
1000	A	14	H	2	15	17	118.95	3830.0						62.14	29.86
1000	A	14	H	2	24	26	119.04	3832.0	4.96	30.4	1.43	0.17	0.24	30.24	37.78
1000	A	14	H	2	35	37	119.15	3834.2						46.24	29.04
1000	A	14	H	2	44	46	119.24	3836.2						39.90	25.89
1000	A	14	H	2	55	57	119.35	3838.4						30.07	8.71
1000	A	14	H	2	65	67	119.45	3840.6						27.19	11.15
1000	A	14	H	2	75	77	119.55	3842.6						32.84	4.69
1000	A	14	H	2	85	87	119.65	3844.8						42.48	16.75
1000	A	14	H	2	95	97	119.75	3846.8						48.54	20.25
1000	A	14	H	2	104	106	119.84	3848.7						51.64	23.91
1000	A	14	H	2	114	116	119.94	3850.7	5.96	32.9	1.56	0.20	0.36	49.46	29.38
1000	A	14	H	2	124	126	120.04	3852.9						55.40	36.06
1000	A	14	H	2	135	137	120.15	3855.1						51.19	12.21
1000	A	14	H	2	145	147	120.25	3857.3						47.83	21.51
1000	A	14	H	3	5	7	120.35	3859.3						41.17	12.23
1000	A	14	H	3	15	17	120.45	3861.5						40.68	12.30
1000	A	14	H	3	25	27	120.55	3863.5						40.43	10.78
1000	A	14	H	3	35	37	120.65	3865.7						43.58	14.87
1000	A	14	H	3	45	47	120.75	3867.7						50.02	18.75
1000	A	14	H	3	55	57	120.85	3869.9	3.96	27.5	1.40	0.09	0.13	62.11	33.81
1000	A	14	H	3	65	67	120.95	3871.9						68.49	40.11
1000	A	14	H	3	75	77	121.05	3874.1	3.82	27.0	1.38	0.08	0.16	72.66	22.29
1000	A	14	H	3	85	87	121.15	3876.1						70.43	34.85
1000	A	14	H	3	94	96	121.24	3878.1						69.84	37.24
1000	A	14	H	3	105	107	121.35	3880.2						66.41	37.47
1000	A	14	H	3	115	117	121.45	3882.2						62.08	38.94
1000	A	14	H	3	125	127	121.55	3884.4	4.68	29.7	1.50	0.13	0.21	58.30	30.75
1000	A	14	H	3	135	137	121.65	3886.4						54.52	27.42
1000	A	14	H	3	145	147	121.75	3888.6						44.29	10.14

Appendix B (continued)

Site	Hole	Core	Type	Sec.	Top (cm)	Bot (cm)	Depth (corr. msbf)	Age (ka)	Mg/Ca (mmol/mol)	Temperature (°C)	Sr/Ca (mmol/mol)	Mn/Ca (mmol/mol)	Fe/Ca (mmol/mol)	Aragonite <63 (%)	*F.profunda* (%)
1000	A	14	H	4	5	7	121.85	3890.6						39.09	16.16
1000	A	14	H	4	15	17	121.95	3892.8						46.08	3.61
1000	A	14	H	4	25	27	122.05	3894.8	5.78	32.4	1.58			55.43	22.10
1000	A	14	H	4	35	37	122.15	3897.0	5.00	30.5	1.50	0.12	0.23	60.91	30.71
1000	A	14	H	4	45	47	122.25	3899.5	4.76	29.9	1.48	0.12	0.25	62.96	30.50
1000	A	14	H	4	55	57	122.35	3902.3						54.12	14.40
1000	A	14	H	4	65	67	122.45	3904.8						48.38	11.60
1000	A	14	H	4	75	77	122.55	3907.6						44.58	8.07
1000	A	14	H	4	85	87	122.65	3910.2						44.08	6.34
1000	A	14	H	4	95	97	122.75	3913.0	6.24	33.5	1.54			45.05	8.59
1000	A	14	H	4	106	108	122.86	3915.8	6.66	34.3	1.49			42.53	11.01
1000	A	14	H	4	115	117	122.95	3918.3	5.79	32.5	1.49			48.49	31.70
1000	A	14	H	4	125	127	123.05	3920.8	5.12	30.9	1.45			57.71	30.21
1000	A	14	H	4	135	137	123.15	3923.6	4.52	29.2	1.42	0.12	0.20	64.98	18.21
1000	A	14	H	4	145	147	123.25	3926.1	4.40	28.9	1.41			64.24	37.56
1000	A	14	H	5	5	7	123.35	3928.9	4.56	29.3	1.43			61.92	28.73
1000	A	14	H	5	15	17	123.45	3931.4	4.91	30.3	1.46			55.78	26.04
1000	A	14	H	5	25	27	123.55	3934.2	5.65	32.2	1.51			43.04	9.01
1000	A	14	H	5	35	37	123.65	3936.8	5.69	32.2	1.55			38.85	5.59
1000	A	14	H	5	45	47	123.75	3939.3	6.15	33.3	1.57			38.05	6.76
1000	A	14	H	5	55	57	123.85	3942.1						29.46	11.55
1000	A	14	H	5	65	67	123.95	3944.6	6.02	33.0	1.57			43.40	10.59
1000	A	14	H	5	75	77	124.05	3947.4	5.12	30.9	1.40			62.12	29.44
1000	A	14	H	5	85	87	124.15	3949.9	4.95	30.4	1.40			66.46	29.16
1000	A	14	H	5	95	97	124.25	3952.7	4.30	28.6	1.39			64.84	29.37
1000	A	14	H	5	105	107	124.35	3955.2	5.50	31.8	1.48			47.92	18.00
1000	A	14	H	5	115	117	124.45	3958.1	6.57	34.1	1.58			33.99	9.47
1000	A	14	H	5	125	127	124.55	3960.6	6.87	34.7	1.54			30.64	3.66
1000	A	14	H	5	135	137	124.65	3963.4	5.70	32.3	1.49			43.68	11.05
1000	A	14	H	5	145	147	124.75	3965.9	4.39	28.8	1.38			61.27	27.18
1000	A	14	H	6	5	7	124.85	3968.7	5.03	30.6	1.41			43.58	40.73
1000	A	14	H	6	15	17	124.95	3971.2	5.61	32.1	1.47			51.97	26.95
1000	A	14	H	6	25	27	125.05	3974.0	5.41	31.6	1.48			52.04	14.32
1000	A	14	H	6	35	37	125.15	3976.5	6.16	33.3	1.48			46.24	16.45
1000	A	14	H	6	45	47	125.25	3979.3	6.33	33.7	1.53			48.69	17.37
1000	A	14	H	6	55	57	125.35	3981.9	5.95	32.8	1.51			53.35	18.64
1000	A	14	H	6	65	67	125.45	3984.7	5.96	32.8	1.46			48.61	19.03
1000	A	14	H	6	75	77	125.55	3987.2	5.54	31.9	1.43			49.75	17.02
1000	A	14	H	6	85	87	125.65	3990.0	5.29	31.3	1.43			51.22	24.93
1000	A	14	H	6	95	97	125.75	3992.5	5.31	31.3	1.45			54.41	23.96
1000	A	14	H	6	105	107	125.85	3995.3	4.51	29.2	1.37			56.24	26.46
1000	A	14	H	6	115	117	125.95	3997.7	4.35	28.7	1.38			59.78	
1000	A	14	H	6	125	127	126.05	4000.4	4.67	29.7	1.39			60.74	35.31
1000	A	14	H	6	135	137	126.15	4002.8	5.26	31.2	1.43			56.97	36.04
1000	A	14	H	6	145	147	126.25	4005.2	5.59	32.0	1.45			50.60	22.06
1000	A	14	H	7	5	7	126.35	4007.9	5.72	32.3	1.43			44.42	19.26
1000	A	14	H	7	15	17	126.45	4010.3	6.34	33.7	1.47			42.02	27.67
1000	A	14	H	7	25	27	126.55	4012.9	5.79	32.5	1.44				24.56
1000	A	14	H	7	35	37	126.65	4015.4	5.20	31.1	1.40			58.45	25.81
1000	A	14	H	7	45	47	126.75	4018.0	4.77	29.9	1.39			54.36	29.93
1000	A	14	H	7	55	57	126.85	4020.4	5.62	32.1	1.46			48.71	26.77
1000	A	14	H	7	65	67	126.95	4023.1	5.58	32.0	1.47			38.96	26.01
1000	A	14	H	0	5	7	127	4029.0	5.58	32.0	1.43			31.80	
1000	A	15	H	1	8	10	127.08	4076.0	4.38	28.8	1.35			33.30	34.59
1000	A	15	H	1	15	17	127.15	4077.7	3.85	27.1	1.35				34.75
1000	A	15	H	1	25	27	127.25	4080.6	3.90	27.3					39.95
1000	A	15	H	1	35	37	127.35	4083.6	4.18	28.2	1.39			33.42	40.22
1000	A	15	H	1	45	47	127.45	4086.2	4.04	27.7					31.40
1000	A	15	H	1	55	57	127.55	4089.1	4.30	28.5					33.47
1000	A	15	H	1	65	67	127.65	4092.0	4.09	27.9	1.36			34.31	34.81
1000	A	15	H	1	75	77	127.75	4094.6	3.96	27.5					32.73
1000	A	15	H	1	85	87	127.85	4097.5	4.10	27.9	1.33				31.92
1000	A	15	H	1	95	97	127.95	4100.4	4.38	28.8	1.34			37.09	27.83
1000	A	15	H	1	105	107	128.05	4103.0	4.27	28.5	1.33				28.41
1000	A	15	H	1	115	117	128.15	4105.9	4.65	29.6	1.38				21.45
1000	A	15	H	1	125	127	128.25	4108.8	5.16	30.9	1.40			3.03	18.12

Appendix B (continued)

Site	Hole	Core	Type	Sec.	Top (cm)	Bot (cm)	Depth (corr. msbf)	Age (ka)	Mg/Ca (mmol/mol)	Temperature (°C)	Sr/Ca (mmol/mol)	Mn/Ca (mmol/mol)	Fe/Ca (mmol/mol)	Aragonite <63 (%)	*F.profunda* (%)
1000	A	15	H	1	135	137	128.35	4111.4	5.38	31.5	1.41				21.27
1000	A	15	H	1	145	147	128.45	4114.3	5.22	31.1	1.40				19.55
1000	A	15	H	2	5	7	128.55	4117.2	4.48	29.1	1.37			28.19	34.20
1000	A	15	H	2	15	17	128.65	4119.8	4.70	29.7	1.38				35.78
1000	A	15	H	2	25	27	128.75	4122.7	4.32	28.6	1.36				31.76
1000	A	15	H	2	35	37	128.85	4125.6	4.82	30.1	1.39			11.25	36.12
1000	A	15	H	2	45	47	128.95	4128.2	4.70	29.7	1.39				24.70
1000	A	15	H	2	55	57	129.05	4131.1	5.63	32.1	1.42				16.73
1000	A	15	H	2	65	67	129.15	4133.7	5.22	31.1	1.43			2.96	26.51
1000	A	15	H	2	75	77	129.25	4136.6	4.53	29.2	1.37				36.34
1000	A	15	H	2	85	87	129.35	4139.6	4.44	29.0	1.35				40.55
1000	A	15	H	2	95	97	129.45	4142.2	4.22	28.3	1.35			21.37	30.96
1000	A	15	H	2	105	107	129.55	4145.1	4.67	29.7	1.38				31.29
1000	A	15	H	2	115	117	129.65	4148.0	4.45	29.0	1.37				21.52
1000	A	15	H	2	125	127	129.75	4150.6	4.96	30.4	1.43			2.92	20.00
1000	A	15	H	2	135	137	129.85	4153.5	4.53	29.3	1.40				19.96
1000	A	15	H	2	145	147	129.95	4156.4	4.22	28.3	1.37				28.26
1000	A	15	H	3	5	7	130.05	4159.0	4.21	28.3	1.37			24.70	31.01
1000	A	15	H	3	15	17	130.15	4162.3	4.28	28.5	1.35				29.26
1000	A	15	H	3	25	27	130.25	4165.5	4.25	28.4	1.36				29.87
1000	A	15	H	3	35	37	130.35	4168.4	4.39	28.8	1.35			14.75	33.88
1000	A	15	H	3	45	47	130.45	4171.7	4.30	28.6	1.37				28.96
1000	A	15	H	3	55	57	130.55	4175.0	4.24	28.4	1.36				28.21
1000	A	15	H	3	65	67	130.65	4177.9	4.55	29.3	1.37			0.82	30.56
1000	A	15	H	3	75	77	130.75	4181.1	4.26	28.5	1.36				17.89
1000	A	15	H	3	85	87	130.85	4184.4	4.16	28.1	1.35				29.26
1000	A	15	H	3	95	97	130.95	4187.3	4.36	28.7	1.37			17.50	23.51
1000	A	15	H	3	105	107	131.05	4190.6	4.22	28.3	1.35				35.82
1000	A	15	H	3	115	117	131.15	4193.5	4.10	27.9	1.32				34.39
1000	A	15	H	3	125	127	131.25	4196.8	4.54	29.3	1.36			7.50	
1000	A	15	H	3	135	137	131.35	4200.0	4.50	29.2	1.40				35.21
1000	A	15	H	3	143	145	131.43	4202.3	4.39	28.8	1.38				40.22
1000	A	15	H	4	5	7	131.55	4206.2	4.26	28.4	1.36			27.49	37.55
1000	A	15	H	4	15	17	131.65	4209.5	4.07	27.8	1.35				44.25
1000	A	15	H	4	25	27	131.75	4212.4	4.17	28.2	1.36				47.39
1000	A	15	H	4	35	37	131.85	4215.7	4.49	29.1	1.36			21.80	45.18
1000	A	15	H	4	45	47	131.95	4218.9	4.37	28.8	1.36				40.53
1000	A	15	H	4	55	57	132.05	4221.9	4.57	29.4	1.41				35.35
1000	A	15	H	4	65	67	132.15	4225.1	4.74	29.8	1.40			0.36	30.91
1000	A	15	H	4	75	77	132.25	4228.4	4.41	28.9	1.38				37.75
1000	A	15	H	4	85	87	132.35	4231.3	4.54	29.3	1.37				45.85
1000	A	15	H	4	95	97	132.45	4234.6	4.50	29.2	1.38			28.53	49.44
1000	A	15	H	4	105	107	132.55	4237.8	4.32	28.6	1.38				43.32
1000	A	15	H	4	115	117	132.65	4240.7	4.39	28.8	1.37				44.51
1000	A	15	H	4	125	127	132.75	4244.0	4.45	29.0	1.37			10.71	45.99
1000	A	15	H	4	135	137	132.85	4246.7	3.99	27.6	1.36				50.10
1000	A	15	H	4	145	147	132.95	4249.2	4.09	27.9	1.34				54.49
1000	A	15	H	5	5	7	133.05	4252.0	4.29	28.5	1.35			34.36	54.22
1000	A	15	H	5	15	17	133.15	4254.4	4.50	29.1	1.34				50.69
1000	A	15	H	5	25	27	133.25	4257.2	4.30	28.6	1.34				44.61
1000	A	15	H	5	35	37	133.35	4259.9	5.02	30.6	1.38			13.95	35.81
1000	A	15	H	5	45	47	133.45	4262.4	4.75	29.9	1.40				33.58
1000	A	15	H	5	55	57	133.55	4265.1	4.99	30.5	1.41				26.53
1000	A	15	H	5	65	67	133.65	4267.9	4.76	29.9	1.40			9.19	36.53
1000	A	15	H	5	75	77	133.75	4270.4	4.54	29.3	1.38				35.82
1000	A	15	H	5	85	87	133.85	4273.1	4.27	28.5	1.34				41.63
1000	A	15	H	5	95	97	133.95	4275.8	4.37	28.8	1.34			34.04	46.58
1000	A	15	H	5	105	107	134.05	4278.3	4.07	27.8	1.35				46.93
1000	A	15	H	5	115	117	134.15	4281.0	4.68	29.7	1.35				42.19
1000	A	15	H	5	125	127	134.25	4283.8	4.53	29.3	1.35			29.81	42.46
1000	A	15	H	5	135	137	134.35	4286.3	4.84	30.1	1.36				37.11
1000	A	15	H	5	145	147	134.45	4289.0	4.63	29.5	1.33				45.39
1000	A	15	H	6	5	7	134.55	4291.8	4.62	29.5	1.34			19.90	40.29
1000	A	15	H	6	15	17	134.65	4294.2	4.18	28.2	1.33				45.89
1000	A	15	H	6	25	27	134.75	4297.0	4.24	28.4	1.33				48.68
1000	A	15	H	6	35	37	134.85	4299.7	4.15	28.1	1.33			32.69	50.98

Appendix B (continued)

Site	Hole	Core	Type	Sec.	Top (cm)	Bot (cm)	Depth (corr. msbf)	Age (ka)	Mg/Ca (mmol/mol)	Temperature (°C)	Sr/Ca (mmol/mol)	Mn/Ca (mmol/mol)	Fe/Ca (mmol/mol)	Aragonite <63 (%)	*F.profunda* (%)
1000	A	15	H	6	45	47	134.95	4302.2	4.62	29.5	1.37				47.36
1000	A	15	H	6	55	57	135.05	4304.9	4.77	29.9	1.40				39.06
1000	A	15	H	6	65	67	135.15	4307.4	4.90	30.3	1.39			5.61	34.24
1000	A	15	H	6	75	77	135.25	4310.1	4.94	30.4	1.39				32.91
1000	A	15	H	6	85	87	135.35	4312.9	4.49	29.1	1.38				44.42
1000	A	15	H	6	95	97	135.45	4315.4	3.99	27.6	1.37			41.69	49.06
1000	A	15	H	6	105	107	135.55	4318.1	4.03	27.7	1.34				46.05
1000	A	15	H	6	115	117	135.65	4320.8	4.41	28.9	1.35				50.95
1000	A	15	H	6	125	127	135.75	4323.3	4.34	28.7	1.39			6.63	46.14
1000	A	15	H	6	135	137	135.85	4326.1	4.45	29.0	1.36				45.04
1000	A	15	H	6	145	147	135.95	4328.8	4.46	29.1	1.37				41.94
1000	A	15	H	7	5	7	136.05	4331.8	4.19	28.2	1.36			23.90	45.86
1000	A	15	H	7	15	17	136.15	4335.0	4.54	29.3	1.35				36.99
1000	A	15	H	7	25	27	136.25	4338.3	4.87	30.2	1.37				28.48
1000	A	15	H	7	35	37	136.35	4341.2	4.26	28.4	1.33			11.56	36.68
1000	A	15	H	7	45	47	136.45	4344.5	4.18	28.2	1.32				34.95
1000	A	15	H	7	55	57	136.55	4347.8	3.92	27.3	1.32				37.87
1000	A	15	H	7	63	65	136.63	4350.1	4.05	27.8	1.33			33.84	43.58
1000	A	15	H	0	5	7	136.65	4352.7	4.33	28.6	1.32				46.76
1000	A	16	H	1	5	7	136.75	4424.0	3.72	26.6	1.34			8.93	39.66
1000	A	16	H	1	15	17	136.85	4427.3	4.15	28.1	1.34				39.84
1000	A	16	H	1	25	27	136.95	4430.9	4.13	28.0	1.34				41.23
1000	A	16	H	1	35	37	137.05	4434.2	4.31	28.6	1.36			2.07	40.69
1000	A	16	H	1	45	47	137.15	4437.8	4.03	27.7	1.33				36.91
1000	A	16	H	1	55	57	137.25	4441.1	3.78	26.9	1.32				39.76
1000	A	16	H	1	65	67	137.35	4444.8	4.78	30.0	1.35			0.20	42.10
1000	A	16	H	1	75	77	137.45	4448.0	3.99	27.6	1.31				40.77
1000	A	16	H	1	85	87	137.55	4451.7	3.96	27.5	1.32				38.90
1000	A	16	H	1	95	97	137.65	4455.0	4.07	27.8	1.32			14.58	36.59
1000	A	16	H	1	105	107	137.75	4458.6	3.74	26.7	1.31				39.92
1000	A	16	H	1	115	117	137.85	4461.9	3.96	27.5	1.32				37.97
1000	A	16	H	1	125	127	137.95	4465.5	3.90	27.3	1.32			2.52	44.81
1000	A	16	H	1	135	137	138.05	4468.8	3.95	27.4	1.34				43.80
1000	A	16	H	1	145	147	138.15	4472.1	3.96	27.5	1.32				41.48
1000	A	16	H	2	5	7	138.25	4475.7	3.76	26.8	1.33			1.92	29.49
1000	A	16	H	2	15	17	138.35	4479.0	3.93	27.4	1.33				27.06
1000	A	16	H	2	25	27	138.45	4481.6	3.95	27.4	1.32				40.80
1000	A	16	H	2	35	37	138.55	4484.0	3.44	25.6	1.30			2.77	
1000	A	16	H	2	45	47	138.65	4486.6	3.46	25.7	1.29				
1000	A	16	H	2	55	57	138.75	4488.9	3.43	25.6	1.30				
1000	A	16	H	2	65	67	138.85	4491.5	3.89	27.2	1.29			2.22	
1000	A	16	H	2	75	77	138.95	4493.9	3.76	26.8	1.29				
1000	A	16	H	2	85	87	139.05	4496.5	3.84	27.1	1.28				
1000	A	16	H	2	95	97	139.15	4498.9	3.42	25.5	1.28			1.58	
1000	A	16	H	2	105	107	139.25	4501.5	3.91	27.3	1.30				
1000	A	16	H	2	115	117	139.35	4503.8	3.74	26.7	1.29				
1000	A	16	H	2	125	127	139.45	4506.5	3.77	26.8	1.29			2.37	
1000	A	16	H	2	135	137	139.55	4508.8	3.93	27.4	1.30				
1000	A	16	H	2	145	147	139.65	4511.4	3.76	26.8	1.30				
1000	A	16	H	3	5	7	139.75	4513.8	4.24	28.4	1.34			2.16	
1000	A	16	H	3	15	17	139.85	4516.4	3.96	27.5	1.29				
1000	A	16	H	3	25	27	139.95	4518.7	3.59	26.2	1.28				
1000	A	16	H	3	35	37	140.05	4521.4	4.14	28.1	1.32			1.79	
1000	A	16	H	3	45	47	140.15	4523.7	4.28	28.5	1.30				
1000	A	16	H	3	55	57	140.25	4526.3	4.05	27.8	1.29				
1000	A	16	H	3	65	67	140.35	4528.7	4.28	28.5	1.30			1.66	
1000	A	16	H	3	75	77	140.45	4531.3	4.11	28.0	1.30				
1000	A	16	H	3	85	87	140.55	4533.6	4.19	28.2	1.31				
1000	A	16	H	3	95	97	140.65	4536.0	3.71	26.6	1.27			2.12	
1000	A	16	H	3	115	117	140.85	4542.3	3.75	26.8	1.27				
1000	A	16	H	3	125	127	140.95	4545.5	3.73	26.7	1.28			2.30	
1000	A	16	H	3	135	137	141.05	4548.5	3.58	26.2	1.27				
1000	A	16	H	3	145	147	141.15	4551.8	3.55	26.0	1.26				
1000	A	16	H	4	5	7	141.25	4554.8	3.79	26.9	1.33			1.65	
1000	A	16	H	4	15	17	141.35	4558.0	4.04	27.7	1.37				
1000	A	16	H	4	25	27	141.45	4561.0	3.95	27.4	1.32				

Appendix B (continued)

Site	Hole	Core	Type	Sec.	Top (cm)	Bot (cm)	Depth (corr. msbf)	Age (ka)	Mg/Ca (mmol/mol)	Temperature (°C)	Sr/Ca (mmol/mol)	Mn/Ca (mmol/mol)	Fe/Ca (mmol/mol)	Aragonite <63 (%)	*F.profunda* (%)
1000	A	16	H	4	35	37	141.55	4564.3	3.72	26.6	1.34			2.03	
1000	A	16	H	4	45	47	141.65	4567.2	3.74	26.7	1.34				
1000	A	16	H	4	55	57	141.75	4570.5	3.85	27.1	1.35				
1000	A	16	H	4	65	67	141.85	4573.5	4.33	28.7	1.37			1.38	
1000	A	16	H	4	75	77	141.95	4576.8	5.39	31.5	1.34				
1000	A	16	H	4	85	87	142.05	4579.7	3.76	26.8	1.33				
1000	A	16	H	4	95	97	142.15	4583.0	3.88	27.2	1.35			2.42	
1000	A	16	H	4	105	107	142.25	4586.0	3.86	27.1	1.31				
1000	A	16	H	4	115	117	142.35	4589.3	3.99	27.6	1.35				
1000	A	16	H	4	125	127	142.45	4592.2	3.88	27.2	1.33			1.70	
1000	A	16	H	4	135	137	142.55	4595.5	3.84	27.1	1.32				
1000	A	16	H	4	145	147	142.65	4598.5	3.86	27.1	1.36				
1000	A	16	H	5	5	7	142.75	4601.8	3.74	26.7	1.36			2.33	
1000	A	16	H	5	15	17	142.85	4604.8	3.88	27.2	1.34				
1000	A	16	H	5	25	27	142.95	4608.0	3.66	26.4	1.33				
1000	A	16	H	5	35	37	143.05	4611.0	4.05	27.8	1.36			2.41	
1000	A	16	H	5	45	47	143.15	4614.1	4.13	28.0	1.38				
1000	A	16	H	5	55	57	143.25	4617.6	3.94	27.4	1.37				
1000	A	16	H	5	65	67	143.35	4620.7	3.93	27.4	1.29			1.10	
1000	A	16	H	5	75	77	143.45	4624.2	3.97	27.5	1.28				
1000	A	16	H	5	85	87	143.55	4627.3	3.70	26.6	1.26				
1000	A	16	H	5	95	97	143.65	4630.8	4.00	27.6	1.28			2.45	
1000	A	16	H	5	105	107	143.75	4633.9	3.91	27.3	1.26				
1000	A	16	H	5	115	117	143.85	4637.4	4.15	28.1	1.29				
1000	A	16	H	5	125	127	143.95	4640.5	4.23	28.4	1.30			1.48	
1000	A	16	H	5	135	137	144.05	4644.0	3.84	27.1	1.29				
1000	A	16	H	5	145	147	144.15	4647.1	3.71	26.6	1.28				
1000	A	16	H	6	5	7	144.25	4650.6	3.93	27.4	1.28			2.96	
1000	A	16	H	6	15	17	144.35	4653.7	3.78	26.9	1.28				
1000	A	16	H	6	25	27	144.45	4657.1	3.82	27.0	1.26				
1000	A	16	H	6	35	37	144.55	4660.3	3.39	25.4	1.23			2.50	
1000	A	16	H	6	45	47	144.65	4663.8	3.91	27.3	1.25				
1000	A	16	H	6	55	57	144.75	4666.9	4.13	28.0	1.28				
1000	A	16	H	6	65	67	144.85	4670.3	4.32	28.6	1.28			0.81	
1000	A	16	H	6	75	77	144.95	4673.5	3.97	27.5	1.27				
1000	A	16	H	6	85	87	145.05	4676.9	3.77	26.8	1.26				
1000	A	16	H	6	95	97	145.15	4680.1	3.70	26.6	1.28			1.21	
1000	A	16	H	6	105	107	145.25	4683.5	3.69	26.6	1.28				
1000	A	16	H	6	115	117	145.35	4686.6	3.84	27.1	1.25				
1000	A	16	H	6	125	127	145.45	4690.1	3.88	27.2	1.26			1.31	
1000	A	16	H	6	135	137	145.55	4693.2	3.78	26.9	1.25				
1000	A	16	H	6	145	147	145.65	4696.4	3.81	27.0	1.27				
1000	A	16	H	7	5	7	145.75	4699.8	3.88	27.2	1.26			1.43	
1000	A	16	H	7	15	17	145.85	4703.0	3.60	26.2	1.29				
1000	A	16	H	7	25	27	145.95	4706.4	3.80	26.9	1.27				
1000	A	16	H	7	35	37	146.05	4709.6	3.55	26.0	1.30			1.79	
1000	A	16	H	7	45	47	146.15	4713.0	3.66	26.4	1.31				
1000	A	16	H	7	55	57	146.25	4716.1	3.78	26.9	1.29				
1000	A	16	H	7	66	68	146.36	4720.0	3.91	27.3	1.28				
1000	A	16	H	7	75	77	146.45	4722.7	4.11	28.0	1.30				
1000	A	17	H	1	5	7	146.55	4733.5	3.85	27.1	1.33			0.00	
1000	A	17	H	1	15	17	146.65	4736.9	3.69	26.5	1.28				
1000	A	17	H	1	25	27	146.75	4740.6	3.75	26.8	1.25				
1000	A	17	H	1	35	37	146.85	4743.9	3.80	26.9	1.28				
1000	A	17	H	1	45	47	146.95	4747.7	4.02	27.7	1.29				
1000	A	17	H	1	55	57	147.05	4751.4	3.91	27.3	1.29				
1000	A	17	H	1	65	67	147.15	4754.7	4.14	28.1	1.31				
1000	A	17	H	1	75	77	147.25	4758.5	4.02	27.7	1.31				
1000	A	17	H	1	85	87	147.35	4761.8	4.46	29.0	1.32				
1000	A	17	H	1	95	97	147.45	4765.5	4.23	28.3	1.33			0.00	
1000	A	17	H	1	105	107	147.55	4768.9	3.99	27.6	1.31				
1000	A	17	H	1	115	117	147.65	4772.6	3.74	26.7	1.32				
1000	A	17	H	1	125	127	147.75	4776.4	3.56	26.1	1.27				
1000	A	17	H	1	135	137	147.85	4779.7	3.41	25.5	1.26				
1000	A	17	H	1	145	147	147.97	4783.4	4.01	27.6	1.30				
1000	A	17	H	2	5	7	148.05	4786.8	3.77	26.8	1.26				

Appendix B (continued)

Site	Hole	Core	Type	Sec.	Top (cm)	Bot (cm)	Depth (corr. msbf)	Age (ka)	Mg/Ca (mmol/mol)	Temperature (°C)	Sr/Ca (mmol/mol)	Mn/Ca (mmol/mol)	Fe/Ca (mmol/mol)	Aragonite <63 (%)	*F.profunda* (%)
1000	A	17	H	2	15	17	148.15	4790.5	3.95	27.4	1.29				
1000	A	17	H	2	25	27	148.25	4793.9	3.74	26.7	1.30				
1000	A	17	H	2	35	37	148.35	4797.6	3.89	27.2	1.29			0.00	
1000	A	17	H	2	45	47	148.45	4801.3	3.91	27.3	1.30				
1000	A	17	H	2	55	57	148.55	4804.7	4.21	28.3	1.32				
1000	A	17	H	2	65	67	148.65	4808.4	4.23	28.4	1.32				
1000	A	17	H	2	75	77	148.75	4811.7	4.26	28.4	1.31				
1000	A	17	H	2	85	87	148.85	4815.5	4.09	27.9	1.28				
1000	A	17	H	2	95	97	148.95	4818.8	4.09	27.9	1.28				
1000	A	17	H	2	105	107	149.05	4822.5	4.08	27.9	1.28				
1000	A	17	H	2	115	117	149.15	4826.3	3.92	27.3	1.29				
1000	A	17	H	2	125	127	149.25	4829.6	3.97	27.5	1.29			0.00	
1000	A	17	H	2	135	137	149.35	4833.4	4.10	27.9	1.32				
1000	A	17	H	2	145	147	149.45	4836.7	4.26	28.4	1.31				
1000	A	17	H	3	5	7	149.55	4840.4	4.04	27.7	1.30				
1000	A	17	H	3	15	17	149.65	4843.8	4.06	27.8	1.31				
1000	A	17	H	3	25	27	149.75	4847.5	3.91	27.3	1.30				
1000	A	17	H	3	35	37	149.85	4851.2	3.65	26.4	1.29				
1000	A	17	H	3	45	47	149.95	4854.6	4.05	27.8	1.31				
1000	A	17	H	3	55	57	150.05	4858.3	4.69	29.7	1.28				
1000	A	17	H	3	65	67	150.15	4861.7	4.35	28.7	1.30			0.00	
1000	A	17	H	3	75	77	150.25	4865.4	4.11	28.0	1.31				
1000	A	17	H	3	85	87	150.35	4868.8	4.49	29.1	1.29				
1000	A	17	H	3	95	97	150.45	4872.5	4.32	28.6	1.30				
1000	A	17	H	3	105	107	150.55	4876.2	4.23	28.3	1.29				
1000	A	17	H	3	115	117	150.65	4879.5	4.52	29.2	1.31				
1000	A	17	H	3	125	127	150.75	4883.3	4.34	28.7	1.33				
1000	A	17	H	3	135	137	150.85	4886.6	4.06	27.8	1.33				
1000	A	17	H	3	145	147	150.95	4890.4	3.97	27.5	1.33				
1000	A	17	H	4	5	7	151.05	4893.7	3.98	27.5	1.38			14.53	
1000	A	17	H	4	15	17	151.15	4897.4	4.16	28.1	1.35				
1000	A	17	H	4	25	27	151.25	4901.2	4.29	28.5	1.36				
1000	A	17	H	4	35	37	151.35	4904.5	4.43	28.9	1.39				
1000	A	17	H	4	45	47	151.45	4908.2	4.20	28.2	1.35				
1000	A	17	H	4	55	57	151.55	4911.6	4.11	28.0	1.34				
1000	A	17	H	4	65	67	151.65	4915.3	4.03	27.7	1.33				
1000	A	17	H	4	75	77	151.75	4918.7	4.55	29.3	1.31				
1000	A	17	H	4	85	87	151.85	4922.4	4.82	30.1	1.36				
1000	A	17	H	4	95	97	151.95	4925.4	4.49	29.1	1.35			0.00	
1000	A	17	H	4	105	107	152.05	4928.0	4.14	28.1	1.35				
1000	A	17	H	4	115	117	152.15	4931.0	4.15	28.1	1.35				
1000	A	17	H	4	125	127	152.25	4933.6	4.41	28.9	1.35				
1000	A	17	H	4	135	137	152.35	4936.6	3.92	27.4	1.37				
1000	A	17	H	4	145	147	152.45	4939.2	4.28	28.5	1.35				
1000	A	17	H	5	5	7	152.55	4942.2	3.55	26.0	1.26				
1000	A	17	H	5	15	17	152.65	4945.1	3.59	26.2	1.28				
1000	A	17	H	5	25	27	152.75	4947.8	3.79	26.9	1.29				
1000	A	17	H	5	35	37	152.85	4950.7	3.89	27.2	1.31			0.00	
1000	A	17	H	5	45	47	152.95	4953.4	4.00	27.6	1.30				
1000	A	17	H	5	55	57	153.05	4956.3	3.81	27.0	1.30				
1000	A	17	H	5	65	67	153.15	4959.0	4.03	27.7	1.30				
1000	A	17	H	5	75	77	153.25	4961.9	3.79	26.9	1.29				
1000	A	17	H	5	85	87	153.35	4964.9	3.81	27.0	1.30				
1000	A	17	H	5	95	97	153.45	4967.5	4.10	27.9	1.31				
1000	A	17	H	5	105	107	153.55	4970.5	4.13	28.0	1.32				
1000	A	17	H	5	115	117	153.65	4973.1	4.05	27.8	1.31				
1000	A	17	H	5	125	127	153.75	4976.1	3.96	27.5	1.27			0.00	
1000	A	17	H	5	135	137	153.85	4978.7	3.56	26.1	1.25				
1000	A	17	H	5	145	147	153.95	4981.7	4.15	28.1	1.32				
1000	A	17	H	6	5	7	154.05	4984.6	3.82	27.0	1.27				
1000	A	17	H	6	15	17	154.15	4987.3	4.42	28.9	1.29				
1000	A	17	H	6	25	27	154.25	4990.2	4.16	28.1	1.28				
1000	A	17	H	6	35	37	154.35	4992.9	3.75	26.8	1.27			0.00	
1000	A	17	H	6	45	47	154.45	4995.8	3.69	26.5	1.27				
1000	A	17	H	6	55	57	154.55	4998.5	3.86	27.1	1.26				
1000	A	17	H	6	65	67	154.65	5001.4	3.99	27.6	1.27				

Appendix B (continued)

Site	Hole	Core	Type	Sec.	Top (cm)	Bot (cm)	Depth (corr. msbf)	Age (ka)	Mg/Ca (mmol/mol)	Temperature (°C)	Sr/Ca (mmol/mol)	Mn/Ca (mmol/mol)	Fe/Ca (mmol/mol)	Aragonite <63 (%)	*F.profunda* (%)
1000	A	17	H	6	75	77	154.75	5004.4	3.91	27.3	1.29				
1000	A	17	H	6	85	87	154.85	5007.0	4.08	27.9	1.30				
1000	A	17	H	6	95	97	154.95	5010.0	4.11	28.0	1.31				
1000	A	17	H	6	105	107	155.05	5012.6	4.12	28.0	1.31				
1000	A	17	H	6	115	117	155.15	5015.6	3.73	26.7	1.26				
1000	A	17	H	6	125	127	155.25	5018.3	4.32	28.6	1.30				
1000	A	17	H	6	135	137	155.35	5021.4	4.01	27.6	1.28				
1000	A	17	H	6	145	147	155.45	5024.4	4.06	27.8	1.27				
1000	A	17	H	7	5	7	155.55	5027.1	3.76	26.8	1.27			0.00	
1000	A	17	H	7	15	17	155.65	5030.2	3.89	27.3	1.25				
1000	A	17	H	7	25	27	155.75	5032.9	4.30	28.6	1.28				
1000	A	17	H	7	35	37	155.85	5035.9	4.21	28.3	1.30				
1000	A	17	H	7	45	47	155.95	5038.7	4.14	28.1	1.28				
1000	A	17	H	7	55	57	156.05	5041.7	3.90	27.3	1.28				
1000	A	17	H	0	7	9	156.1	5045.3	4.03	27.7	1.27				
1000	A	17	H	0	15	17	156.2	5047.8	4.36	28.7	1.27				
1000	A	17	H	0	25	27	156.3	5050.8	4.39	28.8	1.29				
1000	A	18	H	1	5	7	156.35	5054.1	4.20	28.2	1.28			17.40	
1000	A	18	H	1	15	17	156.45	5056.9	3.58	26.2	1.24				
1000	A	18	H	1	25	27	156.55	5059.9	4.25	28.4	1.28				
1000	A	18	H	1	35	37	156.65	5062.6	4.06	27.8	1.27				
1000	A	18	H	1	45	47	156.75	5065.7	4.22	28.3	1.27				
1000	A	18	H	1	55	57	156.85	5068.4	4.19	28.2	1.26				
1000	A	18	H	1	65	67	156.95	5071.4	4.05	27.8	1.25				
1000	A	18	H	1	75	77	157.05	5074.2	3.99	27.6	1.25				
1000	A	18	H	1	85	87	157.15	5077.2	4.29	28.5	1.26				
1000	A	18	H	1	95	97	157.25	5079.9	4.07	27.8	1.25			0.00	
1000	A	18	H	1	105	107	157.35	5083.0	4.06	27.8	1.28				
1000	A	18	H	1	115	117	157.45	5085.7	4.17	28.2	1.27				
1000	A	18	H	1	125	127	157.55	5088.7	4.17	28.2	1.25				
1000	A	18	H	1	135	137	157.65	5091.5	4.07	27.8	1.28				
1000	A	18	H	1	145	147	157.75	5094.5	4.05	27.8	1.36				
1000	A	18	H	2	5	7	157.85	5097.2	3.86	27.2	1.34				
1000	A	18	H	2	15	17	157.95	5100.3	4.04	27.7	1.35				
1000	A	18	H	2	25	27	158.05	5103.0	3.57	26.1	1.33				
1000	A	18	H	2	35	37	158.15	5106.4	3.99	27.6	1.33			0.00	
1000	A	18	H	2	45	47	158.25	5109.4	3.65	26.4	1.29				
1000	A	18	H	2	55	57	158.35	5112.7	3.97	27.5	1.30				
1000	A	18	H	2	65	67	158.45	5115.7	4.27	28.5	1.35				
1000	A	18	H	2	75	77	158.55	5119.1	4.54	29.3	1.36				
1000	A	18	H	2	85	87	158.65	5122.1	4.30	28.6	1.37				
1000	A	18	H	2	95	97	158.75	5125.5	4.24	28.4	1.37				
1000	A	18	H	2	105	107	158.85	5128.5	4.05	27.8	1.37				
1000	A	18	H	2	115	117	158.95	5131.5	4.10	27.9	1.34				
1000	A	18	H	2	125	127	159.05	5134.8	3.99	27.6	1.34			1.00	
1000	A	18	H	2	135	137	159.15	5137.9	3.83	27.0	1.32				
1000	A	18	H	2	145	147	159.25	5141.2	4.25	28.4	1.36				
1000	A	18	H	3	5	7	159.35	5144.2	4.35	28.7	1.37				
1000	A	18	H	3	15	17	159.45	5147.6	4.23	28.4	1.36				
1000	A	18	H	3	25	27	159.55	5150.6	4.14	28.1	1.36				
1000	A	18	H	3	35	37	159.65	5154.0	4.46	29.0	1.35				
1000	A	18	H	3	45	47	159.75	5157.0	4.28	28.5	1.36				
1000	A	18	H	3	55	57	159.85	5160.3	4.86	30.2	1.34				
1000	A	18	H	3	65	67	159.95	5163.3	4.51	29.2	1.34			1.00	
1000	A	18	H	3	75	77	160.05	5166.7	4.07	27.8	1.37				
1000	A	18	H	3	85	87	160.15	5169.7	3.93	27.4	1.33				
1000	A	18	H	3	95	97	160.25	5173.0	3.76	26.8	1.32				
1000	A	18	H	3	105	107	160.35	5176.1	4.41	28.9	1.36				
1000	A	18	H	3	115	117	160.45	5179.4	4.28	28.5	1.35				
1000	A	18	H	3	125	127	160.55	5182.4	4.24	28.4	1.35				
1000	A	18	H	3	135	137	160.65	5185.8	4.28	28.5	1.33				
1000	A	18	H	3	143	145	160.73	5188.1	4.32	28.6	1.33				
1000	A	18	H	4	5	7	160.85	5192.2	4.25	28.4	1.37			0.99	
1000	A	18	H	4	15	17	160.95	5195.2	4.36	28.8	1.35				
1000	A	18	H	4	25	27	161.05	5198.5	4.40	28.9	1.38				
1000	A	18	H	4	35	37	161.15	5201.5	4.01	27.6	1.33				

Appendix B (continued)

Site	Hole	Core	Type	Sec.	Top (cm)	Bot (cm)	Depth (corr. msbf)	Age (ka)	Mg/Ca (mmol/mol)	Temperature (°C)	Sr/Ca (mmol/mol)	Mn/Ca (mmol/mol)	Fe/Ca (mmol/mol)	Aragonite <63 (%)	*F.profunda* (%)
1000	A	18	H	4	45	47	161.25	5204.9	4.47	29.1	1.37				
1000	A	18	H	4	55	57	161.35	5207.9	4.42	28.9	1.39				
1000	A	18	H	4	65	67	161.45	5211.3	4.58	29.4	1.40				
1000	A	18	H	4	75	77	161.55	5214.3	4.43	29.0	1.36				
1000	A	18	H	4	85	87	161.65	5217.6	4.38	28.8	1.36				
1000	A	18	H	4	95	97	161.75	5220.6	3.98	27.5	1.37			9.06	
1000	A	18	H	4	105	107	161.85	5224.0	4.19	28.2	1.36				
1000	A	18	H	4	115	117	161.95	5226.2	3.93	27.4	1.36				
1000	A	18	H	4	125	127	162.05	5228.7	4.09	27.9	1.32				
1000	A	18	H	4	135	137	162.15	5230.9	4.22	28.3	1.39				
1000	A	18	H	4	145	147	162.25	5233.4	4.11	28.0	1.33				
1000	A	18	H	5	5	7	162.35	5235.6	4.14	28.1	1.34				
1000	A	18	H	5	15	17	162.45	5238.1	4.29	28.5	1.38				
1000	A	18	H	5	25	27	162.55	5240.3	3.80	26.9	1.35				
1000	A	18	H	5	35	37	162.65	5242.8	3.95	27.5	1.34				
1000	A	18	H	5	45	47	162.75	5245.0	3.90	27.3	1.32				
1000	A	18	H	5	55	57	162.85	5247.5	4.28	28.5	1.37				
1000	A	18	H	5	65	67	162.95	5249.7	4.39	28.8	1.36			5.81	
1000	A	18	H	5	75	77	163.05	5252.2	4.11	28.0	1.34				
1000	A	18	H	5	85	87	163.15	5254.5	4.07	27.8	1.36				
1000	A	18	H	5	95	97	163.25	5256.9	4.01	27.7	1.35				
1000	A	18	H	5	105	107	163.45	5259.1	3.67	26.5	1.33				
1000	A	18	H	5	115	117	163.55	5261.6	3.84	27.1	1.35				
1000	A	18	H	5	125	127	163.65	5263.9	4.00	27.6	1.35				
1000	A	18	H	5	135	137	163.75	5266.3	3.86	27.1	1.29				
1000	A	18	H	5	145	147	163.85	5268.5	4.29	28.5	1.35				
1000	A	18	H	6	5	7	163.95	5270.8	3.81	27.0	1.35			0.00	
1000	A	18	H	6	15	17	164.05	5273.3	4.55	29.3	1.35				
1000	A	18	H	6	25	27	164.15	5275.5	4.51	29.2	1.35				
1000	A	18	H	6	35	37	164.25	5278.0	4.32	28.6	1.34				
1000	A	18	H	6	45	47	164.35	5280.2	4.16	28.1	1.33				
1000	A	18	H	6	55	57	164.45	5282.7	3.98	27.5	1.34				
1000	A	18	H	6	65	67	164.55	5284.9	4.06	27.8	1.33				
1000	A	18	H	6	75	77	164.65	5287.4	4.38	28.8	1.36				
1000	A	18	H	6	85	87	164.75	5289.6	4.51	29.2	1.36				
1000	A	18	H	6	95	97	164.85	5292.1	4.32	28.6	1.35			1.00	
1000	A	18	H	6	105	107	164.95	5294.3	4.61	29.5	1.36				
1000	A	18	H	6	115	117	165.05	5296.8	4.50	29.2	1.38				
1000	A	18	H	6	125	127	165.15	5299.0	3.81	27.0	1.33				
1000	A	18	H	6	135	137	165.25	5301.9	3.64	26.4	1.32				
1000	A	18	H	6	145	147	165.35	5304.4	4.45	29.0	1.36				
1000	A	18	H	7	5	7	165.45	5307.3	4.46	29.1	1.37				
1000	A	18	H	7	15	17	165.55	5309.8	3.64	26.4	1.33				
1000	A	18	H	7	25	27	165.65	5312.7	4.14	28.1	1.36				
1000	A	18	H	7	35	37	165.75	5315.2	3.99	27.6	1.32			1.00	
1000	A	18	H	7	45	47	165.85	5318.1	4.44	29.0	1.35				
1000	A	18	H	7	55	57	165.95	5320.6	4.26	28.4	1.36				
1000	A	18	H	7	65	67	166.05	5323.5	4.20	28.3	1.32				
1000	A	18	H	0	5	7	166.1	5326.9	4.23	28.3	1.36				
1000	A	18	H	0	15	17	166.2	5329.8	4.05	27.8	1.35				
1000	A	18	H	0	25	27	166.3	5332.3	4.38	28.8	1.33				
1000	A	19	H	1	9	11	166.35	5335.7	4.21	28.3	1.35			0.00	
1000	A	19	H	1	15	17	166.45	5337.2	3.80	26.9	1.32				
1000	A	19	H	1	25	27	166.55	5340.0	4.19	28.2	1.34				
1000	A	19	H	1	35	37	166.65	5342.6	4.07	27.8	1.33				
1000	A	19	H	1	45	47	166.75	5345.4	4.24	28.4	1.33				
1000	A	19	H	1	55	57	166.85	5348.3	4.48	29.1	1.34				
1000	A	19	H	1	65	67	166.95	5350.8	4.30	28.6	1.32				
1000	A	19	H	1	75	77	167.05	5353.7	4.32	28.6	1.31				
1000	A	19	H	1	85	87	167.15	5356.3	3.99	27.6	1.27				
1000	A	19	H	1	95	97	167.25	5359.1	3.99	27.6	1.32			0.00	
1000	A	19	H	1	105	107	167.35	5361.7	4.31	28.6	1.32				
1000	A	19	H	1	115	117	167.45	5364.5	4.05	27.8	1.31				
1000	A	19	H	1	125	127	167.55	5367.1	3.84	27.1	1.30				
1000	A	19	H	1	135	137	167.65	5369.9	4.31	28.6	1.31				
1000	A	19	H	1	145	147	167.75	5372.5	4.15	28.1	1.31				

Appendix B (continued)

Site	Hole	Core	Type	Sec.	Top (cm)	Bot (cm)	Depth (corr. msbf)	Age (ka)	Mg/Ca (mmol/mol)	Temperature (°C)	Sr/Ca (mmol/mol)	Mn/Ca (mmol/mol)	Fe/Ca (mmol/mol)	Aragonite <63 (%)	*F.profunda* (%)
1000	A	19	H	2	5	7	167.85	5375.3	3.85	27.1	1.31				
1000	A	19	H	2	15	17	167.95	5378.2	4.44	29.0	1.33				
1000	A	19	H	2	25	27	168.05	5380.7	4.29	28.5	1.29				
1000	A	19	H	2	35	37	168.15	5383.6	4.05	27.8	1.28			0.00	
1000	A	19	H	2	45	47	168.25	5386.1	3.71	26.6	1.29				
1000	A	19	H	2	55	57	168.35	5389.0	3.84	27.1	1.27				
1000	A	19	H	2	65	67	168.45	5391.4	4.14	28.0	1.28				
1000	A	19	H	2	75	77	168.55	5394.1	3.86	27.1	1.24				
1000	A	19	H	2	85	87	168.65	5396.5	4.16	28.1	1.30				
1000	A	19	H	2	95	97	168.75	5399.1	4.24	28.4	1.29				
1000	A	19	H	2	105	107	168.85	5401.8	4.32	28.6	1.29				
1000	A	19	H	2	115	117	168.95	5404.2	4.04	27.8	1.30				
1000	A	19	H	2	125	127	169.05	5406.9	4.09	27.9	1.29			0.00	
1000	A	19	H	2	135	137	169.15	5409.3	3.90	27.3	1.25				
1000	A	19	H	2	145	147	169.25	5411.9	3.93	27.4	1.26				
1000	A	19	H	3	5	7	169.35	5414.3	4.08	27.9	1.28				
1000	A	19	H	3	15	17	169.45	5417.0	4.21	28.3	1.29				
1000	A	19	H	3	25	27	169.55	5419.4	3.68	26.5	1.29				
1000	A	19	H	3	35	37	169.65	5422.1	4.41	28.9	1.30				
1000	A	19	H	3	45	47	169.75	5424.5	4.64	29.6	1.31				
1000	A	19	H	3	55	57	169.85	5427.1	4.52	29.2	1.33				
1000	A	19	H	3	65	67	169.95	5429.8	4.24	28.4	1.32			0.00	
1000	A	19	H	3	75	77	170.05	5432.2	4.25	28.4	1.33				
1000	A	19	H	3	85	87	170.15	5434.9	3.79	26.9	1.27				
1000	A	19	H	3	95	97	170.25	5437.3	4.17	28.2	1.27				
1000	A	19	H	3	105	107	170.35	5440.0	4.11	28.0	1.30				
1000	A	19	H	3	115	117	170.45	5442.4	4.28	28.5	1.29				
1000	A	19	H	3	125	127	170.56	5445.0	3.87	27.2	1.25				
1000	A	19	H	3	135	137	170.65	5447.4	3.77	26.8	1.25				
1000	A	19	H	3	145	147	170.75	5450.1	4.39	28.8	1.31				
1000	A	19	H	4	5	7	170.85	5452.8	4.40	28.9	1.36			0.00	
1000	A	19	H	4	15	17	170.95	5455.2	4.38	28.8	1.36				
1000	A	19	H	4	25	27	171.05	5457.8	4.07	27.8	1.33				
1000	A	19	H	4	55	57	171.35	5465.3	4.31	28.6	1.33				
1000	A	19	H	4	65	67	171.45	5468.0	4.17	28.2	1.33				
1000	A	19	H	4	75	77	171.55	5470.4	4.04	27.7	1.32				
1000	A	19	H	4	85	87	171.65	5473.0	4.07	27.8	1.31				
1000	A	19	H	4	95	97	171.75	5475.4	3.74	26.7	1.32			3.28	
1000	A	19	H	4	105	107	171.85	5478.1	3.68	26.5	1.31				
1000	A	19	H	4	115	117	171.95	5480.8	4.06	27.8	1.34				
1000	A	19	H	4	126	128	172.05	5483.4	3.86	27.2	1.31				
1000	A	19	H	4	135	137	172.15	5485.8	3.79	26.9	1.32				
1000	A	19	H	4	145	147	172.25	5488.2	4.03	27.7	1.33				
1000	A	19	H	5	5	7	172.35	5490.9	4.03	27.7	1.33				
1000	A	19	H	5	15	17	172.45	5493.3	4.17	28.2	1.35				
1000	A	19	H	5	25	27	172.55	5496.0	4.45	29.0	1.29				
1000	A	19	H	5	35	37	172.65	5498.4	4.15	28.1	1.28			1.00	
1000	A	19	H	5	45	47	172.75	5501.0	3.87	27.2	1.30				
1000	A	19	H	5	55	57	172.85	5503.7	4.15	28.1	1.30				
1000	A	19	H	5	65	67	172.95	5506.1	3.88	27.2	1.28				
1000	A	19	H	5	75	77	173.05	5508.8	3.53	26.0	1.26				
1000	A	19	H	5	85	87	173.15	5511.2	3.70	26.6	1.26				
1000	A	19	H	5	95	97	173.25	5513.8	3.79	26.9	1.28				
1000	A	19	H	5	105	107	173.35	5516.2	4.08	27.9	1.29				
1000	A	19	H	5	115	117	173.45	5518.9	4.40	28.9	1.30				
1000	A	19	H	5	125	127	173.55	5521.3	3.82	27.0	1.28			4.63	
1000	A	19	H	5	135	137	173.65	5524.0	4.01	27.6	1.30				
1000	A	19	H	5	145	147	173.75	5526.4	3.92	27.3	1.30				
1000	A	19	H	6	5	7	173.85	5529.0	4.26	28.4	1.31				
1000	A	19	H	6	15	17	173.95	5531.7	4.40	28.9	1.32				
1000	A	19	H	6	25	27	174.05	5534.1	4.37	28.8	1.29				
1000	A	19	H	6	35	37	174.15	5536.8	4.70	29.7	1.31				
1000	A	19	H	6	45	47	174.25	5539.2	4.46	29.1	1.30				
1000	A	19	H	6	55	57	174.35	5541.9	3.75	26.8	1.28				
1000	A	19	H	6	65	67	174.45	5544.2	4.24	28.4	1.28			1.00	
1000	A	19	H	6	75	77	174.55	5546.9	4.18	28.2	1.30				

Appendix B (continued)

Site	Hole	Core	Type	Sec.	Top (cm)	Bot (cm)	Depth (corr. msbf)	Age (ka)	Mg/Ca (mmol/mol)	Temperature (°C)	Sr/Ca (mmol/mol)	Mn/Ca (mmol/mol)	Fe/Ca (mmol/mol)	Aragonite <63 (%)	*F.profunda* (%)
1000	A	19	H	6	95	97	174.75	5552.0	4.57	29.4	1.29				
1000	A	19	H	6	105	107	174.85	5554.7	4.26	28.4	1.27				
1000	A	19	H	6	115	117	174.95	5557.1	4.03	27.7	1.27				
1000	A	19	H	6	125	127	175.05	5559.7	4.29	28.5	1.29				
1000	A	19	H	6	135	137	175.15	5562.1	4.71	29.8	1.32				
1000	A	19	H	6	145	147	175.25	5564.8	4.59	29.4	1.32				
1000	A	19	H	7	5	7	175.35	5567.2	4.44	29.0	1.33			13.52	
1000	A	19	H	7	15	17	175.45	5569.9	4.45	29.0	1.32				
1000	A	19	H	7	25	27	175.55	5572.3	4.15	28.1	1.30				
1000	A	19	H	7	35	37	175.65	5574.9	3.95	27.4	1.28				
1000	A	19	H	7	45	47	175.75	5577.3	4.36	28.7	1.32				
1000	A	19	H	7	57	59	175.87	5580.0	4.11	28.0	1.31				
1000	A	19	H	7	64	66	175.94	5582.4	3.93	27.4	1.28				
1000	A	19	H	0	5	7	176	5584.5	3.96	27.5	1.29			69.64	
1000	A	19	H	0	15	17	176.1	5587.2	3.98	27.5	1.29				
1000	A	19	H	0	24	26	176.2	5589.6	4.19	28.2	1.27				

Appendix C $\delta^{18}O_{G.\ sacculifer}$, Mg/Ca and temperature for Site 1241. Sr/Ca, Mn/Ca, and Fe/Ca were monitored as quality control.

Site	Hole	Core	T	Sec.	Top (cm)	Bot (cm)	Depth (corr. msbf)	Age (ka)	$\delta^{18}O_{G.\ Sacculifer}$ (‰)	Mg/Ca (mmol/mol)	Temperature (°C)	Sr/Ca (mmol/mol)	Mn/Ca (mmol/mol)	Fe/Ca (mmol/mol)
1241	A	6	H	1	110	112	49.17	2116.0	-1.338	3.15	24.5	1.32	0.41	0.18
1241	A	6	H	1	122	124	49.29	2121.4	-1.565					
1241	A	6	H	1	130	132	49.37	2125.0	-1.348	3.08	24.2	1.36	0.61	0.05
1241	A	6	H	1	140	142	49.47	2129.5	-1.611					
1241	A	6	H	2	0	2	49.58	2134.5	-1.482	3.43	25.6	1.32	0.66	0.06
1241	A	6	H	2	10	12	49.68	2139.0	-1.441					
1241	A	6	H	2	20	22	49.78	2142.2	-1.496	3.02	23.9	1.32	0.33	0.05
1241	A	6	H	2	30	32	49.88	2145.5	-0.869					
1241	A	6	H	2	38	40	49.96	2148.1	-0.910	3.20	24.7	1.33	0.30	0.00
1241	A	6	H	2	50	52	50.08	2152.0	-0.864					
1241	A	6	H	2	60	62	50.18	2155.2	-1.060	2.84	23.1	1.32	0.59	0.13
1241	A	6	H	2	70	72	50.28	2158.5	-1.038					
1241	A	6	H	2	82	84	50.40	2162.4	-1.263	3.16	24.5	1.36	0.62	0.00
1241	A	6	H	2	90	92	50.48	2165.0	-1.057					
1241	A	6	H	2	100	102	50.58	2168.2	-1.329	3.17	24.5	1.32	0.63	0.37
1241	A	6	H	2	110	112	50.68	2171.5	-1.345					
1241	A	6	H	2	122	124	50.80	2175.4	-1.544	3.30	25.1	1.33	0.68	0.02
1241	A	6	H	2	130	132	50.88	2178.0	-1.623					
1241	A	6	H	2	140	142	50.98	2181.2	-1.517	3.33	25.2	1.32	0.57	0.05
1241	A	6	H	3	0	2	51.08	2184.5	-1.278					
1241	A	6	H	3	10	12	51.18	2187.8	-1.472	3.12	24.4	1.34	0.59	0.08
1241	A	6	H	3	20	22	51.28	2191.0	-1.359					
1241	A	6	H	3	30	32	51.38	2194.3	-1.222	3.05	24.1	1.35	0.57	0.06
1241	A	6	H	3	42	44	51.50	2198.1	-1.444					
1241	A	6	H	3	50	52	51.58	2200.8	-1.593	3.01	23.9	1.34	0.61	0.03
1241	A	6	H	3	60	62	51.68	2204.0	-1.724					
1241	A	6	H	3	70	72	51.78	2207.2	-1.505	3.18	24.6	1.34	0.59	0.04
1241	A	6	H	3	82	84	51.90	2211.1	-1.831					
1241	A	6	H	3	90	92	51.98	2213.7	-1.446	2.84	23.1	1.32	0.60	0.01
1241	A	6	H	3	100	102	52.08	2217.0	-1.684					
1241	A	6	H	3	110	112	52.18	2220.6	-1.681	3.15	24.5	1.32	0.59	0.00
1241	A	6	H	3	122	124	52.30	2224.9	-2.002					
1241	A	6	H	3	130	132	52.38	2227.7	-1.517	2.98	23.7	1.33	0.57	0.00
1241	A	6	H	3	140	142	52.48	2231.3	-1.231					
1241	A	6	H	4	0	2	52.58	2234.9	-1.472	3.07	24.1	1.34	0.58	0.03
1241	A	6	H	4	10	12	52.68	2238.5	-1.169					
1241	A	6	H	4	20	22	52.78	2242.1	-1.428	3.01	23.9	1.34	0.58	0.00
1241	A	6	H	4	30	32	52.88	2245.7	-1.274					
1241	A	6	H	4	42	44	53.00	2250.0	-1.256	2.88	23.3	1.28	0.00	0.00
1241	A	6	H	4	50	52	53.08	2252.8	-1.232					
1241	A	6	H	4	60	62	53.18	2256.4	-1.429	2.94	23.6	1.30	0.48	0.02
1241	A	6	H	4	70	72	53.28	2260.0	-1.716					
1241	A	6	H	4	82	84	53.40	2264.2	-1.771	2.86	23.2	1.30	0.12	0.05
1241	A	6	H	4	90	92	53.48	2266.9	-1.450					
1241	A	6	H	4	100	102	53.58	2270.4	-1.328	3.22	24.8	1.33	0.48	0.03
1241	A	6	H	4	110	112	53.68	2273.9	-1.215					
1241	A	6	H	4	122	124	53.80	2278.0	-0.701	2.82	23.0	1.30	0.55	0.03
1241	A	6	H	4	130	132	53.88	2280.8	-0.744					
1241	A	6	H	4	140	142	53.98	2284.3	-1.212	3.11	24.3	1.30	0.54	0.01
1241	A	6	H	5	2	4	54.10	2288.4	-1.380					
1241	A	6	H	5	10	12	54.18	2291.2	-1.310	3.15	24.5	1.31	0.46	0.06
1241	A	6	H	5	20	22	54.28	2294.7	-1.454					
1241	A	6	H	5	30	32	54.38	2298.1	-1.582	3.17	24.5	1.31	0.57	0.02
1241	A	6	H	5	42	44	54.50	2302.3	-1.511					
1241	A	6	H	5	50	52	54.58	2305.1	-1.465	3.07	24.1	1.31	0.61	0.03
1241	A	6	H	5	60	62	54.68	2308.5	-1.312					
1241	A	6	H	5	70	72	54.78	2312.0	-1.362	2.89	23.3	1.28	0.42	0.01
1241	A	6	H	5	82	84	54.90	2316.1	-1.296					
1241	A	6	H	5	90	92	54.98	2318.9	-1.397	2.93	23.5	1.30	0.44	0.02
1241	A	6	H	5	100	102	55.08	2322.4	-1.268					
1241	A	6	H	5	110	112	55.18	2325.9	-1.370	2.88	23.3	1.29	0.48	0.01
1241	A	6	H	5	122	124	55.30	2330.0	-1.221					
1241	A	6	H	5	130	132	55.38	2332.8	-1.527	3.01	23.9	1.30	0.52	0.10
1241	A	6	H	5	140	142	55.48	2336.3	-1.533					
1241	A	6	H	6	0	2	55.59	2340.1	-1.235	3.00	23.8	1.29	0.43	0.07
1241	A	6	H	6	10	12	55.69	2343.5	-1.430					
1241	A	6	H	6	20	22	55.79	2347.0	-1.453	3.17	24.6	1.31	0.40	0.04
1241	A	6	H	6	30	32	55.89	2350.5	-1.444					
1241	A	6	H	6	38	40	55.97	2353.2	-1.341	2.84	23.1	1.31	0.30	0.01

Appendix C (continued)

Site	Hole	Core	T	Sec.	Top (cm)	Bot (cm)	Depth (corr. msbf)	Age (ka)	$\delta^{18}O_{G.\ Sacculifer}$ (‰)	Mg/Ca (mmol/mol)	Temperature (°C)	Sr/Ca (mmol/mol)	Mn/Ca (mmol/mol)	Fe/Ca (mmol/mol)
1241	C	3	H	2	82	84	56.02	2355.0	-1.139					
1241	C	3	H	2	90	92	56.10	2357.7	-1.195	3.10	24.3	1.32	0.41	0.13
1241	C	3	H	2	100	102	56.20	2361.2	-1.359					
1241	C	3	H	2	110	112	56.30	2364.7	-1.124	2.87	23.2	1.29	0.20	0.00
1241	C	3	H	2	122	124	56.42	2368.8	-1.128					
1241	C	3	H	2	130	132	56.50	2371.6	-1.289	2.88	23.3	1.30	0.44	0.06
1241	C	3	H	2	140	142	56.60	2375.1	-1.349					
1241	C	3	H	3	0	2	56.70	2378.5	-1.421	3.21	24.7	1.30	0.38	0.03
1241	C	3	H	3	10	12	56.80	2382.0	-1.384					
1241	C	3	H	3	20	22	56.90	2385.4	-1.492	2.93	23.5	1.27	0.34	0.01
1241	C	3	H	3	30	32	57.00	2388.9	-1.452					
1241	C	3	H	3	42	44	57.12	2393.0	-1.271	3.17	24.6	1.26	0.38	0.08
1241	C	3	H	3	50	52	57.20	2395.7	-1.121					
1241	C	3	H	3	60	62	57.30	2399.1	-1.324	2.99	23.8	1.27	0.38	0.03
1241	C	3	H	3	70	72	57.40	2402.6	-1.279					
1241	C	3	H	3	82	84	57.52	2406.7	-1.416	3.06	24.1	1.30	0.46	0.03
1241	C	3	H	3	90	92	57.60	2409.4	-1.525					
1241	C	3	H	3	100	102	57.70	2412.9	-1.561	3.00	23.8	1.28	0.41	0.03
1241	C	3	H	3	110	112	57.80	2416.3	-1.245					
1241	C	3	H	3	122	124	57.92	2420.4	-0.998	2.94	23.6	1.31	0.34	0.08
1241	C	3	H	3	130	132	58.00	2423.1	-1.067					
1241	C	3	H	3	140	142	58.10	2426.6	-0.667	2.67	22.3	1.28	0.28	0.02
1241	C	3	H	4	0	2	58.21	2443.0		2.66	22.2	1.29	0.31	0.00
1241	C	3	H	4	10	12	58.31	2445.7	-0.938	2.60	21.9	1.29	0.31	0.01
1241	C	3	H	4	20	22	58.41	2448.4	-0.931					
1241	C	3	H	4	30	32	58.51	2451.1	-0.988	2.50	21.4	1.26	0.32	0.05
1241	C	3	H	4	40	42	58.61	2453.8	-1.045					
1241	C	3	H	4	50	52	58.71	2456.4	-1.121	2.65	22.2	1.29	0.44	0.02
1241	C	3	H	4	60	62	58.81	2459.1	-1.231					
1241	C	3	H	4	70	72	58.91	2461.8	-1.467	2.72	22.5	1.27	0.49	0.03
1241	C	3	H	4	80	82	59.01	2464.5						
1241	C	3	H	4	90	92	59.11	2467.2	-1.615	3.09	24.2	1.30	0.40	0.01
1241	C	3	H	4	100	102	59.21	2469.9	-1.860	3.17	24.5	1.36	0.33	0.01
1241	C	3	H	4	110	112	59.31	2472.6	-1.667	3.08	24.2	1.30	0.40	0.00
1241	C	3	H	4	120	122	59.41	2475.3	-1.321					
1241	C	3	H	4	130	132	59.51	2478.0	-1.302					
1241	C	3	H	4	140	142	59.61	2480.7	-1.346	2.72	22.5	1.30	0.34	0.02
1241	C	3	H	5	0	2	59.72	2483.6	-1.163					
1241	C	3	H	5	10	12	59.82	2486.3	-0.554	2.81	22.9	1.31	0.46	0.06
1241	C	3	H	5	20	22	59.92	2489.0	-1.323					
1241	C	3	H	5	30	32	60.02	2493.1	-1.125	2.81	22.9	1.31	0.61	0.02
1241	C	3	H	5	40	42	60.12	2497.2	-1.219	2.88	23.3	1.29	0.67	0.03
1241	C	3	H	5	50	52	60.22	2501.4		3.08	24.2	1.29	0.40	0.02
1241	C	3	H	5	60	62	60.32	2505.5	-1.440					
1241	C	3	H	5	70	72	60.42	2509.6		3.08	24.1	1.33	0.40	0.00
1241	C	3	H	5	80	82	60.52	2513.7	-1.390					
1241	C	3	H	5	90	92	60.62	2517.8	-1.454	3.11	24.3	1.33	0.51	0.04
1241	C	3	H	5	100	102	60.72	2521.9	-1.387					
1241	C	3	H	5	110	112	60.82	2526.0	-1.057	2.69	22.4	1.29	0.44	0.00
1241	C	3	H	5	120	122	60.92	2530.1	-0.801					
1241	C	3	H	5	130	132	61.02	2534.3	-0.940	2.59	21.9	1.30	0.45	0.00
1241	C	3	H	5	140	142	61.12	2538.4	-1.248					
1241	C	3	H	6	0	2	61.23	2542.9	-2.019	2.95	23.6	1.32	0.48	0.00
1241	C	3	H	6	10	12	61.33	2547.0	-1.608					
1241	C	3	H	6	20	22	61.43	2551.1	-1.777	3.40	25.4	1.31	0.53	0.00
1241	C	3	H	6	30	32	61.53	2555.3	-1.911					
1241	A	7	H	3	10	12	61.55	2556.1	-1.512	3.10	24.2	1.31	0.55	0.01
1241	A	7	H	3	20	22	61.65	2560.2	-1.476					
1241	A	7	H	3	30	32	61.75	2564.3	-1.406	2.86	23.2	1.29	0.52	0.00
1241	A	7	H	3	40	42	61.85	2568.4	-1.406					
1241	A	7	H	3	50	52	61.95	2572.5	-1.496	3.02	23.9	1.31	0.51	0.03
1241	A	7	H	3	60	62	62.05	2576.6	-1.746					
1241	A	7	H	3	70	72	62.15	2580.8	-1.564	3.21	24.7	1.30	0.55	0.00
1241	A	7	H	3	80	82	62.25	2584.9	-1.570					
1241	A	7	H	3	90	92	62.35	2589.0	-1.667	3.32	25.2	1.31	0.48	0.02
1241	A	7	H	3	100	102	62.45	2592.9	-1.541					
1241	A	7	H	3	110	112	62.55	2596.7	-1.099	3.01	23.9	1.30	0.49	0.00
1241	A	7	H	3	120	122	62.65	2600.6	-1.154	3.00	23.8	1.30	0.49	0.02
1241	A	7	H	3	130	132	62.75	2604.4	-1.505					

Appendix C (continued)

Site	Hole	Core	T	Sec.	Top (cm)	Bot (cm)	Depth (corr. msbf)	Age (ka)	$\delta^{18}O_{G.\ Sacculifer}$ (‰)	Mg/Ca (mmol/mol)	Temperature (°C)	Sr/Ca (mmol/mol)	Mn/Ca (mmol/mol)	Fe/Ca (mmol/mol)
1241	A	7	H	3	140	142	62.85	2608.3	-1.473	3.01	23.8	1.32	0.46	0.00
1241	A	7	H	4	0	2	62.94	2611.7	-1.273					
1241	A	7	H	4	10	12	63.04	2615.6	-1.309	3.29	25.0	1.31	0.42	0.00
1241	A	7	H	4	20	22	63.14	2619.4	-1.775					
1241	A	7	H	4	30	32	63.24	2623.3	-1.309	2.99	23.8	1.29	0.41	0.00
1241	A	7	H	4	40	42	63.34	2627.1	-1.290					
1241	A	7	H	4	50	52	63.44	2631.0	-1.076	2.90	23.4	1.29	0.47	0.00
1241	A	7	H	4	60	62	63.54	2634.8	-1.360					
1241	A	7	H	4	70	72	63.64	2638.7	-1.395	2.91	23.4	1.29	0.44	0.06
1241	A	7	H	4	80	82	63.74	2642.5	-1.326					
1241	A	7	H	4	90	92	63.84	2646.4	-1.348	2.89	23.3	1.30	0.46	0.03
1241	A	7	H	4	100	102	63.94	2650.2	-1.438					
1241	A	7	H	4	110	112	64.04	2654.1	-1.657	3.02	23.9	1.30	0.49	0.00
1241	A	7	H	4	120	122	64.14	2657.9	-1.744					
1241	A	7	H	4	130	132	64.24	2661.8	-1.771	3.00	23.8	1.27	0.43	0.00
1241	A	7	H	4	140	142	64.34	2665.6	-2.004					
1241	A	7	H	5	0	2	64.45	2669.9	-1.235	3.24	24.8	1.30	0.47	0.00
1241	A	7	H	5	10	12	64.55	2673.7	-1.695					
1241	A	7	H	5	20	22	64.65	2677.6	-1.540	2.95	23.6	1.29	0.56	0.01
1241	A	7	H	5	30	32	64.75	2681.4	-1.236					
1241	A	7	H	5	40	42	64.85	2685.3		2.92	23.5	1.30	0.56	0.01
1241	A	7	H	5	50	52	64.95	2689.1	-1.567					
1241	A	7	H	5	60	62	65.05	2693.0	-1.028	3.29	25.0	1.31	0.55	0.00
1241	A	7	H	5	70	72	65.15	2696.5	-1.333					
1241	A	7	H	5	80	82	65.25	2700.0	-1.186	3.13	24.4	1.31	0.57	0.00
1241	A	7	H	5	90	92	65.35	2703.5	-0.945					
1241	A	7	H	5	100	102	65.45	2707.0	-1.037	3.11	24.3	1.30	0.52	0.02
1241	A	7	H	5	110	112	65.55	2710.5	-1.165					
1241	A	7	H	5	120	122	65.65	2714.1	-1.063	2.96	23.6	1.25	0.31	0.07
1241	A	7	H	5	130	132	65.75	2717.6	-1.270					
1241	A	7	H	5	140	142	65.85	2721.1	-1.035	2.88	23.3	1.31	0.30	0.00
1241	A	7	H	6	0	2	65.96	2724.9	-1.041					
1241	A	7	H	6	10	12	66.06	2728.4	-1.221	3.10	24.3	1.24	0.29	0.02
1241	A	7	H	6	20	22	66.16	2731.9	-1.373					
1241	A	7	H	6	30	32	66.26	2735.5	-1.075	3.64	26.4	1.31	0.46	0.00
1241	A	7	H	6	40	42	66.36	2739.0	-1.393					
1241	C	4	H	2	30	32	66.46	2742.5	-1.706	3.03	24.0	1.29	0.50	0.00
1241	C	4	H	2	40	42	66.56	2746.0	-1.265	3.12	24.3	1.25	0.33	0.01
1241	C	4	H	2	50	52	66.66	2749.5	-1.438	2.88	23.3	1.26	0.46	0.00
1241	C	4	H	2	60	62	66.76	2753.0	-1.657					
1241	C	4	H	2	70	72	66.86	2757.2	-1.347	3.19	24.6	1.29	0.47	0.01
1241	C	4	H	2	80	82	66.96	2761.3	-1.689	2.98	23.7	1.25	0.51	0.01
1241	C	4	H	2	90	92	67.06	2765.5	-1.529					
1241	C	4	H	2	100	102	67.16	2769.6	-1.351	2.91	23.4	1.30	0.60	0.01
1241	C	4	H	2	110	112	67.26	2773.8	-1.267					
1241	C	4	H	2	120	122	67.36	2777.9	-0.989	3.07	24.1	1.29	0.51	0.01
1241	C	4	H	2	130	132	67.46	2782.1	-0.871					
1241	C	4	H	2	140	142	67.56	2786.3	-1.567	3.19	24.6	1.30	0.52	0.02
1241	C	4	H	3	0	2	67.67	2790.8	-1.549					
1241	C	4	H	3	10	12	67.77	2795.0	-1.441	3.37	25.3	1.29	0.58	0.01
1241	C	4	H	3	20	22	67.87	2798.7	-1.456					
1241	C	4	H	3	30	32	67.97	2802.4	-1.410	3.17	24.5	1.31	0.50	0.00
1241	C	4	H	3	40	42	68.07	2806.1	-1.448					
1241	C	4	H	3	50	52	68.17	2809.8	-0.949	2.74	22.6	1.28	0.63	0.03
1241	C	4	H	3	60	62	68.27	2813.5	-1.235					
1241	C	4	H	3	70	72	68.37	2817.2	-1.218	3.14	24.4	1.32	0.80	0.00
1241	C	4	H	3	80	82	68.47	2820.9	-1.429					
1241	C	4	H	3	90	92	68.57	2824.7	-1.452	3.28	25.0	1.30	0.78	0.04
1241	C	4	H	3	100	102	68.67	2828.4	-1.227					
1241	C	4	H	3	110	112	68.77	2832.1	-1.189	3.12	24.3	1.29	0.57	0.00
1241	C	4	H	3	120	122	68.87	2835.8	-1.643					
1241	C	4	H	3	130	132	68.97	2839.5	-1.762	3.38	25.4	1.30	0.63	0.02
1241	C	4	H	3	140	142	69.07	2843.2	-1.602					
1241	C	4	H	4	0	2	69.19	2847.6	-1.630	3.17	24.5	1.29	0.68	0.03
1241	C	4	H	4	10	12	69.29	2851.3	-1.395					
1241	C	4	H	4	20	22	69.39	2855.1	-1.185	2.85	23.1	1.27	0.67	0.00
1241	C	4	H	4	30	32	69.49	2858.8	-1.634					
1241	C	4	H	4	40	42	69.59	2862.5	-1.551	3.00	23.8	1.29	0.79	0.02
1241	C	4	H	4	50	52	69.69	2866.2	-1.624					

Appendix C (continued)

Site	Hole	Core	T	Sec.	Top (cm)	Bot (cm)	Depth (corr. msbf)	Age (ka)	$\delta^{18}O_{G.\ Sacculifer}$ (‰)	Mg/Ca (mmol/mol)	Temperature (°C)	Sr/Ca (mmol/mol)	Mn/Ca (mmol/mol)	Fe/Ca (mmol/mol)
1241	C	4	H	4	60	62	69.79	2869.9	-1.454	3.02	23.9	1.30	0.67	0.02
1241	C	4	H	4	70	72	69.89	2873.6	-1.755					
1241	C	4	H	4	80	82	69.99	2877.3	-1.081	3.06	24.1	1.30	0.53	0.00
1241	C	4	H	4	90	92	70.09	2881.0	-1.551					
1241	C	4	H	4	100	102	70.19	2884.7	-1.289	3.01	23.8	1.29	0.57	0.05
1241	C	4	H	4	110	112	70.29	2888.4	-1.543					
1241	C	4	H	4	120	122	70.39	2892.1	-1.434	3.08	24.1	1.32	0.70	0.02
1241	C	4	H	4	130	132	70.49	2895.8	-1.475					
1241	C	4	H	4	140	142	70.59	2899.5	-1.578	3.23	24.8	1.31	0.73	0.04
1241	C	4	H	5	0	2	70.70	2903.6	-1.591					
1241	C	4	H	5	10	12	70.80	2907.3	-1.772	2.96	23.7	1.32	0.73	0.00
1241	C	4	H	5	20	22	70.90	2911.0	-1.476					
1241	C	4	H	5	30	32	71.00	2914.7	-1.340	3.05	24.0	1.30	0.70	0.03
1241	C	4	H	5	40	42	71.10	2918.4	-1.632					
1241	C	4	H	5	50	52	71.20	2922.1	-1.496	3.02	23.9	1.31	0.66	0.00
1241	C	4	H	5	60	62	71.30	2925.6	-1.279					
1241	C	4	H	5	70	72	71.40	2928.9	-1.258	2.84	23.1	1.31	0.76	0.05
1241	C	4	H	5	80	82	71.50	2932.1	-1.259					
1241	C	4	H	5	90	92	71.60	2935.4	-1.311	2.86	23.2	1.30	0.68	0.02
1241	C	4	H	5	100	102	71.70	2938.6	-1.534					
1241	C	4	H	5	110	112	71.80	2941.9	-1.569	3.23	24.8	1.29	0.78	0.05
1241	C	4	H	5	120	122	71.90	2945.1	-1.608					
1241	C	4	H	5	130	132	72.00	2948.4	-1.422	3.23	24.8	1.28	0.64	0.00
1241	C	4	H	5	140	142	72.10	2951.6	-1.641					
1241	C	4	H	6	0	2	72.21	2955.2	-1.469	3.43	25.6	1.29	0.67	0.06
1241	C	4	H	6	10	12	72.31	2958.5	-1.794					
1241	C	4	H	6	20	22	72.41	2961.7	-1.780	3.67	26.5	1.34	0.73	0.01
1241	C	4	H	6	30	32	72.51	2965.0	-1.483					
1241	C	4	H	6	40	42	72.61	2968.2	-1.676	3.40	25.5	1.33	0.75	0.04
1241	C	4	H	6	50	52	72.71	2971.5	-1.466					
1241	C	4	H	6	60	62	72.81	2974.7	-1.517	3.33	25.2	1.32	0.83	0.00
1241	C	4	H	6	70	72	72.91	2978.0	-1.277					
1241	C	4	H	6	80	82	73.01	2981.2	-0.999	3.32	25.1	1.32	0.84	0.00
1241	C	4	H	6	90	92	73.11	2984.5	-1.311					
1241	B	8	H	2	100	102	73.16	2986.1	-1.610	3.32	25.2	1.39	0.54	0.04
1241	B	8	H	2	110	112	73.26	2989.4	-1.579					
1241	B	8	H	2	120	122	73.36	2992.6	-1.443	3.14	24.4	1.29	0.83	0.01
1241	B	8	H	2	130	132	73.46	2995.9	-1.539					
1241	B	8	H	2	140	142	73.56	2999.1	-1.464	3.35	25.3	1.38	0.55	0.07
1241	B	8	H	3	0	2	73.67	3002.7	-1.338					
1241	B	8	H	3	10	12	73.77	3006.0	-1.304	3.18	24.6	1.32	0.73	0.03
1241	B	8	H	3	20	22	73.87	3009.3	-1.066					
1241	B	8	H	3	30	32	73.97	3012.5	-1.178	3.00	23.8	1.30	0.76	0.01
1241	B	8	H	3	40	42	74.07	3015.8	-1.427					
1241	B	8	H	3	50	52	74.17	3019.0	-1.385	3.24	24.8	1.31	0.76	0.07
1241	B	8	H	3	60	62	74.27	3022.3	-1.441					
1241	B	8	H	3	70	72	74.37	3025.5	-1.254	3.02	23.9	1.34	0.75	0.00
1241	B	8	H	3	80	82	74.47	3028.8	-1.432					
1241	B	8	H	3	90	92	74.57	3032.1	-1.466	2.87	23.3	1.32	0.69	0.06
1241	B	8	H	3	100	102	74.67	3035.3	-1.434					
1241	B	8	H	3	110	112	74.77	3038.6	-1.647	3.26	24.9	1.31	0.76	0.03
1241	B	8	H	3	120	122	74.87	3041.8	-1.297					
1241	B	8	H	3	130	132	74.97	3045.1	-1.610	3.26	24.9	1.32	0.70	0.04
1241	B	8	H	3	140	142	75.07	3048.4	-1.523					
1241	B	8	H	4	0	2	75.17	3051.6	-1.562	3.26	24.9	1.33	0.64	0.00
1241	B	8	H	4	10	12	75.27	3054.9	-1.677					
1241	B	8	H	4	20	22	75.37	3058.1	-1.501	3.12	24.4	1.34	0.72	0.02
1241	B	8	H	4	30	32	75.47	3061.4	-1.462					
1241	B	8	H	4	40	42	75.57	3064.6	-1.679	3.06	24.1	1.31	0.71	0.01
1241	B	8	H	4	50	52	75.67	3067.9	-1.700					
1241	B	8	H	4	60	62	75.77	3071.2	-1.971	3.01	23.9	1.32	0.69	0.03
1241	B	8	H	4	70	72	75.87	3074.4	-1.732					
1241	B	8	H	4	80	82	75.97	3077.7	-1.522	3.42	25.5	1.32	0.81	0.00
1241	B	8	H	4	90	92	76.07	3080.9	-1.718					
1241	B	8	H	4	100	102	76.17	3084.2	-1.684	3.25	24.9	1.31	0.71	0.00
1241	B	8	H	4	110	112	76.27	3087.4	-1.607					
1241	B	8	H	4	120	122	76.37	3090.7	-1.762	3.27	24.9	1.31	0.70	0.00
1241	B	8	H	4	130	132	76.47	3094.0	-1.902					
1241	B	8	H	4	140	142	76.57	3097.2	-1.536	2.97	23.7	1.30	0.76	0.00

Appendix C (continued)

Site	Hole	Core	T	Sec.	Top (cm)	Bot (cm)	Depth (corr. msbf)	Age (ka)	$\delta^{18}O_{G.\ Sacculifer}$ (‰)	Mg/Ca (mmol/mol)	Temperature (°C)	Sr/Ca (mmol/mol)	Mn/Ca (mmol/mol)	Fe/Ca (mmol/mol)
1241	B	8	H	5	0	2	76.67	3100.5	-1.507					
1241	B	8	H	5	10	12	76.77	3103.7	-1.604	3.22	24.8	1.32	0.77	0.02
1241	B	8	H	5	20	22	76.87	3107.0	-1.273					
1241	B	8	H	5	30	32	76.97	3109.7	-1.484	3.15	24.4	1.30	0.70	0.00
1241	B	8	H	5	40	42	77.07	3112.4	-1.692					
1241	B	8	H	5	43	45	77.10	3113.2	-1.256	3.38	25.4	1.28	0.70	0.00
1241	B	8	H	5	50	52	77.17	3115.1	-1.543					
1241	B	8	H	5	60	62	77.27	3117.8	-1.696	3.34	25.2	1.33	0.61	0.02
1241	B	8	H	5	70	72	77.37	3120.5	-1.732					
1241	B	8	H	5	80	82	77.47	3123.2	-1.341	3.25	24.9	1.32	0.74	0.00
1241	B	8	H	5	90	92	77.57	3125.9	-1.687					
1241	B	8	H	5	100	102	77.67	3128.6	-1.725	3.13	24.4	1.31	0.67	0.00
1241	B	8	H	5	110	112	77.77	3131.3	-1.567					
1241	B	8	H	5	120	122	77.87	3134.0	-1.564	3.19	24.6	1.30	0.63	0.00
1241	C	5	H	2	140	142	77.95	3136.1	-1.289					
1241	C	5	H	3	0	2	78.06	3139.1	-1.802	3.05	24.1	1.30	0.65	0.05
1241	C	5	H	3	10	12	78.16	3141.8	-1.532					
1241	C	5	H	3	20	22	78.26	3144.5	-1.663	3.31	25.1	1.32	0.65	0.00
1241	C	5	H	3	30	32	78.36	3147.2	-1.807					
1241	C	5	H	3	40	42	78.46	3149.9	-1.756	3.14	24.4	1.32	0.67	0.03
1241	C	5	H	3	50	52	78.56	3152.6	-2.083					
1241	C	5	H	3	60	62	78.66	3155.3	-2.012	3.48	25.8	1.29	0.73	0.00
1241	C	5	H	3	70	72	78.76	3158.0	-1.959					
1241	C	5	H	3	80	82	78.86	3160.7	-2.089	3.39	25.4	1.32	0.63	0.05
1241	C	5	H	3	90	92	78.96	3163.4	-2.187					
1241	C	5	H	3	100	102	79.06	3166.1	-1.892	3.13	24.4	1.31	0.72	0.00
1241	C	5	H	3	110	112	79.16	3168.8	-1.792					
1241	C	5	H	3	120	122	79.26	3171.5	-2.106	3.27	25.0	1.29	0.81	0.01
1241	C	5	H	3	130	132	79.36	3174.2	-1.928					
1241	C	5	H	3	140	142	79.46	3176.9	-1.862	3.22	24.8	1.29	0.70	0.01
1241	C	5	H	4	0	2	79.56	3179.6	-1.835					
1241	C	5	H	4	10	12	79.66	3182.3	-2.089	3.23	24.8	1.32	0.74	0.01
1241	C	5	H	4	20	22	79.76	3185.0	-1.866					
1241	C	5	H	4	30	32	79.86	3188.7	-1.810	3.02	23.9	1.28	0.70	0.02
1241	C	5	H	4	40	42	79.96	3192.4	-1.890					
1241	C	5	H	4	50	52	80.06	3196.1	-1.879	3.20	24.7	1.28	0.70	0.02
1241	C	5	H	4	60	62	80.16	3199.9	-1.631					
1241	C	5	H	4	70	72	80.26	3203.6	-1.699	3.23	24.8	1.30	0.74	0.00
1241	C	5	H	4	80	82	80.36	3207.3	-1.954					
1241	C	5	H	4	90	92	80.46	3211.0	-2.006	3.15	24.5	1.32	0.69	0.00
1241	C	5	H	4	100	102	80.56	3214.1	-1.756					
1241	C	5	H	4	110	112	80.66	3217.3	-1.839	3.16	24.5	1.31	0.68	0.01
1241	C	5	H	4	120	122	80.76	3220.5	-1.745					
1241	C	5	H	4	130	132	80.86	3223.6	-1.494	2.81	22.9	1.30	0.64	0.04
1241	C	5	H	4	140	142	80.96	3226.8	-1.524					
1241	C	5	H	5	0	2	81.06	3229.9	-1.567	3.06	24.1	1.26	0.68	0.03
1241	C	5	H	5	10	12	81.16	3233.1	-1.681					
1241	C	5	H	5	20	22	81.26	3236.2	-1.685	3.03	24.0	1.32	0.63	0.04
1241	C	5	H	5	30	32	81.36	3239.4	-1.708					
1241	C	5	H	5	40	42	81.46	3242.5	-1.911	3.19	24.6	1.32	0.73	0.03
1241	C	5	H	5	50	52	81.56	3245.7	-1.868					
1241	C	5	H	5	60	62	81.66	3248.8	-1.741	3.18	24.6	1.34	0.66	0.01
1241	C	5	H	5	70	72	81.76	3252.0	-1.223					
1241	C	5	H	5	80	82	81.86	3255.1	-1.526	3.29	25.0	1.33	0.69	0.05
1241	C	5	H	5	90	92	81.96	3258.3	-1.551					
1241	C	5	H	5	100	102	82.06	3261.5	-1.634	3.21	24.7	1.29	0.75	0.02
1241	C	5	H	5	110	112	82.16	3264.6	-1.851					
1241	C	5	H	5	120	122	82.26	3267.8	-1.480	3.33	25.2	1.33	0.73	0.04
1241	C	5	H	5	130	132	82.36	3270.9	-1.570					
1241	C	5	H	5	140	142	82.46	3274.1	-1.641	3.35	25.3	1.33	0.57	0.00
1241	C	5	H	6	0	2	82.57	3277.5	-1.162					
1241	C	5	H	6	10	12	82.67	3280.7	-1.061	3.10	24.2	1.31	0.56	0.00
1241	C	5	H	6	20	22	82.77	3283.9	-1.519					
1241	C	5	H	6	30	32	82.87	3287.0	-1.192	3.17	24.5	1.31	0.52	0.00
1241	C	5	H	6	40	42	82.97	3289.7	-1.233					
1241	C	5	H	6	50	52	83.07	3292.3	-0.821	2.79	22.9	1.31	0.43	0.03
1241	C	5	H	6	60	62	83.17	3295.0	-1.021					
1241	C	5	H	6	70	72	83.27	3297.6	-0.896	2.93	23.5	1.30	0.44	0.02
1241	C	5	H	6	80	82	83.37	3300.3	-1.325					

Appendix C (continued)

Site	Hole	Core	T	Sec.	Top (cm)	Bot (cm)	Depth (corr. msbf)	Age (ka)	$\delta^{18}O_{G.\ Sacculifer}$ (‰)	Mg/Ca (mmol/mol)	Temperature (°C)	Sr/Ca (mmol/mol)	Mn/Ca (mmol/mol)	Fe/Ca (mmol/mol)
1241	C	5	H	6	90	92	83.47	3303.0	-1.321	3.03	23.9	1.31	0.43	0.04
1241	A	9	H	3	50	52	83.55	3305.1	-1.638					
1241	A	9	H	3	60	62	83.65	3307.8	-1.587	3.06	24.1	1.34	0.38	0.04
1241	A	9	H	3	70	72	83.75	3310.4	-1.375					
1241	A	9	H	3	80	82	83.85	3313.1	-1.233	3.26	24.9	1.30	0.37	0.05
1241	A	9	H	3	90	92	83.95	3315.7	-1.380					
1241	A	9	H	3	100	102	84.05	3318.4	-1.698	2.97	23.7	1.29	0.44	0.03
1241	A	9	H	3	110	112	84.15	3321.1	-1.468					
1241	A	9	H	3	120	122	84.25	3323.7	-1.771	3.19	24.6	1.30	0.48	0.00
1241	A	9	H	3	130	132	84.35	3326.4	-1.750					
1241	A	9	H	3	140	142	84.45	3329.1	-1.816	3.50	25.8	1.32	0.56	0.02
1241	A	9	H	4	0	2	84.55	3331.7	-1.628					
1241	A	9	H	4	10	12	84.65	3334.4	-1.832	3.23	24.8	1.31	0.49	0.00
1241	A	9	H	4	20	22	84.75	3337.0	-1.491					
1241	A	9	H	4	30	32	84.85	3339.7	-1.785	3.18	24.6	1.31	0.39	0.00
1241	A	9	H	4	40	42	84.95	3342.4	-1.659					
1241	A	9	H	4	50	52	85.05	3345.0	-1.800	3.02	23.9	1.31	0.38	0.04
1241	A	9	H	4	60	62	85.15	3347.7	-1.478					
1241	A	9	H	4	70	72	85.25	3350.4	-1.629	2.90	23.4	1.31	0.21	0.42
1241	A	9	H	4	80	82	85.35	3353.0	-1.635					
1241	A	9	H	4	90	92	85.45	3355.7	-1.758	3.23	24.8	1.32	0.37	0.00
1241	A	9	H	4	100	102	85.55	3358.3	-1.579					
1241	A	9	H	4	110	112	85.65	3361.0	-1.734	3.38	25.4	1.31	0.45	0.01
1241	A	9	H	4	120	122	85.75	3363.7	-1.879					
1241	A	9	H	4	130	132	85.85	3366.4	-1.638	3.26	24.9	1.33	0.40	0.01
1241	A	9	H	4	140	142	85.95	3369.1	-1.362					
1241	A	9	H	5	0	2	86.05	3371.8	-1.190	3.30	25.1	1.32	0.44	0.01
1241	A	9	H	5	10	12	86.15	3374.6	-1.433					
1241	A	9	H	5	20	22	86.25	3377.2	-1.560	3.02	23.9	1.32	0.40	0.00
1241	A	9	H	5	30	32	86.35	3380.0	-1.582					
1241	A	9	H	5	40	42	86.45	3382.7	-1.559	3.18	24.6	1.29	0.46	0.15
1241	A	9	H	5	50	52	86.55	3385.4	-1.700					
1241	A	9	H	5	60	62	86.65	3388.1	-1.784	3.31	25.1	1.32	0.54	0.05
1241	A	9	H	5	70	72	86.75	3390.8	-1.520					
1241	A	9	H	5	80	82	86.85	3393.5	-1.339	3.14	24.4	1.29	0.45	0.09
1241	A	9	H	5	90	92	86.95	3396.2	-1.705					
1241	A	9	H	5	100	102	87.05	3398.9	-1.363	3.04	24.0	1.28	0.49	0.00
1241	A	9	H	5	110	112	87.15	3401.6	-1.587					
1241	A	9	H	5	120	122	87.25	3404.4	-1.775	3.33	25.2	1.31	0.51	0.02
1241	A	9	H	5	130	132	87.35	3407.1	-1.556					
1241	A	9	H	5	140	142	87.45	3409.8	-1.858	3.28	25.0	1.29	0.45	0.01
1241	A	9	H	6	0	2	87.56	3412.7	-1.972					
1241	A	9	H	6	10	12	87.66	3415.4	-1.850	3.21	24.7	1.30	0.50	0.00
1241	A	9	H	6	20	22	87.76	3418.2	-1.780					
1241	A	9	H	6	30	32	87.86	3420.9	-1.734	3.15	24.5	1.29	0.48	0.00
1241	A	9	H	6	40	42	87.96	3423.6	-1.583					
1241	A	9	H	6	50	52	88.06	3426.3	-1.507	3.17	24.5	1.31	0.52	0.00
1241	A	9	H	6	60	62	88.16	3429.0	-1.521					
1241	A	9	H	6	70	72	88.26	3431.5	-1.649	3.05	24.1	1.30	0.55	0.00
1241	A	9	H	6	80	82	88.36	3434.0	-1.621					
1241	A	9	H	6	90	92	88.46	3436.4	-1.962	3.26	24.9	1.29	0.60	0.05
1241	A	9	H	6	100	102	88.56	3438.9	-2.088					
1241	A	9	H	6	110	112	88.66	3441.4	-2.068	3.62	26.3	1.31	0.57	0.00
1241	A	9	H	6	120	122	88.76	3443.9	-1.817					
1241	A	9	H	6	130	132	88.86	3446.4	-1.758	3.24	24.8	1.28	0.49	0.00
1241	A	9	H	6	140	142	88.96	3448.9	-1.995					
1241	A	9	H	7	0	2	89.07	3451.6	-1.820	3.01	23.9	1.29	0.55	0.00
1241	A	9	H	7	10	12	89.17	3454.1	-2.091					
1241	C	6	H	3	20	22	89.23	3455.6	-1.921	3.33	25.2	1.28	0.61	0.04
1241	C	6	H	3	30	32	89.33	3458.0	-1.856					
1241	C	6	H	3	40	42	89.43	3460.5	-1.438	2.99	23.8	1.31	0.51	0.03
1241	C	6	H	3	50	52	89.53	3463.0	-1.605					
1241	C	6	H	3	60	62	89.63	3466.2	-1.578	2.90	23.4	1.28	0.43	0.06
1241	C	6	H	3	70	72	89.73	3469.4	-1.649					
1241	C	6	H	3	80	82	89.83	3472.6	-1.466	3.20	24.6	1.30	0.56	0.04
1241	C	6	H	3	90	92	89.93	3475.8	-1.654					
1241	C	6	H	3	100	102	90.03	3478.9	-2.215	3.39	25.4	1.29	0.56	0.02
1241	C	6	H	3	110	112	90.13	3482.1	-1.782					
1241	C	6	H	3	120	122	90.23	3485.3	-1.793	3.29	25.0	1.29	0.48	0.00

Appendix C (continued)

Site	Hole	Core	T	Sec.	Top (cm)	Bot (cm)	Depth (corr. msbf)	Age (ka)	$\delta^{18}O_{G.\ Sacculifer}$ (‰)	Mg/Ca (mmol/mol)	Temperature (°C)	Sr/Ca (mmol/mol)	Mn/Ca (mmol/mol)	Fe/Ca (mmol/mol)
1241	C	6	H	3	130	132	90.33	3488.5	-2.104					
1241	C	6	H	3	140	142	90.43	3491.7	-1.938	3.21	24.7	1.28	0.49	0.05
1241	C	6	H	4	0	2	90.53	3494.9	-2.089					
1241	C	6	H	4	10	12	90.63	3498.1	-2.018	3.50	25.8	1.32	0.46	0.00
1241	C	6	H	4	20	22	90.73	3501.3	-2.000					
1241	C	6	H	4	30	32	90.83	3504.4	-2.060	3.10	24.3	1.28	0.46	0.03
1241	C	6	H	4	40	42	90.93	3507.6	-1.770					
1241	C	6	H	4	50	52	91.03	3510.8	-1.870	3.21	24.7	1.31	0.52	0.00
1241	C	6	H	4	60	62	91.13	3514.0	-1.810					
1241	C	6	H	4	70	72	91.23	3517.2	-1.720	3.37	25.3	1.29	0.48	0.00
1241	C	6	H	4	80	82	91.33	3520.4	-1.720					
1241	C	6	H	4	90	92	91.43	3523.6	-1.780	3.16	24.5	1.30	0.51	0.00
1241	C	6	H	4	100	102	91.53	3526.7	-1.930					
1241	C	6	H	4	110	112	91.63	3529.9	-1.850	3.39	25.4	1.29	0.53	0.24
1241	C	6	H	4	120	122	91.73	3533.1	-1.800	3.64	26.4	1.35	0.40	0.04
1241	C	6	H	4	130	132	91.83	3536.3	-1.940	3.40	25.5	1.28	0.51	0.08
1241	C	6	H	4	140	142	91.93	3539.5	-1.910					
1241	C	6	H	5	0	2	92.03	3542.7	-1.910	3.28	25.0	1.31	0.57	0.00
1241	C	6	H	5	10	12	92.13	3545.9	-1.710					
1241	A	10	H	2	10	12	92.22	3548.7	-1.640	3.06	24.1	1.29	0.52	0.01
1241	A	10	H	2	20	22	92.32	3551.9	-1.730					
1241	A	10	H	2	30	32	92.42	3555.1	-2.020	3.40	25.5	1.30	0.50	0.02
1241	A	10	H	2	40	42	92.52	3558.3	-1.920					
1241	A	10	H	2	50	52	92.62	3561.5	-1.870	3.29	25.0	1.35	0.51	0.05
1241	A	10	H	2	60	62	92.72	3564.7	-1.730					
1241	A	10	H	2	70	72	92.82	3567.9	-1.990	3.47	25.7	1.30	0.56	0.00
1241	A	10	H	2	80	82	92.92	3571.1	-2.140					
1241	A	10	H	2	90	92	93.02	3574.3	-1.910	3.33	25.2	1.30	0.45	0.00
1241	A	10	H	2	100	102	93.12	3577.4	-1.890					
1241	A	10	H	2	110	112	93.22	3580.6	-1.980	3.00	23.8	1.29	0.54	0.05
1241	A	10	H	2	120	122	93.32	3583.8	-1.940					
1241	A	10	H	2	130	132	93.42	3587.0	-2.030	3.27	24.9	1.31	0.54	0.04
1241	A	10	H	2	140	142	93.52	3590.0	-1.860					
1241	A	10	H	3	0	2	93.62	3593.1	-1.730	3.46	25.7	1.27	0.50	0.00
1241	A	10	H	3	10	12	93.72	3596.1	-1.750					
1241	A	10	H	3	20	22	93.82	3599.1	-1.880	3.29	25.0	1.30	0.51	0.03
1241	A	10	H	3	30	32	93.92	3602.2	-1.950					
1241	A	10	H	3	40	42	94.02	3605.2	-1.963	3.31	25.1	1.30	0.47	0.02
1241	A	10	H	3	50	52	94.12	3608.3	-1.869					
1241	A	10	H	3	60	62	94.22	3611.3	-1.864	3.54	26.0	1.31	0.46	0.00
1241	A	10	H	3	70	72	94.32	3614.4	-1.856					
1241	A	10	H	3	80	82	94.42	3617.4	-1.898	3.22	24.8	1.28	0.43	0.01
1241	A	10	H	3	90	92	94.52	3620.4	-1.961					
1241	A	10	H	3	100	102	94.62	3623.5	-1.497	3.24	24.8	1.30	0.36	0.02
1241	A	10	H	3	110	112	94.72	3626.5	-1.756					
1241	A	10	H	3	120	122	94.82	3629.5	-1.585	3.10	24.2	1.28	0.37	0.00
1241	A	10	H	3	130	132	94.92	3632.6	-1.757					
1241	A	10	H	3	140	142	95.02	3635.6	-1.522	3.19	24.6	1.31	0.36	0.00
1241	A	10	H	4	0	2	95.12	3638.6	-1.843					
1241	A	10	H	4	10	12	95.22	3641.7	-1.743	3.14	24.4	1.25	0.39	0.00
1241	A	10	H	4	20	22	95.32	3644.7	-2.015					
1241	A	10	H	4	30	32	95.42	3647.8	-2.084	3.68	26.5	1.32	0.42	0.00
1241	A	10	H	4	40	42	95.52	3650.8	-2.053					
1241	A	10	H	4	50	52	95.62	3653.9	-1.645	3.71	26.6	1.32	0.48	0.00
1241	A	10	H	4	60	62	95.72	3656.9	-1.526					
1241	A	10	H	4	70	72	95.82	3659.9	-1.838	3.72	26.6	1.34	0.37	0.00
1241	A	10	H	4	80	82	95.92	3663.0	-1.904					
1241	A	10	H	4	90	92	96.02	3666.0	-1.936	3.35	25.3	1.32	0.39	0.00
1241	A	10	H	4	100	102	96.12	3668.9	-1.765					
1241	A	10	H	4	110	112	96.22	3671.9	-1.488	3.32	25.2	1.32	0.49	0.15
1241	A	10	H	4	120	122	96.32	3674.8	-1.647					
1241	A	10	H	4	130	132	96.42	3677.8	-1.411	3.50	25.8	1.33	0.44	0.07
1241	A	10	H	4	140	142	96.52	3680.7	-1.695					
1241	A	10	H	5	0	2	96.62	3683.6	-2.026	3.61	26.3	1.33	0.44	0.00
1241	A	10	H	5	10	12	96.72	3686.6	-1.686					
1241	A	10	H	5	20	22	96.82	3689.5	-1.954	3.58	26.1	1.30	0.53	0.06
1241	A	10	H	5	30	32	96.92	3692.5	-1.831					
1241	A	10	H	5	40	42	97.02	3695.4	-1.538	3.22	24.8	1.31	0.43	0.02
1241	A	10	H	5	50	52	97.12	3698.4	-2.148					

Appendix C (continued)

Site	Hole	Core	T	Sec.	Top (cm)	Bot (cm)	Depth (corr. msbf)	Age (ka)	$\delta^{18}O_{G.\ Sacculifer}$ (‰)	Mg/Ca (mmol/mol)	Temperature (°C)	Sr/Ca (mmol/mol)	Mn/Ca (mmol/mol)	Fe/Ca (mmol/mol)
1241	A	10	H	5	60	62	97.22	3701.3	-1.495	3.51	25.9	1.30	0.44	0.00
1241	A	10	H	5	70	72	97.32	3704.2	-1.811					
1241	A	10	H	5	80	82	97.42	3707.2	-1.523	3.64	26.4	1.31	0.46	0.00
1241	A	10	H	5	90	92	97.52	3710.1	-1.502					
1241	A	10	H	5	100	102	97.62	3713.1	-1.205	3.14	24.4	1.29	0.41	0.01
1241	A	10	H	5	110	112	97.72	3716.0	-1.605					
1241	A	10	H	5	120	122	97.82	3718.8	-1.512	3.36	25.3	1.33	0.39	0.00
1241	A	10	H	5	130	132	97.92	3721.6	-1.581					
1241	A	10	H	5	140	142	98.02	3724.4	-1.621	3.48	25.8	1.30	0.41	0.01
1241	A	10	H	6	0	2	98.12	3727.2	-1.561					
1241	A	10	H	6	10	12	98.22	3730.0	-1.613	3.37	25.4	1.31	0.41	0.09
1241	A	10	H	6	20	22	98.32	3732.8	-1.668					
1241	A	10	H	6	30	32	98.42	3735.6	-1.697	3.46	25.7	1.30	0.43	0.02
1241	A	10	H	6	40	42	98.52	3738.4	-1.777					
1241	A	10	H	6	50	52	98.62	3741.2	-1.797	3.51	25.9	1.31	0.43	0.06
1241	A	10	H	6	60	62	98.72	3744.0	-1.798					
1241	C	7	H	2	100	102	98.82	3746.8	-1.414	3.47	25.7	1.30	0.39	0.00
1241	C	7	H	2	110	112	98.92	3749.6	-1.542					
1241	C	7	H	2	120	122	99.02	3752.4	-1.526	3.43	25.6	1.30	0.40	0.00
1241	C	7	H	2	130	132	99.12	3755.2	-1.623					
1241	C	7	H	2	140	142	99.22	3758.0	-1.586	2.96	23.7	1.27	0.39	0.00
1241	C	7	H	3	0	2	99.32	3760.8	-1.853					
1241	C	7	H	3	10	12	99.42	3763.6	-1.700	2.94	23.6	1.30	0.40	0.03
1241	C	7	H	3	20	22	99.52	3766.4	-1.686					
1241	C	7	H	3	30	32	99.62	3769.2	-1.650	3.41	25.5	1.30	0.42	0.00
1241	C	7	H	3	40	42	99.72	3772.0	-1.604					
1241	C	7	H	3	50	52	99.82	3774.8	-1.818	3.44	25.6	1.29	0.43	0.09
1241	C	7	H	3	60	62	99.92	3777.6	-1.590					
1241	C	7	H	3	70	72	100.02	3780.4	-1.772	3.16	24.5	1.30	0.42	0.00
1241	C	7	H	3	80	82	100.12	3783.2	-1.709					
1241	C	7	H	3	90	92	100.22	3786.0	-1.503	2.96	23.6	1.28	0.46	0.07
1241	C	7	H	3	100	102	100.32	3788.8	-1.738					
1241	C	7	H	3	110	112	100.42	3791.6	-1.795	3.70	26.6	1.29	0.43	0.01
1241	C	7	H	3	120	122	100.52	3794.4	-1.616					
1241	C	7	H	3	130	132	100.62	3797.2	-1.793	3.57	26.1	1.31	0.41	0.01
1241	C	7	H	3	140	142	100.72	3800.0	-1.631					
1241	C	7	H	4	0	2	100.82	3802.8	-1.476	3.55	26.0	1.32	0.40	0.02
1241	C	7	H	4	10	12	100.92	3805.6	-1.555					
1241	C	7	H	4	20	22	101.02	3808.4	-1.458	3.02	23.9	1.30	0.43	0.00
1241	C	7	H	4	30	32	101.12	3811.2	-1.567					
1241	C	7	H	4	40	42	101.22	3814.0	-1.704	3.37	25.4	1.32	0.39	0.01
1241	C	7	H	4	50	52	101.32	3816.8	-2.060					
1241	C	7	H	4	60	62	101.42	3819.6		3.41	25.5	1.34	0.43	0.00
1241	C	7	H	4	70	72	101.52	3822.4						
1241	C	7	H	4	80	82	101.62	3825.2		2.98	23.7	1.28	0.33	0.00
1241	C	7	H	4	90	92	101.72	3828.0						
1241	C	7	H	4	100	102	101.82	3830.8	-1.690	3.07	24.1	1.39	0.40	0.00
1241	C	7	H	4	110	112	101.92	3833.6	-1.720					
1241	C	7	H	4	120	122	102.02	3836.4	-1.591	3.59	26.2	1.31	0.46	0.27
1241	C	7	H	4	130	132	102.12	3839.2	-1.944					
1241	C	7	H	4	140	142	102.22	3842.0	-1.720	3.11	24.3	1.28	0.34	0.00
1241	C	7	H	5	0	2	102.32	3844.8	-1.811	3.32	25.2	1.27	0.23	0.00
1241	C	7	H	5	10	12	102.42	3847.6	-1.754	3.41	25.5	1.27	0.27	0.05
1241	C	7	H	5	20	22	102.52	3850.4	-1.472	3.35	25.3	1.27	0.27	0.00
1241	C	7	H	5	30	32	102.62	3853.2	-1.823	3.38	25.4	1.33	0.28	0.06
1241	C	7	H	5	40	42	102.72	3856.0		3.51	25.9	1.30	0.27	0.05
1241	C	7	H	5	50	52	102.82	3858.8	-1.500	3.39	25.4	1.27	0.24	0.05
1241	C	7	H	5	60	62	102.92	3861.6	-1.650	3.50	25.9	1.26	0.25	0.03
1241	C	7	H	5	70	72	103.02	3864.4	-1.760	3.40	25.5	1.29	0.21	0.00
1241	C	7	H	5	80	82	103.12	3867.2	-1.310	3.51	25.9	1.29	0.22	0.00
1241	C	7	H	5	90	92	103.22	3870.0	-1.620	3.21	24.7	1.30	0.24	0.00
1241	C	7	H	5	100	102	103.32	3872.8	-1.730	3.36	25.3	1.28	0.25	0.03
1241	C	7	H	5	110	112	103.42	3875.6	-1.640	3.22	24.8	1.32	0.25	0.04
1241	C	7	H	5	120	122	103.52	3878.4	-1.570	3.46	25.7	1.29	0.23	0.29
1241	C	7	H	5	130	132	103.62	3881.2	-1.380	3.42	25.5	1.27	0.23	0.05
1241	C	7	H	5	140	142	103.72	3884.0	-1.750	3.64	26.4	1.28	0.26	0.08
1241	C	7	H	6	0	2	103.82	3886.8	-1.560	3.32	25.2	1.28	0.23	0.01
1241	C	7	H	6	10	12	103.92	3889.6	-1.630	3.32	25.2	1.28	0.25	0.10
1241	C	7	H	6	20	22	104.02	3892.4	-1.760	3.20	24.7	1.26	0.25	0.08

Appendix C (continued)

Site	Hole	Core	T	Sec.	Top (cm)	Bot (cm)	Depth (corr. msbf)	Age (ka)	$\delta^{18}O_{G.\ Sacculifer}$ (‰)	Mg/Ca (mmol/mol)	Temperature (°C)	Sr/Ca (mmol/mol)	Mn/Ca (mmol/mol)	Fe/Ca (mmol/mol)
1241	C	7	H	6	30	32	104.12	3895.2	-1.860	3.37	25.4	1.29	0.27	0.06
1241	C	7	H	6	40	42	104.22	3898.0	-1.580	3.37	25.4	1.29	0.24	0.00
1241	C	7	H	6	50	52	104.32	3900.8	-1.700	3.17	25.4	1.28	0.34	0.04
1241	C	7	H	6	60	62	104.42	3903.6	-1.570	3.32	25.1	1.40	0.34	0.06
1241	C	7	H	6	70	72	104.52	3906.4	-1.290	3.31	25.1	1.39	0.36	0.07
1241	C	7	H	6	80	82	104.62	3909.2	-1.810	3.52	25.9	1.41	0.35	0.06
1241	C	7	H	6	90	92	104.72	3912.0	-1.730	3.31	25.1	1.28	0.28	0.00
1241	C	7	H	6	100	102	104.82	3915.5	-1.520	3.28	25.0	1.33	0.31	0.00
1241	C	7	H	6	110	112	104.92	3919.0	-1.780	3.34	25.2	1.29		
1241	C	7	H	6	120	122	105.02	3922.5	-1.560					
1241	C	7	H	6	130	132	105.12	3926.0	-1.590	3.38	25.4	1.36	0.34	0.02
1241	C	7	H	6	140	142	105.22	3929.5	-1.820	3.51	25.9	1.28	0.31	0.06
1241	C	7	H	7	0	2	105.32	3933.0	-1.840	3.85	27.1	1.42	0.33	0.30
1241	C	7	H	7	10	12	105.42	3936.5	-1.900	3.88	27.2	1.36	0.33	0.06
1241	C	7	H	7	20	22	105.52	3939.9	-1.600	3.60	26.2	1.40	0.33	0.06
1241	C	7	H	7	30	32	105.62	3943.4	-1.740	3.13	24.4	1.34	0.32	0.03
1241	C	7	H	7	40	42	105.72	3946.9	-1.710	3.22	24.8	1.27	0.24	0.05
1241	C	7	H	7	50	52	105.82	3950.4	-1.440	3.55	26.0	1.38	0.33	0.12
1241	C	7	H	7	60	62	105.92	3953.9	-1.710	3.38	25.4	1.36	0.34	0.00
1241	A	11	H	4	20	22	105.93	3954.3	-1.930	3.10	24.3	1.31	0.34	0.08
1241	A	11	H	4	30	32	106.03	3957.8	-1.680	3.34	25.2	1.37	0.33	0.07
1241	A	11	H	4	40	42	106.13	3961.3	-1.800	3.34	25.2	1.29	0.27	0.05
1241	A	11	H	4	50	52	106.23	3964.7	-1.550	3.78	26.9	1.40	0.34	0.08
1241	A	11	H	4	60	62	106.33	3968.2	-1.470	3.22	24.8	1.33	0.37	0.12
1241	A	11	H	4	70	72	106.43	3971.7	-1.720	3.13	24.4	1.35	0.33	0.05
1241	A	11	H	4	80	82	106.53	3975.2	-1.220	3.20	24.7	1.29	0.36	0.13
1241	A	11	H	4	90	92	106.63	3978.7	-1.570	3.03	24.0	1.24	0.25	0.07
1241	A	11	H	4	100	102	106.73	3982.2	-1.440	3.16	24.5	1.34	0.36	0.17
1241	A	11	H	4	110	112	106.83	3985.7	-1.350	3.38	25.4	1.38	0.32	0.07
1241	A	11	H	4	120	122	106.93	3989.2	-1.550	3.17	24.6	1.38	0.30	0.03
1241	A	11	H	4	130	132	107.03	3992.7	-1.420	3.04	24.0	1.40	0.30	0.13
1241	A	11	H	4	140	142	107.13	3996.2	-1.490	3.05	24.0	1.29	0.24	0.04
1241	A	11	H	5	0	2	107.24	4000.0	-1.310	2.92	23.5	1.37	0.31	0.04
1241	A	11	H	5	10	12	107.34	4003.5	-1.670	2.71	22.5	1.35	0.28	0.04
1241	A	11	H	5	20	22	107.44	4007.0	-1.580	3.25	24.9	1.39	0.33	0.05
1241	A	11	H	5	30	32	107.54	4010.5	-1.630	3.02	23.9	1.36	0.31	0.01
1241	A	11	H	5	40	42	107.64	4014.0	-1.310	3.10	24.3	1.27	0.25	0.00
1241	A	11	H	5	50	52	107.74	4017.5	-1.450	3.09	24.2	1.39	0.27	0.07
1241	A	11	H	5	60	62	107.84	4021.0	-1.460	3.20	24.7	1.39	0.30	0.10
1241	A	11	H	5	70	72	107.94	4023.9	-1.480	3.15	24.5	1.39	0.26	0.04
1241	A	11	H	5	80	82	108.04	4026.9	-1.410	3.34	25.2	1.41	0.28	0.01
1241	A	11	H	5	90	92	108.14	4029.8	-1.770	3.24	24.9	1.28	0.22	0.05
1241	A	11	H	5	100	102	108.24	4032.7	-1.720	3.25	24.9	1.28	0.26	0.06
1241	A	11	H	5	110	112	108.34	4035.7	-1.630	3.41	25.5	1.42	0.31	0.03
1241	C	8	H	2	0	2	108.36	4036.3	-1.400	3.38	25.4	1.40	0.32	0.06
1241	C	8	H	2	10	12	108.46	4039.2	-1.810	3.20	24.7	1.29	0.24	0.04
1241	C	8	H	2	20	22	108.56	4042.1	-1.360	3.52	25.9	1.42	0.31	0.01
1241	C	8	H	2	30	32	108.66	4045.1	-1.760	3.21	24.7	1.36	0.35	
1241	C	8	H	2	40	42	108.76	4048.0	-1.490	3.37	25.3	1.32	0.31	0.11
1241	C	8	H	2	50	52	108.86	4050.9	-1.710	3.30	25.1	1.39	0.30	0.05
1241	C	8	H	2	60	62	108.96	4053.9	-1.640	3.19	24.6	1.27	0.25	0.06
1241	C	8	H	2	70	72	109.06	4056.8	-1.820	3.36	25.3	1.36	0.32	0.06
1241	C	8	H	2	80	82	109.16	4059.7	-1.770	3.32	25.2	1.36	0.27	0.06
1241	C	8	H	2	90	92	109.26	4062.7	-1.590	3.31	25.1	1.35	0.26	0.01
1241	C	8	H	2	100	102	109.36	4065.6	-1.530	3.47	25.7	1.36	0.29	0.09
1241	C	8	H	2	110	112	109.46	4068.5	-1.520	3.31	25.1	1.27	0.18	0.05
1241	C	8	H	2	120	122	109.56	4071.5	-1.570	3.60	26.2	1.42	0.29	0.08
1241	C	8	H	2	130	132	109.66	4074.4	-1.390	3.54	26.0	1.35	0.30	0.06
1241	C	8	H	2	140	142	109.76	4077.3	-1.360	3.16	24.5	1.37	0.30	0.01
1241	C	8	H	3	0	2	109.86	4080.3	-1.450	3.45	25.7	1.37	0.28	0.07
1241	C	8	H	3	10	12	109.96	4083.2	-1.580	3.15	24.4	1.26	0.25	0.01
1241	C	8	H	3	20	22	110.06	4086.1	-1.460	3.44	25.6	1.38	0.31	0.10
1241	C	8	H	3	30	32	110.16	4089.1	-1.720	2.99	23.8	1.33	0.32	0.00
1241	C	8	H	3	40	42	110.26	4092.0	-1.630	3.12	24.3	1.36	0.33	0.06
1241	C	8	H	3	50	52	110.36	4094.9		3.18	24.6	1.34	0.30	0.08
1241	C	8	H	3	60	62	110.46	4097.9	-1.500	3.17	24.5	1.25	0.22	0.06
1241	C	8	H	3	70	72	110.56	4100.8	-1.520	3.37	25.3	1.34	0.31	0.07
1241	C	8	H	3	80	82	110.66	4103.7	-1.680	3.54	26.0	1.35	0.30	0.01
1241	C	8	H	3	90	92	110.76	4106.7	-1.800	3.48	25.8	1.42	0.35	0.05

Appendix C (continued)

Site	Hole	Core	T	Sec.	Top (cm)	Bot (cm)	Depth (corr. msbf)	Age (ka)	$\delta^{18}O_{G.\ Sacculifer}$ (‰)	Mg/Ca (mmol/mol)	Temperature (°C)	Sr/Ca (mmol/mol)	Mn/Ca (mmol/mol)	Fe/Ca (mmol/mol)
1241	C	8	H	3	100	102	110.86	4109.6	-1.750	3.10	24.3	1.36	0.30	0.00
1241	C	8	H	3	110	112	110.96	4112.5	-1.670	3.30	25.1	1.26	0.27	0.05
1241	C	8	H	3	120	122	111.06	4115.5	-1.690	3.55	26.0	1.33	0.35	0.07
1241	C	8	H	3	130	132	111.16	4118.4	-1.330	2.97	23.7	1.28	0.36	0.01
1241	C	8	H	3	140	142	111.26	4121.3	-1.570	2.95	23.6	1.30	0.33	0.05
1241	C	8	H	4	0	2	111.36	4124.3	-1.710	3.22	24.8	1.38	0.32	0.00
1241	C	8	H	4	10	12	111.46	4127.2	-1.860	3.50	25.9	1.26	0.26	0.02
1241	C	8	H	4	20	22	111.56	4130.1	-1.860	3.51	25.9	1.41	0.29	0.04
1241	C	8	H	4	30	32	111.66	4133.1	-1.700	3.39	25.4	1.36	0.29	0.03
1241	C	8	H	4	40	42	111.76	4136.0	-1.650	3.27	25.0	1.37	0.32	0.00
1241	C	8	H	4	50	52	111.86	4138.5	-1.780	3.59	26.2	1.38	0.33	0.07
1241	C	8	H	4	60	62	111.96	4141.0	-1.780	3.69	26.5	1.24	0.23	0.03
1241	C	8	H	4	70	72	112.06	4143.5	-1.620	3.28	25.0	1.34	0.30	0.10
1241	C	8	H	4	80	82	112.16	4146.0	-1.460	3.33	25.2	1.33	0.31	0.09
1241	C	8	H	4	90	92	112.26	4148.5	-1.670	3.44	25.6	1.41	0.30	0.01
1241	C	8	H	4	100	102	112.36	4150.9	-1.470	3.54	26.0	1.39	0.32	0.04
1241	C	8	H	4	110	112	112.46	4153.4	-1.350	3.22	24.8	1.29	0.26	0.15
1241	C	8	H	4	120	122	112.56	4155.9	-1.330	3.45	25.7	1.39	0.32	0.03
1241	C	8	H	4	130	132	112.66	4158.4	-1.470	3.06	24.1	1.35	0.34	0.03
1241	C	8	H	4	140	142	112.76	4160.9	-1.700	3.14	24.4	1.38	0.30	0.00
1241	C	8	H	5	0	2	112.86	4163.4	-1.750	3.45	25.7	1.38	0.33	0.06
1241	C	8	H	5	10	12	112.96	4165.9	-1.510	3.23	24.8	1.25	0.26	0.02
1241	C	8	H	5	20	22	113.06	4168.4	-1.670	3.33	25.2	1.38	0.32	0.06
1241	C	8	H	5	30	32	113.16	4170.9	-1.560	3.38	25.4	1.37	0.30	0.06
1241	C	8	H	5	40	42	113.26	4173.3	-1.670	3.32	25.2	1.41	0.31	0.00
1241	C	8	H	5	50	52	113.36	4175.8	-1.350	3.11	24.3	1.39	0.30	0.06
1241	C	8	H	5	60	62	113.46	4178.3	-1.470	3.20	24.7	1.23	0.27	0.01
1241	C	8	H	5	70	72	113.56	4180.8	-1.590	3.15	24.4	1.35	0.34	0.02
1241	C	8	H	5	80	82	113.66	4183.3	-1.740	3.44	25.6	1.36	0.33	0.00
1241	C	8	H	5	90	92	113.76	4185.8	-1.630	3.54	26.0	1.39	0.35	0.03
1241	C	8	H	5	100	102	113.86	4188.3	-1.540	3.51	25.9	1.37	0.33	0.03
1241	C	8	H	5	110	112	113.96	4190.8	-1.690	3.51	25.9	1.27	0.25	0.05
1241	C	8	H	5	120	122	114.06	4193.2	-1.640	3.10	24.2	1.33	0.33	0.00
1241	C	8	H	5	130	132	114.16	4195.7	-1.830	3.44	25.6	1.37	0.33	0.04
1241	C	8	H	5	140	142	114.26	4198.2	-1.950	3.82	27.0	1.38	0.32	0.03
1241	C	8	H	6	0	2	114.36	4200.7	-1.770	3.30	25.1	1.37	0.31	0.02
1241	C	8	H	6	10	12	114.46	4203.2	-1.550	3.16	24.5	1.25	0.24	0.05
1241	C	8	H	6	20	22	114.56	4205.7	-1.680	3.02	23.9	1.31	0.31	0.02
1241	C	8	H	6	30	32	114.66	4208.2	-1.900	3.10	24.3	1.33	0.37	0.04
1241	C	8	H	6	40	42	114.76	4210.7	-1.830	3.40	25.5	1.39	0.33	0.06
1241	C	8	H	6	50	52	114.86	4213.2	-1.750	3.23	24.8	1.25	0.25	0.07
1241	C	8	H	6	60	62	114.96	4215.7	-1.690	3.53	26.0	1.38	0.30	0.06
1241	A	12	H	2	140	142	115.01	4216.9	-1.900	2.98	23.7	1.34	0.31	0.06
1241	A	12	H	3	0	2	115.12	4219.6	-1.770	3.17	24.5	1.36	0.28	0.02
1241	A	12	H	3	10	12	115.22	4222.1	-1.700	3.32	25.2	1.24		
1241	A	12	H	3	20	22	115.32	4224.6	-1.480	3.41	25.5	1.26	0.24	0.04
1241	A	12	H	3	30	32	115.42	4227.1	-1.860	3.21	24.7	1.26		
1241	A	12	H	3	40	42	115.52	4229.6	-1.800	3.19	24.6	1.27	0.26	0.07
1241	A	12	H	3	50	52	115.62	4232.1	-1.710	3.09	24.2	1.25		
1241	A	12	H	3	60	62	115.72	4234.6	-1.740	3.30	25.1	1.29	0.25	0.11
1241	A	12	H	3	70	72	115.82	4237.1	-1.550	3.36	25.3	1.26	0.24	0.04
1241	A	12	H	3	80	82	115.92	4239.5	-2.050	3.46	25.7	1.25	0.22	0.07
1241	A	12	H	3	90	92	116.02	4242.0	-1.680	3.05	24.0	1.25	0.22	0.02
1241	A	12	H	3	100	102	116.12	4244.5	-1.850	3.04	24.0	1.34	0.29	0.00
1241	A	12	H	3	110	112	116.22	4247.0	-1.470	3.08	24.2	1.28	0.23	0.02
1241	A	12	H	3	120	122	116.32	4249.5	-1.540	3.26	24.9	1.26	0.26	0.16
1241	A	12	H	3	130	132	116.42	4252.0	-1.860					
1241	A	12	H	3	140	142	116.52	4254.6	-1.570	2.96	23.7	1.26	0.23	0.07
1241	A	12	H	4	0	2	116.63	4257.5	-1.840	3.17	24.5	1.39	0.28	0.00
1241	A	12	H	4	10	12	116.73	4260.1	-1.860	3.29	25.0	1.25	0.23	0.05
1241	A	12	H	4	20	22	116.83	4262.8	-1.920	2.99	23.8	1.26	0.21	0.09
1241	A	12	H	4	30	32	116.93	4265.4	-1.770	3.05	24.0	1.25	0.25	0.14
1241	A	12	H	4	40	42	117.03	4268.0	-1.610			1.23		
1241	A	12	H	4	50	52	117.13	4270.7	-1.760	3.34	25.2	1.37	0.24	0.02
1241	A	12	H	4	60	62	117.23	4273.3	-1.661	3.02	23.9	1.26	0.22	0.04
1241	A	12	H	4	70	72	117.33	4275.9	-1.576	3.27	25.0	1.26	0.22	0.00
1241	A	12	H	4	80	82	117.43	4278.6	-1.882	3.26	24.9	1.25	0.24	0.11
1241	A	12	H	4	90	92	117.53	4281.2	-1.835	3.34	25.2	1.26	0.22	0.04
1241	A	12	H	4	100	102	117.63	4283.8	-1.651	3.30	25.1	1.39	0.26	0.09

Appendix C (continued)

Site	Hole	Core	T	Sec.	Top (cm)	Bot (cm)	Depth (corr. msbf)	Age (ka)	$\delta^{18}O_{G.\ Sacculifer}$ (‰)	Mg/Ca (mmol/mol)	Temperature (°C)	Sr/Ca (mmol/mol)	Mn/Ca (mmol/mol)	Fe/Ca (mmol/mol)
1241	A	12	H	4	110	112	117.73	4286.4						
1241	A	12	H	4	120	122	117.83	4289.1	-1.643	2.98	23.7	1.27	0.21	0.03
1241	A	12	H	4	130	132	117.93	4291.7	-1.603	2.98	23.7	1.24	0.21	0.10
1241	A	12	H	4	140	142	118.03	4294.3	-1.738	3.40	25.5	1.25	0.22	0.02
1241	A	12	H	5	0	2	118.14	4297.2	-1.782	3.21	24.7	1.35	0.29	0.06
1241	A	12	H	5	10	12	118.24	4299.9	-1.442	3.06	24.1	1.23	0.22	0.17
1241	A	12	H	5	20	22	118.34	4302.5	-1.491	3.04	24.0	1.24	0.21	0.01
1241	A	12	H	5	30	32	118.44	4305.1	-1.897	3.43	25.6	1.27	0.24	0.04
1241	A	12	H	5	40	42	118.54	4307.7	-1.696	3.10	24.3	1.25	0.22	0.01
1241	A	12	H	5	50	52	118.64	4310.4	-1.775	3.21	24.7	1.34	0.29	0.03
1241	A	12	H	5	60	62	118.74	4313.0	-1.834	3.42	25.5	1.24	0.22	0.05
1241	A	12	H	5	70	72	118.84	4315.7	-1.906	3.21	24.7	1.24	0.21	0.07
1241	A	12	H	5	80	82	118.94	4318.5	-1.647	2.97	23.7	1.25	0.19	0.03
1241	A	12	H	5	90	92	119.04	4321.2	-1.540	2.91	23.4	1.28	0.18	0.02
1241	A	12	H	5	100	102	119.14	4323.9	-1.759	2.97	23.7	1.34	0.22	0.05
1241	A	12	H	5	110	112	119.24	4326.6	-1.735	2.96	23.7	1.25	0.19	0.00
1241	B	12	H	2	130	132	119.31	4328.5	-1.542	3.15	24.5	1.28	0.15	0.00
1241	B	12	H	2	140	142	119.41	4331.3	-1.569	3.44	25.6	1.23		
1241	B	12	H	3	0	2	119.51	4334.0	-1.747	3.27	25.0	1.25	0.18	0.02
1241	B	12	H	3	10	12	119.61	4336.7	-1.861	3.44	25.6	1.33	0.28	0.03
1241	B	12	H	3	20	22	119.71	4339.5	-1.717			1.25		
1241	B	12	H	3	30	32	119.81	4342.2	-1.743	3.08	24.2	1.25	0.22	0.10
1241	B	12	H	3	40	42	119.91	4344.9	-1.631	3.14	24.4	1.26	0.19	0.02
1241	B	12	H	3	50	52	120.01	4347.6	-1.488	2.84	23.1	1.24	0.23	0.11
1241	B	12	H	3	60	62	120.11	4350.4	-1.469	3.42	25.5	1.35	0.28	0.11
1241	B	12	H	3	70	72	120.21	4353.1	-1.588	3.11	24.3	1.24	0.21	0.09
1241	B	12	H	3	80	82	120.31	4355.8	-1.297	2.84	23.1	1.27	0.23	0.07
1241	B	12	H	3	90	92	120.41	4358.5	-1.349	3.01	23.9	1.25	0.21	0.06
1241	B	12	H	3	100	102	120.51	4361.3	-1.340	2.76	22.7	1.27		
1241	B	12	H	3	110	112	120.61	4364.0	-1.581	2.70	22.4	1.30	0.27	0.04
1241	B	12	H	3	120	122	120.71	4366.7	-1.704	3.21	24.7	1.24	0.23	0.57
1241	B	12	H	3	130	132	120.81	4369.5	-1.322	3.06	24.1	1.23	0.23	0.09
1241	B	12	H	3	140	142	120.91	4372.2	-1.676	3.54	26.0	1.29	0.24	0.01
1241	B	12	H	4	0	2	121.02	4375.2	-1.673	3.19	24.6	1.27	0.18	0.13
1241	B	12	H	4	10	12	121.12	4377.9	-1.749	2.87	23.2	1.25	0.32	0.08
1241	B	12	H	4	20	22	121.22	4380.6	-1.748	3.13	24.4	1.27	0.26	0.06
1241	B	12	H	4	30	32	121.32	4383.4	-1.538					
1241	B	12	H	4	40	42	121.42	4386.1	-1.986	3.55	26.1	1.24	0.25	0.02
1241	B	12	H	4	50	52	121.52	4388.8	-1.792	3.66	26.4	1.26	0.23	0.06
1241	B	12	H	4	60	62	121.62	4391.5	-1.611	3.46	25.7	1.37	0.27	0.03
1241	B	12	H	4	70	72	121.72	4394.3	-1.833	3.13	24.4	1.26	0.22	0.07
1241	B	12	H	4	80	82	121.82	4397.0	-1.894	3.50	25.9	1.24	0.24	0.02
1241	B	12	H	4	90	92	121.92	4399.7	-1.724	3.41	25.5	1.27	0.24	0.08
1241	B	12	H	4	100	102	122.02	4402.5	-1.646	3.41	25.5	1.25	0.24	0.06
1241	B	12	H	4	110	112	122.12	4405.2	-1.344					
1241	B	12	H	4	120	122	122.22	4407.9	-1.688	3.24	24.8	1.24	0.26	0.05
1241	B	12	H	4	130	132	122.32	4410.6	-1.770	3.34	25.2	1.24	0.21	0.11
1241	B	12	H	4	140	142	122.42	4413.4	-1.657	3.23	24.8	1.24	0.22	0.06
1241	B	12	H	5	0	2	122.53	4416.4	-1.763	3.28	25.0	1.22	0.26	0.05
1241	B	12	H	5	10	12	122.63	4419.1	-1.654	3.75	26.8	1.38	0.29	0.00
1241	B	12	H	5	20	22	122.73	4421.8	-1.717	3.49	25.8	1.24	0.22	0.05
1241	B	12	H	5	30	32	122.83	4424.5	-2.224	3.41	25.5	1.26	0.18	0.05
1241	B	12	H	5	40	42	122.93	4427.3	-1.681	3.44	25.6	1.25	0.20	0.11
1241	B	12	H	5	50	52	123.03	4430.0	-1.791	3.41	25.5	1.25	0.17	0.06
1241	B	12	H	5	60	62	123.13	4433.1	-1.919	3.43	25.6	1.35	0.22	0.01
1241	B	12	H	5	70	72	123.23	4436.3	-1.695	3.32	25.1	1.25	0.17	0.12
1241	B	12	H	5	80	82	123.33	4439.4	-1.600	3.32	25.2	1.24	0.17	0.12
1241	B	12	H	5	90	92	123.43	4442.6	-1.440	3.12	24.3	1.23	0.19	0.04
1241	B	12	H	5	100	102	123.53	4445.7	-1.544	3.26	24.9	1.24	0.18	0.08
1241	B	12	H	5	110	112	123.63	4448.9	-1.365	3.15	24.5	1.23	0.19	0.11
1241	B	12	H	5	120	122	123.73	4452.0	-1.597	3.14	24.4	1.24	0.17	0.15
1241	B	12	H	5	130	132	123.83	4455.1	-1.612	3.38	25.4	1.26	0.19	0.13
1241	B	12	H	5	140	142	123.93	4458.3	-1.526	3.34	25.2	1.26	0.21	0.08
1241	B	12	H	6	0	2	124.03	4461.4	-1.786					
1241	B	12	H	6	10	12	124.13	4464.6	-1.552	3.22	24.8	1.22	0.19	0.07
1241	B	12	H	6	20	22	124.23	4467.7	-1.796	3.48	25.8	1.24	0.22	0.09
1241	B	12	H	6	30	32	124.33	4470.9	-1.382	3.07	24.1	1.23	0.19	0.09
1241	B	12	H	6	40	42	124.43	4474.0	-1.957	3.50	25.9	1.26	0.21	0.05
1241	B	12	H	6	50	52	124.53	4477.1	-1.934	3.43	25.6	1.24	0.22	0.03

Appendix C (continued)

Site	Hole	Core	T	Sec.	Top (cm)	Bot (cm)	Depth (corr. msbf)	Age (ka)	$\delta^{18}O_{G.\ Sacculifer}$ (‰)	Mg/Ca (mmol/mol)	Temperature (°C)	Sr/Ca (mmol/mol)	Mn/Ca (mmol/mol)	Fe/Ca (mmol/mol)
1241	B	12	H	6	60	62	124.63	4480.3	-1.571	3.15	24.5	1.24	0.20	0.06
1241	B	12	H	6	70	72	124.73	4483.4	-1.385	3.37	25.3	1.24	0.22	0.07
1241	B	12	H	6	80	82	124.83	4486.6	-1.512	3.31	25.1	1.23	0.21	0.07
1241	B	12	H	6	90	92	124.93	4489.7	-1.818	3.39	25.4	1.26	0.20	0.03
1241	B	12	H	6	100	102	125.03	4492.9	-1.721	3.32	25.1	1.23	0.23	0.10
1241	B	12	H	6	110	112	125.13	4496.0	-1.587	3.52	25.9	1.23	0.25	0.09
1241	B	12	H	6	120	122	125.23	4498.9	-1.776	3.39	25.4	1.24	0.19	0.04
1241	B	12	H	6	130	132	125.33	4501.7	-1.900	3.15	24.5	1.24	0.17	0.11
1241	A	13	H	3	40	42	125.41	4504.0	-1.668	3.11	24.3	1.24	0.18	0.14
1241	A	13	H	3	50	52	125.51	4506.8	-1.754	3.24	24.8	1.24	0.21	0.07
1241	A	13	H	3	60	62	125.61	4509.7	-1.742	3.55	26.0	1.25	0.21	0.08
1241	A	13	H	3	70	72	125.71	4512.5	-1.570	3.45	25.7	1.24	0.21	0.08
1241	A	13	H	3	80	82	125.81	4515.4	-1.625	3.50	25.9	1.26	0.21	0.03
1241	A	13	H	3	90	92	125.91	4518.2	-1.612	3.57	26.1	1.26	0.23	0.00
1241	A	13	H	3	100	102	126.01	4521.1	-1.965	3.28	25.0	1.23	0.22	0.02
1241	A	13	H	3	110	112	126.11	4523.9	-1.367	3.31	25.1	1.23	0.22	0.07
1241	A	13	H	3	120	122	126.21	4526.8	-1.517	3.26	24.9	1.22	0.22	0.09
1241	A	13	H	3	130	132	126.31	4529.6	-1.457	3.31	25.1	1.23	0.19	0.03
1241	A	13	H	3	140	142	126.41	4532.5	-1.352	3.17	24.6	1.23	0.22	0.06
1241	A	13	H	4	0	2	126.52	4535.6	-1.799	3.13	24.4	1.21	0.24	0.10
1241	A	13	H	4	10	12	126.62	4538.5	-1.740	3.17	24.6	1.24	0.21	0.08
1241	A	13	H	4	20	22	126.72	4541.3	-1.676	3.13	24.4	1.22	0.23	0.01
1241	A	13	H	4	30	32	126.82	4544.2	-1.779	3.50	25.8	1.23	0.25	0.05
1241	A	13	H	4	40	42	126.92	4547.0	-1.611	2.98	23.7	1.32	0.28	0.08
1241	A	13	H	4	50	52	127.02	4549.9	-1.505	3.30	25.1	1.26	0.20	0.08
1241	A	13	H	4	60	62	127.12	4552.7	-1.364	3.06	24.1	1.26	0.21	0.09
1241	A	13	H	4	70	72	127.22	4555.6	-1.735	3.40	25.5	1.25	0.21	0.19
1241	A	13	H	4	80	82	127.32	4558.5	-1.724	3.35	25.3	1.22	0.24	0.11
1241	A	13	H	4	90	92	127.42	4561.3	-1.496	3.25	24.9	1.38	0.29	0.07
1241	A	13	H	4	100	102	127.52	4564.1	-1.249	3.18	24.6	1.23	0.19	0.02
1241	A	13	H	4	110	112	127.62	4567.0	-1.127	2.97	23.7	1.17	0.00	1.58
1241	A	13	H	4	120	122	127.72	4570.0	-1.363	3.26	24.9	1.25	0.20	0.09
1241	A	13	H	4	130	132	127.82	4573.0	-1.941	3.21	24.7	1.26	0.20	0.05
1241	A	13	H	4	140	142	127.92	4576.0	-1.345	3.13	24.4	1.34	0.28	0.00
1241	A	13	H	5	0	2	128.02	4579.0	-1.621	3.30	25.1	1.24	0.22	0.09
1241	A	13	H	5	10	12	128.12	4582.0	-1.637	3.27	25.0	1.25	0.21	0.10
1241	A	13	H	5	20	22	128.22	4585.0	-1.178	3.20	24.7	1.25	0.20	0.07
1241	A	13	H	5	30	32	128.32	4588.0	-1.448	3.10	24.2	1.23	0.21	0.00
1241	A	13	H	5	40	42	128.42	4591.0	-1.655	3.32	25.2	1.37	0.28	0.05
1241	A	13	H	5	50	52	128.52	4594.0	-1.590	3.49	25.8	1.25	0.21	0.10
1241	A	13	H	5	60	62	128.62	4597.0	-1.563	2.88	23.3	1.18	0.18	0.07
1241	A	13	H	5	70	72	128.72	4600.0	-1.450	2.97	23.7	1.17	0.18	0.02
1241	A	13	H	5	80	82	128.82	4602.4	-1.805	3.17	24.6	1.22	0.19	0.04
1241	A	13	H	5	90	92	128.92	4604.8	-1.766	3.49	25.8	1.31	0.28	0.05
1241	A	13	H	5	100	102	129.02	4607.2	-1.043	2.84	23.1	1.20	0.20	0.00
1241	A	13	H	5	110	112	129.12	4609.6	-1.706	3.17	24.5	1.23	0.14	0.26
1241	C	9	H	3	90	92	129.14	4610.1	-1.100	2.85	23.2	1.22	0.23	0.12
1241	C	9	H	3	100	102	129.24	4612.5	-1.530	2.85	23.1	1.28	0.28	0.00
1241	C	9	H	3	110	112	129.34	4614.9	-1.526			1.19		
1241	C	9	H	3	120	122	129.44	4617.3	-1.847	3.28	25.0	1.24	0.22	0.01
1241	C	9	H	3	130	132	129.54	4619.7	-1.778	3.37	25.3	1.24	0.20	0.01
1241	C	9	H	3	140	142	129.64	4622.1	-1.627	3.02	23.9	1.22	0.22	0.02
1241	C	9	H	4	0	2	129.74	4624.6	-1.342	3.02	23.9	1.32	0.29	0.05
1241	C	9	H	4	10	12	129.84	4627.0	-1.379	2.91	23.4	1.20	0.24	0.06
1241	C	9	H	4	20	22	129.94	4629.4	-1.453	3.26	24.9	1.24	0.26	0.05
1241	C	9	H	4	30	32	130.04	4631.8	-1.554	2.91	23.4	1.19	0.20	0.02
1241	C	9	H	4	40	42	130.14	4634.2	-1.794	3.62	26.3	1.25	0.24	0.01
1241	C	9	H	4	50	52	130.24	4636.6	-1.737	3.53	25.9	1.36	0.28	0.06
1241	C	9	H	4	60	62	130.34	4639.0	-1.690	3.29	25.0	1.23	0.22	0.04
1241	C	9	H	4	70	72	130.44	4642.0	-1.481	3.71	26.6	1.25	0.25	0.00
1241	C	9	H	4	80	82	130.54	4645.0	-1.281	3.08	24.2	1.19	0.25	0.10
1241	C	9	H	4	90	92	130.64	4648.0	-1.470	2.99	23.8	1.18	0.26	0.08
1241	C	9	H	4	100	102	130.74	4651.0	-1.187	3.03	24.0	1.30	0.32	0.04
1241	C	9	H	4	110	112	130.84	4654.0	-0.905	3.14	24.4	1.19	0.27	0.04
1241	C	9	H	4	120	122	130.94	4657.0	-1.539	3.12	24.3	1.19	0.22	0.12
1241	C	9	H	4	130	132	131.04	4659.8	-1.518	3.11	24.3	1.18	0.25	0.03
1241	C	9	H	4	140	142	131.14	4662.6	-1.563	3.26	24.9	1.20	0.27	0.19
1241	C	9	H	5	0	2	131.25	4665.7	-1.521	3.01	23.9	1.29	0.32	0.13
1241	C	9	H	5	10	12	131.35	4668.5	-1.339	3.36	25.3	1.20	0.21	0.06

Appendix C (continued)

Site	Hole	Core	T	Sec.	Top (cm)	Bot (cm)	Depth (corr. msbf)	Age (ka)	$\delta^{18}O_{G.\ Sacculifer}$ (‰)	Mg/Ca (mmol/mol)	Temperature (°C)	Sr/Ca (mmol/mol)	Mn/Ca (mmol/mol)	Fe/Ca (mmol/mol)
1241	C	9	H	5	20	22	131.45	4671.2	-1.326	3.44	25.6	1.20	0.23	0.09
1241	C	9	H	5	30	32	131.55	4674.0	-1.351	3.03	23.9	1.20	0.21	0.06
1241	C	9	H	5	40	42	131.65	4676.8	-1.490	3.09	24.2	1.19	0.21	0.08
1241	C	9	H	5	50	52	131.75	4679.6	-1.584					
1241	C	9	H	5	60	62	131.85	4682.4	-1.542	3.06	24.1	1.20	0.19	0.10
1241	C	9	H	5	70	72	131.95	4685.2	-1.113	3.05	24.0	1.20	0.22	0.20
1241	C	9	H	5	80	82	132.05	4688.0	-1.467	2.95	23.6	1.20	0.19	0.16
1241	C	9	H	5	90	92	132.15	4690.8	-1.433	3.40	25.5	1.22	0.27	0.08
1241	C	9	H	5	100	102	132.25	4693.6	-1.666	2.97	23.7	1.27	0.32	0.00
1241	C	9	H	5	110	112	132.35	4696.4	-1.595	3.09	24.2	1.21	0.22	0.20
1241	C	9	H	5	120	122	132.45	4699.2	-1.608	2.88	23.3	1.20	0.18	0.11
1241	C	9	H	5	130	132	132.55	4702.0	-1.562	3.09	24.2	1.21	0.20	0.21
1241	A	14	H	1	50	52	132.57	4702.5	-1.543	2.99	23.8	1.20	0.16	0.19
1241	A	14	H	1	60	62	132.67	4704.7	-1.497	2.90	23.4	1.27	0.29	0.07
1241	A	14	H	1	70	72	132.77	4707.0	-1.537	3.03	24.0	1.19	0.19	0.07
1241	A	14	H	1	80	82	132.87	4709.3	-1.781	3.12	24.3	1.19	0.21	0.11
1241	A	14	H	1	90	92	132.97	4711.6	-1.570	3.33	25.2	1.21	0.20	0.10
1241	A	14	H	1	100	102	133.07	4713.9	-1.925	3.13	24.4	1.18	0.18	0.05
1241	A	14	H	1	110	112	133.17	4716.2	-1.541	2.90	23.4	1.28	0.23	0.00
1241	A	14	H	1	120	122	133.27	4718.5	-1.557	3.26	24.9	1.18	0.19	0.22
1241	A	14	H	1	130	132	133.37	4720.8	-1.374	2.95	23.6	1.19	0.19	0.09
1241	A	14	H	1	140	142	133.47	4723.1	-1.410	3.04	24.0	1.21	0.19	0.10
1241	A	14	H	2	0	2	133.58	4725.6	-1.183	3.05	24.1	1.21	0.17	0.08
1241	A	14	H	2	10	12	133.68	4727.9	-1.480	2.98	23.7	1.30	0.26	0.04
1241	A	14	H	2	20	22	133.78	4730.2	-1.421	2.77	22.8	1.15	0.14	0.00
1241	A	14	H	2	30	32	133.88	4732.5	-1.225	2.94	23.5	1.17	0.18	0.12
1241	A	14	H	2	40	42	133.98	4734.8	-1.341	3.32	25.2	1.16	0.19	0.05
1241	A	14	H	2	50	52	134.08	4737.1	-1.569	3.15	24.5	1.18	0.22	0.05
1241	A	14	H	2	60	62	134.18	4739.4	-1.623	3.32	25.2	1.31	0.29	0.07
1241	A	14	H	2	70	72	134.28	4741.7	-1.432	3.14	24.4	1.18	0.17	0.06
1241	A	14	H	2	80	82	134.38	4744.0	-1.153	3.17	24.5	1.21	0.16	0.20
1241	A	14	H	2	90	92	134.48	4746.2	-1.477	3.10	24.2	1.21	0.19	0.12
1241	A	14	H	2	100	102	134.58	4748.5	-1.405	3.06	24.1	1.16	0.17	0.09
1241	A	14	H	2	110	112	134.68	4750.8	-1.417	2.99	23.8	1.17	0.18	0.14
1241	A	14	H	2	120	122	134.78	4753.1	-1.496	2.98	23.7	1.17	0.18	0.11
1241	A	14	H	2	130	132	134.88	4755.4	-1.579	3.37	25.4	1.21	0.18	0.07
1241	A	14	H	2	140	142	134.98	4757.7	-1.285	3.18	24.6	1.19	0.18	0.12
1241	A	14	H	3	0	2	135.09	4760.2	-1.733	3.14	24.4	1.20	0.18	0.13
1241	A	14	H	3	10	12	135.19	4762.5	-1.170	3.31	25.1	1.19	0.17	0.04
1241	A	14	H	3	20	22	135.29	4764.8	-1.604	3.10	24.3	1.20	0.20	0.06
1241	A	14	H	3	30	32	135.39	4767.1	-1.431	3.10	24.2	1.20	0.19	0.10
1241	A	14	H	3	40	42	135.49	4769.4	-1.681	3.39	25.4	1.23	0.20	0.18
1241	A	14	H	3	50	52	135.59	4771.7	-1.703	3.16	24.5	1.22	0.17	0.10
1241	A	14	H	3	60	62	135.69	4774.0	-1.298	2.90	23.4	1.22	0.18	0.11
1241	A	14	H	3	70	72	135.79	4776.8	-1.414	3.38	25.4	1.22	0.21	0.16
1241	A	14	H	3	80	82	135.89	4779.5	-1.728	2.88	23.3	1.20	0.21	0.23
1241	A	14	H	3	90	92	135.99	4782.3	-1.423	3.08	24.2	1.28	0.20	0.00
1241	A	14	H	3	100	102	136.09	4785.1	-1.328					
1241	A	14	H	3	110	112	136.19	4787.9	-1.337	2.98	23.7	1.24	0.14	0.00
1241	A	14	H	3	120	122	136.29	4790.6	-1.435					
1241	A	14	H	3	130	132	136.39	4793.4	-1.501	3.03	24.0	1.21	0.22	0.02
1241	A	14	H	3	140	142	136.49	4796.2	-1.548					
1241	A	14	H	4	0	2	136.60	4799.2	-1.526	2.89	23.3	1.24	0.19	0.01
1241	A	14	H	4	10	12	136.70	4802.0	-1.531					
1241	A	14	H	4	20	22	136.80	4804.8	-1.504	3.22	24.7	1.25	0.21	0.00
1241	A	14	H	4	30	32	136.90	4807.6	-1.581					
1241	A	14	H	4	40	42	137.00	4810.4	-1.243	3.08	24.2	1.25	0.20	0.00
1241	A	14	H	4	50	52	137.10	4813.1	-1.541					
1241	A	14	H	4	60	62	137.20	4815.9	-1.504	3.19	24.6	1.26	0.24	0.00
1241	A	14	H	4	70	72	137.30	4818.7	-1.544					
1241	A	14	H	4	80	82	137.40	4821.5	-1.266	2.91	23.4	1.21	0.20	0.05
1241	A	14	H	4	90	92	137.50	4824.2	-1.366					
1241	A	14	H	4	100	102	137.60	4827.0	-1.330	2.95	23.6	1.22	0.16	0.01
1241	A	14	H	4	110	112	137.70	4829.8	-1.478					
1241	A	14	H	4	120	122	137.80	4832.5	-1.332	3.06	24.1	1.24	0.19	0.06
1241	A	14	H	4	130	132	137.90	4835.3	-1.425					
1241	A	14	H	4	140	142	138.00	4838.1	-1.311	3.16	24.5	1.26	0.17	0.07
1241	A	14	H	5	0	2	138.11	4841.1	-1.190					
1241	A	14	H	5	10	12	138.21	4843.9	-1.319	2.90	23.4	1.24	0.18	0.04

Appendix C (continued)

Site	Hole	Core	T	Sec.	Top (cm)	Bot (cm)	Depth (corr. msbf)	Age (ka)	$\delta^{18}O_{G.\ Sacculifer}$ (‰)	Mg/Ca (mmol/mol)	Temperature (°C)	Sr/Ca (mmol/mol)	Mn/Ca (mmol/mol)	Fe/Ca (mmol/mol)
1241	A	14	H	5	20	22	138.31	4846.7	-1.249					
1241	A	14	H	5	30	32	138.41	4849.5	-1.229	3.09	24.2	1.26	0.19	0.00
1241	A	14	H	5	40	42	138.51	4852.2	-1.575					
1241	A	14	H	5	50	52	138.61	4855.0	-1.553	3.16	24.5	1.27	0.19	0.03
1241	A	14	H	5	60	62	138.71	4857.8	-1.575					
1241	A	14	H	5	70	72	138.81	4860.6	-1.290	3.27	24.9	1.21	0.06	0.08
1241	A	14	H	5	80	82	138.91	4863.4	-1.393					
1241	A	14	H	5	90	92	139.01	4866.1	-1.466	3.38	25.4	1.24	0.15	0.03
1241	A	14	H	5	100	102	139.11	4868.9	-1.848					
1241	A	14	H	5	110	112	139.21	4871.7	-1.451	3.39	25.4	1.25	0.18	0.06
1241	A	14	H	5	120	122	139.31	4874.5	-1.326					
1241	A	14	H	5	130	132	139.41	4877.2	-1.526	3.58	26.2	1.26	0.18	0.06
1241	A	14	H	5	140	142	139.51	4880.0	-1.329					
1241	A	14	H	6	0	2	139.62	4882.7	-1.474	3.38	25.4	1.24	0.17	0.03
1241	A	14	H	6	10	12	139.72	4885.2	-1.243					
1241	A	14	H	6	20	22	139.82	4887.7	-1.288	3.09	24.2	1.25	0.13	0.05
1241	A	14	H	6	30	32	139.92	4890.1	-1.094	2.89	23.3	1.26	0.15	0.02
1241	A	14	H	6	40	42	140.02	4892.6	-1.251	2.89	23.3	1.26	0.14	0.02
1241	A	14	H	6	50	52	140.12	4895.1	-0.987					
1241	A	14	H	6	60	62	140.22	4897.6	-1.091	2.96	23.6	1.26	0.16	0.00
1241	A	14	H	6	70	72	140.32	4900.0	-1.110					
1241	B	14	H	2	110	112	140.38	4901.5	-1.177					
1241	B	14	H	2	120	122	140.48	4904.0	-1.500	3.36	25.3	1.17	0.03	0.00
1241	B	14	H	2	130	132	140.58	4906.5	-1.361					
1241	B	14	H	2	140	142	140.68	4909.0	-1.504	3.50	25.9	1.24	0.18	0.00
1241	B	14	H	3	0	2	140.79	4911.7	-1.274					
1241	B	14	H	3	10	12	140.89	4914.1	-1.195	3.59	26.2	1.24	0.17	0.09
1241	B	14	H	3	20	22	140.99	4916.6	-1.367					
1241	B	14	H	3	30	32	141.09	4919.1	-1.622	3.32	25.2	1.23	0.16	0.06
1241	B	14	H	3	40	42	141.19	4921.6	-1.398					
1241	B	14	H	3	50	52	141.29	4924.0	-1.503	3.36	25.3	1.26	0.16	0.03
1241	B	14	H	3	60	62	141.39	4926.5	-1.520					
1241	B	14	H	3	70	72	141.49	4929.0	-1.409	3.32	25.2	1.26	0.14	0.04
1241	B	14	H	3	80	82	141.59	4931.5	-1.340					
1241	B	14	H	3	90	92	141.69	4934.0	-1.234	3.14	24.4	1.22	0.16	0.06
1241	B	14	H	3	100	102	141.79	4936.4	-1.424					
1241	B	14	H	3	110	112	141.89	4938.9	-1.124	3.09	24.2	1.24	0.14	0.03
1241	B	14	H	3	120	122	141.99	4941.4	-1.319					
1241	B	14	H	3	130	132	142.09	4943.9	-1.480	3.22	24.7	1.27	0.16	0.00
1241	B	14	H	3	140	142	142.19	4946.3	-1.446					
1241	B	14	H	4	0	2	142.30	4949.0	-1.435	3.33	25.2	1.30	0.16	0.02
1241	B	14	H	4	10	12	142.40	4951.5	-1.708					
1241	B	14	H	4	20	22	142.50	4954.0	-1.606	3.29	25.1	1.25	0.16	0.00
1241	B	14	H	4	30	32	142.60	4956.3	-1.449					
1241	B	14	H	4	40	42	142.70	4958.6	-1.647	3.51	25.9	1.25	0.15	0.02
1241	B	14	H	4	50	52	142.80	4960.9	-1.431					
1241	B	14	H	4	60	62	142.90	4963.2	-1.569	3.29	25.0	1.25	0.15	0.00
1241	B	14	H	4	70	72	143.00	4965.6	-1.007	3.44	25.6	1.28	0.18	0.06
1241	B	14	H	4	80	82	143.10	4967.9	-1.351	3.18	24.6	1.29	0.15	0.00
1241	B	14	H	4	90	92	143.20	4970.2	-1.409					
1241	B	14	H	4	100	102	143.30	4972.5	-1.291	3.05	24.0	1.24	0.17	0.00
1241	B	14	H	4	110	112	143.40	4974.8	-1.660					
1241	B	14	H	4	120	122	143.50	4977.1	-1.353	3.46	25.7	1.28	0.17	0.02
1241	B	14	H	4	130	132	143.60	4979.4	-1.772					
1241	B	14	H	4	140	142	143.70	4981.7	-1.431	3.29	25.1	1.25	0.18	0.13
1241	B	14	H	5	0	2	143.81	4984.3	-1.689					
1241	B	14	H	5	10	12	143.91	4986.6	-1.830	3.01	23.9	1.24	0.17	0.06
1241	B	14	H	5	20	22	144.01	4988.9	-1.442					
1241	B	14	H	5	30	32	144.11	4991.2	-1.771	3.28	25.0	1.28	0.17	0.01
1241	B	14	H	5	40	42	144.21	4993.5	-1.464					
1241	B	14	H	5	50	52	144.31	4995.8	-1.311	3.17	24.5	1.27	0.17	0.06
1241	B	14	H	5	60	62	144.41	4998.1	-1.478					
1241	B	14	H	5	70	72	144.51	5000.5	-1.722	3.04	24.0	1.23	0.16	0.00
1241	B	14	H	5	80	82	144.61	5002.8	-1.665					
1241	B	14	H	5	90	92	144.71	5005.1	-1.725	3.39	25.4	1.26	0.17	0.04
1241	B	14	H	5	100	102	144.81	5007.4	-1.460					
1241	B	14	H	5	110	112	144.91	5009.7	-1.710	3.33	25.2	1.26	0.17	0.00
1241	B	14	H	5	120	122	145.01	5012.0	-1.322					
1241	B	14	H	5	130	132	145.11	5014.3		3.34	25.2	1.26	0.15	0.09

Appendix C (continued)

Site	Hole	Core	T	Sec.	Top (cm)	Bot (cm)	Depth (corr. msbf)	Age (ka)	$\delta^{18}O_{G.\ Sacculifer}$ (‰)	Mg/Ca (mmol/mol)	Temperature (°C)	Sr/Ca (mmol/mol)	Mn/Ca (mmol/mol)	Fe/Ca (mmol/mol)
1241	A	15	H	3	0	2	145.14	5015.0		3.23	24.8	1.25	0.12	0.10
1241	A	15	H	3	10	12	145.24	5017.3	-1.933					
1241	A	15	H	3	20	22	145.34	5019.6	-1.916	3.48	25.8	1.28	0.15	0.07
1241	A	15	H	3	30	32	145.44	5022.0	-1.277					
1241	A	15	H	3	40	42	145.54	5024.3	-1.859	3.39	25.4	1.24	0.18	0.06
1241	A	15	H	3	50	52	145.64	5026.6	-1.738					
1241	A	15	H	3	60	62	145.74	5028.9	-1.703	3.52	25.9	1.24	0.18	0.09
1241	A	15	H	3	70	72	145.84	5031.2	-1.821					
1241	A	15	H	3	80	82	145.94	5033.5	-1.116	3.61	26.3	1.24	0.15	0.03
1241	A	15	H	3	90	92	146.04	5035.8	-1.580					
1241	A	15	H	3	100	102	146.14	5038.1	-1.803	3.59	26.2	1.27	0.15	0.02
1241	A	15	H	3	110	112	146.24	5040.4	-1.787					
1241	A	15	H	3	120	122	146.34	5042.7	-1.484	3.58	26.1	1.26	0.16	0.02
1241	A	15	H	3	130	132	146.44	5045.1	-1.777					
1241	A	15	H	3	140	142	146.54	5047.4	-2.091	3.80	26.9	1.27	0.16	0.04
1241	A	15	H	4	0	2	146.65	5049.9	-1.781					
1241	A	15	H	4	10	12	146.75	5052.2	-1.763	3.58	26.1	1.27	0.17	0.00
1241	A	15	H	4	20	22	146.85	5054.5	-1.426					
1241	A	15	H	4	30	32	146.95	5056.8	-1.196	3.65	26.4	1.31	0.20	0.06
1241	A	15	H	4	40	42	147.05	5059.0	-1.173					
1241	A	15	H	4	50	52	147.15	5061.0	-1.826	3.39	25.4	1.29	0.15	0.00
1241	A	15	H	4	60	62	147.25	5063.1	-1.768	3.22	24.7	1.26	0.14	0.06
1241	A	15	H	4	70	72	147.35	5065.1	-1.185	3.45	25.7	1.27	0.15	0.04
1241	A	15	H	4	80	82	147.45	5067.2						
1241	A	15	H	4	90	92	147.55	5069.2		3.65	26.4	1.28	0.17	0.06
1241	A	15	H	4	100	102	147.65	5071.2	-1.681					
1241	A	15	H	4	110	112	147.75	5073.3	-1.719	3.37	25.4	1.25	0.16	0.10
1241	A	15	H	4	120	122	147.85	5075.3	-1.542					
1241	A	15	H	4	130	132	147.95	5077.3	-1.531	3.20	24.7	1.21	0.14	0.02
1241	A	15	H	4	140	142	148.05	5079.4	-1.594					
1241	A	15	H	5	0	2	148.16	5081.6	-1.576	3.33	25.2	1.27	0.15	0.08
1241	A	15	H	5	10	12	148.26	5083.6	-1.651					
1241	A	15	H	5	20	22	148.36	5085.7	-1.877	3.59	26.2	1.29	0.17	0.00
1241	A	15	H	5	30	32	148.46	5087.7	-1.501					
1241	A	15	H	5	40	42	148.56	5089.8	-1.531	3.35	25.3	1.28	0.17	0.10
1241	A	15	H	5	50	52	148.66	5091.8	-1.465					
1241	A	15	H	5	60	62	148.76	5093.8	-1.556	3.39	25.4	1.28	0.15	0.03
1241	A	15	H	5	70	72	148.86	5095.9	-1.161					
1241	A	15	H	5	80	82	148.96	5097.9	-1.507	3.19	24.6	1.28	0.17	0.05
1241	A	15	H	5	93	95	149.09	5100.5	-1.341					
1241	A	15	H	5	100	102	149.16	5102.0	-1.018	3.10	24.2	1.27	0.16	0.07
1241	A	15	H	5	110	112	149.26	5104.0	-1.255					
1241	A	15	H	5	120	122	149.36	5106.0	-1.295	3.08	24.2	1.26	0.15	0.04
1241	A	15	H	5	130	132	149.46	5108.0	-1.568					
1241	A	15	H	5	140	142	149.56	5110.1	-1.555	3.20	24.7	1.27	0.14	0.05
1241	A	15	H	6	0	2	149.67	5112.3	-1.499					
1241	A	15	H	6	10	12	149.77	5114.3	-1.171	3.26	24.9	1.28	0.16	0.04
1241	A	15	H	6	20	22	149.87	5116.3	-1.497					
1241	A	15	H	6	30	32	149.97	5118.4		3.38	25.4	1.26	0.18	0.01
1241	A	15	H	6	40	42	150.07	5120.4	-1.717					
1241	A	15	H	6	50	52	150.17	5122.4	-1.682	3.69	26.6	1.28	0.17	0.05
1241	A	15	H	6	60	62	150.27	5124.4	-1.777					
1241	A	15	H	6	70	72	150.37	5126.5	-1.567	3.45	25.7	1.29	0.19	0.03
1241	A	15	H	6	80	82	150.47	5128.5	-1.579					
1241	A	15	H	6	90	92	150.57	5130.5	-1.544	3.52	25.9	1.28	0.18	0.08
1241	A	15	H	6	100	102	150.67	5132.5	-1.340					
1241	A	15	H	6	110	112	150.77	5134.5	-1.415	3.46	25.7	1.27	0.18	0.06
1241	A	15	H	6	120	122	150.87	5136.6	-1.585					
1241	C	11	H	2	90	92	150.97	5138.6	-1.872	3.44	25.6	1.26	0.18	0.03
1241	C	11	H	2	100	102	151.07	5140.6	-1.628					
1241	C	11	H	2	110	112	151.17	5142.6	-1.701	3.45	25.7	1.27	0.17	0.05
1241	C	11	H	2	120	122	151.27	5144.7	-1.468					
1241	C	11	H	2	130	132	151.37	5146.7	-1.421	3.24	24.9	1.27	0.17	0.04
1241	C	11	H	2	140	142	151.47	5148.7	-1.768					
1241	C	11	H	3	0	2	151.57	5150.7	-1.466	3.48	25.8	1.30	0.18	0.00
1241	C	11	H	3	10	12	151.67	5152.8	-1.581					
1241	C	11	H	3	20	22	151.77	5154.8	-1.175	3.22	24.8	1.24	0.14	0.01
1241	C	11	H	3	30	32	151.87	5156.8	-1.830					
1241	C	11	H	3	40	42	151.97	5158.8	-1.528	3.28	25.0	1.24	0.15	0.08

Appendix C (continued)

Site	Hole	Core	T	Sec.	Top (cm)	Bot (cm)	Depth (corr. msbf)	Age (ka)	$\delta^{18}O_{G.\ Sacculifer}$ (‰)	Mg/Ca (mmol/mol)	Temperature (°C)	Sr/Ca (mmol/mol)	Mn/Ca (mmol/mol)	Fe/Ca (mmol/mol)
1241	C	11	H	3	50	52	152.07	5160.9	-1.645					
1241	C	11	H	3	60	62	152.17	5162.9	-1.513	3.75	26.7	1.28	0.16	0.06
1241	C	11	H	3	70	72	152.27	5164.9	-1.865					
1241	C	11	H	3	80	82	152.37	5166.9	-0.917	3.60	26.2	1.30	0.19	0.04
1241	C	11	H	3	90	92	152.47	5169.0	-1.379					
1241	C	11	H	3	100	102	152.57	5171.0	-1.562	3.34	25.2	1.29	0.16	0.02
1241	C	11	H	3	110	112	152.67	5173.0	-1.549					
1241	C	11	H	3	120	122	152.77	5175.7	-1.202					
1241	C	11	H	3	130	132	152.87	5178.4	-1.390					
1241	C	11	H	3	140	142	152.97	5181.0	-1.589	3.14	24.4	1.28	0.15	0.07
1241	C	11	H	4	0	2	153.07	5183.7	-1.678					
1241	C	11	H	4	10	12	153.17	5186.4	-1.649	3.35	25.3	1.27	0.15	0.03
1241	C	11	H	4	20	22	153.27	5189.1	-1.078					
1241	C	11	H	4	30	32	153.37	5191.7	-1.137					
1241	C	11	H	4	40	42	153.47	5194.4	-1.577					
1241	C	11	H	4	50	52	153.57	5197.1	-0.990	2.97	23.7	1.23	0.13	0.00
1241	C	11	H	4	60	62	153.67	5199.8	-0.930					
1241	C	11	H	4	70	72	153.77	5202.4	-0.994	3.21	24.7	1.24	0.15	0.00
1241	C	11	H	4	80	82	153.87	5205.1	-1.289					
1241	C	11	H	4	90	92	153.97	5207.8	-1.496	3.33	25.2	1.26	0.17	0.03
1241	C	11	H	4	100	102	154.07	5210.5	-1.344					
1241	C	11	H	4	110	112	154.17	5213.1	-1.406	3.45	25.7	1.27	0.18	0.04
1241	C	11	H	4	120	122	154.27	5215.8	-1.366					
1241	C	11	H	4	130	132	154.37	5218.5	-1.228	3.43	25.6	1.26	0.17	0.03
1241	C	11	H	4	140	142	154.47	5221.2	-1.280					
1241	C	11	H	5	0	2	154.57	5223.9	-1.421	3.24	24.8	1.25	0.17	0.05
1241	C	11	H	5	10	12	154.67	5226.5	-1.265					
1241	C	11	H	5	20	22	154.77	5229.2	-1.162	3.18	24.6	1.24	0.17	0.07
1241	C	11	H	5	30	32	154.87	5231.9	-1.315					
1241	C	11	H	5	40	42	154.97	5234.6	-1.489	3.56	26.1	1.27	0.18	0.00
1241	C	11	H	5	50	52	155.07	5237.2	-1.395					
1241	C	11	H	5	60	62	155.17	5239.9	-1.701	3.62	26.3	1.27	0.20	0.01
1241	C	11	H	5	70	72	155.27	5242.6	-1.516					
1241	C	11	H	5	80	82	155.37	5245.3	-1.559	3.60	26.2	1.28	0.19	0.00
1241	C	11	H	5	90	92	155.47	5248.0	-1.291					
1241	C	11	H	5	100	102	155.57	5250.6	-1.367	3.51	25.9	1.28	0.19	0.03
1241	C	11	H	5	110	112	155.67	5253.3	-1.524					
1241	C	11	H	5	120	122	155.77	5256.0	-1.549	3.62	26.3	1.30	0.20	0.04
1241	C	11	H	5	130	132	155.87	5258.6	-1.387					
1241	C	11	H	5	140	142	155.97	5261.3	-1.397	3.35	25.3	1.30	0.19	0.02
1241	C	11	H	6	0	2	156.08	5264.3	-1.247					
1241	C	11	H	6	10	12	156.18	5267.0	-1.469	3.44	25.6	1.28	0.18	0.06
1241	C	11	H	6	20	22	156.28	5269.6	-1.960					
1241	C	11	H	6	30	32	156.38	5272.3	-1.727	3.32	25.2	1.25	0.18	0.04
1241	C	11	H	6	40	42	156.48	5275.0	-1.790					
1241	C	11	H	6	50	52	156.58	5277.7	-1.714	3.60	26.2	1.26	0.19	0.01
1241	C	11	H	6	60	62	156.68	5280.3	-1.201					
1241	C	11	H	6	70	72	156.78	5283.0	-1.596	3.69	26.6	1.29	0.19	0.09
1241	C	11	H	6	80	82	156.88	5285.7	-1.541					
1241	C	11	H	6	90	92	156.98	5288.4	-1.952	3.91	27.3	1.31	0.19	0.03
1241	C	11	H	6	100	102	157.08	5291.0	-1.338					
1241	C	11	H	6	110	112	157.18	5293.7	-1.364	3.52	25.9	1.23	0.18	0.02
1241	C	11	H	6	120	122	157.28	5296.4	-1.562					
1241	C	11	H	6	130	132	157.38	5299.1	-1.271	3.16	24.5	1.25	0.16	0.03
1241	C	11	H	6	140	142	157.48	5301.8	-1.294					
1241	C	11	H	7	0	2	157.58	5304.4	-1.444	3.28	25.0	1.24	0.18	0.04
1241	C	11	H	7	10	12	157.68	5307.1	-1.673					
1241	C	11	H	7	20	22	157.78	5310.0	-1.802	3.60	26.2	1.29	0.18	0.05
1241	A	16	H	4	80	82	157.86	5312.3	-1.714					
1241	A	16	H	4	90	92	157.96	5315.2	-1.672	3.58	26.1	1.29	0.23	0.00
1241	A	16	H	4	100	102	158.06	5318.1	-1.601					
1241	A	16	H	4	110	112	158.16	5321.0	-1.548	3.43	25.6	1.26	0.19	0.08
1241	A	16	H	4	120	122	158.26	5324.0	-1.637					
1241	A	16	H	4	130	132	158.36	5326.9	-1.569	3.25	24.9	1.26	0.20	0.00
1241	A	16	H	4	140	142	158.46	5329.8	-1.522					
1241	A	16	H	5	0	2	158.57	5333.0	-1.169	3.45	25.7	1.28	0.21	0.02
1241	A	16	H	5	10	12	158.67	5335.9	-1.748					
1241	A	16	H	5	20	22	158.77	5338.8	-1.783	3.75	26.7	1.29	0.19	0.02
1241	A	16	H	5	30	32	158.87	5341.7	-1.610					

Appendix C (continued)

Site	Hole	Core	T	Sec.	Top (cm)	Bot (cm)	Depth (corr. msbf)	Age (ka)	$\delta^{18}O_{G.\ Sacculifer}$ (‰)	Mg/Ca (mmol/mol)	Temperature (°C)	Sr/Ca (mmol/mol)	Mn/Ca (mmol/mol)	Fe/Ca (mmol/mol)
1241	A	16	H	5	40	42	158.97	5344.6	-1.320	3.27	24.9	1.28	0.20	0.05
1241	A	16	H	5	50	52	159.07	5347.5	-1.662					
1241	A	16	H	5	60	62	159.17	5350.2	-1.645	3.37	25.4	1.29	0.20	0.00
1241	A	16	H	5	70	72	159.27	5352.9	-1.570					
1241	A	16	H	5	80	82	159.37	5355.5	-1.691	3.54	26.0	1.28	0.19	0.03
1241	A	16	H	5	90	92	159.47	5358.2	-1.708					
1241	A	16	H	5	100	102	159.57	5360.9	-1.867	3.65	26.4	1.28	0.20	0.03
1241	A	16	H	5	110	112	159.67	5363.6	-1.195					
1241	A	16	H	5	120	122	159.77	5366.2	-1.610	3.24	24.9	1.28	0.21	0.00
1241	A	16	H	5	130	132	159.87	5368.9	-1.396					
1241	A	16	H	5	140	142	159.97	5371.6	-1.667	3.73	26.7	1.30	0.21	0.06
1241	A	16	H	6	0	2	160.08	5374.5	-1.121					
1241	A	16	H	6	10	12	160.18	5377.2	-1.426	2.95	23.6	1.26	0.15	0.02
1241	A	16	H	6	20	22	160.28	5379.9	-1.340					
1241	A	16	H	6	30	32	160.38	5382.6	-1.141	3.35	25.3	1.29	0.22	0.02
1241	A	16	H	6	40	42	160.48	5385.3	-1.288					
1241	A	16	H	6	50	52	160.58	5387.9	-1.042	2.98	23.7	1.29	0.19	0.01
1241	A	16	H	6	60	62	160.68	5390.6	-1.359					
1241	A	16	H	6	70	72	160.78	5393.3	-1.281	3.12	24.3	1.27	0.20	0.11
1241	A	16	H	6	80	82	160.88	5396.0	-1.208					
1241	A	16	H	6	90	92	160.98	5398.6	-1.576					
1241	B	16	H	2	30	32	161.03	5400.0	-1.268					
1241	B	16	H	2	45	47	161.18	5404.0	-1.345	3.15	24.5	1.24	0.19	0.05
1241	B	16	H	2	60	62	161.33	5408.1	-1.903					
1241	B	16	H	2	75	77	161.48	5412.1	-1.585	3.62	26.3	1.27	0.18	0.06
1241	B	16	H	2	90	92	161.63	5416.2	-1.531					
1241	B	16	H	2	105	107	161.78	5420.3	-1.395					
1241	B	16	H	2	120	122	161.93	5424.3	-1.434	3.17	24.6	1.29	0.18	0.03
1241	B	16	H	2	135	137	162.08	5428.4	-1.653	3.48	25.8	1.27	0.19	0.03
1241	B	16	H	3	0	2	162.24	5432.7	-1.421					
1241	B	16	H	3	15	17	162.39	5436.8	-1.283	3.33	25.2	1.28	0.21	0.07
1241	B	16	H	3	30	32	162.54	5440.9	-1.181					
1241	B	16	H	3	45	47	162.69	5444.9	-1.378	3.30	25.1	1.28	0.20	0.03
1241	B	16	H	3	60	62	162.84	5449.0	-1.455					
1241	B	16	H	3	75	77	162.99	5452.5	-1.627	4.04	27.8	1.31	0.19	0.03
1241	B	16	H	3	90	92	163.14	5455.9	-1.113					
1241	B	16	H	3	105	107	163.29	5459.4	-1.269	3.62	26.3	1.29	0.18	0.02
1241	B	16	H	3	120	122	163.44	5462.8	-1.231					
1241	B	16	H	3	135	137	163.59	5466.3	-1.257	3.61	26.3	1.27	0.20	0.02
1241	B	16	H	4	0	2	163.75	5470.0	-1.363					
1241	B	16	H	4	15	17	163.90	5473.4	-1.601	3.52	25.9	1.29	0.21	0.13
1241	B	16	H	4	30	32	164.05	5476.9	-1.095					
1241	B	16	H	4	45	47	164.20	5480.3	-1.321					
1241	B	16	H	4	60	62	164.35	5483.8	-1.433	3.44	25.6	1.26	0.19	0.02
1241	B	16	H	4	75	77	164.50	5487.3	-1.069					
1241	B	16	H	4	90	92	164.65	5490.7	-1.241					
1241	B	16	H	4	105	107	164.80	5494.2	-1.348	3.40	25.4	1.24	0.19	0.12
1241	B	16	H	4	120	122	164.95	5497.6	-1.285					
1241	B	16	H	4	135	137	165.10	5501.1	-1.228	3.69	26.5	1.25	0.20	0.21
1241	B	16	H	5	0	2	165.25	5504.5	-1.358					
1241	B	16	H	5	15	17	165.40	5508.0	-1.371	3.27	25.0	1.26	0.18	0.06
1241	B	16	H	5	30	32	165.55	5511.3	-1.337					
1241	B	16	H	5	45	47	165.70	5514.6	-1.253	3.26	24.9	1.25	0.18	0.00
1241	B	16	H	5	60	62	165.85	5518.0	-1.649					
1241	B	16	H	5	75	77	166.00	5521.3	-1.388	3.96	27.5	1.26	0.16	0.01
1241	B	16	H	5	90	92	166.15	5524.6	-1.288					
1241	B	16	H	5	105	107	166.30	5528.0	-1.110	3.24	24.9	1.25	0.17	0.05
1241	B	16	H	5	120	122	166.45	5531.3	-1.276					
1241	B	16	H	5	135	137	166.60	5534.6	-1.380	3.52	25.9	1.25	0.19	0.04
1241	B	16	H	6	0	2	166.74	5537.7	-1.276					
1241	B	16	H	6	15	17	166.89	5541.0	-1.274	3.54	26.0	1.26	0.19	0.05
1241	B	16	H	6	30	32	167.04	5544.4	-1.131					
1241	B	16	H	6	45	47	167.19	5547.7	-1.098	2.92	23.5	1.23	0.15	0.06
1241	B	16	H	6	60	62	167.34	5551.0	-0.837					
1241	A	17	H	4	30	32	167.43	5553.0	-1.125	3.07	24.1	1.26	0.16	0.15
1241	A	17	H	4	45	47	167.58	5556.4	-0.781					
1241	A	17	H	4	60	62	167.73	5559.7	-1.485	3.65	26.4	1.26	0.21	0.04
1241	A	17	H	4	75	77	167.88	5563.1	-1.112					
1241	A	17	H	4	90	92	168.03	5566.4	-1.116	3.49	25.8	1.23	0.19	0.02

Appendix D Correction of Mg/Ca of Site 1000 (<4.5 Ma) for the influence of salinity.

Age (ka)	$\delta^{18}O_{G.\ Sacculifer}$ (‰)	Mg/Ca (mmol/mol)	$\delta^{18}O$_Temp-corr (‰)	Salinity change	Δ(Mg/Ca) (7%/1 sal.unit)	Mg/Ca_corr (mmol/mol)	Temp_corr (°C)
3894.3	-0.622	5.78	-0.31	2.66	18.6	4.70	29.7
3897.0	-1.371	5.00	-1.29	0.70	4.9	4.75	29.9
3899.1	-1.242	4.76	-1.12	1.04	7.3	4.41	28.9
3910.3	0.031	6.24	0.52	4.20	29.4	4.40	28.9
3912.6	-0.018	6.66	0.48	4.24	29.6	4.69	29.7
3914.7	-0.384	5.79	0.00	3.28	23.0	4.46	29.0
3916.9	-0.664	5.12	-0.37	2.55	17.8	4.21	28.3
3919.2	-0.885	4.52	-0.65	1.97	13.8	3.90	27.3
3921.3	-0.863	4.40	-0.63	2.03	14.2	3.78	26.9
3923.6	-1.326	4.56	-1.23	0.82	5.7	4.30	28.6
3925.7	-0.909	4.91	-0.69	1.91	13.4	4.26	28.4
3928.1	-0.225	5.65	0.21	3.69	25.9	4.19	28.2
3930.1	-0.309	5.69	0.10	3.48	24.3	4.31	28.6
3932.3	-0.114	6.15	0.35	3.98	27.9	4.43	29.0
3936.7	-0.678	6.02	-0.38	2.51	17.6	4.96	30.4
3939.0	-1.440	5.12	-1.38	0.52	3.7	4.93	30.4
3941.1	-1.528	4.95	-1.49	0.29	2.1	4.85	30.1
3943.5	-1.259	4.30	-1.14	1.00	7.0	4.00	27.6
3945.6	-1.373	5.50	-1.29	0.70	4.9	5.23	31.1
3947.9	-0.432	6.57	-0.06	3.16	22.1	5.12	30.9
3950.0	-0.187	6.87	0.26	3.79	26.6	5.05	30.7
3953.2	-0.564	5.70	-0.24	2.81	19.7	4.58	29.4
3956.0	-0.970	4.39	-0.77	1.75	12.2	3.85	27.1
3959.2	-1.379	5.03	-1.30	0.68	4.8	4.79	30.0
3962.0	-0.934	5.61	-0.72	1.84	12.9	4.89	30.2
3965.2	-0.916	5.41	-0.70	1.89	13.2	4.69	29.7
3968.0	-0.369	6.16	0.02	3.32	23.2	4.73	29.8
3971.2	-0.284	6.33	0.13	3.54	24.8	4.76	29.9
3974.0	-0.185	5.95	0.26	3.80	26.6	4.37	28.8
3977.2	-0.831	5.96	-0.58	2.11	14.8	5.08	30.7
3980.0	-0.535	5.54	-0.20	2.88	20.2	4.42	28.9
3983.2	-0.880	5.29	-0.65	1.99	13.9	4.55	29.3
3986.0	-1.042	5.31	-0.86	1.56	10.9	4.73	29.8
3989.2	-1.242	4.51	-1.12	1.04	7.3	4.18	28.2
3992.0	-0.862	4.35	-0.62	2.03	14.2	3.73	26.7
3995.2	-0.741	4.67	-0.47	2.35	16.4	3.90	27.3
3998.0	-0.617	5.26	-0.30	2.67	18.7	4.28	28.5
4004.0	-0.388	5.72	-0.01	3.27	22.9	4.41	28.9
4006.9	-0.533	6.34	-0.20	2.89	20.2	5.06	30.7
4010.0	-0.626	5.79	-0.32	2.65	18.5	4.72	29.8
4012.9	-0.497	5.20	-0.15	2.98	20.9	4.11	28.0
4016.0	-0.935	4.77	-0.72	1.84	12.9	4.15	28.1
4018.9	-0.662	5.62	-0.36	2.55	17.9	4.62	29.5
4022.1	-0.681	5.58	-0.39	2.50	17.5	4.60	29.5
4029.0	-0.455	5.58	-0.09	3.09	21.7	4.37	28.8
4064.0	-1.166	4.38	-1.02	1.24	8.7	4.00	27.6
4065.9	-0.873	3.85	-0.64	2.00	14.0	3.31	25.1
4069.2	-1.112	3.90	-0.95	1.38	9.7	3.52	25.9
4072.4	-0.801	4.18	-0.54	2.19	15.3	3.54	26.0
4075.4	-0.778	4.04	-0.51	2.25	15.8	3.40	25.5
4078.6	-0.840	4.30	-0.60	2.09	14.6	3.67	26.5
4081.8	-1.226	4.09	-1.10	1.08	7.6	3.78	26.9
4084.8	-0.934	3.96	-0.72	1.84	12.9	3.45	25.7
4088.0	-1.413	4.10	-1.34	0.59	4.2	3.93	27.4
4091.0	-1.056	4.38	-0.88	1.52	10.7	3.91	27.3
4093.7	-0.757	4.27	-0.49	2.31	16.1	3.58	26.1
4096.7	-0.537	4.65	-0.20	2.88	20.2	3.71	26.6
4099.8	-0.364	5.16	0.03	3.33	23.3	3.96	27.5
4102.5	-0.876	5.38	-0.64	1.99	14.0	4.63	29.5
4105.5	-0.565	5.22	-0.24	2.81	19.6	4.19	28.2
4108.5	-1.030	4.48	-0.84	1.59	11.2	3.98	27.5
4111.2	-1.256	4.70	-1.14	1.00	7.0	4.37	28.8
4114.3	-1.168	4.32	-1.02	1.23	8.6	3.95	27.4
4117.3	-1.168	4.82	-1.02	1.23	8.6	4.40	28.9
4120.0	-0.313	4.70	0.09	3.46	24.3	3.56	26.1
4123.5	-0.769	5.63	-0.50	2.27	15.9	4.73	29.8

Appendix D (continued)

Age (ka)	$\delta^{18}O_{G.\ Sacculifer}$ (‰)	Mg/Ca (mmol/mol)	$\delta^{18}O$_Temp-corr (‰)	Salinity change	Δ(Mg/Ca) (7%/1 sal.unit)	Mg/Ca_corr (mmol/mol)	Temp_corr (°C)
4126.6	-0.842	5.22	-0.60	2.08	14.6	4.46	29.0
4130.1	-1.478	4.53	-1.43	0.42	3.0	4.40	28.8
4133.6	-1.565	4.44	-1.54	0.20	1.4	4.38	28.8
4136.8	-1.463	4.22	-1.41	0.46	3.2	4.08	27.9
4140.2	-0.886	4.67	-0.66	1.97	13.8	4.03	27.7
4143.7	-1.079	4.45	-0.91	1.46	10.3	3.99	27.6
4146.9	-0.774	4.96	-0.51	2.26	15.8	4.17	28.2
4150.4	-0.651	4.53	-0.35	2.58	18.1	3.71	26.6
4153.9	-1.179	4.22	-1.04	1.21	8.4	3.86	27.1
4157.0	-1.498	4.21	-1.45	0.37	2.6	4.10	27.9
4161.5	-1.213	4.28	-1.08	1.12	7.8	3.95	27.4
4166.0	-1.137	4.25	-0.98	1.31	9.2	3.86	27.1
4170.1	-1.138	4.39	-0.98	1.31	9.2	3.99	27.6
4174.6	-1.286	4.30	-1.18	0.93	6.5	4.02	27.7
4179.2	-1.460	4.24	-1.41	0.47	3.3	4.10	27.9
4183.2	-1.020	4.55	-0.83	1.62	11.3	4.03	27.7
4187.8	-1.081	4.26	-0.91	1.46	10.2	3.82	27.0
4192.3	-0.999	4.16	-0.80	1.67	11.7	3.67	26.5
4196.4	-1.367	4.36	-1.28	0.71	5.0	4.14	28.1
4200.9	-1.194	4.22	-1.06	1.17	8.2	3.88	27.2
4205.0	-1.390	4.10	-1.31	0.65	4.6	3.91	27.3
4209.5	-0.830	4.54	-0.58	2.12	14.8	3.87	27.2
4214.0	-0.989	4.50	-0.79	1.70	11.9	3.96	27.5
4216.6	-1.027	4.39	-0.84	1.60	11.2	3.90	27.3
4221.0	-1.436	4.26	-1.37	0.53	3.7	4.10	27.9
4224.7	-1.209	4.07	-1.08	1.13	7.9	3.75	26.8
4228.1	-1.320	4.17	-1.22	0.84	5.9	3.93	27.4
4231.8	-1.423	4.49	-1.36	0.57	4.0	4.31	28.6
4235.5	-1.205	4.37	-1.07	1.14	8.0	4.02	27.7
4238.8	-0.754	4.57	-0.48	2.31	16.2	3.83	27.0
4242.5	-0.665	4.74	-0.37	2.55	17.8	3.90	27.3
4246.2	-1.330	4.41	-1.23	0.81	5.7	4.16	28.1
4249.6	-1.310	4.54	-1.21	0.86	6.0	4.27	28.5
4253.3	-1.010	4.50	-0.82	1.65	11.5	3.98	27.5
4257.0	-1.434	4.32	-1.37	0.54	3.8	4.16	28.1
4260.3	-1.138	4.39	-0.99	1.31	9.2	3.99	27.6
4264.0	-1.023	4.45	-0.83	1.61	11.3	3.95	27.4
4266.7	-1.060	3.99	-0.88	1.52	10.6	3.57	26.1
4269.2	-1.287	4.09	-1.18	0.92	6.5	3.83	27.0
4272.0	-1.211	4.29	-1.08	1.12	7.9	3.95	27.4
4274.4	-1.308	4.50	-1.21	0.87	6.1	4.23	28.3
4277.2	-1.272	4.30	-1.16	0.96	6.7	4.01	27.6
4279.9	-0.985	5.02	-0.78	1.71	12.0	4.42	28.9
4282.4	-0.896	4.75	-0.67	1.94	13.6	4.10	27.9
4285.1	-1.250	4.99	-1.13	1.02	7.1	4.63	29.5
4287.8	-0.677	4.76	-0.38	2.52	17.6	3.92	27.3
4290.3	-0.954	4.54	-0.74	1.79	12.5	3.97	27.5
4293.0	-1.093	4.27	-0.93	1.43	10.0	3.84	27.1
4295.8	-1.380	4.37	-1.30	0.68	4.8	4.16	28.1
4298.3	-1.406	4.07	-1.33	0.61	4.3	3.90	27.3
4301.0	-1.109	4.68	-0.95	1.39	9.7	4.23	28.3
4303.7	-1.548	4.53	-1.52	0.24	1.7	4.45	29.0
4306.2	-1.641	4.84	-1.64	0.00	0.0	4.84	30.1
4309.0	-1.002	4.63	-0.81	1.67	11.7	4.09	27.9
4311.7	-0.950	4.62	-0.74	1.80	12.6	4.04	27.7
4314.2	-1.417	4.18	-1.35	0.58	4.1	4.01	27.6
4316.9	-1.354	4.24	-1.27	0.75	5.2	4.02	27.7
4319.6	-1.353	4.15	-1.27	0.75	5.3	3.93	27.4
4322.1	-1.563	4.62	-1.54	0.20	1.4	4.55	29.3
4324.8	-1.001	4.77	-0.81	1.67	11.7	4.21	28.3
4327.3	-0.965	4.90	-0.76	1.76	12.3	4.30	28.5
4330.0	-0.947	4.94	-0.74	1.81	12.7	4.31	28.6
4332.8	-1.208	4.49	-1.08	1.13	7.9	4.14	28.0
4335.3	-1.218	3.99	-1.09	1.10	7.7	3.68	26.5
4338.0	-1.379	4.03	-1.30	0.68	4.8	3.84	27.1
4340.4	-1.315	4.41	-1.22	0.85	5.9	4.15	28.1

Appendix D (continued)

Age (ka)	$\delta^{18}O_{G.\ Sacculifer}$ (‰)	Mg/Ca (mmol/mol)	$\delta^{18}O$_Temp-corr (‰)	Salinity change	Δ(Mg/Ca) (7%/1 sal.unit)	Mg/Ca_corr (mmol/mol)	Temp_corr (°C)
4342.6	-0.886	4.34	-0.66	1.97	13.8	3.74	26.7
4345.0	-0.891	4.45	-0.66	1.96	13.7	3.84	27.1
4347.4	-0.916	4.46	-0.70	1.89	13.2	3.87	27.2
4349.6	-0.855	4.19	-0.62	2.05	14.4	3.59	26.2
4352.0	-1.085	4.54	-0.92	1.45	10.2	4.08	27.9
4354.4	-0.891	4.87	-0.66	1.96	13.7	4.20	28.3
4356.6	-0.810	4.26	-0.56	2.17	15.2	3.61	26.3
4359.0	-0.935	4.18	-0.72	1.84	12.9	3.64	26.4
4361.4	-1.454	3.92	-1.40	0.49	3.4	3.79	26.9
4363.1	-1.300	4.05	-1.20	0.89	6.2	3.80	26.9
4365.0	-1.367	4.33	-1.28	0.72	5.0	4.11	28.0
4424.0	-1.512	3.72	-1.47	0.34	2.4	3.63	26.3
4427.3	-1.390	4.15	-1.31	0.65	4.6	3.96	27.5
4430.9	-1.519	4.13	-1.48	0.32	2.2	4.04	27.7
4434.2	-1.371	4.31	-1.29	0.71	4.9	4.10	27.9
4437.8	-1.620	4.03	-1.61	0.05	0.4	4.01	27.7
4441.1	-1.581	3.78	-1.56	0.16	1.1	3.74	26.7
4444.8	-1.417	4.78	-1.35	0.59	4.1	4.58	29.4
4448.0	-1.252	3.99	-1.13	1.01	7.1	3.71	26.6
4451.7	-1.044	3.96	-0.86	1.56	10.9	3.53	26.0
4455.0	-1.302	4.07	-1.20	0.88	6.2	3.82	27.0
4458.6	-0.998	3.74	-0.80	1.68	11.7	3.30	25.1
4461.9	-1.316	3.96	-1.22	0.85	5.9	3.73	26.7
4465.5	-0.984	3.90	-0.78	1.71	12.0	3.43	25.6
4468.8	-1.522	3.95	-1.49	0.31	2.2	3.86	27.2
4472.1	-1.185	3.96	-1.05	1.19	8.3	3.63	26.3
4475.7	-1.092	3.76	-0.93	1.43	10.0	3.38	25.4
4479.0	-0.647	3.93	-0.34	2.59	18.2	3.22	24.7
4481.6	-1.112	3.95	-0.95	1.38	9.7	3.57	26.1
4484.0	-1.365	3.44	-1.28	0.72	5.0	3.27	24.9
4486.6	-1.263	3.46	-1.15	0.99	6.9	3.22	24.8
4488.9	-1.469	3.43	-1.42	0.45	3.1	3.32	25.2
4491.5	-1.375	3.89	-1.29	0.69	4.9	3.70	26.6
4493.9	-1.388	3.76	-1.31	0.66	4.6	3.59	26.2
4496.5	-1.534	3.84	-1.50	0.28	2.0	3.76	26.8
4498.9	-1.068	3.42	-0.89	1.49	10.5	3.06	24.1
4501.5	-1.503	3.91	-1.46	0.36	2.5	3.81	27.0

Appendix E Sea level estimation for the Pliocene and $\delta^{18}O_{water}$ and $\delta^{18}O_{salinity}$ for Site 1241

Age (ka)	Smoothed Benthic $\delta^{18}O$ (‰)	Sea level correction 50 m (‰)	$\delta^{18}O$ *(G. sacc.)* (‰)	SST (Mg/Ca) (°C)	$\delta^{18}O$ (water) (‰)	$\delta^{18}O$ (salinity) (‰)
2446	3.76	0.55	-0.94	21.8	0.44	-0.11
2449	3.69	0.52	-0.95	21.6	0.38	-0.14
2452	3.59	0.47	-1.01	21.6	0.31	-0.17
2455	3.47	0.42	-1.08	22.0	0.32	-0.09
2458	3.24	0.31	-1.19	22.3	0.28	-0.03
2461	3.02	0.22	-1.39	22.5	0.12	-0.09
2464	2.82	0.12	-1.53	23.2	0.14	0.02
2467	2.76	0.09	-1.63	24.1	0.22	0.13
2470	2.89	0.15	-1.80	24.4	0.13	-0.03
2473	3.06	0.23	-1.60	24.1	0.25	0.02
2476	3.25	0.32	-1.33	23.5	0.40	0.08
2479	3.43	0.40	-1.32	22.9	0.27	-0.13
2482	3.54	0.45	-1.26	22.6	0.28	-0.17
2485	3.61	0.48	-0.85	22.9	0.74	0.26
2488	3.57	0.46	-1.02	22.9	0.59	0.12
2491	3.45	0.41	-1.23	22.9	0.38	-0.03
2494	3.34	0.36	-1.15	23.0	0.48	0.12
2497	3.17	0.28	-1.22	23.3	0.47	0.19
2500	3.00	0.20	-1.29	23.9	0.51	0.31
2503	2.87	0.15	-1.37	24.2	0.50	0.35
2506	2.87	0.14	-1.43	24.2	0.44	0.29
2509	2.98	0.19	-1.42	24.2	0.45	0.26
2512	3.13	0.26	-1.40	24.2	0.47	0.21
2515	3.28	0.33	-1.41	24.2	0.47	0.14
2518	3.43	0.40	-1.44	24.2	0.43	0.03
2521	3.55	0.45	-1.40	23.5	0.34	-0.12
2524	3.60	0.48	-1.22	22.8	0.37	-0.11
2527	3.61	0.48	-1.00	22.3	0.48	-0.01
2530	3.60	0.47	-0.84	22.1	0.60	0.12
2533	3.48	0.42	-0.90	22.0	0.50	0.08
2536	3.29	0.34	-1.07	22.2	0.39	0.05
2539	3.09	0.25	-1.36	22.8	0.22	-0.03
2542	2.92	0.17	-1.85	23.4	-0.14	-0.31
2545	2.79	0.11	-1.81	24.1	0.04	-0.07
2548	2.77	0.10	-1.66	24.7	0.34	0.24
2551	2.83	0.13	-1.77	25.3	0.33	0.21
2554	2.95	0.18	-1.87	24.7	0.13	-0.05
2557	3.03	0.22	-1.53	24.1	0.33	0.11
2560	3.08	0.24	-1.48	23.7	0.31	0.06
2563	3.07	0.24	-1.43	23.4	0.27	0.03
2566	3.02	0.21	-1.41	23.3	0.29	0.08
2569	2.95	0.18	-1.42	23.6	0.33	0.14
2572	2.89	0.16	-1.49	23.9	0.31	0.16
2575	2.85	0.14	-1.65	24.1	0.22	0.08
2578	2.81	0.12	-1.69	24.4	0.24	0.12
2581	2.77	0.10	-1.58	24.7	0.41	0.31
2584	2.74	0.09	-1.57	24.9	0.45	0.37
2587	2.77	0.10	-1.62	25.1	0.44	0.34
2590	2.83	0.12	-1.63	25.0	0.41	0.29
2593	2.90	0.16	-1.50	24.5	0.44	0.28
2596	2.99	0.20	-1.19	24.0	0.64	0.44
2599	3.12	0.26	-1.13	23.8	0.67	0.41
2602	3.17	0.28	-1.28	23.8	0.51	0.23
2605	3.13	0.27	-1.49	23.8	0.31	0.05
2608	3.07	0.24	-1.46	23.9	0.35	0.11
2611	3.04	0.22	-1.32	24.3	0.57	0.35
2614	3.00	0.20	-1.29	24.8	0.70	0.50
2617	2.93	0.17	-1.48	24.8	0.52	0.35
2620	2.90	0.16	-1.67	24.3	0.23	0.07
2623	2.94	0.18	-1.37	23.8	0.43	0.25
2626	2.98	0.19	-1.29	23.6	0.46	0.27
2629	2.96	0.19	-1.19	23.5	0.54	0.35
2632	2.98	0.19	-1.16	23.4	0.55	0.36
2635	3.03	0.22	-1.34	23.4	0.36	0.14
2638	3.03	0.22	-1.39	23.4	0.32	0.10

Appendix E (continued)

Age (ka)	Smoothed Benthic $\delta^{18}O$ (‰)	Sea level correction 50 m (‰)	$\delta^{18}O$ *(G. sacc.)* (‰)	SST (Mg/Ca) (°C)	$\delta^{18}O$ (water) (‰)	$\delta^{18}O$ (salinity) (‰)
2641	3.07	0.23	-1.35	23.4	0.35	0.12
2644	3.20	0.29	-1.33	23.4	0.36	0.07
2647	3.34	0.36	-1.36	23.4	0.34	-0.02
2650	3.35	0.36	-1.44	23.6	0.31	-0.06
2653	3.21	0.30	-1.59	23.8	0.20	-0.10
2656	3.04	0.22	-1.70	23.9	0.11	-0.12
2659	2.89	0.15	-1.75	23.8	0.05	-0.10
2662	2.74	0.08	-1.80	23.9	0.01	-0.08
2665	2.68	0.06	-1.93	24.2	-0.05	-0.11
2668	2.83	0.13	-1.57	24.6	0.39	0.26
2671	3.03	0.22	-1.38	24.7	0.60	0.38
2674	3.16	0.28	-1.64	24.2	0.23	-0.05
2677	3.26	0.32	-1.56	23.7	0.22	-0.11
2680	3.34	0.36	-1.35	23.6	0.39	0.03
2683	3.39	0.38	-1.31	23.5	0.42	0.04
2686	3.38	0.38	-1.43	23.6	0.32	-0.06
2689	3.32	0.35	-1.50	24.2	0.38	0.03
2692	3.33	0.36	-1.18	24.8	0.83	0.48
2695	3.33	0.35	-1.20	24.8	0.81	0.46
2698	3.27	0.33	-1.27	24.6	0.68	0.36
2701	3.21	0.30	-1.12	24.4	0.80	0.50
2704	3.19	0.29	-0.97	24.3	0.93	0.64
2707	3.17	0.28	-1.04	24.3	0.85	0.56
2710	3.13	0.26	-1.14	24.0	0.70	0.44
2713	3.13	0.26	-1.10	23.7	0.68	0.42
2716	3.18	0.29	-1.18	23.5	0.56	0.27
2719	3.22	0.30	-1.18	23.4	0.52	0.22
2722	3.22	0.30	-1.04	23.4	0.66	0.36
2725	3.22	0.30	-1.06	23.8	0.73	0.42
2728	3.26	0.32	-1.20	24.2	0.69	0.37
2731	3.24	0.31	-1.33	25.0	0.73	0.41
2734	3.11	0.25	-1.20	25.9	1.04	0.79
2737	2.97	0.19	-1.21	25.8	1.01	0.82
2740	2.83	0.13	-1.48	24.8	0.52	0.40
2743	2.73	0.08	-1.61	24.1	0.24	0.17
2746	2.68	0.06	-1.33	24.2	0.54	0.48
2749	2.72	0.08	-1.42	23.5	0.32	0.24
2752	2.81	0.12	-1.59	23.7	0.19	0.07
2755	2.90	0.16	-1.51	24.2	0.38	0.22
2758	2.91	0.16	-1.43	24.4	0.50	0.33
2761	2.91	0.16	-1.64	23.8	0.17	0.00
2764	2.92	0.17	-1.59	23.6	0.17	0.01
2767	2.93	0.17	-1.46	23.5	0.27	0.10
2770	2.96	0.18	-1.35	23.5	0.38	0.20
2773	2.96	0.19	-1.28	23.7	0.50	0.31
2776	2.93	0.17	-1.12	24.0	0.71	0.54
2779	2.86	0.14	-0.96	24.2	0.92	0.77
2782	2.77	0.10	-0.94	24.4	0.98	0.88
2785	2.72	0.08	-1.35	24.5	0.60	0.52
2788	2.66	0.05	-1.56	24.8	0.44	0.39
2791	2.57	0.01	-1.54	25.0	0.51	0.50
2794	2.59	0.02	-1.47	25.2	0.63	0.61
2797	2.65	0.05	-1.45	25.1	0.62	0.58
2800	2.75	0.09	-1.44	24.8	0.56	0.47
2803	2.91	0.16	-1.42	24.4	0.49	0.33
2806	3.11	0.25	-1.40	23.6	0.35	0.10
2809	3.26	0.32	-1.07	22.9	0.52	0.20
2812	3.29	0.34	-1.12	23.1	0.53	0.20
2815	3.28	0.33	-1.23	23.9	0.58	0.25
2818	3.29	0.34	-1.27	24.4	0.66	0.33
2821	3.22	0.30	-1.41	24.7	0.57	0.27
2824	3.12	0.26	-1.44	24.9	0.59	0.33
2827	3.05	0.23	-1.31	24.8	0.69	0.46
2830	2.97	0.19	-1.21	24.5	0.73	0.54
2833	2.85	0.14	-1.31	24.5	0.63	0.49

Appendix E (continued)

Age (ka)	Smoothed Benthic $\delta^{18}O$ (‰)	Sea level correction 50 m (‰)	$\delta^{18}O$ *(G. sacc.)* (‰)	SST (Mg/Ca) (°C)	$\delta^{18}O$ (water) (‰)	$\delta^{18}O$ (salinity) (‰)
2836	2.76	0.09	-1.62	24.9	0.40	0.31
2839	2.76	0.10	-1.73	25.3	0.37	0.28
2842	2.82	0.12	-1.65	25.1	0.42	0.30
2845	2.88	0.15	-1.61	24.8	0.40	0.24
2848	2.98	0.19	-1.59	24.5	0.34	0.15
2851	3.08	0.24	-1.42	23.9	0.40	0.16
2854	3.14	0.27	-1.25	23.3	0.44	0.18
2857	3.13	0.27	-1.42	23.3	0.27	0.01
2860	3.09	0.24	-1.60	23.6	0.14	-0.10
2863	3.01	0.21	-1.57	23.8	0.23	0.02
2866	2.95	0.18	-1.60	23.8	0.20	0.02
2869	2.90	0.16	-1.50	23.9	0.31	0.15
2872	2.86	0.14	-1.63	23.9	0.20	0.06
2875	2.88	0.15	-1.50	24.0	0.34	0.19
2878	2.90	0.16	-1.20	24.1	0.64	0.48
2881	2.95	0.18	-1.48	24.0	0.35	0.17
2884	3.12	0.26	-1.35	23.9	0.46	0.20
2887	3.22	0.30	-1.45	23.9	0.38	0.07
2890	3.25	0.32	-1.50	24.1	0.35	0.03
2893	3.19	0.29	-1.45	24.2	0.44	0.14
2896	3.05	0.23	-1.49	24.5	0.45	0.23
2899	2.93	0.17	-1.56	24.7	0.43	0.26
2902	2.81	0.12	-1.59	24.4	0.34	0.22
2905	2.81	0.12	-1.66	24.0	0.18	0.06
2908	2.94	0.18	-1.70	23.7	0.07	-0.11
2911	3.00	0.20	-1.49	23.8	0.31	0.10
2914	3.02	0.21	-1.38	24.0	0.45	0.24
2917	2.99	0.20	-1.52	24.0	0.31	0.11
2920	2.97	0.19	-1.57	23.9	0.25	0.06
2923	2.96	0.19	-1.44	23.8	0.35	0.17
2926	2.96	0.19	-1.29	23.4	0.43	0.24
2929	2.94	0.18	-1.26	23.1	0.39	0.21
2932	2.94	0.18	-1.26	23.1	0.39	0.21
2935	2.94	0.18	-1.32	23.2	0.36	0.18
2938	2.89	0.15	-1.48	23.8	0.32	0.16
2941	2.81	0.12	-1.56	24.6	0.39	0.28
2944	2.72	0.08	-1.59	24.8	0.41	0.33
2947	2.56	0.01	-1.50	24.8	0.50	0.49
2950	2.49	-0.03	-1.53	25.0	0.51	0.53
2953	2.45	-0.04	-1.57	25.3	0.54	0.59
2956	2.48	-0.03	-1.56	25.7	0.63	0.66
2959	2.56	0.00	-1.77	26.1	0.50	0.50
2962	2.64	0.04	-1.73	26.3	0.60	0.55
2965	2.70	0.07	-1.54	25.9	0.71	0.64
2968	2.71	0.07	-1.63	25.5	0.53	0.46
2971	2.73	0.08	-1.51	25.3	0.61	0.53
2974	2.88	0.15	-1.50	25.2	0.60	0.45
2977	3.05	0.22	-1.35	25.2	0.74	0.51
2980	3.13	0.26	-1.11	25.2	0.98	0.71
2983	3.13	0.26	-1.17	25.2	0.91	0.65
2986	3.01	0.21	-1.53	25.1	0.55	0.34
2989	2.83	0.13	-1.58	24.8	0.44	0.31
2992	2.68	0.06	-1.48	24.5	0.47	0.41
2995	2.65	0.04	-1.51	24.7	0.48	0.44
2998	2.74	0.08	-1.49	25.1	0.59	0.50
3001	2.87	0.15	-1.40	25.1	0.67	0.53
3004	2.99	0.20	-1.32	24.8	0.68	0.48
3007	3.06	0.23	-1.23	24.5	0.71	0.48
3010	3.04	0.22	-1.10	24.1	0.76	0.53
3013	3.00	0.20	-1.22	23.9	0.60	0.40
3016	2.95	0.18	-1.40	24.4	0.52	0.33
3019	2.93	0.17	-1.40	24.7	0.60	0.42
3022	2.95	0.18	-1.42	24.4	0.51	0.33
3025	2.96	0.19	-1.30	24.0	0.53	0.35
3028	2.95	0.18	-1.38	23.7	0.38	0.20

Appendix E (continued)

Age (ka)	Smoothed Benthic $\delta^{18}O$ (‰)	Sea level correction 50 m (‰)	$\delta^{18}O$ *(G. sacc.)* (‰)	SST (Mg/Ca) (°C)	$\delta^{18}O$ (water) (‰)	$\delta^{18}O$ (salinity) (‰)
3031	2.91	0.16	-1.45	23.4	0.25	0.08
3034	2.84	0.13	-1.45	23.7	0.33	0.20
3037	2.74	0.09	-1.54	24.5	0.40	0.31
3040	2.63	0.04	-1.49	24.9	0.53	0.50
3043	2.61	0.03	-1.41	24.9	0.61	0.59
3046	2.64	0.04	-1.58	24.9	0.45	0.41
3049	2.73	0.08	-1.54	24.9	0.49	0.41
3052	2.85	0.13	-1.58	24.9	0.44	0.30
3055	2.91	0.16	-1.64	24.6	0.33	0.16
3058	2.90	0.16	-1.52	24.4	0.39	0.23
3061	2.84	0.13	-1.48	24.2	0.40	0.27
3064	2.75	0.09	-1.63	24.1	0.23	0.14
3067	2.71	0.07	-1.70	24.0	0.14	0.06
3070	2.67	0.05	-1.87	23.9	-0.06	-0.11
3073	2.70	0.07	-1.84	24.3	0.07	0.00
3076	2.77	0.10	-1.63	25.1	0.44	0.34
3079	2.84	0.13	-1.60	25.4	0.53	0.40
3082	2.83	0.13	-1.70	25.1	0.36	0.23
3085	2.79	0.11	-1.66	24.9	0.36	0.25
3088	2.72	0.08	-1.64	24.9	0.38	0.31
3091	2.66	0.05	-1.77	24.8	0.24	0.19
3094	2.60	0.02	-1.84	24.3	0.05	0.03
3097	2.57	0.01	-1.59	23.8	0.20	0.19
3100	2.60	0.02	-1.52	24.1	0.34	0.32
3103	2.71	0.07	-1.57	24.6	0.40	0.32
3106	2.73	0.08	-1.38	24.6	0.59	0.51
3109	2.72	0.08	-1.43	24.5	0.51	0.44
3112	2.70	0.07	-1.55	25.1	0.51	0.45
3115	2.69	0.06	-1.50	25.3	0.62	0.56
3118	2.66	0.05	-1.69	25.2	0.41	0.36
3121	2.64	0.04	-1.63	25.0	0.42	0.38
3124	2.63	0.04	-1.47	24.8	0.54	0.50
3127	2.65	0.04	-1.70	24.5	0.24	0.20
3130	2.66	0.05	-1.64	24.4	0.28	0.23
3133	2.67	0.06	-1.56	24.6	0.39	0.34
3136	2.70	0.07	-1.40	24.4	0.52	0.45
3139	2.72	0.08	-1.70	24.2	0.17	0.10
3142	2.71	0.07	-1.58	24.6	0.38	0.31
3145	2.67	0.05	-1.69	25.0	0.35	0.30
3148	2.55	0.00	-1.79	24.7	0.19	0.19
3151	2.44	-0.05	-1.89	24.7	0.09	0.14
3154	2.38	-0.08	-2.05	25.4	0.10	0.17
3157	2.33	-0.10	-1.98	25.7	0.21	0.31
3160	2.33	-0.10	-2.05	25.4	0.09	0.19
3163	2.36	-0.09	-2.14	25.0	-0.10	-0.02
3166	2.40	-0.07	-1.93	24.5	0.02	0.08
3169	2.42	-0.06	-1.86	24.7	0.13	0.19
3172	2.41	-0.06	-2.04	24.9	-0.01	0.05
3175	2.44	-0.05	-1.91	24.8	0.10	0.15
3178	2.47	-0.04	-1.85	24.8	0.15	0.18
3181	2.50	-0.02	-1.97	24.8	0.03	0.06
3184	2.55	0.00	-1.95	24.5	0.00	0.00
3187	2.59	0.02	-1.84	24.1	0.03	0.01
3190	2.59	0.02	-1.84	24.1	0.01	-0.01
3193	2.60	0.02	-1.88	24.4	0.03	0.01
3196	2.60	0.02	-1.86	24.6	0.11	0.09
3199	2.56	0.00	-1.69	24.7	0.29	0.29
3202	2.53	-0.01	-1.67	24.8	0.33	0.34
3205	2.52	-0.02	-1.80	24.7	0.19	0.21
3208	2.48	-0.03	-1.96	24.6	0.00	0.03
3211	2.46	-0.04	-1.97	24.5	-0.03	0.01
3214	2.45	-0.04	-1.80	24.5	0.14	0.18
3217	2.48	-0.03	-1.82	24.4	0.11	0.14
3220	2.52	-0.02	-1.75	23.8	0.05	0.07
3223	2.52	-0.02	-1.55	23.1	0.10	0.11

Appendix E (continued)

Age (ka)	Smoothed Benthic $\delta^{18}O$ (‰)	Sea level correction 50 m (‰)	$\delta^{18}O$ *(G. sacc.)* (‰)	SST (Mg/Ca) (°C)	$\delta^{18}O$ (water) (‰)	$\delta^{18}O$ (salinity) (‰)
3226	2.54	0.00	-1.52	23.4	0.18	0.19
3229	2.56	0.00	-1.56	23.9	0.26	0.25
3232	2.53	-0.01	-1.64	24.0	0.20	0.21
3235	2.50	-0.02	-1.68	24.0	0.15	0.17
3238	2.49	-0.03	-1.70	24.2	0.17	0.20
3241	2.50	-0.02	-1.81	24.5	0.12	0.14
3244	2.51	-0.02	-1.89	24.6	0.07	0.09
3247	2.51	-0.02	-1.81	24.6	0.14	0.16
3250	2.54	-0.01	-1.54	24.7	0.43	0.44
3253	2.57	0.01	-1.33	24.9	0.69	0.68
3256	2.60	0.02	-1.53	25.0	0.51	0.49
3259	2.62	0.03	-1.57	24.8	0.44	0.41
3262	2.63	0.03	-1.68	24.8	0.32	0.29
3265	2.62	0.03	-1.77	25.0	0.27	0.24
3268	2.59	0.02	-1.53	25.2	0.56	0.54
3271	2.54	0.00	-1.57	25.2	0.53	0.53
3274	2.53	-0.01	-1.59	25.2	0.51	0.52
3277	2.57	0.01	-1.25	24.8	0.76	0.75
3280	2.64	0.04	-1.10	24.4	0.81	0.77
3283	2.73	0.08	-1.38	24.3	0.53	0.45
3286	2.85	0.13	-1.30	24.5	0.63	0.50
3289	2.93	0.17	-1.20	23.9	0.61	0.44
3292	3.00	0.21	-0.92	23.1	0.71	0.50
3295	3.01	0.21	-0.97	23.2	0.68	0.47
3298	2.98	0.19	-1.00	23.5	0.73	0.54
3301	2.95	0.18	-1.31	23.8	0.48	0.30
3304	2.93	0.17	-1.47	24.0	0.35	0.18
3307	2.86	0.14	-1.60	24.1	0.25	0.11
3310	2.84	0.13	-1.41	24.4	0.51	0.38
3313	2.81	0.12	-1.27	24.8	0.73	0.61
3316	2.76	0.10	-1.43	24.3	0.46	0.36
3319	2.63	0.04	-1.62	23.9	0.19	0.15
3322	2.64	0.04	-1.59	24.3	0.32	0.28
3325	2.70	0.07	-1.76	24.9	0.27	0.20
3328	2.75	0.09	-1.79	25.6	0.38	0.29
3331	2.75	0.09	-1.69	25.5	0.45	0.36
3334	2.77	0.10	-1.76	24.9	0.27	0.17
3337	2.76	0.09	-1.58	24.7	0.40	0.31
3340	2.72	0.08	-1.73	24.5	0.21	0.13
3343	2.66	0.05	-1.70	24.2	0.16	0.11
3346	2.74	0.08	-1.67	23.8	0.12	0.03
3349	2.76	0.09	-1.55	23.5	0.18	0.08
3352	2.73	0.08	-1.63	23.8	0.16	0.07
3355	2.72	0.08	-1.71	24.6	0.24	0.17
3358	2.69	0.06	-1.63	25.0	0.42	0.36
3361	2.68	0.06	-1.73	25.3	0.38	0.32
3364	2.71	0.07	-1.82	25.1	0.25	0.18
3367	2.74	0.09	-1.57	24.9	0.46	0.37
3370	2.78	0.10	-1.31	25.0	0.74	0.64
3373	2.82	0.12	-1.30	24.8	0.71	0.59
3376	2.80	0.12	-1.50	24.2	0.37	0.26
3379	2.77	0.10	-1.57	24.1	0.29	0.19
3382	2.71	0.07	-1.57	24.5	0.37	0.29
3385	2.65	0.04	-1.67	24.8	0.33	0.29
3388	2.57	0.01	-1.74	25.0	0.32	0.31
3391	2.51	-0.02	-1.52	24.8	0.48	0.50
3394	2.47	-0.04	-1.44	24.4	0.48	0.52
3397	2.49	-0.03	-1.58	24.2	0.28	0.31
3400	2.52	-0.01	-1.46	24.2	0.43	0.44
3403	2.54	0.00	-1.68	24.9	0.34	0.35
3406	2.54	-0.01	-1.65	25.1	0.43	0.43
3409	2.50	-0.02	-1.76	25.0	0.29	0.31
3412	2.44	-0.05	-1.94	24.9	0.09	0.14
3415	2.40	-0.07	-1.87	24.7	0.12	0.19
3418	2.40	-0.07	-1.79	24.6	0.18	0.24

Appendix E (continued)

Age (ka)	Smoothed Benthic $\delta^{18}O$ (‰)	Sea level correction 50 m (‰)	$\delta^{18}O$ *(G. sacc.)* (‰)	SST (Mg/Ca) (°C)	$\delta^{18}O$ (water) (‰)	$\delta^{18}O$ (salinity) (‰)
3421	2.41	-0.07	-1.72	24.5	0.22	0.29
3424	2.40	-0.07	-1.58	24.5	0.37	0.43
3427	2.39	-0.07	-1.51	24.5	0.42	0.49
3430	2.36	-0.09	-1.57	24.2	0.30	0.39
3433	2.31	-0.11	-1.64	24.3	0.26	0.37
3436	2.27	-0.13	-1.89	24.9	0.13	0.26
3439	2.29	-0.12	-2.07	25.6	0.11	0.23
3442	2.40	-0.07	-2.00	26.0	0.27	0.34
3445	2.45	-0.05	-1.79	25.3	0.31	0.35
3448	2.45	-0.05	-1.90	24.5	0.05	0.10
3451	2.45	-0.05	-1.88	24.0	-0.04	0.01
3454	2.44	-0.05	-2.01	24.7	-0.03	0.01
3457	2.40	-0.07	-1.88	24.8	0.12	0.19
3460	2.41	-0.06	-1.56	24.0	0.27	0.33
3463	2.42	-0.06	-1.58	23.6	0.17	0.23
3466	2.50	-0.02	-1.59	23.5	0.13	0.15
3469	2.53	-0.01	-1.62	23.9	0.19	0.20
3472	2.52	-0.01	-1.52	24.5	0.43	0.44
3475	2.50	-0.02	-1.62	25.0	0.42	0.44
3478	2.44	-0.05	-2.03	25.3	0.08	0.13
3481	2.33	-0.10	-1.93	25.3	0.18	0.28
3484	2.26	-0.13	-1.79	25.1	0.28	0.41
3487	2.23	-0.15	-1.96	24.9	0.08	0.22
3490	2.23	-0.14	-2.03	24.8	-0.02	0.12
3493	2.26	-0.13	-2.00	25.0	0.04	0.17
3496	2.34	-0.10	-2.06	25.5	0.08	0.18
3499	2.45	-0.05	-2.01	25.6	0.16	0.21
3502	2.50	-0.02	-2.02	24.9	0.00	0.03
3505	2.51	-0.02	-1.99	24.4	-0.08	-0.06
3508	2.51	-0.02	-1.81	24.5	0.14	0.15
3511	2.52	-0.01	-1.85	24.7	0.14	0.15
3514	2.49	-0.03	-1.81	25.0	0.25	0.27
3517	2.42	-0.06	-1.73	25.3	0.37	0.43
3520	2.38	-0.08	-1.72	25.0	0.32	0.39
3523	2.35	-0.09	-1.77	24.6	0.19	0.28
3526	2.29	-0.12	-1.89	24.9	0.13	0.25
3529	2.24	-0.14	-1.87	25.3	0.24	0.38
3532	2.23	-0.15	-1.82	26.0	0.44	0.59
3535	2.24	-0.14	-1.88	25.8	0.34	0.48
3538	2.30	-0.12	-1.92	25.3	0.20	0.31
3541	2.34	-0.10	-1.91	25.1	0.16	0.26
3544	2.38	-0.08	-1.83	24.8	0.17	0.25
3547	2.40	-0.07	-1.68	24.3	0.22	0.29
3550	2.39	-0.07	-1.68	24.4	0.23	0.31
3553	2.42	-0.06	-1.83	25.0	0.22	0.28
3556	2.44	-0.05	-1.98	25.4	0.14	0.19
3559	2.44	-0.05	-1.91	25.2	0.18	0.23
3562	2.42	-0.06	-1.84	25.1	0.23	0.29
3565	2.39	-0.07	-1.78	25.4	0.35	0.42
3568	2.36	-0.09	-1.98	25.7	0.20	0.29
3571	2.35	-0.09	-2.10	25.5	0.05	0.14
3574	2.37	-0.08	-1.95	25.2	0.14	0.22
3577	2.43	-0.06	-1.90	24.6	0.06	0.12
3580	2.48	-0.03	-1.96	24.0	-0.12	-0.09
3583	2.50	-0.02	-1.95	24.2	-0.07	-0.05
3586	2.48	-0.03	-2.00	24.8	0.00	0.03
3589	2.40	-0.07	-1.92	25.2	0.17	0.24
3592	2.31	-0.11	-1.78	25.5	0.39	0.49
3595	2.29	-0.12	-1.74	25.5	0.40	0.52
3598	2.27	-0.13	-1.83	25.2	0.25	0.38
3601	2.25	-0.14	-1.92	25.1	0.14	0.27
3604	2.25	-0.14	-1.96	25.1	0.11	0.24
3607	2.26	-0.13	-1.91	25.4	0.21	0.35
3610	2.27	-0.13	-1.87	25.8	0.35	0.47
3613	2.28	-0.12	-1.86	25.6	0.32	0.45

Appendix E (continued)

Age (ka)	Smoothed Benthic $\delta^{18}O$ (‰)	Sea level correction 50 m (‰)	$\delta^{18}O$ *(G. sacc.)* (‰)	SST (Mg/Ca) (°C)	$\delta^{18}O$ (water) (‰)	$\delta^{18}O$ (salinity) (‰)
3616	2.34	-0.10	-1.88	25.0	0.18	0.28
3619	2.45	-0.04	-1.93	24.8	0.07	0.11
3622	2.57	0.01	-1.72	24.8	0.29	0.28
3625	2.67	0.06	-1.63	24.7	0.36	0.30
3628	2.74	0.09	-1.67	24.4	0.25	0.16
3631	2.75	0.09	-1.67	24.3	0.24	0.15
3634	2.69	0.06	-1.65	24.5	0.30	0.24
3637	2.57	0.01	-1.67	24.6	0.28	0.28
3640	2.43	-0.06	-1.80	24.5	0.14	0.19
3643	2.32	-0.10	-1.86	24.9	0.15	0.26
3646	2.25	-0.14	-2.04	25.9	0.19	0.32
3649	2.23	-0.15	-2.07	26.5	0.29	0.44
3652	2.27	-0.13	-1.89	26.6	0.49	0.61
3655	2.34	-0.10	-1.60	26.6	0.78	0.88
3658	2.41	-0.06	-1.64	26.6	0.74	0.81
3661	2.46	-0.04	-1.86	26.4	0.48	0.52
3664	2.45	-0.05	-1.91	25.7	0.29	0.33
3667	2.47	-0.04	-1.87	25.3	0.23	0.26
3670	2.48	-0.03	-1.66	25.2	0.43	0.46
3673	2.47	-0.04	-1.55	25.3	0.55	0.59
3676	2.45	-0.04	-1.55	25.6	0.63	0.68
3679	2.40	-0.07	-1.53	25.9	0.71	0.78
3682	2.34	-0.10	-1.84	26.1	0.44	0.54
3685	2.29	-0.12	-1.87	26.2	0.44	0.56
3688	2.22	-0.15	-1.82	26.2	0.48	0.63
3691	2.21	-0.15	-1.89	25.8	0.32	0.48
3694	2.25	-0.14	-1.68	25.1	0.39	0.52
3697	2.30	-0.11	-1.86	25.1	0.20	0.31
3700	2.33	-0.10	-1.79	25.6	0.39	0.49
3703	2.37	-0.08	-1.68	26.0	0.58	0.66
3706	2.46	-0.04	-1.64	26.3	0.67	0.71
3709	2.54	-0.01	-1.51	25.8	0.70	0.71
3712	2.56	0.01	-1.32	24.8	0.69	0.68
3715	2.52	-0.01	-1.46	24.7	0.53	0.54
3718	2.47	-0.04	-1.54	25.2	0.54	0.58
3721	2.37	-0.08	-1.56	25.5	0.59	0.67
3724	2.28	-0.13	-1.61	25.7	0.59	0.71
3727	2.26	-0.13	-1.58	25.6	0.59	0.73
3730	2.28	-0.12	-1.61	25.4	0.52	0.64
3733	2.32	-0.11	-1.67	25.5	0.49	0.60
3736	2.33	-0.10	-1.71	25.7	0.48	0.58
3739	2.31	-0.11	-1.78	25.8	0.44	0.54
3742	2.34	-0.10	-1.80	25.8	0.43	0.52
3745	2.40	-0.07	-1.65	25.8	0.56	0.63
3748	2.46	-0.04	-1.47	25.7	0.72	0.76
3751	2.53	-0.01	-1.53	25.6	0.64	0.65
3754	2.54	-0.01	-1.58	25.0	0.47	0.48
3757	2.54	-0.01	-1.60	24.0	0.23	0.24
3760	2.50	-0.02	-1.76	23.6	-0.01	0.02
3763	2.40	-0.07	-1.74	23.6	0.02	0.08
3766	2.35	-0.09	-1.69	24.4	0.23	0.32
3769	2.37	-0.08	-1.65	25.3	0.47	0.55
3772	2.31	-0.11	-1.64	25.6	0.53	0.64
3775	2.32	-0.10	-1.76	25.5	0.40	0.50
3778	2.33	-0.10	-1.65	25.0	0.40	0.50
3781	2.34	-0.10	-1.75	24.4	0.18	0.27
3784	2.33	-0.10	-1.65	24.0	0.18	0.28
3787	2.26	-0.13	-1.59	24.2	0.28	0.41
3790	2.27	-0.13	-1.76	25.7	0.44	0.57
3793	2.34	-0.09	-1.71	26.4	0.64	0.74
3796	2.31	-0.11	-1.71	26.2	0.59	0.69
3799	2.37	-0.08	-1.69	26.1	0.59	0.67
3802	2.40	-0.07	-1.53	26.0	0.73	0.80
3805	2.44	-0.05	-1.53	25.2	0.56	0.61
3808	2.45	-0.05	-1.49	24.2	0.39	0.43

Appendix E (continued)

Age (ka)	Smoothed Benthic $\delta^{18}O$ (‰)	Sea level correction 50 m (‰)	$\delta^{18}O$ *(G. sacc.)* (‰)	SST (Mg/Ca) (°C)	$\delta^{18}O$ (water) (‰)	$\delta^{18}O$ (salinity) (‰)
3811	2.40	-0.07	-1.56	24.6	0.40	0.47
3814	2.36	-0.09	-1.73	25.3	0.37	0.46
3817	2.35	-0.09	-2.01	25.4	0.13	0.22
3820	2.32	-0.11	-1.98	25.3	0.13	0.24
3823	2.34	-0.10	-1.90	24.4	0.03	0.12
3826	2.35	-0.09	-1.82	23.8	-0.02	0.07
3829	2.41	-0.07	-1.74	24.0	0.10	0.16
3832	2.42	-0.06	-1.70	24.6	0.25	0.31
3835	2.35	-0.09	-1.66	25.7	0.53	0.62
3838	2.25	-0.14	-1.79	25.6	0.39	0.53
3841	2.17	-0.17	-1.80	24.7	0.17	0.35
3844	2.17	-0.17	-1.78	24.9	0.25	0.42
3847	2.24	-0.14	-1.76	25.4	0.37	0.52
3850	2.32	-0.11	-1.56	25.3	0.56	0.67
3853	2.38	-0.08	-1.75	25.4	0.39	0.47
3856	2.36	-0.09	-1.66	25.8	0.55	0.63
3859	2.29	-0.12	-1.54	25.5	0.62	0.74
3862	2.27	-0.13	-1.66	25.7	0.54	0.67
3865	2.26	-0.13	-1.64	25.6	0.53	0.66
3868	2.36	-0.09	-1.42	25.5	0.73	0.82
3871	2.47	-0.04	-1.66	24.9	0.38	0.41
3874	2.56	0.01	-1.69	25.1	0.37	0.36
3877	2.62	0.03	-1.60	25.2	0.49	0.46
3880	2.58	0.01	-1.46	25.6	0.71	0.70
3883	2.49	-0.03	-1.61	26.0	0.65	0.68
3886	2.40	-0.07	-1.62	25.5	0.54	0.60
3889	2.32	-0.10	-1.62	25.1	0.46	0.56
3892	2.33	-0.10	-1.74	24.8	0.27	0.37
3895	2.33	-0.10	-1.81	25.2	0.28	0.38
3898	2.32	-0.10	-1.63	25.4	0.49	0.59
3901	2.35	-0.09	-1.67	25.3	0.45	0.54
3904	2.37	-0.08	-1.52	25.2	0.56	0.64
3907	2.36	-0.09	-1.44	25.3	0.68	0.76
3910	2.38	-0.08	-1.77	25.7	0.41	0.49
3913	2.41	-0.06	-1.67	25.1	0.40	0.46
3916	2.47	-0.03	-1.58	25.0	0.48	0.51
3919	2.49	-0.03	-1.73	25.2	0.36	0.39
3922	2.45	-0.05	-1.60	25.3	0.50	0.55
3925	2.41	-0.06	-1.58	25.4	0.54	0.60
3928	2.34	-0.09	-1.72	25.7	0.47	0.56
3931	2.28	-0.13	-1.83	26.4	0.51	0.64
3934	2.24	-0.14	-1.86	27.1	0.63	0.77
3937	2.25	-0.14	-1.84	27.0	0.63	0.76
3940	2.30	-0.11	-1.65	26.1	0.63	0.74
3943	2.37	-0.08	-1.71	24.7	0.27	0.35
3946	2.44	-0.05	-1.71	24.7	0.26	0.31
3949	2.50	-0.02	-1.55	25.5	0.61	0.63
3952	2.47	-0.04	-1.56	25.7	0.64	0.67
3955	2.38	-0.08	-1.83	24.7	0.16	0.24
3958	2.28	-0.12	-1.72	25.2	0.36	0.48
3961	2.24	-0.14	-1.76	25.3	0.35	0.49
3964	2.26	-0.13	-1.61	26.4	0.74	0.87
3967	2.32	-0.11	-1.50	25.5	0.65	0.76
3970	2.40	-0.07	-1.60	24.5	0.35	0.42
3973	2.47	-0.04	-1.53	24.5	0.40	0.44
3976	2.49	-0.03	-1.32	24.5	0.62	0.65
3979	2.47	-0.04	-1.53	24.1	0.33	0.37
3982	2.46	-0.04	-1.45	24.5	0.49	0.53
3985	2.47	-0.04	-1.38	25.2	0.71	0.75
3988	2.50	-0.02	-1.48	24.8	0.54	0.56
3991	2.54	-0.01	-1.48	24.3	0.41	0.41
3994	2.61	0.03	-1.45	24.0	0.39	0.36
3997	2.68	0.06	-1.45	23.9	0.37	0.31
4000	2.72	0.08	-1.37	23.4	0.35	0.27
4003	2.69	0.06	-1.60	22.8	-0.03	-0.09

Appendix E (continued)

Age (ka)	Smoothed Benthic $\delta^{18}O$ (‰)	Sea level correction 50 m (‰)	$\delta^{18}O$ *(G. sacc.)* (‰)	SST (Mg/Ca) (°C)	$\delta^{18}O$ (water) (‰)	$\delta^{18}O$ (salinity) (‰)
4006	2.60	0.02	-1.61	24.1	0.26	0.23
4009	2.50	-0.02	-1.61	24.3	0.29	0.31
4012	2.41	-0.06	-1.49	24.0	0.35	0.42
4015	2.35	-0.09	-1.36	24.2	0.53	0.62
4018	2.35	-0.09	-1.45	24.3	0.45	0.55
4021	2.36	-0.09	-1.46	24.6	0.50	0.59
4024	2.36	-0.09	-1.47	24.6	0.49	0.58
4027	2.37	-0.08	-1.47	25.1	0.60	0.68
4030	2.38	-0.08	-1.73	24.9	0.30	0.38
4033	2.43	-0.06	-1.71	25.0	0.34	0.39
4036	2.51	-0.02	-1.56	25.3	0.56	0.58
4039	2.55	0.00	-1.70	24.9	0.33	0.33
4042	2.56	0.01	-1.47	25.6	0.70	0.70
4045	2.51	-0.02	-1.67	25.0	0.36	0.38
4048	2.44	-0.05	-1.55	25.2	0.54	0.59
4051	2.38	-0.08	-1.68	25.0	0.38	0.46
4054	2.34	-0.10	-1.67	24.8	0.33	0.42
4057	2.33	-0.10	-1.79	25.2	0.30	0.40
4060	2.34	-0.10	-1.74	25.2	0.34	0.44
4063	2.37	-0.08	-1.59	25.2	0.50	0.58
4066	2.42	-0.06	-1.53	25.6	0.63	0.69
4069	2.47	-0.03	-1.53	25.4	0.60	0.63
4072	2.53	-0.01	-1.53	26.1	0.75	0.77
4075	2.55	0.00	-1.39	25.6	0.78	0.78
4078	2.55	0.00	-1.39	24.8	0.63	0.63
4081	2.52	-0.01	-1.48	25.3	0.62	0.63
4084	2.48	-0.03	-1.54	24.8	0.47	0.51
4087	2.41	-0.06	-1.55	25.0	0.50	0.57
4090	2.31	-0.11	-1.69	24.0	0.15	0.25
4093	2.26	-0.13	-1.61	24.4	0.31	0.45
4096	2.26	-0.13	-1.54	24.6	0.41	0.54
4099	2.28	-0.12	-1.51	24.8	0.51	0.63
4102	2.33	-0.10	-1.59	25.6	0.59	0.69
4105	2.40	-0.07	-1.73	25.9	0.50	0.57
4108	2.48	-0.03	-1.78	25.1	0.29	0.32
4111	2.50	-0.02	-1.71	24.7	0.26	0.29
4114	2.50	-0.02	-1.68	25.6	0.48	0.51
4117	2.49	-0.03	-1.50	24.8	0.50	0.53
4120	2.47	-0.04	-1.46	23.6	0.30	0.33
4123	2.44	-0.05	-1.65	24.3	0.24	0.29
4126	2.41	-0.06	-1.80	25.4	0.33	0.40
4129	2.38	-0.08	-1.86	25.9	0.37	0.45
4132	2.40	-0.07	-1.76	25.6	0.41	0.48
4135	2.44	-0.05	-1.67	25.1	0.41	0.46
4138	2.47	-0.04	-1.75	25.9	0.49	0.52
4141	2.50	-0.03	-1.76	26.2	0.55	0.58
4144	2.50	-0.02	-1.59	25.1	0.49	0.51
4147	2.48	-0.03	-1.55	25.4	0.58	0.61
4150	2.49	-0.03	-1.55	25.8	0.67	0.70
4153	2.49	-0.03	-1.38	25.1	0.70	0.72
4156	2.49	-0.03	-1.36	25.3	0.75	0.78
4159	2.50	-0.03	-1.53	24.3	0.36	0.39
4162	2.47	-0.04	-1.72	25.0	0.32	0.36
4165	2.45	-0.05	-1.61	25.1	0.47	0.52
4168	2.42	-0.06	-1.62	25.1	0.45	0.51
4171	2.40	-0.07	-1.59	25.3	0.52	0.59
4174	2.39	-0.07	-1.56	24.9	0.46	0.54
4177	2.41	-0.07	-1.41	24.5	0.52	0.59
4180	2.39	-0.07	-1.55	24.6	0.40	0.47
4183	2.39	-0.07	-1.70	25.4	0.44	0.51
4186	2.39	-0.07	-1.63	25.9	0.62	0.69
4189	2.40	-0.07	-1.59	25.9	0.64	0.71
4192	2.38	-0.08	-1.67	25.1	0.40	0.48
4195	2.34	-0.09	-1.77	25.2	0.32	0.41
4198	2.32	-0.10	-1.91	26.5	0.46	0.56

Appendix E (continued)

Age (ka)	Smoothed Benthic $\delta^{18}O$ (‰)	Sea level correction 50 m (‰)	$\delta^{18}O$ *(G. sacc.)* (‰)	SST (Mg/Ca) (°C)	$\delta^{18}O$ (water) (‰)	$\delta^{18}O$ (salinity) (‰)
4201	2.36	-0.09	-1.74	25.1	0.34	0.43
4204	2.40	-0.07	-1.60	24.3	0.30	0.37
4207	2.42	-0.06	-1.79	24.1	0.07	0.12
4210	2.42	-0.06	-1.85	25.1	0.21	0.27
4213	2.40	-0.07	-1.76	25.1	0.30	0.37
4216	2.33	-0.10	-1.78	25.0	0.26	0.37
4219	2.24	-0.14	-1.80	24.3	0.11	0.25
4222	2.22	-0.15	-1.68	25.1	0.38	0.53
4225	2.30	-0.12	-1.59	25.3	0.52	0.63
4228	2.38	-0.08	-1.83	24.7	0.16	0.23
4231	2.43	-0.06	-1.75	24.4	0.17	0.23
4234	2.43	-0.05	-1.72	24.8	0.29	0.35
4237	2.45	-0.05	-1.65	25.3	0.47	0.51
4240	2.43	-0.05	-1.92	25.2	0.18	0.23
4243	2.44	-0.05	-1.76	24.0	0.09	0.14
4246	2.46	-0.04	-1.63	24.1	0.23	0.27
4249	2.50	-0.02	-1.54	24.7	0.44	0.46
4252	2.49	-0.03	-1.77	24.3	0.13	0.16
4255	2.45	-0.04	-1.65	23.9	0.16	0.20
4258	2.40	-0.07	-1.83	24.6	0.13	0.20
4261	2.36	-0.09	-1.88	24.6	0.08	0.16
4264	2.33	-0.10	-1.85	23.9	-0.03	0.07
4267	2.35	-0.09	-1.68	24.4	0.24	0.33
4270	2.37	-0.08	-1.71	25.0	0.33	0.41
4273	2.38	-0.08	-1.67	24.3	0.22	0.30
4276	2.37	-0.08	-1.63	24.8	0.37	0.46
4279	2.36	-0.09	-1.85	25.0	0.20	0.28
4282	2.37	-0.08	-1.77	25.2	0.31	0.39
4285	2.35	-0.09	-1.65	24.8	0.35	0.44
4288	2.37	-0.08	-1.64	24.0	0.19	0.28
4291	2.41	-0.06	-1.62	23.8	0.17	0.24
4294	2.47	-0.04	-1.71	25.0	0.34	0.38
4297	2.50	-0.03	-1.74	24.8	0.26	0.29
4300	2.51	-0.02	-1.49	24.1	0.37	0.39
4303	2.48	-0.03	-1.59	24.4	0.33	0.36
4306	2.42	-0.06	-1.81	25.1	0.25	0.31
4309	2.34	-0.10	-1.73	24.5	0.20	0.30
4312	2.29	-0.12	-1.81	25.2	0.27	0.39
4315	2.26	-0.13	-1.87	24.9	0.15	0.28
4318	2.29	-0.12	-1.70	23.9	0.12	0.23
4321	2.34	-0.10	-1.58	23.5	0.15	0.24
4324	2.37	-0.08	-1.73	23.7	0.03	0.12
4327	2.38	-0.08	-1.68	23.9	0.14	0.22
4330	2.38	-0.08	-1.56	25.1	0.51	0.58
4333	2.39	-0.07	-1.68	25.2	0.42	0.49
4336	2.40	-0.07	-1.82	25.4	0.31	0.38
4339	2.39	-0.07	-1.75	25.0	0.30	0.37
4342	2.40	-0.07	-1.73	24.3	0.18	0.25
4345	2.39	-0.07	-1.62	24.2	0.25	0.33
4348	2.39	-0.07	-1.49	23.7	0.28	0.35
4351	2.41	-0.06	-1.50	25.1	0.56	0.62
4354	2.45	-0.05	-1.48	23.9	0.33	0.38
4357	2.50	-0.02	-1.32	23.4	0.40	0.42
4360	2.53	-0.01	-1.35	23.2	0.33	0.34
4363	2.51	-0.02	-1.49	22.6	0.04	0.05
4366	2.49	-0.03	-1.65	24.0	0.18	0.21
4369	2.43	-0.05	-1.43	24.3	0.47	0.52
4372	2.36	-0.09	-1.61	25.5	0.54	0.63
4375	2.30	-0.11	-1.68	24.7	0.30	0.42
4378	2.29	-0.12	-1.74	23.6	0.01	0.13
4381	2.30	-0.11	-1.70	24.5	0.23	0.35
4384	2.33	-0.10	-1.67	25.4	0.46	0.56
4387	2.35	-0.09	-1.91	26.2	0.38	0.48
4390	2.35	-0.09	-1.71	26.1	0.56	0.65
4393	2.35	-0.09	-1.73	25.0	0.32	0.41

Appendix E (continued)

Age (ka)	Smoothed Benthic $\delta^{18}O$ (‰)	Sea level correction 50 m (‰)	$\delta^{18}O$ *(G. sacc.)* (‰)	SST (Mg/Ca) (°C)	$\delta^{18}O$ (water) (‰)	$\delta^{18}O$ (salinity) (‰)
4396	2.33	-0.10	-1.87	25.3	0.24	0.34
4399	2.36	-0.09	-1.77	25.6	0.40	0.49
4402	2.44	-0.05	-1.65	25.5	0.50	0.55
4405	2.50	-0.02	-1.43	25.2	0.65	0.67
4408	2.54	-0.01	-1.66	24.9	0.37	0.38
4411	2.54	-0.01	-1.74	25.1	0.33	0.33
4414	2.51	-0.02	-1.69	24.9	0.33	0.35
4417	2.48	-0.03	-1.73	25.5	0.42	0.45
4420	2.43	-0.05	-1.68	26.4	0.66	0.71
4423	2.43	-0.05	-1.94	25.7	0.25	0.30
4426	2.45	-0.05	-1.93	25.6	0.23	0.28
4429	2.47	-0.04	-1.75	25.5	0.41	0.45
4432	2.47	-0.04	-1.87	25.5	0.29	0.33
4435	2.47	-0.03	-1.79	25.3	0.33	0.36
4438	2.48	-0.03	-1.64	25.1	0.43	0.47
4441	2.49	-0.03	-1.52	24.7	0.47	0.50
4444	2.49	-0.03	-1.49	24.6	0.47	0.50
4447	2.50	-0.02	-1.47	24.7	0.52	0.54
4450	2.54	-0.01	-1.45	24.4	0.48	0.48
4453	2.57	0.01	-1.60	24.7	0.39	0.39
4456	2.55	0.00	-1.59	25.3	0.53	0.53
4459	2.51	-0.02	-1.60	25.2	0.49	0.51
4462	2.50	-0.02	-1.72	25.0	0.32	0.34
4465	2.49	-0.03	-1.61	25.0	0.43	0.46
4468	2.48	-0.03	-1.71	25.4	0.43	0.46
4471	2.49	-0.03	-1.50	24.5	0.45	0.47
4474	2.53	-0.01	-1.88	25.6	0.29	0.30
4477	2.53	-0.01	-1.90	25.5	0.25	0.26
4480	2.50	-0.02	-1.62	24.7	0.37	0.39
4483	2.49	-0.03	-1.43	25.2	0.65	0.68
4486	2.51	-0.02	-1.50	25.2	0.58	0.61
4489	2.53	-0.01	-1.73	25.3	0.38	0.39
4492	2.52	-0.01	-1.75	25.2	0.35	0.36
4495	2.52	-0.02	-1.63	25.7	0.55	0.56
4498	2.54	-0.01	-1.72	25.6	0.45	0.46
4501	2.49	-0.03	-1.85	24.7	0.14	0.17
4504	2.41	-0.06	-1.72	24.4	0.20	0.26
4507	2.33	-0.10	-1.74	25.0	0.30	0.40
4510	2.28	-0.12	-1.71	25.9	0.52	0.64
4513	2.24	-0.14	-1.59	25.7	0.61	0.75
4516	2.17	-0.17	-1.62	25.9	0.62	0.79
4519	2.17	-0.17	-1.72	25.8	0.49	0.66
4522	2.24	-0.14	-1.75	25.1	0.31	0.45
4525	2.30	-0.11	-1.43	25.0	0.62	0.74
4528	2.35	-0.09	-1.49	25.0	0.56	0.65
4531	2.42	-0.06	-1.41	24.8	0.61	0.67
4534	2.51	-0.02	-1.57	24.5	0.37	0.39
4537	2.57	0.01	-1.77	24.5	0.17	0.16
4540	2.55	0.00	-1.71	24.5	0.23	0.23
4543	2.51	-0.02	-1.73	25.2	0.36	0.37
4546	2.49	-0.03	-1.67	24.5	0.27	0.30
4549	2.44	-0.05	-1.54	24.6	0.42	0.47
4552	2.35	-0.09	-1.42	24.4	0.51	0.60
4555	2.28	-0.13	-1.64	25.1	0.43	0.56
4558	2.33	-0.10	-1.71	25.3	0.39	0.49
4561	2.43	-0.06	-1.52	24.9	0.51	0.57
4564	2.51	-0.02	-1.27	24.5	0.67	0.69
4567	2.57	0.01	-1.17	23.9	0.65	0.64
4570	2.61	0.03	-1.41	24.7	0.58	0.56
4573	2.62	0.03	-1.79	24.7	0.19	0.16
4576	2.56	0.00	-1.45	24.5	0.49	0.48
4579	2.48	-0.03	-1.59	25.0	0.46	0.49
4582	2.49	-0.03	-1.58	24.9	0.46	0.49
4585	2.48	-0.03	-1.27	24.7	0.70	0.74
4588	2.47	-0.04	-1.44	24.4	0.48	0.52

Appendix E (continued)

Age (ka)	Smoothed Benthic $\delta^{18}O$ (‰)	Sea level correction 50 m (‰)	$\delta^{18}O$ *(G. sacc.)* (‰)	SST (Mg/Ca) (°C)	$\delta^{18}O$ (water) (‰)	$\delta^{18}O$ (salinity) (‰)
4591	2.44	-0.05	-1.62	25.1	0.45	0.50
4594	2.42	-0.06	-1.59	25.4	0.54	0.60
4597	2.42	-0.06	-1.55	23.6	0.21	0.27
4600	2.43	-0.05	-1.52	23.8	0.27	0.32
4603	2.49	-0.03	-1.77	24.9	0.25	0.28
4606	2.52	-0.01	-1.41	24.5	0.52	0.54
4609	2.50	-0.02	-1.38	23.8	0.41	0.44
4612	2.49	-0.03	-1.41	23.2	0.26	0.28
4615	2.49	-0.03	-1.58	24.1	0.28	0.30
4618	2.47	-0.04	-1.81	25.1	0.25	0.29
4621	2.45	-0.04	-1.69	24.6	0.26	0.30
4624	2.43	-0.06	-1.43	23.9	0.38	0.44
4627	2.45	-0.05	-1.38	23.7	0.39	0.44
4630	2.42	-0.06	-1.48	24.4	0.43	0.50
4633	2.38	-0.08	-1.67	24.9	0.35	0.43
4636	2.36	-0.09	-1.75	26.0	0.51	0.59
4639	2.34	-0.10	-1.67	25.4	0.45	0.55
4642	2.32	-0.10	-1.48	26.1	0.80	0.90
4645	2.33	-0.10	-1.33	24.4	0.59	0.69
4648	2.38	-0.08	-1.41	23.8	0.39	0.47
4651	2.41	-0.07	-1.19	24.0	0.65	0.71
4654	2.46	-0.04	-1.02	24.4	0.89	0.93
4657	2.47	-0.03	-1.46	24.3	0.45	0.49
4660	2.44	-0.05	-1.53	24.4	0.39	0.44
4663	2.36	-0.09	-1.55	24.7	0.42	0.51
4666	2.28	-0.12	-1.49	24.2	0.39	0.51
4669	2.26	-0.13	-1.35	25.3	0.76	0.90
4672	2.28	-0.12	-1.33	25.1	0.73	0.85
4675	2.30	-0.11	-1.40	24.1	0.44	0.56
4678	2.37	-0.08	-1.53	24.2	0.34	0.42
4681	2.41	-0.06	-1.56	24.1	0.30	0.36
4684	2.46	-0.04	-1.30	24.1	0.55	0.59
4687	2.49	-0.03	-1.34	23.8	0.45	0.48
4690	2.48	-0.03	-1.45	24.8	0.56	0.59
4693	2.46	-0.04	-1.60	24.2	0.27	0.31
4696	2.42	-0.06	-1.61	24.0	0.23	0.29
4699	2.37	-0.08	-1.60	23.5	0.13	0.21
4702	2.33	-0.10	-1.56	23.9	0.25	0.35
4705	2.29	-0.12	-1.51	23.6	0.23	0.35
4708	2.29	-0.12	-1.65	24.1	0.21	0.33
4711	2.30	-0.11	-1.66	24.9	0.36	0.47
4714	2.31	-0.11	-1.80	24.3	0.10	0.20
4717	2.35	-0.09	-1.56	24.0	0.27	0.37
4720	2.38	-0.08	-1.45	24.1	0.42	0.49
4723	2.42	-0.06	-1.37	23.9	0.45	0.51
4726	2.43	-0.06	-1.28	24.0	0.55	0.60
4729	2.40	-0.07	-1.45	23.3	0.23	0.30
4732	2.37	-0.08	-1.29	23.4	0.42	0.51
4735	2.35	-0.09	-1.37	24.8	0.64	0.72
4738	2.34	-0.10	-1.59	24.8	0.41	0.51
4741	2.31	-0.11	-1.49	24.7	0.50	0.60
4744	2.29	-0.12	-1.25	24.5	0.68	0.80
4747	2.27	-0.13	-1.44	24.2	0.44	0.56
4750	2.28	-0.12	-1.42	23.9	0.39	0.51
4753	2.32	-0.11	-1.49	24.0	0.34	0.44
4756	2.36	-0.09	-1.48	25.0	0.57	0.66
4759	2.41	-0.06	-1.51	24.5	0.43	0.49
4762	2.47	-0.04	-1.36	24.8	0.65	0.69
4765	2.54	0.00	-1.51	24.4	0.40	0.40
4768	2.55	0.00	-1.54	24.7	0.45	0.45
4771	2.57	0.01	-1.68	24.8	0.32	0.31
4774	2.60	0.02	-1.38	23.8	0.42	0.39
4777	2.57	0.01	-1.46	24.8	0.54	0.53
4780	2.52	-0.01	-1.64	23.6	0.11	0.13
4783	2.45	-0.05	-1.41	24.1	0.44	0.49

Appendix E (continued)

Age (ka)	Smoothed Benthic $\delta^{18}O$ (‰)	Sea level correction 50 m (‰)	$\delta^{18}O$ *(G. sacc.)* (‰)	SST (Mg/Ca) (°C)	$\delta^{18}O$ (water) (‰)	$\delta^{18}O$ (salinity) (‰)
4786	2.38	-0.08	-1.33	23.9	0.47	0.55
4789	2.37	-0.08	-1.38	23.8	0.41	0.49
4792	2.34	-0.09	-1.47	23.9	0.34	0.44
4795	2.41	-0.07	-1.53	23.8	0.26	0.33
4798	2.48	-0.03	-1.54	23.5	0.19	0.22
4801	2.54	0.00	-1.53	23.8	0.26	0.27
4804	2.62	0.03	-1.51	24.5	0.43	0.40
4807	2.66	0.05	-1.54	24.5	0.40	0.35
4810	2.63	0.04	-1.34	24.2	0.55	0.51
4813	2.57	0.01	-1.49	24.4	0.43	0.42
4816	2.49	-0.03	-1.51	24.5	0.43	0.46
4819	2.42	-0.06	-1.49	24.0	0.34	0.40
4822	2.37	-0.08	-1.31	23.5	0.41	0.50
4825	2.36	-0.09	-1.35	23.5	0.38	0.47
4828	2.40	-0.07	-1.39	23.7	0.38	0.45
4831	2.45	-0.05	-1.41	24.0	0.41	0.46
4834	2.51	-0.02	-1.38	24.2	0.50	0.52
4837	2.55	0.00	-1.36	24.4	0.57	0.57
4840	2.58	0.01	-1.24	24.1	0.63	0.62
4843	2.57	0.01	-1.27	23.6	0.47	0.46
4846	2.56	0.00	-1.27	23.7	0.50	0.49
4849	2.55	0.00	-1.26	24.1	0.60	0.60
4852	2.54	-0.01	-1.51	24.3	0.40	0.40
4855	2.50	-0.02	-1.56	24.5	0.39	0.41
4858	2.47	-0.04	-1.52	24.7	0.47	0.50
4861	2.45	-0.05	-1.33	25.0	0.71	0.76
4864	2.43	-0.06	-1.41	25.2	0.68	0.74
4867	2.40	-0.07	-1.60	25.4	0.53	0.61
4870	2.38	-0.08	-1.68	25.4	0.45	0.53
4873	2.38	-0.08	-1.39	25.6	0.78	0.86
4876	2.42	-0.06	-1.43	26.0	0.82	0.88
4879	2.47	-0.04	-1.40	25.9	0.83	0.87
4882	2.56	0.01	-1.42	25.5	0.73	0.72
4885	2.65	0.05	-1.29	24.9	0.72	0.68
4888	2.73	0.08	-1.24	24.1	0.61	0.53
4891	2.76	0.09	-1.16	23.4	0.54	0.45
4894	2.71	0.07	-1.11	23.4	0.60	0.53
4897	2.59	0.02	-1.06	23.6	0.69	0.67
4900	2.46	-0.04	-1.12	24.3	0.77	0.81
4903	2.40	-0.07	-1.36	25.1	0.70	0.76
4906	2.38	-0.08	-1.41	25.5	0.75	0.83
4909	2.39	-0.07	-1.45	25.8	0.77	0.85
4912	2.43	-0.06	-1.28	26.1	0.99	1.05
4915	2.46	-0.04	-1.26	26.0	0.99	1.03
4918	2.48	-0.03	-1.50	25.4	0.62	0.66
4921	2.44	-0.05	-1.47	25.2	0.62	0.67
4924	2.40	-0.07	-1.49	25.3	0.62	0.69
4927	2.39	-0.08	-1.49	25.2	0.60	0.68
4930	2.39	-0.07	-1.38	25.0	0.67	0.74
4933	2.41	-0.07	-1.28	24.6	0.68	0.74
4936	2.42	-0.06	-1.35	24.3	0.55	0.61
4939	2.44	-0.05	-1.20	24.3	0.70	0.75
4942	2.46	-0.04	-1.36	24.5	0.59	0.64
4945	2.44	-0.05	-1.46	24.8	0.55	0.60
4948	2.37	-0.08	-1.44	25.1	0.62	0.71
4951	2.31	-0.11	-1.63	25.1	0.45	0.56
4954	2.29	-0.12	-1.60	25.1	0.48	0.60
4957	2.26	-0.13	-1.53	25.6	0.65	0.78
4960	2.29	-0.12	-1.52	25.6	0.65	0.77
4963	2.37	-0.08	-1.47	25.2	0.61	0.70
4966	2.45	-0.05	-1.14	25.3	0.96	1.01
4969	2.45	-0.05	-1.37	24.5	0.56	0.60
4972	2.39	-0.07	-1.35	24.2	0.52	0.59
4975	2.36	-0.09	-1.55	24.9	0.48	0.57
4978	2.36	-0.09	-1.54	25.5	0.63	0.71

Appendix E (continued)

Age (ka)	Smoothed Benthic $\delta^{18}O$ (‰)	Sea level correction 50 m (‰)	$\delta^{18}O$ *(G. sacc.)* (‰)	SST (Mg/Ca) (°C)	$\delta^{18}O$ (water) (‰)	$\delta^{18}O$ (salinity) (‰)
4981	2.38	-0.08	-1.56	25.1	0.51	0.59
4984	2.42	-0.06	-1.65	24.5	0.29	0.35
4987	2.43	-0.05	-1.72	24.1	0.13	0.19
4990	2.43	-0.06	-1.60	24.7	0.38	0.44
4993	2.36	-0.09	-1.54	24.8	0.47	0.55
4996	2.30	-0.11	-1.36	24.5	0.58	0.69
4999	2.32	-0.11	-1.57	24.2	0.30	0.41
5002	2.37	-0.08	-1.69	24.5	0.24	0.33
5005	2.44	-0.05	-1.68	25.3	0.43	0.48
5008	2.48	-0.03	-1.56	25.3	0.55	0.58
5011	2.45	-0.05	-1.50	25.2	0.59	0.64
5014	2.41	-0.07	-1.55	25.1	0.52	0.58
5017	2.36	-0.09	-1.87	25.2	0.22	0.31
5020	2.34	-0.09	-1.76	25.7	0.43	0.53
5023	2.36	-0.09	-1.55	25.5	0.61	0.69
5026	2.36	-0.09	-1.77	25.6	0.40	0.49
5029	2.36	-0.08	-1.73	25.9	0.51	0.59
5032	2.34	-0.10	-1.55	26.1	0.74	0.84
5035	2.30	-0.12	-1.41	26.2	0.90	1.01
5038	2.23	-0.15	-1.76	26.2	0.54	0.68
5041	2.16	-0.18	-1.69	26.2	0.60	0.78
5044	2.15	-0.18	-1.64	26.4	0.69	0.87
5047	2.18	-0.17	-1.98	26.8	0.44	0.61
5050	2.25	-0.14	-1.82	26.5	0.54	0.68
5053	2.32	-0.10	-1.63	26.2	0.67	0.77
5056	2.40	-0.07	-1.28	26.3	1.05	1.11
5059	2.42	-0.06	-1.30	25.9	0.94	1.00
5062	2.37	-0.08	-1.78	25.1	0.30	0.38
5065	2.28	-0.12	-1.34	25.5	0.82	0.95
5068	2.20	-0.16	-1.42	26.2	0.87	1.03
5071	2.19	-0.16	-1.65	25.9	0.60	0.76
5074	2.22	-0.15	-1.65	25.2	0.45	0.60
5077	2.26	-0.13	-1.54	24.8	0.46	0.59
5080	2.31	-0.11	-1.58	25.0	0.46	0.57
5083	2.31	-0.11	-1.64	25.5	0.52	0.63
5086	2.32	-0.11	-1.75	26.0	0.51	0.62
5089	2.32	-0.10	-1.52	25.5	0.63	0.73
5092	2.36	-0.09	-1.50	25.4	0.63	0.71
5095	2.44	-0.05	-1.35	25.2	0.74	0.79
5098	2.46	-0.04	-1.42	24.6	0.55	0.59
5101	2.48	-0.03	-1.22	24.3	0.68	0.71
5104	2.48	-0.03	-1.22	24.2	0.66	0.69
5107	2.48	-0.03	-1.43	24.3	0.47	0.51
5110	2.48	-0.03	-1.55	24.6	0.42	0.46
5113	2.48	-0.03	-1.37	24.8	0.64	0.68
5116	2.47	-0.04	-1.42	25.1	0.65	0.68
5119	2.47	-0.04	-1.64	25.6	0.53	0.56
5122	2.43	-0.05	-1.70	26.3	0.62	0.68
5125	2.42	-0.06	-1.70	26.0	0.56	0.62
5128	2.44	-0.05	-1.57	25.8	0.63	0.69
5131	2.46	-0.04	-1.48	25.9	0.75	0.79
5134	2.43	-0.05	-1.40	25.7	0.80	0.85
5137	2.40	-0.07	-1.66	25.7	0.53	0.60
5140	2.38	-0.08	-1.72	25.6	0.46	0.54
5143	2.35	-0.09	-1.63	25.5	0.53	0.62
5146	2.35	-0.09	-1.46	25.0	0.59	0.69
5149	2.36	-0.09	-1.64	25.4	0.48	0.57
5152	2.39	-0.07	-1.52	25.4	0.62	0.69
5155	2.43	-0.05	-1.39	24.9	0.63	0.68
5158	2.44	-0.05	-1.66	25.0	0.39	0.44
5161	2.47	-0.04	-1.60	25.9	0.65	0.69
5164	2.50	-0.03	-1.67	26.6	0.71	0.73
5167	2.51	-0.02	-1.17	26.2	1.12	1.14
5170	2.51	-0.02	-1.46	25.5	0.69	0.70
5173	2.47	-0.04	-1.50	25.1	0.56	0.59

Appendix E (continued)

Age (ka)	Smoothed Benthic $\delta^{18}O$ (‰)	Sea level correction 50 m (‰)	$\delta^{18}O$ *(G. sacc.)* (‰)	SST (Mg/Ca) (°C)	$\delta^{18}O$ (water) (‰)	$\delta^{18}O$ (salinity) (‰)
5176	2.46	-0.04	-1.27	24.8	0.74	0.78
5179	2.46	-0.04	-1.44	24.6	0.52	0.56
5182	2.46	-0.04	-1.62	24.6	0.34	0.38
5185	2.44	-0.05	-1.66	25.1	0.40	0.45
5188	2.43	-0.06	-1.32	25.0	0.74	0.80
5191	2.42	-0.06	-1.14	24.6	0.82	0.88
5194	2.41	-0.07	-1.43	24.1	0.43	0.49
5197	2.39	-0.07	-1.08	23.8	0.72	0.79
5200	2.40	-0.07	-0.95	24.2	0.94	1.01
5203	2.44	-0.05	-1.07	24.8	0.92	0.98
5206	2.45	-0.04	-1.36	25.0	0.70	0.74
5209	2.50	-0.02	-1.43	25.3	0.69	0.71
5212	2.53	-0.01	-1.38	25.6	0.79	0.80
5215	2.54	0.00	-1.37	25.6	0.81	0.81
5218	2.52	-0.01	-1.26	25.6	0.90	0.91
5221	2.48	-0.03	-1.29	25.2	0.81	0.84
5224	2.46	-0.04	-1.38	24.8	0.64	0.68
5227	2.43	-0.06	-1.25	24.7	0.73	0.79
5230	2.43	-0.06	-1.22	24.8	0.80	0.85
5233	2.48	-0.03	-1.39	25.6	0.79	0.83
5236	2.48	-0.03	-1.44	26.1	0.84	0.88
5239	2.48	-0.03	-1.59	26.2	0.72	0.75
5242	2.43	-0.05	-1.57	26.3	0.74	0.80
5245	2.37	-0.08	-1.53	26.2	0.78	0.86
5248	2.33	-0.10	-1.34	26.1	0.93	1.03
5251	2.30	-0.11	-1.40	25.9	0.85	0.96
5254	2.30	-0.11	-1.53	26.1	0.76	0.87
5257	2.32	-0.10	-1.48	26.1	0.79	0.89
5260	2.37	-0.08	-1.39	25.5	0.76	0.85
5263	2.41	-0.06	-1.31	25.4	0.81	0.88
5266	2.44	-0.05	-1.39	25.5	0.77	0.82
5269	2.43	-0.05	-1.81	25.4	0.33	0.39
5272	2.42	-0.06	-1.78	25.3	0.32	0.38
5275	2.42	-0.06	-1.77	25.7	0.42	0.48
5278	2.38	-0.08	-1.61	26.2	0.69	0.76
5281	2.36	-0.09	-1.34	26.4	1.01	1.09
5284	2.34	-0.10	-1.57	26.7	0.83	0.93
5287	2.31	-0.11	-1.74	27.1	0.75	0.86
5290	2.30	-0.11	-1.58	26.9	0.86	0.97
5293	2.32	-0.11	-1.36	26.1	0.92	1.02
5296	2.32	-0.10	-1.50	25.3	0.62	0.72
5299	2.34	-0.10	-1.32	24.6	0.65	0.75
5302	2.31	-0.11	-1.32	24.8	0.68	0.79
5305	2.24	-0.14	-1.50	25.1	0.58	0.72
5308	2.18	-0.17	-1.71	25.8	0.50	0.67
5311	2.13	-0.19	-1.76	26.2	0.54	0.73
5314	2.13	-0.19	-1.69	26.2	0.60	0.79
5317	2.23	-0.15	-1.63	26.0	0.62	0.77
5320	2.30	-0.11	-1.57	25.7	0.62	0.74
5323	2.36	-0.08	-1.60	25.4	0.52	0.60
5326	2.41	-0.07	-1.59	25.0	0.46	0.52
5329	2.43	-0.05	-1.53	25.1	0.55	0.60
5332	2.47	-0.04	-1.29	25.5	0.87	0.91
5335	2.49	-0.03	-1.56	26.0	0.71	0.74
5338	2.53	-0.01	-1.77	26.6	0.61	0.62
5341	2.57	0.01	-1.65	26.1	0.62	0.61
5344	2.54	-0.01	-1.41	25.2	0.68	0.68
5347	2.45	-0.04	-1.58	25.1	0.49	0.54
5350	2.37	-0.08	-1.64	25.4	0.48	0.56
5353	2.30	-0.11	-1.60	25.7	0.59	0.71
5356	2.24	-0.14	-1.69	26.0	0.57	0.72
5359	2.20	-0.16	-1.76	26.2	0.55	0.71
5362	2.24	-0.14	-1.58	26.1	0.69	0.83
5365	2.30	-0.12	-1.42	25.2	0.68	0.79
5368	2.34	-0.10	-1.48	25.5	0.67	0.76

Appendix E (continued)

Age (ka)	Smoothed Benthic $\delta^{18}O$ (‰)	Sea level correction 50 m (‰)	$\delta^{18}O$ *(G. sacc.)* (‰)	SST (Mg/Ca) (°C)	$\delta^{18}O$ (water) (‰)	$\delta^{18}O$ (salinity) (‰)
5371	2.38	-0.08	-1.57	26.4	0.77	0.84
5374	2.44	-0.05	-1.27	25.4	0.86	0.91
5377	2.46	-0.04	-1.36	24.0	0.47	0.51
5380	2.45	-0.04	-1.32	24.5	0.62	0.66
5383	2.44	-0.05	-1.19	25.0	0.86	0.91
5386	2.44	-0.05	-1.21	24.3	0.69	0.74
5389	2.42	-0.06	-1.18	23.9	0.63	0.69
5392	2.36	-0.08	-1.32	24.2	0.55	0.64
5395	2.35	-0.09	-1.24	24.3	0.67	0.76
5398	2.35	-0.09	-1.44	24.4	0.48	0.57
5401	2.31	-0.11	-1.30	24.4	0.63	0.74
5404	2.29	-0.12	-1.39	24.6	0.57	0.68
5407	2.26	-0.13	-1.75	25.2	0.33	0.46
5410	2.25	-0.14	-1.75	25.8	0.47	0.61
5413	2.25	-0.14	-1.58	26.2	0.71	0.85
5416	2.26	-0.13	-1.53	25.7	0.68	0.81
5419	2.30	-0.11	-1.44	25.3	0.68	0.79
5422	2.34	-0.10	-1.41	24.9	0.61	0.71
5425	2.36	-0.09	-1.48	24.8	0.53	0.62
5428	2.37	-0.08	-1.61	25.6	0.56	0.64
5431	2.38	-0.08	-1.51	25.6	0.66	0.73
5434	2.42	-0.06	-1.38	25.4	0.75	0.81
5437	2.44	-0.05	-1.28	25.2	0.81	0.86
5440	2.44	-0.05	-1.21	25.1	0.87	0.92
5443	2.45	-0.04	-1.28	25.1	0.78	0.83
5446	2.44	-0.05	-1.40	25.5	0.75	0.80
5449	2.40	-0.07	-1.47	26.5	0.90	0.97
5452	2.33	-0.10	-1.57	27.5	1.00	1.10
5455	2.28	-0.12	-1.26	27.2	1.25	1.37
5458	2.26	-0.13	-1.21	26.6	1.17	1.31
5461	2.26	-0.13	-1.25	26.3	1.07	1.20
5464	2.30	-0.11	-1.24	26.3	1.07	1.19
5467	2.38	-0.08	-1.28	26.2	1.02	1.10
5470	2.43	-0.06	-1.38	26.1	0.90	0.96
5473	2.45	-0.05	-1.53	26.0	0.72	0.77
5476	2.44	-0.05	-1.24	25.9	0.99	1.04
5479	2.39	-0.07	-1.23	25.8	0.98	1.05
5482	2.36	-0.09	-1.38	25.7	0.82	0.90
5485	2.36	-0.08	-1.31	25.6	0.87	0.96
5488	2.40	-0.07	-1.12	25.6	1.04	1.11
5491	2.41	-0.06	-1.25	25.5	0.91	0.97
5494	2.43	-0.05	-1.33	25.5	0.82	0.88
5497	2.47	-0.04	-1.30	25.9	0.94	0.97
5500	2.49	-0.03	-1.25	26.4	1.08	1.11
5503	2.42	-0.06	-1.30	26.1	0.98	1.04
5506	2.36	-0.09	-1.36	25.4	0.77	0.86
5509	2.35	-0.09	-1.36	25.0	0.68	0.77
5512	2.32	-0.11	-1.32	24.9	0.72	0.82
5515	2.27	-0.13	-1.33	25.1	0.75	0.88
5518	2.24	-0.14	-1.58	26.2	0.73	0.87
5521	2.24	-0.14	-1.42	27.2	1.08	1.22
5524	2.26	-0.13	-1.30	26.4	1.04	1.17
5527	2.25	-0.14	-1.17	25.3	0.94	1.07
5530	2.28	-0.12	-1.21	25.2	0.87	1.00
5533	2.36	-0.09	-1.33	25.7	0.86	0.94
5536	2.41	-0.06	-1.33	25.9	0.91	0.98
5539	2.53	-0.01	-1.28	26.0	0.98	0.99
5542	2.64	0.04	-1.23	25.6	0.94	0.90
5545	2.75	0.09	-1.13	24.5	0.81	0.72
5548	2.78	0.10	-1.06	23.6	0.70	0.60
5551	2.73	0.08	-0.92	23.9	0.89	0.81
5554	2.63	0.04	-1.01	24.5	0.92	0.89
5557	2.53	-0.01	-0.95	25.5	1.20	1.21
5560	2.44	-0.05	-1.37	26.3	0.94	0.99
5563	2.42	-0.06	-1.16	26.1	1.12	1.18

Appendix F $\delta^{18}O_{water}$ and $\delta^{18}O_{salinity}$ for Sites 999 and 1000 and the $\delta^{18}O_{water}$ gradients 999-1241 and 1000-1241.

SL-correction 50 m (‰)	999 age (ka)	$\delta^{18}O$ (*G. sacc*) (‰)	Temperature (Mg/Ca) (°C)	$\delta^{18}O$ (water) (‰)	$\delta^{18}O$ (salinity) (‰)	$\delta^{18}O_{water}$ grad. 999-1241 (‰)	1000 Age (ka)	$\delta^{18}O$ (*G. sacc*) (‰)	Temperature (Mg/Ca) (°C)	$\delta^{18}O$ (water) (‰)	$\delta^{18}O$ (salinity) (‰)	$\delta^{18}O_{water}$ grad. 1000-1241 (‰)
0.55	2203	-0.71	25.6	1.46								
0.52	2206	-0.85	25.7	1.34								
0.47	2209	-0.91	25.7	1.28								
0.42	2212	-1.02	25.2	1.07								
0.31	2215	-0.99	24.9	1.03								
0.22	2218	-0.91	25.3	1.19								
0.12	2221	-1.00	25.6	1.17								
0.09	2224	-1.17	25.5	0.97								
0.15	2227	-1.21	25.2	0.89								
0.23	2230	-1.12	25.1	0.96								
0.32	2233	-1.03	25.1	1.03								
0.40	2236	-0.80	25.2	1.30								
0.45	2239	-0.67	25.4	1.47								
0.48	2242	-0.55	25.0	1.49								
0.46	2245	-0.56	24.3	1.34								
0.41	2248	-0.76	24.1	1.08								
0.36	2251	-0.88	24.1	0.98								
0.28	2254	-0.95	24.3	0.96								
0.20	2257	-1.09	24.6	0.88								
0.15	2260	-1.09	25.2	1.00								
0.14	2263	-0.97	25.6	1.21								
0.19	2266	-0.94	25.2	1.16								
0.26	2269	-0.89	24.8	1.13								
0.33	2272	-0.68	24.5	1.26								
0.40	2275	-0.45	24.3	1.44								
0.45	2278	-0.71	24.5	1.24								
0.48	2281	-0.71	25.0	1.34								
0.48	2284	-0.68	25.5	1.48								
0.47	2287	-0.89	26.0	1.38								
0.42	2290	-1.11	25.7	1.08								
0.34	2293	-1.10	24.9	0.93								
0.25	2296	-1.10	24.7	0.88								
0.17	2299	-1.01	24.9	1.01								
0.11	2302	-0.82	25.2	1.26								
0.10	2305	-0.82	25.7	1.37								
0.13	2308	-0.90	25.6	1.28								
0.18	2311	-0.80	24.6	1.16								
0.22	2314	-0.77	23.8	1.03								
0.24	2317	-0.88	24.3	1.02								
0.24	2320	-0.73	24.9	1.29								
0.21	2323	-1.00	24.4	0.92								
0.18	2326	-0.91	23.6	0.84								
0.16	2329	-0.78	23.5	0.96								
0.14	2332	-0.86	23.8	0.92								
0.12	2335	-0.84	24.3	1.06								
0.10	2338	-0.79	25.2	1.31								
0.09	2341	-1.02	25.7	1.17								
0.10	2344	-1.10	25.2	0.98								
0.12	2347	-1.27	24.6	0.69								
0.16	2350	-1.20	24.2	0.68								
0.20	2353	-1.08	23.9	0.73								
0.26	2356	-1.04	24.2	0.85								
0.28	2359	-1.05	24.8	0.95								
0.27	2362	-0.86	24.8	1.15								
0.24	2365	-0.64	24.7	1.34								
0.22	2368	-0.60	24.8	1.39								
0.20	2371	-0.55	25.2	1.53								
0.17	2374	-0.34	25.5	1.82								
0.16	2377	-0.38	25.8	1.84								
0.18	2380	-0.65	25.8	1.56								
0.19	2383	-0.83	25.1	1.25								
0.19	2386	-0.99	24.7	1.00								
0.19	2389	-1.16	24.8	0.84								
0.22	2392	-1.09	25.1	0.97								
0.22	2395	-1.15	25.5	1.01								
0.23	2398	-1.28	26.8	1.15								
0.29	2401	-1.23	26.2	1.08								

Appendix F (continued)

SL-correction 50 m (‰)	999 age (ka)	$\delta^{18}O$ (*G. sacc*) (‰)	Temperature (Mg/Ca) (°C)	$\delta^{18}O$ (water) (‰)	$\delta^{18}O$ (salinity) (‰)	$\delta^{18}O_{water}$ grad. 999-1241 (‰)	1000 Age (ka)	$\delta^{18}O$ (*G. sacc*) (‰)	Temperature (Mg/Ca) (°C)	$\delta^{18}O$ (water) (‰)	$\delta^{18}O$ (salinity) (‰)	$\delta^{18}O_{water}$ grad. 1000-1241 (‰)
0.36	2404	-0.82	25.4	1.31								
0.36	2407	-0.67	24.6	1.28								
0.30	2410	-0.76	24.7	1.23								
0.22	2413	-0.92	26.1	1.37								
0.15	2416	-1.05	26.5	1.31								
0.08	2419	-0.98	26.0	1.27								
0.06	2422	-0.84	25.5	1.32								
0.13	2425	-1.08	25.4	1.06								
0.22	2428	-0.81	25.5	1.35								
0.28	2431	-0.86	25.9	1.38								
0.32	2434	-0.88	26.9	1.57								
0.36	2437	-0.83	26.4	1.52								
0.38	2440	-0.45	24.6	1.52								
0.38	2443	-0.29	24.0	1.54								
0.35	2446	-0.48	24.2	1.40	0.85	0.96						
0.36	2449	-0.53	24.6	1.42	0.91	1.05						
0.35	2452	-0.67	24.4	1.25	0.78	0.94						
0.33	2455	-0.68	23.7	1.08	0.66	0.76						
0.30	2458	-0.86	23.0	0.76	0.45	0.48						
0.29	2461	-0.92	23.4	0.79	0.58	0.67						
0.28	2464	-0.90	24.2	0.98	0.86	0.84						
0.26	2467	-0.81	25.0	1.23	1.14	1.01						
0.26	2470	-0.77	25.2	1.31	1.16	1.18						
0.29	2473	-0.86	24.5	1.09	0.86	0.84						
0.30	2476	-0.58	23.9	1.24	0.92	0.84						
0.30	2479	-0.67	24.1	1.18	0.78	0.91						
0.30	2482	-0.67	24.6	1.29	0.84	1.01						
0.32	2485	-0.46	25.7	1.73	1.25	0.99						
0.31	2488	-0.28	26.1	1.99	1.52	1.40						
0.25	2491	-0.25	25.8	1.97	1.57	1.59						
0.19	2494	-0.50	25.6	1.67	1.31	1.20						
0.13	2497	-0.59	25.4	1.53	1.25	1.06						
0.08	2500	-0.51	25.2	1.57	1.36	1.05						
0.06	2503	-0.56	24.9	1.48	1.33	0.98						
0.08	2506	-0.67	24.9	1.36	1.21	0.92						
0.12	2509	-0.77	25.2	1.32	1.13	0.87						
0.16	2512	-0.81	25.4	1.32	1.06	0.85						
0.16	2515	-0.72	25.4	1.41	1.08	0.94						
0.16	2518	-0.51	25.3	1.60	1.21	1.18						
0.17	2521	-0.41	25.4	1.72	1.27	1.38						
0.17	2524	-0.37	25.5	1.78	1.30	1.41						
0.18	2527	-0.42	25.6	1.75	1.27	1.27						
0.19	2530	-0.61	25.7	1.58	1.10	0.98						
0.17	2533	-0.70	25.5	1.46	1.04	0.95						
0.14	2536	-0.73	24.8	1.28	0.95	0.89						
0.10	2539	-0.87	24.5	1.08	0.83	0.86						
0.08	2542	-1.28	24.9	0.75	0.58	0.89						
0.05	2545	-1.50	24.8	0.51	0.40	0.47						
0.01	2548	-0.61	23.8	1.19	1.09	0.85						
0.02	2551	-0.79	23.5	0.95	0.82	0.61						
0.05	2554	-1.05	24.4	0.88	0.70	0.75						
0.09	2557	-0.96	25.2	1.14	0.92	0.81						
0.16	2560	-0.85	25.8	1.36	1.12	1.06						
0.25	2563	-0.77	25.8	1.45	1.22	1.18						
0.32	2566	-0.87	25.2	1.22	1.00	0.93						
0.34	2569	-1.03	24.8	0.98	0.80	0.65						
0.33	2572	-1.04	25.2	1.05	0.89	0.73						
0.34	2575	-1.02	25.2	1.07	0.93	0.85						
0.30	2578	-1.11	24.4	0.81	0.69	0.57						
0.26	2581	-1.11	23.9	0.70	0.60	0.29						
0.23	2584	-1.05	23.8	0.75	0.66	0.29						
0.19	2587	-0.87	23.8	0.91	0.82	0.48						
0.14	2590	-0.73	23.7	1.03	0.91	0.62						
0.09	2593	-0.69	23.7	1.07	0.92	0.64						
0.10	2596	-0.75	23.8	1.04	0.84	0.40						
0.12	2599	-0.88	23.9	0.93	0.68	0.27						
0.15	2602	-0.87	24.3	1.03	0.75	0.52						

Appendix F (continued)

SL-correction 50 m (‰)	999 age (ka)	$\delta^{18}O$ (*G. sacc*) (‰)	Temperature (Mg/Ca) (°C)	$\delta^{18}O$ (water) (‰)	$\delta^{18}O$ (salinity) (‰)	$\delta^{18}O_{water}$ grad. 999-1241 (‰)	1000 Age (ka)	$\delta^{18}O$ (*G. sacc*) (‰)	Temperature (Mg/Ca) (°C)	$\delta^{18}O$ (water) (‰)	$\delta^{18}O$ (salinity) (‰)	$\delta^{18}O_{water}$ grad. 1000-1241 (‰)
0.19	2605	-0.75	25.1	1.31	1.04	1.00						
0.24	2608	-0.95	25.8	1.25	1.02	0.91						
0.27	2611	-1.16	26.2	1.13	0.90	0.56						
0.27	2614	-1.18	26.5	1.19	0.98	0.48						
0.24	2617	-1.15	25.6	1.02	0.85	0.50						
0.21	2620	-1.15	24.1	0.72	0.56	0.49						
0.18	2623	-1.10	23.5	0.63	0.45	0.20						
0.16	2626	-0.99	24.4	0.94	0.74	0.47						
0.14	2629	-0.89	25.2	1.21	1.02	0.67						
0.15	2632	-0.87	25.2	1.23	1.03	0.68						
0.16	2635	-0.86	25.0	1.19	0.97	0.83						
0.18	2638	-0.91	24.7	1.08	0.86	0.76						
0.26	2641	-0.86	24.4	1.06	0.82	0.71						
0.30	2644	-0.74	24.3	1.17	0.88	0.81						
0.32	2647	-0.82	25.0	1.23	0.87	0.89						
0.29	2650	-0.95	25.7	1.25	0.89	0.94						
0.23	2653	-1.03	25.8	1.18	0.88	0.98						
0.17	2656	-1.20	25.6	0.97	0.74	0.86						
0.12	2659	-1.17	25.0	0.88	0.73	0.83						
0.12	2662	-1.32	24.4	0.60	0.52	0.60						
0.18	2665	-1.29	24.3	0.60	0.54	0.65						
0.20	2668	-1.22	24.4	0.71	0.58	0.32						
0.21	2671	-1.00	24.7	0.98	0.76	0.38						
0.20	2674	-1.02	24.6	0.95	0.68	0.72						
0.19	2677	-0.85	23.9	0.96	0.64	0.75						
0.19	2680	-0.75	23.1	0.89	0.53	0.49						
0.19	2683	-0.71	22.3	0.76	0.38	0.34						
0.18	2686	-0.78	22.4	0.72	0.34	0.40						
0.18	2689	-0.88	22.7	0.69	0.34	0.31						
0.18	2692	-0.63	22.9	0.96	0.61	0.13						
0.15	2695	-0.69	23.0	0.92	0.57	0.11						
0.12	2698	-0.62	23.0	1.01	0.68	0.32						
0.08	2701	-0.67	23.1	0.97	0.67	0.17						
0.01	2704	-0.69	23.4	1.01	0.72	0.08						
-0.03	2707	-0.58	23.7	1.19	0.91	0.34						
-0.04	2710	-0.53	23.7	1.24	0.98	0.54						
-0.03	2713	-0.52	23.5	1.21	0.94	0.53						
0.00	2716	-0.51	23.2	1.15	0.87	0.59						
0.04	2719	-0.46	22.9	1.13	0.83	0.61						
0.07	2722	-0.60	23.0	1.01	0.71	0.35						
0.07	2725	-0.87	24.2	1.01	0.70	0.28						
0.08	2728	-0.84	25.1	1.23	0.91	0.54						
0.15	2731	-0.86	24.7	1.12	0.81	0.40						
0.22	2734	-1.20	24.5	0.75	0.49	-0.29						
0.26	2737	-1.12	24.8	0.89	0.70	-0.12						
0.26	2740	-1.05	25.1	1.01	0.88	0.49						
0.21	2743	-1.22	25.0	0.84	0.76	0.59						
0.13	2746	-1.07	25.0	0.98	0.92	0.44						
0.06	2749	-0.93	25.2	1.17	1.09	0.85						
0.04	2752	-1.01	25.3	1.10	0.98	0.91						
0.08	2755	-1.07	24.6	0.89	0.74	0.52						
0.15	2758	-1.11	24.0	0.72	0.56	0.22						
0.20	2761	-1.09	24.7	0.90	0.73	0.73						
0.23	2764	-1.06	25.6	1.12	0.95	0.95						
0.22	2767	-1.02	25.3	1.08	0.91	0.81						
0.20	2770	-0.93	24.6	1.03	0.85	0.65						
0.18	2773	-0.77	24.5	1.17	0.98	0.67						
0.17	2776	-0.82	24.6	1.15	0.97	0.44						
0.18	2779	-0.85	24.7	1.13	0.99	0.21						
0.19	2782	-1.03	24.7	0.96	0.86	-0.01						
0.18	2785	-1.04	24.9	0.99	0.91	0.39						
0.16	2788	-1.07	25.2	1.02	0.98	0.59						
0.13	2791	-1.05	25.4	1.07	1.06	0.56						
0.09	2794	-0.96	25.4	1.17	1.15	0.53						
0.04	2797	-0.94	25.3	1.16	1.11	0.54						
0.03	2800	-0.88	25.1	1.18	1.09	0.62						
0.04	2803	-0.66	25.1	1.41	1.24	0.91						

Appendix F (continued)

SL-correction 50 m (‰)	999 age (ka)	$\delta^{18}O$ (*G. sacc*) (‰)	Temperature (Mg/Ca) (°C)	$\delta^{18}O$ (water) (‰)	$\delta^{18}O$ (salinity) (‰)	$\delta^{18}O_{water}$ grad. 999-1241 (‰)	1000 Age (ka)	$\delta^{18}O$ (*G. sacc*) (‰)	Temperature (Mg/Ca) (°C)	$\delta^{18}O$ (water) (‰)	$\delta^{18}O$ (salinity) (‰)	$\delta^{18}O_{water}$ grad. 1000-1241 (‰)
0.08	2806	-0.65	25.4	1.48	1.23	1.13						
0.13	2809	-0.86	25.6	1.31	0.99	0.79						
0.16	2812	-0.74	25.7	1.45	1.12	0.92						
0.16	2815	-0.76	25.8	1.46	1.12	0.88						
0.13	2818	-0.89	26.0	1.37	1.04	0.71						
0.09	2821	-0.86	26.2	1.43	1.13	0.86						
0.07	2824	-0.76	25.7	1.42	1.16	0.83						
0.05	2827	-0.83	25.0	1.22	0.99	0.53						
0.07	2830	-0.86	24.6	1.11	0.92	0.37						
0.10	2833	-0.74	24.5	1.21	1.07	0.58						
0.13	2836	-1.01	24.5	0.92	0.83	0.52						
0.13	2839	-1.01	24.5	0.93	0.83	0.56						
0.11	2842	-1.11	24.5	0.84	0.72	0.42						
0.08	2845	-1.21	24.6	0.76	0.61	0.37						
0.05	2848	-0.96	24.8	1.04	0.85	0.70						
0.02	2851	-0.98	24.9	1.05	0.81	0.65						
0.01	2854	-0.91	25.0	1.12	0.86	0.68						
0.02	2857	-0.86	24.9	1.16	0.90	0.89						
0.07	2860	-0.93	24.8	1.07	0.82	0.92						
0.08	2863	-0.98	24.5	0.96	0.75	0.73						
0.08	2866	-0.77	24.2	1.10	0.92	0.90						
0.07	2869	-0.73	24.2	1.15	1.00	0.85						
0.06	2872	-0.85	24.7	1.14	1.00	0.94						
0.05	2875	-0.80	25.2	1.28	1.12	0.94						
0.04	2878	-0.85	25.0	1.20	1.04	0.55						
0.04	2881	-0.91	24.7	1.07	0.88	0.72						
0.04	2884	-0.97	24.4	0.96	0.70	0.50						
0.05	2887	-1.03	24.4	0.89	0.59	0.52						
0.06	2890	-0.99	24.4	0.94	0.62	0.59						
0.07	2893	-0.97	24.2	0.92	0.63	0.49						
0.08	2896	-1.09	23.8	0.69	0.47	0.24						
0.07	2899	-0.87	23.3	0.81	0.64	0.38						
0.05	2902	-0.82	23.5	0.90	0.78	0.56						
0.00	2905	-0.86	23.9	0.96	0.84	0.78						
-0.05	2908	-0.90	24.3	0.99	0.81	0.91						
-0.08	2911	-0.90	24.4	1.01	0.80	0.70						
-0.10	2914	-0.96	24.4	0.95	0.74	0.50						
-0.10	2917	-1.06	24.2	0.82	0.63	0.51						
-0.09	2920	-0.94	23.9	0.87	0.68	0.62						
-0.07	2923	-0.87	23.2	0.79	0.60	0.44						
-0.06	2926	-0.61	22.9	0.99	0.80	0.57						
-0.06	2929	-0.85	23.8	0.95	0.77	0.56						
-0.05	2932	-0.79	24.4	1.14	0.96	0.75						
-0.04	2935	-0.68	24.2	1.19	1.02	0.84						
-0.02	2938	-0.80	24.1	1.05	0.89	0.73						
0.00	2941	-0.96	24.1	0.90	0.78	0.51						
0.02	2944	-0.93	24.3	0.98	0.90	0.57						
0.02	2947	-1.08	24.9	0.94	0.94	0.44						
0.02	2950	-1.13	25.2	0.97	0.99	0.46						
0.02	2953	-1.43	24.9	0.59	0.64	0.05						
0.00	2956	-1.28	24.7	0.70	0.74	0.07						
-0.01	2959	-1.18	25.3	0.93	0.92	0.42						
-0.02	2962	-1.26	25.6	0.90	0.86	0.30						
-0.03	2965	-1.18	25.1	0.90	0.83	0.19						
-0.04	2968	-1.00	24.5	0.94	0.87	0.42						
-0.04	2971	-0.96	23.5	0.77	0.69	0.16						
-0.03	2974	-1.09	23.3	0.59	0.44	-0.01						
-0.02	2977	-1.06	24.4	0.86	0.64	0.12						
-0.02	2980	-0.78	25.0	1.27	1.00	0.29						
0.00	2983	-0.80	25.1	1.27	1.00	0.36						
0.00	2986	-1.00	24.6	0.97	0.76	0.42						
-0.01	2989	-0.92	23.8	0.86	0.74	0.43						
-0.02	2992	-1.06	23.4	0.64	0.58	0.17						
-0.03	2995	-1.15	23.2	0.52	0.47	0.03						
-0.02	2998	-1.11	23.1	0.53	0.45	-0.05						
-0.02	3001	-1.08	23.0	0.55	0.40	-0.12						
-0.02	3004	-0.90	23.7	0.87	0.67	0.19						

Appendix F (continued)

SL-correction 50 m (‰)	999 age (ka)	$\delta^{18}O$ (*G. sacc*) (‰)	Temperature (Mg/Ca) (°C)	$\delta^{18}O$ (water) (‰)	$\delta^{18}O$ (salinity) (‰)	$\delta^{18}O_{water}$ grad. 999-1241 (‰)	1000 Age (ka)	$\delta^{18}O$ (*G. sacc*) (‰)	Temperature (Mg/Ca) (°C)	$\delta^{18}O$ (water) (‰)	$\delta^{18}O$ (salinity) (‰)	$\delta^{18}O_{water}$ grad. 1000-1241 (‰)
-0.01	3007	-0.94	24.3	0.97	0.74	0.26						
0.01	3010	-1.07	23.6	0.68	0.45	-0.08						
0.02	3013	-1.03	22.8	0.54	0.34	-0.06						
0.03	3016	-1.04	23.1	0.60	0.41	0.08						
0.03	3019	-1.07	23.6	0.68	0.51	0.08						
0.03	3022	-1.01	24.3	0.89	0.71	0.39						
0.02	3025	-0.85	24.9	1.17	0.98	0.64						
0.00	3028	-0.86	24.8	1.14	0.96	0.77						
-0.01	3031	-0.85	24.8	1.15	0.99	0.90						
0.01	3034	-0.94	25.2	1.14	1.01	0.81						
0.04	3037	-1.03	25.3	1.08	0.99	0.68						
0.08	3040	-1.16	24.7	0.82	0.78	0.28						
0.13	3043	-1.17	24.2	0.70	0.67	0.09						
0.17	3046	-1.15	24.2	0.72	0.68	0.27						
0.21	3049	-1.41	23.7	0.35	0.27	-0.14						
0.21	3052	-1.19	21.9	0.19	0.06	-0.24						
0.19	3055	-0.97	20.9	0.20	0.04	-0.12						
0.18	3058	-0.83	21.6	0.48	0.32	0.09						
0.17	3061	-0.92	22.1	0.51	0.38	0.11						
0.14	3064	-0.90	22.5	0.62	0.53	0.40						
0.13	3067	-1.15	23.1	0.49	0.42	0.35						
0.12	3070	-1.20	23.9	0.61	0.55	0.66						
0.10	3073	-1.05	23.8	0.75	0.68	0.68						
0.04	3076	-1.06	23.4	0.64	0.54	0.20						
0.04	3079	-1.04	23.5	0.69	0.56	0.16						
0.07	3082	-1.04	23.6	0.72	0.59	0.35						
0.09	3085	-1.12	23.6	0.64	0.53	0.28						
0.09	3088	-1.19	23.5	0.54	0.46	0.15						
0.10	3091	-0.82	23.6	0.92	0.87	0.68						
0.09	3094	-1.03	23.8	0.77	0.75	0.71						
0.08	3097	-1.24	24.3	0.66	0.65	0.45						
0.05	3100	-1.23	24.9	0.80	0.77	0.45						
0.08	3103	-1.20	25.1	0.86	0.79	0.47						
0.09	3106	-1.10	25.0	0.94	0.86	0.36						
0.08	3109	-1.23	24.6	0.73	0.66	0.22						
0.08	3112	-1.35	24.1	0.50	0.44	-0.01						
0.06	3115	-1.24	24.2	0.63	0.56	0.01						
0.06	3118	-1.14	24.5	0.81	0.76	0.40						
0.07	3121	-1.22	24.7	0.76	0.72	0.35						
0.09	3124	-1.29	24.8	0.72	0.68	0.18						
0.10	3127	-1.17	24.5	0.78	0.74	0.54						
0.12	3130	-1.02	24.2	0.86	0.80	0.57						
0.12	3133	-1.10	24.2	0.78	0.73	0.39						
0.10	3136	-1.05	24.4	0.87	0.80	0.35						
0.07	3139	-1.18	24.0	0.65	0.58	0.48						
0.04	3142	-1.16	23.5	0.57	0.50	0.19						
0.01	3145	-0.91	23.4	0.80	0.75	0.45						
-0.02	3148	-1.05	23.3	0.65	0.65	0.46						
-0.04	3151	-1.15	23.9	0.66	0.71	0.56						
-0.03	3154	-1.08	24.7	0.90	0.97	0.80						
-0.01	3157	-0.96	25.2	1.13	1.23	0.92						
0.00	3160	-0.96	25.1	1.12	1.21	1.03						
-0.01	3163	-1.13	25.1	0.94	1.03	1.04						
-0.02	3166	-1.00	25.2	1.10	1.16	1.08						
-0.05	3169	-1.35	25.3	0.77	0.83	0.64						
-0.07	3172	-1.65	25.4	0.48	0.54	0.49						
-0.07	3175	-1.61	25.4	0.52	0.57	0.42						
-0.07	3178	-1.40	25.5	0.75	0.78	0.60						
-0.07	3181	-1.31	25.6	0.86	0.88	0.83						
-0.07	3184	-1.31	25.7	0.88	0.88	0.88						
-0.09	3187	-1.15	25.9	1.08	1.07	1.05						
-0.11	3190	-1.32	26.1	0.95	0.93	0.94						
-0.13	3193	-1.40	25.9	0.83	0.81	0.81						
-0.12	3196	-1.27	25.0	0.78	0.76	0.67						
-0.07	3199	-1.18	24.4	0.73	0.73	0.44						
-0.05	3202	-1.28	24.6	0.69	0.70	0.36						
-0.05	3205	-1.38	24.9	0.65	0.66	0.45						

Appendix F (continued)

SL-correction 50 m (‰)	999 age (ka)	$\delta^{18}O$ (*G. sacc*) (‰)	Temperature (Mg/Ca) (°C)	$\delta^{18}O$ (water) (‰)	$\delta^{18}O$ (salinity) (‰)	$\delta^{18}O_{water}$ grad. 999-1241 (‰)	1000 Age (ka)	$\delta^{18}O$ (*G. sacc*) (‰)	Temperature (Mg/Ca) (°C)	$\delta^{18}O$ (water) (‰)	$\delta^{18}O$ (salinity) (‰)	$\delta^{18}O_{water}$ grad. 1000-1241 (‰)
-0.05	3208	-1.37	24.7	0.61	0.64	0.61						
-0.05	3211	-1.34	24.4	0.58	0.62	0.61						
-0.07	3214	-1.32	24.6	0.65	0.69	0.51						
-0.06	3217	-1.29	25.0	0.76	0.80	0.65						
-0.06	3220	-1.33	25.1	0.74	0.76	0.69						
-0.02	3223	-1.38	24.8	0.63	0.64	0.53						
-0.01	3226	-1.27	24.4	0.65	0.66	0.47						
-0.01	3229	-1.44	23.7	0.33	0.32	0.07						
-0.02	3232	-1.35	23.0	0.28	0.29	0.08						
-0.05	3235	-1.21	23.4	0.49	0.51	0.34						
-0.10	3238	-1.13	23.9	0.69	0.72	0.52						
-0.13	3241	-1.18	24.5	0.76	0.79	0.64						
-0.15	3244	-1.15	25.1	0.92	0.94	0.85						
-0.14	3247	-1.09	25.2	1.00	1.02	0.86						
-0.13	3250	-1.25	24.4	0.67	0.68	0.24						
-0.10	3253	-1.47	23.7	0.31	0.30	-0.38						
-0.05	3256	-1.46	23.4	0.25	0.23	-0.26						
-0.02	3259	-1.35	23.3	0.33	0.30	-0.11						
-0.02	3262	-1.38	23.7	0.39	0.36	0.07						
-0.02	3265	-1.41	24.3	0.49	0.45	0.21						
-0.01	3268	-1.37	24.3	0.54	0.52	-0.02						
-0.03	3271	-1.35	24.1	0.52	0.52	-0.01						
-0.06	3274	-1.32	23.9	0.50	0.51	-0.01						
-0.08	3277	-1.22	23.8	0.56	0.55	-0.20						
-0.09	3280	-1.15	23.7	0.62	0.58	-0.19						
-0.12	3283	-0.99	24.0	0.84	0.76	0.31						
-0.14	3286	-0.83	24.2	1.05	0.91	0.42						
-0.15	3289	-0.83	23.8	0.97	0.79	0.36						
-0.14	3292	-0.81	23.3	0.88	0.67	0.17						
-0.12	3295	-0.93	22.6	0.61	0.40	-0.07						
-0.10	3298	-0.98	21.9	0.41	0.22	-0.32						
-0.08	3301	-0.90	21.4	0.38	0.20	-0.10						
-0.07	3304	-0.87	21.3	0.38	0.21	0.03						
-0.07	3307	-0.77	21.3	0.49	0.35	0.24						
-0.06	3310	-0.92	21.7	0.42	0.28	-0.10						
-0.05	3313	-0.92	22.1	0.51	0.39	-0.22						
-0.05	3316	-0.80	22.9	0.79	0.69	0.33						
-0.06	3319	-1.07	23.5	0.66	0.62	0.47						
-0.07	3322	-1.14	23.0	0.48	0.44	0.16						
-0.09	3325	-0.92	22.2	0.53	0.46	0.26						
-0.09	3328	-0.81	22.3	0.65	0.56	0.27						
-0.08	3331	-0.72	22.7	0.83	0.74	0.38						
-0.06	3334	-0.70	23.1	0.94	0.84	0.67						
-0.03	3337	-0.78	23.5	0.94	0.84	0.54						
-0.02	3340	-0.85	23.2	0.82	0.74	0.61						
-0.03	3343	-0.91	22.7	0.63	0.59	0.47						
-0.07	3346	-0.96	22.5	0.56	0.47	0.44						
-0.11	3349	-0.98	23.8	0.81	0.72	0.64						
-0.12	3352	-0.97	25.0	1.08	1.00	0.93						
-0.13	3355	-1.11	24.6	0.86	0.78	0.61						
-0.14	3358	-1.07	24.0	0.76	0.70	0.34						
-0.14	3361	-1.07	23.8	0.73	0.67	0.35						
-0.13	3364	-1.08	23.8	0.71	0.64	0.46						
-0.13	3367	-0.99	23.8	0.80	0.71	0.34						
-0.12	3370	-0.87	23.7	0.90	0.80	0.16						
-0.10	3373	-0.81	23.0	0.81	0.69	0.10						
-0.04	3376	-0.84	22.4	0.65	0.53	0.28						
0.01	3379	-0.99	23.1	0.66	0.56	0.37						
0.06	3382	-1.03	23.9	0.78	0.71	0.41						
0.09	3385	-1.02	24.5	0.92	0.87	0.59						
0.09	3388	-1.02	24.8	0.99	0.98	0.67						
0.06	3391	-1.09	24.9	0.95	0.97	0.47						
0.01	3394	-1.21	24.8	0.79	0.83	0.32						
-0.06	3397	-1.22	24.7	0.76	0.78	0.47						
-0.10	3400	-1.22	24.5	0.73	0.74	0.30						
-0.14	3403	-1.23	24.2	0.64	0.65	0.30						
-0.15	3406	-1.19	23.9	0.62	0.62	0.19						

Appendix F (continued)

SL-correction 50 m (‰)	999 age (ka)	$\delta^{18}O$ (*G. sacc*) (‰)	Temperature (Mg/Ca) (°C)	$\delta^{18}O$ (water) (‰)	$\delta^{18}O$ (salinity) (‰)	$\delta^{18}O_{water}$ grad. 999-1241 (‰)	1000 Age (ka)	$\delta^{18}O$ (*G. sacc*) (‰)	Temperature (Mg/Ca) (°C)	$\delta^{18}O$ (water) (‰)	$\delta^{18}O$ (salinity) (‰)	$\delta^{18}O_{water}$ grad. 1000-1241 (‰)
-0.13	3409	-1.11	23.6	0.63	0.65	0.34						
-0.10	3412	-1.15	23.7	0.63	0.68	0.54						
-0.06	3415	-1.18	24.0	0.65	0.72	0.53						
-0.04	3418	-1.15	24.3	0.75	0.82	0.57						
-0.05	3421	-1.21	24.7	0.77	0.83	0.54						
-0.04	3424	-1.30	25.1	0.76	0.83	0.40						
-0.03	3427	-1.30	25.4	0.85	0.92	0.43						
-0.04	3430	-1.28	24.9	0.75	0.83	0.45						
-0.04	3433	-1.27	24.1	0.58	0.69	0.32						
-0.07	3436	-1.28	23.7	0.49	0.61	0.35						
-0.10	3439	-1.35	24.2	0.54	0.65	0.43						
-0.12	3442	-1.38	24.8	0.63	0.70	0.36						
-0.15	3445	-1.47	24.9	0.56	0.61	0.26						
-0.15	3448	-1.50	24.8	0.50	0.55	0.45						
-0.14	3451	-1.44	24.7	0.53	0.58	0.57						
-0.11	3454	-1.38	24.4	0.53	0.58	0.57						
-0.10	3457	-1.37	24.1	0.48	0.55	0.36						
-0.08	3460	-1.25	24.1	0.62	0.68	0.35						
-0.04	3463	-1.01	24.4	0.90	0.96	0.73						
-0.01	3466	-0.82	24.4	1.11	1.13	0.98						
0.01	3469	-0.92	24.0	0.92	0.93	0.73						
-0.01	3472	-1.09	23.6	0.65	0.67	0.23						
-0.04	3475	-1.00	23.8	0.79	0.81	0.37						
-0.08	3478	-1.02	24.4	0.90	0.95	0.82						
-0.13	3481	-1.23	24.6	0.73	0.83	0.55						
-0.13	3484	-1.31	24.2	0.56	0.70	0.29						
-0.12	3487	-1.42	23.9	0.40	0.55	0.33						
-0.11	3490	-1.48	24.0	0.37	0.51	0.39						
-0.10	3493	-1.40	24.2	0.47	0.60	0.43						
-0.11	3496	-1.19	24.4	0.72	0.82	0.63						
-0.10	3499	-1.29	24.6	0.67	0.71	0.51						
-0.07	3502	-1.26	24.8	0.75	0.78	0.75						
-0.04	3505	-1.29	25.1	0.79	0.81	0.87						
-0.01	3508	-1.19	24.9	0.83	0.85	0.69						
-0.01	3511	-1.26	24.4	0.66	0.67	0.52						
-0.01	3514	-1.12	24.2	0.76	0.79	0.52						
-0.02	3517	-1.19	24.2	0.68	0.74	0.31						
-0.07	3520	-1.15	24.4	0.78	0.86	0.46						
-0.09	3523	-1.11	24.8	0.88	0.98	0.69						
-0.08	3526	-1.05	24.9	0.98	1.10	0.85						
-0.11	3529	-1.09	25.0	0.95	1.09	0.71						
-0.10	3532	-1.10	24.8	0.91	1.06	0.47						
-0.10	3535	-1.13	24.7	0.86	1.00	0.52						
-0.10	3538	-1.20	24.6	0.76	0.88	0.56						
-0.10	3541	-1.27	24.4	0.65	0.75	0.49						
-0.13	3544	-1.39	24.3	0.52	0.59	0.34						
-0.13	3547	-1.52	24.4	0.40	0.47	0.17						
-0.09	3550	-1.51	24.6	0.44	0.51	0.21						
-0.11	3553	-1.41	25.0	0.63	0.69	0.41						
-0.08	3556	-1.42	25.5	0.74	0.79	0.59						
-0.07	3559	-1.34	25.7	0.86	0.91	0.68						
-0.05	3562	-1.26	25.8	0.95	1.01	0.72						
-0.05	3565	-1.55	25.7	0.64	0.71	0.29						
-0.07	3568	-1.65	25.4	0.49	0.58	0.28						
-0.09	3571	-1.53	25.4	0.61	0.70	0.56						
-0.09	3574	-1.41	25.6	0.77	0.85	0.63						
-0.11	3577	-1.35	25.3	0.77	0.82	0.70						
-0.10	3580	-1.13	24.7	0.85	0.88	0.97						
-0.09	3583	-1.13	24.6	0.82	0.84	0.89						
-0.07	3586	-1.35	24.7	0.64	0.67	0.64						
-0.06	3589	-1.47	24.9	0.55	0.62	0.38						
-0.09	3592	-1.51	24.8	0.49	0.60	0.10						
-0.14	3595	-1.55	24.3	0.36	0.48	-0.05						
-0.17	3598	-1.60	24.1	0.25	0.38	0.01						
-0.17	3601	-1.40	24.1	0.45	0.58	0.31						
-0.14	3604	-1.27	24.0	0.57	0.71	0.46						
-0.11	3607	-1.48	24.0	0.35	0.48	0.14						

Appendix F (continued)

SL-correction 50 m (‰)	999 age (ka)	$\delta^{18}O$ (*G. sacc*) (‰)	Temperature (Mg/Ca) (°C)	$\delta^{18}O$ (water) (‰)	$\delta^{18}O$ (salinity) (‰)	$\delta^{18}O_{water}$ grad. 999-1241 (‰)	1000 Age (ka)	$\delta^{18}O$ (*G. sacc*) (‰)	Temperature (Mg/Ca) (°C)	$\delta^{18}O$ (water) (‰)	$\delta^{18}O$ (salinity) (‰)	$\delta^{18}O_{water}$ grad. 1000-1241 (‰)
-0.08	3610	-1.50	24.3	0.41	0.53	0.06						
-0.09	3613	-1.49	25.0	0.57	0.69	0.24						
-0.12	3616	-1.52	25.0	0.52	0.62	0.35						
-0.13	3619	-1.57	24.1	0.29	0.33	0.22						
-0.13	3622	-1.45	23.5	0.28	0.27	-0.01						
-0.09	3625	-1.21	23.2	0.45	0.39	0.09						
-0.04	3628	-1.29	22.9	0.30	0.21	0.05						
0.01	3631	-1.16	22.5	0.35	0.27	0.12						
0.03	3634	-1.15	22.4	0.35	0.28	0.05						
0.01	3637	-1.07	22.9	0.54	0.54	0.26						
-0.03	3640	-1.01	23.4	0.69	0.74	0.55						
-0.07	3643	-1.22	23.3	0.47	0.57	0.32						
-0.10	3646	-1.23	23.2	0.45	0.58	0.26						
-0.10	3649	-1.29	24.3	0.60	0.75	0.31						
-0.10	3652	-1.33	25.7	0.86	0.99	0.38						
-0.10	3655	-1.37	25.9	0.86	0.95	0.08						
-0.09	3658	-1.45	25.0	0.60	0.67	-0.14						
-0.08	3661	-1.36	24.3	0.53	0.57	0.05						
-0.09	3664	-1.07	23.7	0.70	0.75	0.42						
-0.08	3667	-1.11	23.2	0.54	0.58	0.31						
-0.06	3670	-1.16	22.7	0.39	0.42	-0.04						
-0.03	3673	-1.11	22.4	0.38	0.42	-0.17						
-0.03	3676	-1.08	23.5	0.66	0.70	0.03						
-0.05	3679	-1.23	24.9	0.79	0.86	0.08						
-0.06	3682	-1.40	25.5	0.76	0.85	0.31						
-0.09	3685	-1.49	25.9	0.75	0.87	0.31						
-0.13	3688	-1.47	25.6	0.70	0.85	0.22						
-0.14	3691	-1.41	24.8	0.59	0.75	0.27						
-0.14	3694	-1.34	24.6	0.63	0.77	0.24						
-0.11	3697	-1.33	25.6	0.85	0.96	0.65						
-0.08	3700	-1.36	26.3	0.97	1.07	0.58						
-0.05	3703	-1.24	26.2	1.06	1.14	0.47						
-0.02	3706	-1.37	25.9	0.87	0.91	0.20						
-0.04	3709	-1.41	25.2	0.67	0.68	-0.03						
-0.08	3712	-1.27	24.4	0.66	0.65	-0.03						
-0.12	3715	-1.09	24.4	0.83	0.85	0.30						
-0.14	3718	-0.99	24.7	1.00	1.04	0.46						
-0.13	3721	-0.95	24.8	1.06	1.14	0.48						
-0.11	3724	-1.01	24.5	0.94	1.06	0.35						
-0.07	3727	-1.24	24.2	0.63	0.77	0.04						
-0.04	3730	-1.39	24.2	0.48	0.61	-0.04						
-0.03	3732	-1.46	24.4	0.46	0.57	-0.03						
-0.04	3735	-1.45	24.7	0.52	0.63	0.04						
-0.04	3738	-1.14	24.9	0.88	0.99	0.45						
-0.04	3741	-1.00	25.2	1.08	1.17	0.65						
-0.02	3744	-1.07	25.5	1.07	1.14	0.51						
-0.01	3747	-1.03	25.7	1.17	1.21	0.44						
0.03	3750	-1.12	25.5	1.03	1.04	0.39						
0.06	3753	-1.34	25.1	0.73	0.74	0.26						
0.08	3756	-1.51	24.8	0.50	0.50	0.26						
0.06	3759	-1.11	25.0	0.93	0.96	0.94						
0.02	3762	-1.05	25.2	1.05	1.12	1.03						
-0.02	3765	-1.13	25.2	0.96	1.05	0.72						
-0.06	3768	-1.17	24.8	0.83	0.92	0.36						
-0.09	3771	-1.12	24.4	0.81	0.92	0.28						
-0.09	3774	-1.08	24.6	0.88	0.98	0.48						
-0.09	3777	-1.09	25.0	0.95	1.05	0.55						
-0.09	3780	-1.16	25.1	0.92	1.02	0.74						
-0.08	3783	-1.23	24.4	0.68	0.78	0.50						
-0.08	3786	-1.27	23.8	0.53	0.66	0.25						
-0.06	3789	-1.10	24.7	0.89	1.01	0.45						
-0.02	3792	-1.14	25.5	1.01	1.11	0.37						
0.00	3795	-1.29	25.9	0.95	1.06	0.36						
0.01	3798	-1.40	26.0	0.86	0.95	0.28						
-0.02	3801	-1.14	25.6	1.05	1.11	0.31						
-0.05	3804	-1.11	25.6	1.05	1.10	0.49						
-0.08	3807	-1.22	25.7	0.97	1.02	0.58						

Appendix F (continued)

SL-correction 50 m (‰)	999 age (ka)	$\delta^{18}O$ (*G. sacc*) (‰)	Temperature (Mg/Ca) (°C)	$\delta^{18}O$ (water) (‰)	$\delta^{18}O$ (salinity) (‰)	$\delta^{18}O_{water}$ grad. 999-1241 (‰)	1000 Age (ka)	$\delta^{18}O$ (*G. sacc*) (‰)	Temperature (Mg/Ca) (°C)	$\delta^{18}O$ (water) (‰)	$\delta^{18}O$ (salinity) (‰)	$\delta^{18}O_{water}$ grad. 1000-1241 (‰)
-0.10	3810	-1.18	25.0	0.86	0.93	0.47						
-0.10	3813	-1.15	23.9	0.67	0.75	0.29						
-0.10	3816	-1.17	24.4	0.76	0.84	0.63						
-0.08	3819	-1.30	25.3	0.82	0.93	0.69						
-0.06	3822	-1.32	25.3	0.78	0.87	0.75						
-0.03	3825	-1.46	25.0	0.58	0.68	0.61	3826	-1.09	29.2	1.83	1.92	1.51
-0.01	3828	-1.53	24.4	0.39	0.45	0.29	3900	-1.24	29.9	1.82	1.92	1.58
0.00	3831	-1.41	24.2	0.47	0.53	0.22	3924	-0.88	29.2	2.03	2.12	1.63
0.00	3834	-1.24	25.4	0.88	0.98	0.35	3926	-0.86	28.9	1.99	2.05	1.49
-0.01	3837	-1.31	26.4	1.04	1.17	0.65	3929	-1.33	29.3	1.61	1.63	0.96
-0.03	3840	-1.35	26.4	1.00	1.17	0.83	3953	-1.26	28.6	1.53	1.53	1.15
-0.06	3843	-1.44	26.2	0.87	1.04	0.63	3966	-0.97	28.8	1.87	1.88	1.55
-0.11	3846	-1.36	25.4	0.76	0.90	0.38	3969	-1.38	30.6	1.83	1.85	1.50
-0.13	3849	-1.51	24.4	0.42	0.52	-0.14	3995	-1.24	29.2	1.67	1.71	1.26
-0.13	3852	-1.46	24.2	0.41	0.49	0.02	3998	-0.86	28.7	1.96	2.01	1.29
-0.12	3855	-1.35	24.2	0.53	0.61	-0.02	4000	-0.74	29.7	2.27	2.32	2.02
-0.10	3858	-1.39	24.9	0.63	0.75	0.02	4078	-0.87	27.1	1.62	1.66	1.38
-0.07	3861	-1.34	25.9	0.89	1.02	0.36	4084	-0.80	28.2	1.91	1.95	1.50
-0.03	3864	-1.42	24.8	0.58	0.71	0.05	4086	-0.78	27.7	1.84	1.88	1.55
-0.02	3867	-1.43	22.8	0.15	0.23	-0.58	4089	-0.84	28.5	1.94	1.98	1.62
-0.02	3870	-0.59	22.5	0.92	0.95	0.54	4092	-1.23	27.9	1.42	1.46	0.99
-0.03	3873	-0.48	22.5	1.04	1.03	0.67	4095	-0.93	27.5	1.63	1.66	1.16
-0.04	3876	-0.84	23.2	0.82	0.79	0.33	4098	-1.41	27.9	1.24	1.27	0.77
-0.05	3879	-0.78	24.1	1.08	1.06	0.37	4123	-1.17	28.6	1.63	1.65	1.11
-0.06	3882	-1.11	24.6	0.85	0.88	0.20	4140	-1.56	29.0	1.31	1.31	0.83
-0.08	3885	-1.12	24.9	0.91	0.98	0.37	4142	-1.46	28.3	1.27	1.26	0.88
-0.07	3888	-1.40	24.7	0.58	0.68	0.12	4184	-1.00	28.1	1.70	1.70	1.17
-0.05	3891	-1.43	24.1	0.43	0.53	0.16	4187	-1.37	28.7	1.45	1.47	0.97
-0.04	3894	-1.47	23.9	0.34	0.44	0.05	4191	-1.19	28.3	1.54	1.57	1.23
-0.03	3897	-1.33	23.8	0.45	0.56	-0.03	4194	-1.39	27.9	1.27	1.29	0.84
-0.02	3900	-1.21	24.0	0.63	0.72	0.18	4210	-1.21	27.8	1.43	1.46	1.00
-0.03	3903	-1.31	24.7	0.67	0.75	0.11	4212	-1.32	28.2	1.39	1.41	0.94
-0.03	3906	-1.30	25.0	0.75	0.84	0.07	4247	-1.06	27.6	1.53	1.54	1.24
-0.03	3909	-1.52	24.8	0.48	0.56	0.06	4249	-1.29	27.9	1.37	1.38	1.11
-0.03	3912	-1.22	24.6	0.75	0.81	0.35	4315	-1.22	27.6	1.37	1.39	1.00
-0.03	3915	-0.91	24.8	1.08	1.12	0.61	4318	-1.38	27.7	1.23	1.26	0.58
-0.04	3918	-1.06	24.9	0.96	0.99	0.60	4424	-1.51	26.6	0.88	0.90	0.29
-0.05	3921	-1.16	24.7	0.83	0.88	0.33	4441	-1.58	26.9	0.86	0.87	0.48
-0.06	3924	-1.05	24.6	0.91	0.97	0.37	4459	-1.00	26.7	1.41	1.42	1.06
-0.07	3927	-0.99	24.4	0.92	1.02	0.45	4484	-1.36	25.6	0.82	0.83	0.27
-0.07	3930	-1.17	24.2	0.71	0.84	0.20	4487	-1.26	25.7	0.93	0.94	0.48
-0.07	3933	-1.22	24.4	0.69	0.83	0.06	4489	-1.47	25.6	0.70	0.73	0.56
-0.07	3936	-1.18	24.6	0.79	0.92	0.16	4504	-1.36	26.7	1.05	1.11	0.85
-0.07	3939	-1.26	25.0	0.79	0.91	0.17	4507	-1.28	27.0	1.18	1.28	0.88
-0.07	3942	-1.32	25.5	0.83	0.92	0.56	4510	-1.12	27.1	1.37	1.50	0.86
-0.07	3945	-1.46	25.6	0.71	0.76	0.45	4513	-1.15	27.8	1.47	1.61	0.87
-0.08	3948	-1.58	25.3	0.52	0.55	-0.08	4516	-1.23	27.6	1.36	1.53	0.73
-0.09	3951	-1.49	25.1	0.58	0.62	-0.06	4519	-1.28	26.7	1.12	1.29	0.63
-0.10	3954	-1.49	25.1	0.59	0.67	0.43	4522	-1.30	28.1	1.39	1.53	1.08
-0.09	3957	-1.56	25.1	0.51	0.63	0.15	4525	-1.28	28.1	1.42	1.54	0.80
-0.07	3960	-1.49	25.0	0.57	0.71	0.21	4528	-1.30	28.2	1.42	1.51	0.86
-0.06	3963	-1.57	24.9	0.45	0.59	-0.28	4531	-1.39	28.1	1.30	1.36	0.69
-0.06	3966	-1.62	24.7	0.36	0.46	-0.29	4534	-1.29	27.8	1.34	1.36	0.97
-0.07	3969	-1.47	24.3	0.44	0.51	0.08	4537	-1.29	26.7	1.11	1.10	0.94
-0.10	3972	-1.45	23.7	0.33	0.36	-0.08	4540	-1.09	26.7	1.32	1.32	1.09
-0.14	3975	-1.46	23.2	0.20	0.23	-0.42	4543	-1.02	26.7	1.39	1.40	1.03
-0.15	3978	-1.35	23.4	0.36	0.40	0.03	4546	-1.28	26.6	1.10	1.13	0.82
-0.12	3981	-1.37	23.7	0.40	0.44	-0.10	4549	-1.29	26.2	1.00	1.05	0.58
-0.08	3984	-1.49	23.1	0.16	0.20	-0.55	4552	-1.10	26.2	1.19	1.28	0.68
-0.06	3987	-1.34	22.4	0.15	0.17	-0.39	4555	-1.16	26.9	1.29	1.42	0.86
-0.05	3990	-1.20	21.9	0.19	0.20	-0.22	4558	-1.09	27.6	1.49	1.59	1.10
-0.05	3993	-1.23	21.6	0.09	0.06	-0.30	4561	-1.16	27.4	1.38	1.44	0.87
-0.05	3996	-1.27	21.8	0.10	0.04	-0.26	4564	-1.39	26.8	1.03	1.05	0.36
-0.05	3999	-1.25	22.5	0.26	0.19	-0.08	4567	-1.10	26.7	1.31	1.30	0.66
-0.04	4002	-1.15	22.7	0.40	0.34	0.43	4570	-1.22	27.1	1.27	1.24	0.68
-0.02	4005	-1.12	22.6	0.41	0.38	0.15	4573	-1.28	28.4	1.48	1.45	1.29
-0.03	4008	-1.23	22.9	0.38	0.40	0.09	4576	-1.10	30.6	2.10	2.10	1.61

Appendix F (continued)

SL-correction 50 m (‰)	999 age (ka)	$\delta^{18}O$ (*G. sacc*) (‰)	Temperature (Mg/Ca) (°C)	$\delta^{18}O$ (water) (‰)	$\delta^{18}O$ (salinity) (‰)	$\delta^{18}O_{water}$ grad. 999-1241 (‰)	1000 Age (ka)	$\delta^{18}O$ (*G. sacc*) (‰)	Temperature (Mg/Ca) (°C)	$\delta^{18}O$ (water) (‰)	$\delta^{18}O$ (salinity) (‰)	$\delta^{18}O_{water}$ grad. 1000-1241 (‰)
-0.04	4011	-1.42	24.1	0.44	0.51	0.09	4579	-1.35	28.2	1.37	1.40	0.91
-0.07	4014	-1.59	25.0	0.46	0.55	-0.07	4582	-1.05	27.1	1.43	1.46	0.98
-0.09	4017	-1.43	25.1	0.63	0.72	0.17	4585	-0.83	27.2	1.67	1.70	0.96
-0.10	4020	-1.18	24.9	0.84	0.93	0.34	4588	-1.06	27.4	1.49	1.52	1.00
-0.09	4023	-0.96	24.2	0.91	1.00	0.42	4591	-0.98	27.4	1.56	1.61	1.11
-0.08	4026	-1.17	23.4	0.54	0.63	-0.05	4594	-0.94	27.1	1.55	1.61	1.01
-0.08	4029	-1.18	22.7	0.38	0.45	0.08	4597	-1.14	27.1	1.35	1.41	1.14
-0.08	4032	-1.21	22.1	0.22	0.27	-0.12	4600	-1.21	26.9	1.25	1.30	0.98
-0.09	4035	-1.09	22.8	0.48	0.50	-0.08	4603	-1.19	26.9	1.25	1.28	1.00
-0.08	4038	-1.02	23.7	0.75	0.75	0.42	4606	-1.10	26.9	1.35	1.36	0.83
-0.09	4041	-1.06	23.5	0.66	0.66	-0.04	4609	-1.11	26.9	1.33	1.35	0.91
-0.08	4044	-1.25	22.7	0.31	0.33	-0.06	4612	-1.28	27.8	1.36	1.39	1.10
-0.06	4047	-1.45	23.0	0.17	0.22	-0.37	4615	-1.25	27.8	1.39	1.42	1.12
-0.04	4050	-1.43	24.1	0.43	0.51	0.05	4618	-1.36	27.4	1.20	1.23	0.94
-0.03	4053	-1.31	24.8	0.70	0.80	0.37	4621	-1.11	27.4	1.44	1.49	1.18
-0.02	4056	-1.26	25.1	0.80	0.90	0.50	4624	-1.06	27.4	1.49	1.54	1.11
-0.03	4059	-1.22	25.1	0.84	0.93	0.50	4627	-1.23	26.8	1.20	1.25	0.82
-0.06	4062	-1.23	23.5	0.49	0.57	-0.01	4630	-1.45	27.3	1.08	1.14	0.64
-0.10	4065	-1.15	23.5	0.57	0.63	-0.06	4633	-1.47	27.4	1.09	1.16	0.74
-0.12	4068	-1.05	23.6	0.71	0.74	0.11	4636	-1.37	27.7	1.25	1.33	0.74
-0.13	4071	-1.05	23.7	0.73	0.74	-0.02	4639	-1.04	28.2	1.68	1.77	1.23
-0.12	4074	-1.13	23.7	0.63	0.63	-0.15	4642	-1.03	27.9	1.61	1.71	0.81
-0.10	4077	-1.20	23.5	0.52	0.52	-0.11	4645	-1.46	27.0	1.00	1.10	0.40
-0.08	4080	-1.05	23.5	0.68	0.69	0.06	4648	-1.35	26.8	1.08	1.16	0.69
-0.08	4083	-0.90	23.7	0.87	0.90	0.40	4651	-1.27	27.2	1.24	1.30	0.59
-0.08	4086	-0.98	23.6	0.77	0.83	0.26	4654	-1.25	26.9	1.20	1.24	0.31
-0.07	4089	-1.14	23.2	0.51	0.62	0.37	4657	-1.60	26.8	0.84	0.87	0.39
-0.07	4092	-1.20	23.0	0.41	0.54	0.10	4660	-1.23	25.8	0.99	1.05	0.60
-0.07	4095	-1.19	23.2	0.48	0.61	0.07	4663	-1.08	26.8	1.34	1.43	0.92
-0.07	4098	-1.08	23.5	0.65	0.77	0.15	4666	-1.14	27.8	1.48	1.60	1.09
-0.07	4101	-1.05	24.0	0.78	0.88	0.19	4669	-1.29	28.4	1.46	1.60	0.70
-0.07	4104	-1.20	24.4	0.72	0.79	0.22	4672	-1.32	28.1	1.37	1.49	0.64
-0.06	4107	-1.26	24.6	0.71	0.74	0.42	4675	-1.32	27.2	1.19	1.31	0.75
-0.05	4110	-1.17	24.5	0.77	0.80	0.51	4678	-1.43	26.8	0.99	1.07	0.65
-0.02	4113	-1.13	24.4	0.80	0.82	0.32	4681	-1.48	26.6	0.90	0.97	0.61
-0.01	4116	-0.39	24.5	1.55	1.58	1.05	4684	-1.31	26.6	1.08	1.12	0.54
-0.02	4119	-0.47	24.6	1.48	1.52	1.18	4687	-1.08	27.0	1.39	1.42	0.94
-0.03	4122	-1.16	24.6	0.81	0.87	0.57	4690	-1.28	27.2	1.22	1.25	0.66
-0.05	4125	-1.32	24.8	0.68	0.74	0.35	4693	-1.02	26.9	1.44	1.48	1.17
-0.09	4128	-1.35	24.9	0.67	0.75	0.30	4696	-1.19	26.9	1.26	1.32	1.03
-0.11	4131	-1.38	24.8	0.62	0.69	0.21	4699	-1.43	27.1	1.05	1.13	0.92
-0.12	4134	-1.42	24.7	0.56	0.61	0.15	4702	-1.46	26.6	0.92	1.02	0.67
-0.11	4137	-1.44	24.8	0.57	0.60	0.08	4705	-1.30	26.6	1.08	1.20	0.85
-0.10	4140	-1.41	24.7	0.57	0.60	0.02	4708	-1.25	26.5	1.12	1.24	0.91
-0.09	4143	-1.37	24.5	0.57	0.59	0.08	4711	-1.25	26.2	1.04	1.16	0.68
-0.09	4146	-1.27	24.2	0.61	0.64	0.04	4714	-1.22	26.5	1.15	1.26	1.05
-0.09	4149	-1.05	23.9	0.77	0.80	0.10	4717	-1.45	27.0	1.00	1.09	0.73
-0.10	4152	-1.26	23.7	0.50	0.53	-0.20	4720	-1.31	27.3	1.22	1.29	0.80
-0.09	4155	-1.41	23.6	0.35	0.37	-0.40	4723	-1.14	27.9	1.51	1.57	1.06
-0.05	4158	-1.38	23.7	0.39	0.42	0.03	4726	-1.23	27.7	1.38	1.44	0.83
-0.02	4161	-1.20	23.8	0.61	0.64	0.28	4729	-1.37	27.5	1.20	1.27	0.96
-0.01	4164	-1.29	24.1	0.56	0.61	0.09	4732	-1.28	27.2	1.24	1.32	0.81
-0.01	4167	-1.29	24.3	0.60	0.66	0.15	4735	-1.28	26.9	1.17	1.26	0.53
-0.02	4170	-1.24	24.0	0.60	0.67	0.07	4738	-1.40	26.6	0.99	1.09	0.58
-0.03	4173	-1.22	23.3	0.46	0.53	0.00	4741	-1.30	26.8	1.12	1.23	0.63
-0.05	4176	-1.11	25.0	0.95	1.01	0.42	4744	-1.48	27.0	0.97	1.09	0.29
-0.05	4179	-1.24	25.5	0.91	0.98	0.51	4747	-1.41	27.5	1.15	1.28	0.72
-0.05	4182	-1.43	25.0	0.62	0.70	0.19	4750	-1.58	27.5	0.98	1.10	0.59
-0.04	4185	-1.50	24.6	0.46	0.54	-0.15	4753	-1.62	27.6	0.97	1.08	0.64
-0.04	4188	-1.56	24.4	0.36	0.43	-0.28	4756	-1.38	27.9	1.28	1.37	0.71
-0.03	4191	-1.42	24.3	0.47	0.55	0.08	4759	-1.22	27.9	1.43	1.49	1.00
-0.03	4194	-1.43	24.2	0.45	0.55	0.13	4762	-1.11	28.8	1.73	1.76	1.08
-0.03	4197	-1.59	24.2	0.30	0.41	-0.16	4765	-1.25	28.5	1.52	1.53	1.13
-0.03	4200	-1.43	24.5	0.52	0.61	0.18	4768	-1.15	27.8	1.49	1.49	1.04
-0.02	4203	-1.43	24.2	0.44	0.51	0.14	4771	-1.10	27.1	1.39	1.38	1.07
-0.01	4206	-1.50	24.0	0.34	0.40	0.28	4774	-1.24	26.5	1.13	1.11	0.71
0.01	4209	-1.58	24.6	0.38	0.44	0.17	4777	-1.40	26.0	0.86	0.85	0.32

Appendix F (continued)

SL-correction 50 m (‰)	999 age (ka)	$\delta^{18}O$ (*G. sacc*) (‰)	Temperature (Mg/Ca) (°C)	$\delta^{18}O$ (water) (‰)	$\delta^{18}O$ (salinity) (‰)	$\delta^{18}O_{water}$ grad. 999-1241 (‰)	1000 Age (ka)	$\delta^{18}O$ (*G. sacc*) (‰)	Temperature (Mg/Ca) (°C)	$\delta^{18}O$ (water) (‰)	$\delta^{18}O$ (salinity) (‰)	$\delta^{18}O_{water}$ grad. 1000-1241 (‰)
0.00	4212	-1.65	25.1	0.42	0.49	0.12	4780	-1.23	25.8	0.98	1.00	0.87
-0.02	4215	-1.64	25.5	0.52	0.63	0.26	4783	-1.31	27.2	1.19	1.23	0.75
-0.02	4218	-1.58	25.8	0.63	0.77	0.52	4786	-1.34	27.1	1.14	1.22	0.67
-0.03	4221	-1.71	26.0	0.54	0.69	0.16	4789	-1.42	27.1	1.07	1.16	0.67
-0.03	4224	-1.96	25.4	0.18	0.30	-0.34	4792	-1.47	27.2	1.03	1.13	0.69
-0.03	4227	-1.83	24.7	0.15	0.23	0.00	4795	-1.39	26.9	1.05	1.11	0.79
-0.01	4230	-1.52	24.2	0.36	0.42	0.19	4798	-1.28	27.2	1.23	1.26	1.04
-0.01	4233	-1.48	24.6	0.48	0.54	0.19	4801	-1.10	27.3	1.44	1.44	1.18
-0.02	4236	-1.45	25.0	0.59	0.64	0.13	4804	-1.38	28.0	1.29	1.26	0.86
-0.03	4239	-1.52	24.8	0.49	0.54	0.31	4807	-1.53	28.3	1.21	1.16	0.81
-0.02	4242	-1.67	24.2	0.20	0.25	0.12	4810	-1.50	28.4	1.25	1.21	0.70
-0.01	4245	-1.81	23.6	-0.07	-0.03	-0.30	4813	-1.47	28.3	1.26	1.25	0.83
-0.01	4248	-1.85	23.0	-0.23	-0.20	-0.66	4816	-1.46	27.9	1.20	1.23	0.76
-0.02	4251	-1.86	22.5	-0.36	-0.33	-0.49	4819	-1.32	27.9	1.32	1.38	0.98
-0.01	4254	-1.86	22.4	-0.37	-0.32	-0.53	4822	-1.37	27.9	1.27	1.35	0.86
-0.03	4257	-1.82	23.1	-0.17	-0.11	-0.31	4825	-1.32	27.6	1.26	1.35	0.88
-0.06	4260	-1.78	23.8	0.01	0.10	-0.06	4828	-1.31	27.4	1.24	1.31	0.86
-0.10	4263	-1.75	23.7	0.02	0.12	0.05	4831	-1.44	27.6	1.16	1.20	0.74
-0.12	4266	-1.71	23.1	-0.06	0.03	-0.30	4834	-1.55	28.0	1.12	1.14	0.63
-0.14	4269	-1.66	22.7	-0.11	-0.03	-0.44	4837	-1.43	28.3	1.31	1.31	0.74
-0.17	4272	-1.61	22.7	-0.06	0.02	-0.28	4840	-1.18	27.9	1.47	1.46	0.84
-0.17	4275	-1.57	22.8	0.00	0.09	-0.37	4843	-1.14	27.8	1.49	1.48	1.02
-0.14	4278	-1.59	23.0	0.04	0.13	-0.16	4846	-0.99	27.5	1.59	1.59	1.09
-0.11	4281	-1.69	23.4	0.01	0.09	-0.30	4849	-0.99	27.0	1.48	1.48	0.88
-0.09	4284	-1.67	22.5	-0.16	-0.07	-0.50	4852	-1.28	26.7	1.13	1.13	0.73
-0.06	4287	-1.49	22.4	-0.01	0.08	-0.20	4855	-1.22	27.9	1.42	1.44	1.03
-0.02	4290	-1.45	22.7	0.12	0.18	-0.06	4858	-1.09	29.3	1.84	1.88	1.37
0.01	4293	-1.67	23.1	-0.01	0.02	-0.36	4861	-1.06	29.0	1.82	1.87	1.12
0.00	4296	-1.87	23.9	-0.06	-0.04	-0.33	4864	-1.25	28.3	1.49	1.54	0.80
-0.02	4299	-1.71	24.0	0.11	0.13	-0.26	4867	-1.55	28.4	1.20	1.27	0.67
-0.03	4302	-1.53	24.1	0.34	0.37	0.01	4870	-1.70	29.0	1.17	1.25	0.72
-0.05	4305	-1.53	24.9	0.49	0.55	0.24	4873	-1.51	28.6	1.29	1.37	0.51
-0.09	4308	-1.51	25.6	0.67	0.76	0.46	4876	-1.37	28.4	1.39	1.45	0.57
-0.13	4311	-1.49	25.0	0.56	0.68	0.29	4879	-1.52	29.0	1.35	1.38	0.51
-0.10	4314	-1.49	23.7	0.27	0.40	0.12	4882	-1.63	28.9	1.23	1.23	0.50
-0.06	4317	-1.55	22.6	-0.01	0.11	-0.12	4885	-1.60	28.3	1.14	1.10	0.42
-0.02	4320	-1.60	22.7	-0.05	0.05	-0.20	4888	-1.44	27.7	1.18	1.10	0.57
0.01	4323	-1.56	22.8	0.03	0.11	-0.01	4891	-1.26	27.5	1.31	1.22	0.77
0.03	4326	-1.47	23.3	0.22	0.30	0.08	4894	-1.41	27.6	1.18	1.11	0.58
0.03	4329	-1.43	24.2	0.46	0.53	-0.05	4897	-1.50	28.0	1.18	1.16	0.49
0.00	4332	-1.57	25.1	0.49	0.56	0.07	4900	-1.48	28.4	1.26	1.30	0.50
-0.03	4335	-1.55	24.6	0.41	0.48	0.10	4903	-1.42	28.7	1.40	1.47	0.70
-0.03	4338	-1.45	23.7	0.31	0.38	0.01	4906	-1.35	28.7	1.47	1.55	0.72
-0.03	4341	-1.38	22.9	0.22	0.29	0.04	4909	-1.39	28.2	1.33	1.40	0.55
-0.04	4344	-1.37	22.7	0.19	0.27	-0.06	4912	-1.71	28.0	0.96	1.01	-0.04
-0.05	4347	-1.37	23.3	0.31	0.38	0.03	4915	-1.55	27.8	1.08	1.12	0.09
-0.06	4350	-1.32	22.8	0.26	0.32	-0.30	4918	-1.27	28.8	1.56	1.60	0.94
-0.06	4353	-1.22	21.7	0.11	0.16	-0.22	4921	-1.15	29.7	1.87	1.92	1.25
-0.05	4356	-1.15	22.6	0.40	0.42	0.00	4924	-1.16	29.7	1.86	1.93	1.24
-0.03	4359	-1.49	23.2	0.17	0.19	-0.15	4927	-1.22	28.6	1.58	1.66	0.98
-0.01	4362	-1.63	23.5	0.10	0.12	0.06	4930	-1.29	28.1	1.40	1.47	0.73
-0.02	4365	-1.44	23.8	0.36	0.39	0.18	4933	-1.31	28.5	1.47	1.54	0.80
-0.03	4368	-1.29	24.1	0.56	0.62	0.09	4936	-1.31	27.9	1.34	1.40	0.79
-0.03	4371	-1.34	24.4	0.57	0.65	0.02	4939	-1.38	28.1	1.30	1.35	0.61
-0.04	4374	-1.46	23.5	0.27	0.38	-0.04	4942	-1.44	26.6	0.95	0.99	0.35
-0.04	4377	-1.50	21.9	-0.11	0.02	-0.11	4945	-1.25	26.2	1.05	1.10	0.50
-0.06	4380	-1.33	23.0	0.29	0.41	0.06	4948	-1.13	26.8	1.30	1.38	0.67
-0.05	4383	-1.28	22.3	0.20	0.30	-0.26	4951	-1.40	27.2	1.11	1.22	0.67
-0.06	4386	-1.26	21.7	0.09	0.18	-0.30	4954	-1.66	27.4	0.90	1.02	0.42
-0.08	4389	-1.27	21.9	0.12	0.21	-0.44	4957	-1.53	27.2	0.97	1.10	0.32
-0.09	4392	-1.35	22.9	0.24	0.34	-0.07	4960	-1.17	27.5	1.40	1.51	0.74
-0.10	4395	-1.44	23.9	0.37	0.47	0.13	4963	-1.28	26.9	1.17	1.26	0.56
-0.10	4398	-1.53	24.6	0.43	0.52	0.02	4966	-1.46	27.2	1.06	1.10	0.09
-0.10	4401	-1.57	24.7	0.41	0.47	-0.09	4969	-1.45	28.0	1.22	1.26	0.66
-0.08	4404	-1.47	23.9	0.34	0.36	-0.32	4972	-1.46	27.9	1.19	1.26	0.67
-0.07	4407	-1.36	24.1	0.48	0.49	0.11	4975	-1.31	27.6	1.28	1.37	0.80
-0.04	4410	-1.36	24.5	0.58	0.59	0.25	4978	-1.36	26.7	1.05	1.13	0.42

Appendix F (continued)

SL-correction 50 m (‰)	999 age (ka)	$\delta^{18}O$ (*G. sacc*) (‰)	Temperature (Mg/Ca) (°C)	$\delta^{18}O$ (water) (‰)	$\delta^{18}O$ (salinity) (‰)	$\delta^{18}O_{water}$ grad. 999-1241 (‰)	1000 Age (ka)	$\delta^{18}O$ (*G. sacc*) (‰)	Temperature (Mg/Ca) (°C)	$\delta^{18}O$ (water) (‰)	$\delta^{18}O$ (salinity) (‰)	$\delta^{18}O_{water}$ grad. 1000-1241 (‰)
-0.03	4413	-1.43	24.4	0.49	0.51	0.16	4981	-1.62	27.3	0.91	0.99	0.39
-0.05	4416	-1.50	23.0	0.13	0.16	-0.29	4984	-1.54	27.4	1.02	1.08	0.73
-0.09	4419	-1.53	23.8	0.26	0.31	-0.40	4987	-1.51	28.3	1.23	1.28	1.09
-0.12	4422	-1.55	25.0	0.50	0.55	0.25	4990	-1.60	28.3	1.13	1.19	0.75
-0.13	4425	-1.57	25.7	0.62	0.67	0.39	4993	-1.64	27.0	0.84	0.92	0.37
-0.12	4428	-1.60	25.2	0.48	0.52	0.07	4996	-1.48	26.6	0.91	1.02	0.33
-0.11	4431	-1.63	24.6	0.33	0.37	0.04	4999	-1.48	27.1	1.01	1.11	0.71
-0.08	4434	-1.63	24.0	0.20	0.24	-0.13	5002	-1.40	27.5	1.16	1.25	0.92
-0.06	4437	-1.62	23.8	0.17	0.21	-0.26	5005	-1.45	27.4	1.11	1.16	0.68
-0.04	4440	-1.61	24.2	0.28	0.31	-0.19	5008	-1.46	27.9	1.18	1.22	0.63
-0.03	4443	-1.58	23.9	0.24	0.27	-0.23	5011	-1.52	28.0	1.15	1.19	0.55
-0.03	4446	-1.45	23.5	0.29	0.31	-0.23	5014	-1.44	27.6	1.15	1.21	0.63
-0.04	4449	-1.37	23.3	0.33	0.33	-0.15	5017	-1.71	27.4	0.84	0.93	0.61
-0.06	4452	-1.46	23.6	0.30	0.29	-0.10	5020	-1.68	28.2	1.04	1.14	0.61
-0.08	4455	-1.46	24.0	0.37	0.37	-0.16	5023	-1.61	27.7	1.01	1.09	0.40
-0.10	4458	-1.43	25.0	0.60	0.62	0.12	5026	-1.39	27.4	1.15	1.24	0.75
-0.12	4461	-1.51	26.1	0.76	0.79	0.45	5029	-1.39	27.0	1.07	1.16	0.57
-0.12	4464	-1.56	25.7	0.64	0.67	0.21	5032	-1.41	27.9	1.24	1.34	0.50
-0.11	4467	-1.50	24.4	0.42	0.45	-0.01	5035	-1.48	28.4	1.27	1.39	0.38
-0.11	4470	-1.43	25.3	0.67	0.70	0.22	5038	-1.48	28.2	1.22	1.37	0.69
-0.09	4473	-1.38	24.7	0.61	0.62	0.32	5041	-1.56	27.6	1.03	1.21	0.43
-0.08	4476	-1.52	24.1	0.33	0.35	0.08	5044	-1.48	27.5	1.08	1.26	0.39
-0.06	4479	-1.60	23.9	0.21	0.23	-0.16	5047	-1.26	28.2	1.45	1.62	1.01
-0.06	4482	-1.57	23.4	0.14	0.17	-0.51	5050	-1.15	28.8	1.68	1.82	1.14
-0.07	4485	-1.55	22.6	0.00	0.02	-0.59	5052	-1.30	28.5	1.48	1.59	0.81
-0.08	4488	-1.52	22.9	0.09	0.10	-0.29	5055	-1.53	27.2	0.97	1.04	-0.07
-0.09	4491	-1.49	23.7	0.29	0.31	-0.06	5058	-1.48	27.3	1.06	1.12	0.12
-0.10	4494	-1.46	23.4	0.24	0.26	-0.31	5061	-1.31	28.1	1.38	1.46	1.08
-0.11	4497	-1.43	22.7	0.13	0.14	-0.32	5064	-1.16	28.1	1.53	1.65	0.71
-0.12	4500	-1.41	23.0	0.21	0.24	0.07	5067	-0.98	28.2	1.75	1.91	0.87
-0.13	4503	-1.65	23.5	0.07	0.14	-0.13	5070	-1.14	27.9	1.52	1.68	0.92
-0.12	4506	-1.66	23.6	0.08	0.18	-0.21	5073	-1.11	27.7	1.50	1.65	1.04
-0.11	4509	-1.55	23.7	0.21	0.33	-0.31	5076	-1.41	28.2	1.31	1.45	0.85
-0.09	4512	-1.57	24.3	0.34	0.48	-0.27	5079	-1.58	28.0	1.09	1.20	0.63
-0.06	4515	-1.61	25.1	0.46	0.63	-0.16	5082	-1.44	27.8	1.19	1.30	0.67
-0.04	4518	-1.50	25.1	0.57	0.75	0.09	5085	-1.09	28.1	1.60	1.71	1.09
0.00	4521	-1.42	25.0	0.62	0.77	0.32	5088	-1.56	28.1	1.14	1.24	0.51
0.00	4524	-1.74	25.1	0.32	0.43	-0.31	5091	-1.29	27.9	1.35	1.44	0.73
0.01	4527	-1.72	25.1	0.35	0.44	-0.21	5094	-1.31	27.7	1.30	1.35	0.56
0.02	4530	-1.63	24.7	0.36	0.42	-0.25	5097	-1.30	27.3	1.22	1.26	0.68
0.01	4533	-1.56	24.1	0.31	0.32	-0.06	5100	-1.39	27.4	1.16	1.19	0.48
-0.01	4536	-1.54	23.1	0.10	0.09	-0.06	5103	-1.24	26.5	1.12	1.15	0.46
-0.05	4539	-1.52	23.0	0.10	0.10	-0.13	5106	-1.41	27.3	1.11	1.15	0.64
-0.08	4542	-1.51	22.3	-0.04	-0.03	-0.40	5109	-1.14	26.7	1.26	1.29	0.83
-0.08	4545	-1.50	22.3	-0.02	0.01	-0.29	5112	-1.17	27.4	1.38	1.41	0.74
-0.09	4548	-1.48	23.2	0.17	0.22	-0.25	5115	-1.08	28.4	1.67	1.70	1.02
-0.07	4551	-1.47	23.1	0.17	0.26	-0.34	5118	-0.99	29.1	1.90	1.94	1.38
-0.03	4554	-1.45	22.8	0.13	0.26	-0.30	5121	-1.04	28.7	1.78	1.83	1.15
0.00	4557	-1.44	24.2	0.43	0.53	0.03	5124	-1.43	28.4	1.33	1.38	0.77
0.03	4560	-1.43	23.2	0.24	0.30	-0.27	5127	-1.36	28.0	1.31	1.36	0.67
0.05	4563	-1.41	22.6	0.12	0.14	-0.55	5130	-1.17	27.9	1.47	1.51	0.72
0.04	4566	-1.40	23.0	0.21	0.20	-0.44	5133	-1.11	27.7	1.50	1.56	0.70
0.01	4569	-1.39	23.2	0.28	0.26	-0.30	5136	-1.15	27.3	1.37	1.44	0.84
-0.03	4572	-1.37	23.1	0.26	0.23	0.08	5139	-1.13	27.7	1.48	1.55	1.02
-0.06	4575	-1.36	23.7	0.42	0.41	-0.07	5142	-1.19	28.5	1.59	1.68	1.06
-0.08	4578	-1.35	25.1	0.72	0.75	0.26	5145	-1.49	28.6	1.30	1.39	0.71
-0.09	4581	-1.33	24.6	0.64	0.67	0.18	5148	-1.50	28.3	1.23	1.32	0.75
-0.07	4584	-1.32	24.7	0.65	0.69	-0.05	5151	-1.27	28.3	1.47	1.54	0.84
-0.05	4587	-1.31	25.0	0.73	0.77	0.25	5154	-1.32	28.9	1.53	1.59	0.91
-0.02	4590	-1.29	25.3	0.81	0.86	0.35	5157	-1.22	28.8	1.62	1.67	1.24
0.00	4593	-1.28	25.6	0.89	0.95	0.35	5160	-1.03	29.9	2.02	2.06	1.37
0.01	4596	-1.27	25.8	0.95	1.01	0.74	5163	-1.15	29.1	1.76	1.78	1.05
0.01	4599	-1.26	24.4	0.66	0.72	0.40	5166	-1.12	28.0	1.55	1.57	0.43
0.00	4602	-1.36	23.6	0.40	0.43	0.15	5169	-1.22	27.4	1.33	1.35	0.64
0.00	4605	-1.44	23.8	0.34	0.35	-0.18	5172	-1.37	27.0	1.10	1.14	0.54
-0.01	4608	-1.40	23.9	0.42	0.44	0.00	5175	-1.43	28.3	1.30	1.35	0.57
-0.02	4611	-1.15	24.1	0.70	0.73	0.45	5178	-1.64	28.6	1.16	1.20	0.64

Appendix F (continued)

SL-correction 50 m (‰)	999 age (ka)	$\delta^{18}O$ (*G. sacc*) (‰)	Temperature (Mg/Ca) (°C)	$\delta^{18}O$ (water) (‰)	$\delta^{18}O$ (salinity) (‰)	$\delta^{18}O_{water}$ grad. 999-1241 (‰)	1000 Age (ka)	$\delta^{18}O$ (*G. sacc*) (‰)	Temperature (Mg/Ca) (°C)	$\delta^{18}O$ (water) (‰)	$\delta^{18}O$ (salinity) (‰)	$\delta^{18}O_{water}$ grad. 1000-1241 (‰)
-0.04	4614	-1.14	24.9	0.90	0.93	0.62	5181	-1.52	28.4	1.24	1.28	0.90
-0.05	4617	-1.16	25.2	0.92	0.95	0.66	5184	-1.61	28.4	1.15	1.20	0.75
-0.06	4620	-1.16	25.5	0.99	1.04	0.73	5187	-1.61	28.6	1.18	1.24	0.44
-0.07	4623	-1.50	26.4	0.84	0.90	0.46	5190	-1.49	28.5	1.29	1.34	0.46
-0.08	4626	-1.69	25.6	0.48	0.52	0.09	5193	-1.41	28.5	1.37	1.43	0.94
-0.08	4629	-1.65	25.5	0.50	0.56	0.07	5196	-1.40	28.8	1.43	1.51	0.72
-0.06	4632	-1.34	25.6	0.83	0.91	0.48	5199	-1.37	28.5	1.40	1.47	0.46
-0.04	4635	-1.45	25.3	0.66	0.75	0.16	5202	-1.16	28.1	1.52	1.57	0.60
0.01	4638	-1.47	25.1	0.60	0.70	0.15	5205	-1.40	28.9	1.46	1.51	0.76
0.05	4641	-1.53	25.0	0.53	0.63	-0.27	5208	-1.46	29.0	1.42	1.44	0.74
0.08	4644	-1.61	25.2	0.47	0.57	-0.12	5211	-1.44	29.3	1.49	1.50	0.70
0.09	4647	-1.68	25.5	0.48	0.56	0.09	5214	-1.43	29.0	1.45	1.45	0.64
0.07	4650	-1.62	25.3	0.50	0.57	-0.15	5217	-1.27	28.7	1.55	1.56	0.65
0.02	4653	-1.32	25.1	0.74	0.78	-0.15	5220	-1.51	27.8	1.12	1.15	0.31
-0.04	4656	-1.23	26.0	1.03	1.06	0.58	5223	-1.51	28.0	1.16	1.21	0.53
-0.07	4659	-1.31	25.5	0.84	0.89	0.45	5226	-1.50	27.6	1.09	1.14	0.36
-0.08	4662	-1.56	25.5	0.59	0.68	0.17	5229	-1.30	28.0	1.37	1.43	0.58
-0.07	4665	-1.80	24.9	0.23	0.35	-0.16	5232	-1.20	28.1	1.49	1.53	0.70
-0.06	4668	-1.56	25.1	0.51	0.65	-0.25	5235	-1.34	28.1	1.35	1.38	0.51
-0.04	4671	-1.46	24.9	0.56	0.68	-0.17	5238	-1.18	28.1	1.51	1.54	0.79
-0.03	4674	-1.41	25.0	0.64	0.75	0.19	5241	-1.04	27.2	1.46	1.51	0.71
-0.05	4677	-1.60	24.7	0.38	0.46	0.04	5244	-1.25	27.4	1.30	1.38	0.52
-0.07	4680	-1.50	24.3	0.40	0.47	0.11	5247	-1.28	28.3	1.46	1.56	0.53
-0.08	4683	-1.52	24.0	0.31	0.36	-0.23	5250	-1.39	28.6	1.40	1.51	0.54
-0.07	4686	-1.54	23.5	0.19	0.22	-0.26	5253	-1.41	27.9	1.25	1.36	0.49
-0.07	4689	-1.57	23.1	0.08	0.11	-0.48	5256	-1.31	27.6	1.28	1.39	0.49
-0.06	4692	-1.56	23.5	0.17	0.21	-0.10	5259	-1.49	26.7	0.92	1.00	0.16
-0.05	4695	-1.56	24.4	0.36	0.41	0.13	5262	-1.55	27.2	0.97	1.03	0.16
-0.04	4698	-1.51	24.6	0.46	0.54	0.33	5265	-1.36	27.4	1.17	1.22	0.40
-0.05	4701	-1.43	24.2	0.46	0.56	0.21	5268	-1.29	28.0	1.39	1.44	1.06
-0.08	4704	-1.46	24.5	0.49	0.60	0.26	5271	-1.04	27.7	1.57	1.63	1.25
-0.11	4707	-1.51	25.0	0.53	0.65	0.31	5274	-1.05	29.2	1.87	1.93	1.45
-0.12	4710	-1.54	25.3	0.57	0.69	0.21	5277	-1.10	28.8	1.73	1.81	1.05
-0.13	4713	-1.48	25.2	0.62	0.72	0.52	5280	-1.18	28.1	1.51	1.60	0.51
-0.12	4716	-1.66	25.5	0.49	0.58	0.21	5283	-1.37	27.7	1.23	1.32	0.39
-0.08	4719	-1.85	25.8	0.37	0.45	-0.04	5286	-1.49	28.4	1.25	1.36	0.50
-0.05	4722	-1.34	25.4	0.79	0.85	0.34	5289	-1.68	29.0	1.21	1.32	0.35
-0.05	4725	-1.37	25.2	0.73	0.79	0.19	5292	-1.29	28.9	1.56	1.67	0.65
-0.07	4728	-1.50	25.1	0.57	0.64	0.34	5295	-1.48	29.3	1.46	1.57	0.84
-0.09	4731	-1.44	25.8	0.76	0.85	0.34	5298	-1.71	27.8	0.92	1.02	0.27
-0.09	4734	-1.41	26.1	0.87	0.96	0.23	5301	-1.72	26.6	0.67	0.78	0.00
-0.08	4737	-1.37	25.7	0.82	0.92	0.41	5304	-1.48	28.5	1.30	1.45	0.72
-0.06	4740	-1.48	25.4	0.64	0.75	0.15	5307	-1.30	28.7	1.51	1.68	1.01
-0.05	4743	-1.74	25.0	0.31	0.43	-0.38	5310	-1.31	26.9	1.14	1.33	0.60
-0.06	4746	-1.74	24.7	0.25	0.38	-0.19	5313	-1.23	27.8	1.40	1.59	0.80
-0.09	4749	-1.55	25.3	0.55	0.68	0.16	5316	-1.28	28.1	1.42	1.56	0.79
-0.11	4752	-1.69	25.7	0.51	0.61	0.17	5319	-1.58	28.7	1.24	1.36	0.62
-0.11	4755	-1.83	24.4	0.09	0.18	-0.48	5322	-1.65	28.3	1.09	1.18	0.58
-0.08	4758	-1.74	25.1	0.32	0.38	-0.11	5325	-1.52	28.3	1.21	1.27	0.75
-0.05	4761	-1.44	25.5	0.72	0.76	0.07	5328	-1.39	28.1	1.29	1.34	0.74
-0.03	4764	-1.23	24.5	0.70	0.70	0.30	5331	-1.22	28.3	1.52	1.56	0.65
-0.05	4767	-1.14	24.0	0.69	0.70	0.25	5334	-0.99	28.5	1.79	1.81	1.08
-0.07	4770	-1.42	24.0	0.41	0.40	0.09	5337	-1.09	27.4	1.47	1.48	0.86
-0.09	4773	-1.57	25.5	0.58	0.56	0.16	5340	-1.17	28.0	1.50	1.50	0.88
-0.09	4776	-1.28	24.5	0.65	0.64	0.11	5343	-1.16	28.0	1.50	1.51	0.83
-0.09	4779	-1.33	25.1	0.73	0.74	0.61	5346	-1.42	28.6	1.37	1.41	0.88
-0.09	4782	-1.35	25.4	0.79	0.84	0.35	5349	-1.52	28.9	1.33	1.41	0.85
-0.08	4785	-1.62	26.0	0.64	0.72	0.17	5352	-1.50	28.6	1.29	1.40	0.69
-0.10	4788	-1.70	26.6	0.68	0.77	0.28	5355	-1.32	28.0	1.36	1.50	0.78
-0.12	4791	-1.57	25.4	0.56	0.66	0.22	5358	-1.39	27.6	1.20	1.36	0.65
-0.15	4794	-1.40	25.0	0.64	0.70	0.38	5361	-1.55	28.3	1.18	1.32	0.49
-0.18	4797	-1.47	24.6	0.50	0.53	0.31	5364	-1.47	27.9	1.17	1.29	0.50
-0.18	4800	-1.62	24.1	0.23	0.23	-0.04	5367	-1.43	27.4	1.12	1.22	0.45
-0.17	4803	-1.62	24.0	0.22	0.19	-0.21	5370	-1.52	28.3	1.23	1.31	0.46
-0.14	4806	-1.53	24.2	0.35	0.30	-0.06	5373	-1.27	27.8	1.36	1.42	0.50
-0.10	4809	-1.48	25.0	0.57	0.53	0.02	5376	-1.26	27.7	1.36	1.40	0.89
-0.07	4812	-1.55	26.0	0.71	0.70	0.28	5379	-1.42	28.8	1.41	1.45	0.79

Appendix F (continued)

SL-correction 50 m (‰)	999 age (ka)	$\delta^{18}O$ (*G. sacc*) (‰)	Temperature (Mg/Ca) (°C)	$\delta^{18}O$ (water) (‰)	$\delta^{18}O$ (salinity) (‰)	$\delta^{18}O_{water}$ grad. 999-1241 (‰)	1000 Age (ka)	$\delta^{18}O$ (*G. sacc*) (‰)	Temperature (Mg/Ca) (°C)	$\delta^{18}O$ (water) (‰)	$\delta^{18}O$ (salinity) (‰)	$\delta^{18}O_{water}$ grad. 1000-1241 (‰)
-0.06	4815	-1.42	25.6	0.74	0.77	0.31	5382	-1.34	28.1	1.36	1.41	0.49
-0.08	4818	-1.51	25.4	0.61	0.67	0.27	5385	-1.38	27.1	1.10	1.15	0.41
-0.12	4821	-1.56	25.2	0.54	0.62	0.12	5388	-1.42	26.9	1.04	1.10	0.41
-0.16	4824	-1.69	25.0	0.37	0.45	-0.02	5391	-1.45	27.7	1.17	1.26	0.62
-0.16	4827	-1.63	25.1	0.45	0.52	0.07	5394	-1.34	27.4	1.21	1.30	0.55
-0.15	4830	-1.70	25.3	0.42	0.47	0.01	5397	-1.42	28.1	1.28	1.37	0.80
-0.13	4833	-1.64	25.0	0.40	0.42	-0.09	5400	-1.36	28.5	1.41	1.52	0.78
-0.11	4836	-1.51	24.9	0.51	0.51	-0.06	5403	-1.72	28.1	0.98	1.10	0.42
-0.11	4839	-1.46	25.2	0.63	0.62	0.00	5406	-1.78	27.8	0.86	0.99	0.53
-0.11	4842	-1.28	25.2	0.80	0.79	0.33	5409	-1.63	27.4	0.92	1.05	0.45
-0.10	4845	-1.45	25.1	0.62	0.62	0.13	5412	-1.35	27.5	1.21	1.35	0.50
-0.09	4848	-1.38	24.8	0.63	0.63	0.03	5415	-1.48	28.0	1.20	1.33	0.52
-0.05	4851	-1.43	24.5	0.51	0.51	0.11	5418	-1.33	27.4	1.23	1.34	0.55
-0.04	4854	-1.44	25.1	0.63	0.65	0.25	5421	-1.25	28.0	1.43	1.53	0.82
-0.03	4857	-1.63	25.8	0.58	0.62	0.12	5424	-1.49	29.4	1.46	1.55	0.93
-0.03	4860	-1.78	25.7	0.41	0.46	-0.30	5427	-1.45	29.1	1.46	1.54	0.90
-0.03	4863	-1.78	25.9	0.46	0.52	-0.22	5430	-1.32	28.4	1.44	1.52	0.78
-0.03	4866	-1.81	26.7	0.59	0.66	0.05	5433	-1.39	27.8	1.25	1.31	0.50
-0.03	4869	-1.54	26.6	0.85	0.92	0.40	5436	-1.40	27.5	1.18	1.23	0.37
-0.04	4872	-1.41	26.1	0.88	0.95	0.10	5439	-0.91	28.0	1.77	1.82	0.90
-0.04	4875	-1.62	26.8	0.80	0.86	-0.02	5442	-1.19	28.3	1.54	1.58	0.75
-0.05	4878	-1.55	27.5	1.03	1.07	0.19	5445	-1.38	27.3	1.14	1.19	0.39
-0.06	4881	-1.38	26.2	0.91	0.91	0.19	5448	-1.43	27.4	1.13	1.20	0.23
-0.05	4884	-1.09	24.8	0.91	0.87	0.19	5451	-1.38	28.8	1.46	1.56	0.46
-0.04	4887	-1.32	24.1	0.53	0.45	-0.08	5454	-1.42	28.8	1.42	1.55	0.17
-0.05	4890	-1.39	23.8	0.40	0.31	-0.14	5457	-1.27	28.1	1.43	1.56	0.26
-0.07	4893	-1.43	24.1	0.42	0.34	-0.18	5460	-1.25	28.1	1.44	1.57	0.37
-0.08	4896	-1.41	24.8	0.59	0.57	-0.10	5463	-1.32	28.4	1.43	1.54	0.35
-0.09	4899	-1.32	25.7	0.88	0.92	0.11	5466	-1.42	28.4	1.34	1.42	0.31
-0.09	4902	-1.33	26.3	0.99	1.06	0.30	5469	-1.48	28.0	1.19	1.24	0.29
-0.09	4905	-1.29	26.1	0.99	1.07	0.24	5472	-1.47	27.8	1.16	1.20	0.44
-0.07	4908	-1.26	26.1	1.02	1.09	0.25	5475	-1.54	27.0	0.92	0.97	-0.07
-0.05	4911	-1.39	26.4	0.96	1.02	-0.03	5478	-1.45	26.7	0.96	1.03	-0.02
-0.05	4914	-1.46	26.7	0.94	0.98	-0.06	5481	-1.30	27.5	1.28	1.36	0.46
-0.04	4917	-1.49	26.7	0.91	0.94	0.28	5484	-1.30	27.1	1.18	1.27	0.31
-0.03	4920	-1.60	26.5	0.77	0.82	0.15	5487	-1.40	27.3	1.13	1.20	0.09
-0.02	4923	-1.66	26.0	0.60	0.67	-0.02	5490	-1.25	27.7	1.37	1.43	0.46
-0.02	4926	-1.87	25.5	0.29	0.36	-0.32	5493	-1.09	28.1	1.62	1.67	0.79
-0.04	4929	-1.61	25.9	0.62	0.70	-0.04	5496	-1.52	28.7	1.31	1.34	0.37
-0.04	4932	-1.69	26.3	0.63	0.70	-0.04	5499	-1.61	27.8	1.03	1.06	-0.06
-0.04	4935	-1.43	25.6	0.75	0.81	0.20	5502	-1.54	27.5	1.04	1.10	0.06
-0.04	4938	-1.42	24.6	0.55	0.60	-0.15	5505	-1.18	27.6	1.41	1.50	0.64
-0.05	4941	-1.62	25.5	0.54	0.58	-0.06	5508	-1.31	26.4	1.03	1.12	0.35
-0.06	4944	-1.82	25.4	0.32	0.36	-0.24	5511	-1.23	26.5	1.13	1.24	0.42
-0.06	4947	-1.75	25.5	0.40	0.48	-0.22	5514	-1.17	27.1	1.31	1.44	0.56
-0.07	4950	-1.58	26.4	0.76	0.87	0.31	5517	-1.14	28.2	1.57	1.71	0.84
-0.07	4953	-1.84	26.6	0.54	0.66	0.06	5520	-1.29	27.9	1.36	1.51	0.29
-0.07	4956	-1.78	26.1	0.49	0.62	-0.16	5523	-1.36	27.4	1.19	1.32	0.15
-0.05	4959	-1.41	25.8	0.80	0.92	0.15	5526	-1.36	27.5	1.21	1.35	0.27
-0.04	4962	-1.47	25.7	0.72	0.81	0.11	5529	-1.45	28.3	1.29	1.42	0.42
-0.02	4965	-1.68	25.6	0.49	0.54	-0.47	5532	-1.40	28.8	1.44	1.52	0.58
-0.01	4968	-1.72	25.4	0.42	0.47	-0.14	5535	-1.06	29.1	1.84	1.91	0.93
0.00	4971	-1.57	25.3	0.53	0.60	0.01	5538	-1.09	29.4	1.86	1.87	0.88
-0.01	4974	-1.57	25.1	0.49	0.58	0.01	5541	-1.27	27.6	1.32	1.28	0.37
-0.03	4977	-1.83	24.9	0.20	0.29	-0.42	5544	-1.34	28.0	1.34	1.25	0.53
-0.04	4980	-1.99	25.0	0.06	0.14	-0.45	5547	-1.32	28.3	1.41	1.30	0.71
-0.06	4983	-1.69	25.1	0.38	0.44	0.09	5550	-1.35	28.8	1.49	1.41	0.60
-0.06	4986	-1.83	25.2	0.25	0.30	0.12	5553	-1.44	29.0	1.43	1.40	0.51
-0.03	4989	-1.65	25.2	0.45	0.50	0.07	5556	-1.41	28.0	1.28	1.29	0.08
-0.03	4992	-1.45	25.8	0.76	0.85	0.29	5559	-1.55	28.3	1.19	1.24	0.25
-0.03	4995	-1.55	26.3	0.78	0.89	0.20	5562	-1.70	29.5	1.28	1.34	0.16
-0.05	4998	-1.87	26.3	0.45	0.55	0.15	5565	-1.32	29.4	1.63	1.70	0.52
-0.08	5001	-1.80	26.1	0.48	0.56	0.23	5568	-1.19	29.0	1.69		
-0.10	5004	-1.70	25.4	0.43	0.49	0.01	5571	-1.07	28.6	1.72		
-0.11	5007	-1.68	24.2	0.19	0.22	-0.36	5574	-1.15	27.7	1.46		
-0.11	5010	-1.62	23.5	0.12	0.17	-0.47	5577	-1.32	28.4	1.43		
-0.10	5013	-1.49	23.9	0.32	0.38	-0.20	5580	-1.57	28.0	1.10		

Appendix F (continued)

SL-correction 50 m (‰)	999 age (ka)	$\delta^{18}O$ (*G. sacc*) (‰)	Temperature (Mg/Ca) (°C)	$\delta^{18}O$ (water) (‰)	$\delta^{18}O$ (salinity) (‰)	$\delta^{18}O_{water}$ grad. 999-1241 (‰)	1000 Age (ka)	$\delta^{18}O$ (*G. sacc*) (‰)	Temperature (Mg/Ca) (°C)	$\delta^{18}O$ (water) (‰)	$\delta^{18}O$ (salinity) (‰)	$\delta^{18}O_{water}$ grad. 1000-1241 (‰)
-0.08	5016	-1.37	24.2	0.51	0.60	0.29	5583	-1.18	27.4	1.37		
-0.06	5019	-1.54	25.3	0.58	0.67	0.15	5586	-1.23	27.5	1.34		
-0.05	5022	-1.76	26.6	0.62	0.70	0.01	5589	-1.26	27.9	1.39		
-0.05	5025	-1.90	27.4	0.66	0.74	0.26						
-0.06	5028	-1.91	27.2	0.59	0.68	0.09						
-0.06	5031	-1.87	26.8	0.55	0.64	-0.19						
-0.08	5034	-1.82	26.4	0.52	0.63	-0.38						
-0.09	5037	-1.79	26.1	0.48	0.63	-0.05						
-0.10	5040	-1.90	25.8	0.31	0.49	-0.28						
-0.11	5043	-1.63	26.0	0.62	0.80	-0.07						
-0.11	5046	-1.48	26.3	0.85	1.02	0.41						
-0.11	5049	-1.78	26.6	0.60	0.74	0.06						
-0.10	5052	-1.73	26.6	0.65	0.75	-0.02						
-0.10	5055	-1.55	26.4	0.80	0.87	-0.25						
-0.11	5058	-1.39	26.5	0.97	1.03	0.03						
-0.14	5061	-1.33	26.8	1.10	1.18	0.80						
-0.17	5064	-1.40	27.1	1.09	1.22	0.27						
-0.19	5067	-1.47	26.9	0.98	1.14	0.11						
-0.19	5070	-1.55	26.7	0.86	1.02	0.26						
-0.15	5073	-1.63	26.8	0.79	0.94	0.34						
-0.11	5076	-1.70	26.9	0.74	0.87	0.28						
-0.08	5079	-1.88	26.4	0.46	0.57	0.00						
-0.07	5082	-1.88	25.2	0.20	0.31	-0.32						
-0.05	5085	-1.51	24.6	0.46	0.56	-0.05						
-0.04	5088	-1.37	25.4	0.76	0.87	0.14						
-0.03	5091	-1.41	26.1	0.88	0.96	0.25						
-0.01	5094	-1.47	25.9	0.77	0.82	0.03						
0.01	5097	-1.92	25.5	0.23	0.27	-0.31						
-0.01	5100	-1.95	25.1	0.12	0.15	-0.56						
-0.04	5103	-1.75	24.7	0.22	0.25	-0.44						
-0.08	5106	-1.58	24.6	0.38	0.42	-0.09						
-0.11	5109	-1.46	25.2	0.62	0.66	0.20						
-0.14	5112	-1.55	25.0	0.49	0.52	-0.15						
-0.16	5115	-1.59	25.0	0.46	0.50	-0.19						
-0.14	5118	-1.55	25.5	0.59	0.63	0.07						
-0.12	5121	-1.54	25.9	0.69	0.75	0.07						
-0.10	5124	-1.58	25.8	0.64	0.70	0.09						
-0.08	5127	-1.59	25.7	0.61	0.66	-0.02						
-0.05	5130	-1.56	25.5	0.58	0.62	-0.17						
-0.04	5133	-1.55	25.0	0.49	0.55	-0.31						
-0.04	5136	-1.56	24.5	0.39	0.46	-0.14						
-0.05	5139	-1.59	25.0	0.45	0.53	-0.01						
-0.05	5142	-1.63	25.9	0.61	0.70	0.08						
-0.06	5145	-1.66	26.6	0.72	0.81	0.13						
-0.08	5148	-1.63	25.8	0.59	0.68	0.11						
-0.09	5151	-1.61	24.9	0.41	0.48	-0.22						
-0.09	5154	-1.69	24.6	0.27	0.32	-0.36						
-0.11	5157	-1.82	25.0	0.24	0.29	-0.15						
-0.12	5160	-1.78	25.5	0.37	0.41	-0.28						
-0.13	5163	-1.72	25.8	0.48	0.51	-0.22						
-0.14	5166	-1.66	26.0	0.59	0.61	-0.54						
-0.14	5169	-1.53	26.2	0.77	0.79	0.09						
-0.13	5172	-1.17	26.6	1.22	1.26	0.67						
-0.11	5175	-1.20	27.1	1.29	1.33	0.55						
-0.10	5178	-1.50	27.2	1.00	1.04	0.48						
-0.09	5181	-1.80	26.9	0.65	0.69	0.31						
-0.08	5184	-1.81	26.7	0.59	0.64	0.20						
-0.08	5187	-1.77	26.4	0.58	0.63	-0.16						
-0.06	5190	-1.70	24.6	0.27	0.33	-0.56						
-0.05	5193	-1.61	22.8	-0.03	0.04	-0.45						
-0.05	5196	-1.54	23.6	0.20	0.28	-0.51						
-0.04	5199	-1.58	24.4	0.34	0.41	-0.60						
-0.05	5202	-1.67	25.5	0.48	0.53	-0.44						
-0.07	5205	-1.74	26.7	0.67	0.71	-0.03						
-0.10	5208	-1.73	27.8	0.90	0.92	0.21						
-0.12	5211	-1.69	27.7	0.92	0.93	0.13						
-0.13	5214	-1.60	27.4	0.94	0.94	0.13						

Appendix F (continued)

SL-correction 50 m (‰)	999 age (ka)	$\delta^{18}O$ (*G. sacc*) (‰)	Temperature (Mg/Ca) (°C)	$\delta^{18}O$ (water) (‰)	$\delta^{18}O$ (salinity) (‰)	$\delta^{18}O_{water}$ grad. 999-1241 (‰)	1000 Age (ka)	$\delta^{18}O$ (*G. sacc*) (‰)	Temperature (Mg/Ca) (°C)	$\delta^{18}O$ (water) (‰)	$\delta^{18}O$ (salinity) (‰)	$\delta^{18}O_{water}$ grad. 1000-1241 (‰)
-0.13	5217	-1.57	27.0	0.90	0.91	0.00						
-0.11	5220	-1.71	26.8	0.70	0.73	-0.11						
-0.08	5223	-1.73	26.5	0.63	0.67	-0.01						
-0.06	5226	-1.68	26.3	0.64	0.70	-0.09						
-0.05	5229	-1.60	26.2	0.70	0.75	-0.10						
-0.05	5232	-1.52	26.1	0.75	0.78	-0.05						
-0.07	5235	-1.63	26.1	0.65	0.68	-0.20						
-0.09	5238	-1.59	26.2	0.70	0.74	-0.02						
-0.08	5241	-1.61	26.2	0.69	0.74	-0.05						
-0.07	5244	-1.87	26.3	0.45	0.53	-0.33						
-0.06	5247	-1.81	26.4	0.53	0.63	-0.40						
-0.05	5250	-1.58	26.6	0.80	0.91	-0.05						
-0.04	5253	-1.51	26.9	0.92	1.04	0.16						
-0.03	5256	-1.71	27.1	0.77	0.87	-0.02						

Curriculum Vitae

Name: Jeroen Groeneveld

Date of Birth: February 5th, 1976, Rotterdam, Netherlands

Nationality: Dutch

Academic Career:

1988-1994: Gymnasium Camphusianum, Gorinchem, Netherlands

1994-2000: Geology Studies Institute of Earth Sciences, University of Utrecht, Netherlands
Master thesis: „A high resolution record of the Arabian monsoon variability and the Oxygen Minimum Zone from the Pakistan Margin“
Supervision: Dr. W.J. Zachariasse, Dr. G.J. Reichart

2000-2001: Backpacking Australia

Autumn 2001: Mammoet Company, Project Lifting Kursk, Utrecht, Netherlands

Since 11/2001: PhD-student at IFM-Geomar, Leibniz Institute of Marine Sciences, Kiel, Germany, DFG-Research Unit „Ocean Gateways“:
“Effect of the Pliocene closure of the Panamanian Gateway on Caribbean and east Pacific sea surface temperatures and salinities by applying combined Mg/Ca and $\delta^{18}O$ measurements (5.6-2.2 Ma)
Supervision: Dr. D. Nürnberg, Dr. R. Tiedemann

Kiel, May 2005